

IGF2BP1 induces high-risk neuroblastoma in
transgenic mice and enhances tumor progression in
synergy with MYCN

Dissertation

zur Erlangung des
Doktorgrades der Naturwissenschaften (Dr. rer. nat.)

der

Naturwissenschaftlichen Fakultät I - Biowissenschaften
der Martin-Luther-Universität Halle-Wittenberg,

vorgelegt

von Herrn Sven Hagemann

Erstgutachter: Prof. Dr. Stefan Hüttelmaier
Zweitgutachterin: PD Dr. Jessica Höll
Drittgutachter: Prof. Dr. Dirk Heckl

Verteidigungsdatum: 18.12.2024

"Working in cancer research is like playing a never-ending game of whack-a-mole: just when you think you've got one problem solved, another one pops up."

ChatGPT 3.5 (2024)

Table of content

1. Summary.....	1
2. Introduction.....	3
2.1 Neuroblastoma.....	3
2.1.1 Origin and clinical presentation.....	3
2.1.2 Diagnosis.....	4
2.1.3 Staging	6
2.1.4 Genetic susceptibility	7
2.1.5 Mutations and altered gene expression.....	9
2.1.6 Genetics.....	18
2.1.7 Epigenetics.....	25
2.1.8 Immunological microenvironment of neuroblastoma	26
2.1.9 Treatment and therapy	27
2.1.10 Genetically engineered mouse models (GEMMs).....	31
2.2 Insulin-like growth factor 2 mRNA binding protein family - IGF2BPs	34
2.2.1 Structural features and RNA binding.....	34
2.2.2 Subcellular localization and mRNA complexes.....	36
2.2.3 Role of IGF2BPs in RNA regulation	36
2.2.4 Control of IGF2BP expression	39
2.2.5 IGF2BPs in development and cancer.....	40
2.2.6 Inhibition of IGF2BP1.....	45
2.2.7 IGF2BP1 mouse models in cancer	45
2.3 Aims of the thesis	47
3. Material and Methods.....	48
3.1 Material	48
3.1.1 Patient samples	48
3.1.2 Animals	48
3.1.3 Bacteria.....	48
3.1.4 Cell lines.....	49
3.1.5 Chemicals and reagents.....	49
3.1.6 Buffers	50
3.1.7 Antibodies.....	51
3.1.8 Plasmids.....	52
3.1.9 Oligonucleotides.....	53

3.1.10	siRNAs	55
3.1.11	Kits and systems	56
3.1.12	Instruments	57
3.2	Animal work.....	58
3.2.1	Mouse xenograft studies.....	58
3.2.2	Patient-derived xenograft study.....	58
3.2.3	Transgenic mouse studies	58
3.2.4	Immunohistochemistry	59
3.3	Cell biological methods	59
3.3.1	Cell culture.....	59
3.3.2	Transfection.....	59
3.3.3	CRISPR/Cas9-mediated knockout.....	59
3.3.4	Luciferase reporter assay	60
3.3.5	Fluorescence reporter assay	60
3.3.6	Lentiviral transduction.....	60
3.3.7	Inhibition of RNA and protein synthesis.....	61
3.3.8	2D growth assay	61
3.3.9	3D spheroid formation assay.....	61
3.3.10	Anoikis resistance assay	61
3.3.11	Cell viability measurement.....	61
3.3.12	Apoptosis measurement	61
3.3.13	Compound testing	62
3.4	Biochemical methods	62
3.4.1	Cloning.....	62
3.4.2	RNA isolation	64
3.4.3	Reverse transcription	65
3.4.4	Quantitative real-time PCR.....	65
3.4.5	Protein extraction.....	65
3.4.6	SDS-PAGE and Western blot analysis.....	66
3.4.7	Mouse tissue preparation	66
3.4.8	RNA immunoprecipitation.....	66
3.4.9	Nascent mRNA capture	67
3.4.10	miTRAP	67
3.4.11	Flow cytometry.....	68
3.5	Bioinformatic methods.....	69
3.5.1	RNA sequencing and differential expression analysis.....	69

3.5.2	Gene set enrichment analysis	71
3.5.3	Shallow whole genome sequencing	71
3.5.4	Kaplan-Meier survival analysis	72
3.5.5	Public data analysis	72
3.6	Statistics and presentation	74
4.	Results	75
4.1	Genome analyses of primary neuroblastoma	75
4.2	Identification of essential candidate genes on chromosome 17q in neuroblastoma.....	78
4.3	IGF2BP1 expression and prognostic significance in neuroblastoma.....	81
4.4	IGF2BP1 and MYCN form a self-promoting feedforward loop.....	83
4.4.1	MYCN as a transcriptional regulator of IGF2BP1 in neuroblastoma	83
4.4.2	Deregulated miRNAs distinguishes <i>MYCN</i> -amplified neuroblastoma.....	84
4.4.3	Evaluation of directly associated miRNAs with MYCN using miTRAP	86
4.4.4	IGF2BP1 is a potent regulator of MYCN mRNA expression.....	87
4.4.5	IGF2BP1 directly binds MYCN mRNA in a 3'UTR- and miRNA-dependent manner	90
4.4.6	IGF2BP1 stabilizes the MYCN mRNA, which is targetable by BTYNB	92
4.4.7	Regulation of MYCN by IGF2BP1 is rather m ⁶ A-independent	93
4.5	Impairment of IGF2BP1 expression reduces neuroblastoma growth <i>in vitro</i> and <i>in vivo</i>	95
4.5.1	IGF2BP1 enhances cell proliferation, viability and self-renewal capacity.....	95
4.5.2	IGF2BP1 promotes neuroblastoma xenograft growth	96
4.6	IGF2BP1 and MYCN share oncogenic downstream targets	99
4.6.1	IGF2BP1 and MYCN enhances expression of chromosome 17q genes.....	99
4.6.2	Modulation of BIRC5 by IGF2BP1 and MYC/N is conserved across cancer types	102
4.6.3	Cell cycle kinases as potential targets of the IGF2BP1/MYCN-driven network	104
4.6.4	IGF2BP1 indirectly influences MYCN protein turnover	106
4.7	Inhibition of the IGF2BP1/MYCN-driven network.....	108
4.7.1	EN4 impairs MYCN transcriptional activity and neuroblastoma cell growth	108
4.7.2	Combined treatment of BRD inhibitors and BTYNB is beneficial	109
4.7.3	HDAC1-3 inhibition is sufficient to reduce IGF2BP1 and MYCN.....	111
4.7.4	Combined inhibition of chromosome 17q target genes and IGF2BP1 is beneficial.....	114
4.8	Establishment of a new neuroblastoma transgenic mouse model.....	116
4.8.1	LSL- <i>IGF2BP1</i> transgenic mice induces neuroblastoma in synergy with MYCN	116
4.8.2	IGF2BP1 induces chromosomal aberrations syntenic to human disease	121
5.	Discussion	123
6.	References.....	V
7.	Appendix.....	XXVII

7.1	Supplementary Tables.....	XXVII
7.2	List of figures	XXXI
7.3	List of tables.....	XXXII
7.4	List of abbreviations	XXXII
7.5	List of publications / presentations.....	XXXIV
7.6	Eidesstattliche Erklärung.....	XXXV
7.7	Curriculum vitae	XXXVI

1. Summary

Neuroblastoma is the most prevalent extracranial solid tumor in infants, contributing to approximately 15% of childhood cancer-related mortalities. Despite diverse therapeutic approaches encompassing surgery, radiation, chemotherapy, stem cell transplantation or immunotherapy, the 5-year survival rate for high-risk patients remains below 50% marked by considerable challenges and over 50% incidence of high-risk neuroblastoma relapses. Currently, there are no established preventive strategies for neuroblastoma. This emphasizes the need to elucidate new drug targets and therapeutic avenues. Genomic anomalies underlie the progression of neuroblastoma, prominently characterized by *MYCN* amplification and chromosome 17q gain. The co-occurrence of these chromosomal aberrations is widely recognized, yet their intricate mechanistic relation remain largely elusive. Recent years have identified several candidate oncogenes residing on chromosome 17q. Among them, *IGF2BP1*, an oncofetal RNA-binding protein, has shown gene gain and suggested *MYCN*-associated roles in neuroblastoma.

For the first time, a transgenic mouse model provides crucial insights into *IGF2BP1*'s role in tumorigenesis. The *IGF2BP1*-induced neuroblastoma model showcases the protein's potential to drive tumor formation, highlighting its synergy with *MYCN* and the importance of genomic instability in this process. These findings add to the existing repertoire of transgenic models that contribute to the understanding of neuroblastoma progression. Exploration of miRNA expression in primary neuroblastoma tumor samples has unveiled a general elevation of *MYCN*-regulatory miRNAs. This suggests a mechanism that uncouples *MYCN* expression from miRNA-directed downregulation, implicating RNA-binding proteins. Evidence points to *IGF2BP1* as a potent and druggable chromosome 17q oncogene that synergizes with *MYCN*. This collaboration establishes a self-reinforcing feedforward loop wherein *MYCN* transcriptionally enhances *IGF2BP1* expression and *IGF2BP1* post-transcriptional impairs *MYCN* downregulation via inhibiting miRNA-directed degradation in a 3'UTR-dependent manner. This intricate regulatory network unleashes an "oncogene storm" and genomic instability reminiscent of high-risk disease. Inhibition of *IGF2BP1*, exemplified by *BTYNB*, disrupts this oncogenic network, rendering cancer cells more susceptible to a spectrum of treatments. Subsequent investigations should advance the efficacy and pharmacological properties of *IGF2BP1* inhibitors to effectively disrupt *IGF2BP1*-dependent oncogenic enhancement. *BTYNB* appears a promising starting point for these endeavors. The presented mouse models will expedite the evaluation of improved *IGF2BP1* inhibitors and provide valuable resources for identifying additional *IGF2BP1*-driven oncogenic effectors for combined cancer treatment. Given *IGF2BP1*'s substantial expression in various cancer types, minimal expression in adult tissue and recurrent occurrence of chromosome 17q gains across cancers, targeting *IGF2BP1* emerges as a promising therapeutic avenue.

Zusammenfassung

Neuroblastom ist der häufigste extrakranielle solide Tumor im Säuglingsalter und trägt zu etwa 15% der krebisbedingten Todesfälle im Kindesalter bei. Trotz verschiedener therapeutischer Ansätze, einschließlich Operation, Stammzelltransplantation, sowie Strahlen-, Chemo- oder Immuntherapie, bleibt die 5-Jahres-Überlebensrate für Hochrisikopatienten unter 50% mit einer Rezidivrate von über 50%. Derzeit gibt es keine etablierten Präventionsstrategien für Neuroblastome. Dies unterstreicht die Notwendigkeit, neue Wirkstoffziele und therapeutische Ansätze zu untersuchen. Genomische Anomalien, wie beispielsweise eine Amplifikation von *MYCN* oder die Zunahme von Chromosom 17q, sind ein wesentlicher Bestandteil der Progression von Neuroblastomen. Das gleichzeitige Auftreten dieser chromosomalen Aberrationen ist weithin anerkannt, aber ihre komplexe mechanistische Beziehung bleibt größtenteils unklar. In den letzten Jahren wurden einige Onkogene identifiziert, die auf Chromosom 17q liegen. Unter diesen liegt *IGF2BP1*, ein onkofetales RNA-bindendes Protein, verstärkt exprimiert vor und besitzt *MYCN*-assoziierte Rollen im Neuroblastom.

Zum ersten Mal liefert ein transgenes Mausmodell entscheidende Einblicke in die Rolle von *IGF2BP1* in der Tumorentstehung von Neuroblastomen, hebt seine Synergie mit *MYCN* und die Bedeutung von genomischer Instabilität in diesem Prozess hervor. Diese Ergebnisse erweitern das bestehende Repertoire an transgenen Modellen, die zum Verständnis der Neuroblastomprogression beitragen. Die Untersuchung der miRNA-Expression in primären Neuroblastomtumorproben legt eine allgemeine Erhöhung der *MYCN*-regulatorischen miRNAs nahe. Dies impliziert einen Mechanismus, der die *MYCN*-Expression von der miRNA-vermittelten Degradation entkoppelt und RNA-bindende Proteine, wie *IGF2BP1*, einschließt. Dabei verstärken sich beide Proteine gegenseitig, wobei *MYCN* die Expression von *IGF2BP1* transkriptionell erhöht und *IGF2BP1* post-transkriptionell die *MYCN* mRNA vor miRNA-vermittelten Degradation in einer 3'UTR-abhängigen Weise schützt. Die Inhibierung von *IGF2BP1*, exemplarisch durch *BTYNB*, unterbricht dieses onkogene Netzwerk und macht Krebszellen anfälliger für eine Vielzahl von Behandlungen. Folgeuntersuchungen sollten die Wirksamkeit und pharmakologischen Eigenschaften von *IGF2BP1*-Inhibitoren vorantreiben, um die *IGF2BP1*-abhängige Tumorprogression effektiv zu unterbinden. *BTYNB* scheint ein vielversprechender Ausgangspunkt für diese Bemühungen zu sein. Die vorgestellten Mausmodelle werden die Bewertung verbesserter *IGF2BP1*-Inhibitoren beschleunigen und eine wertvolle Ressource für die Identifizierung zusätzlicher *IGF2BP1*-getriebener onkogener Effektoren sein. Angesichts der erheblichen Expression von *IGF2BP1* in verschiedenen Krebsarten, der minimalen Expression in adulten Geweben und der Zunahme von genetischem Material von Chromosom 17q bei verschiedenen Krebsarten erweist sich die gezielte Inhibierung von *IGF2BP1* als vielversprechender therapeutischer Ansatz.

2. Introduction

2.1 Neuroblastoma

2.1.1 Origin and clinical presentation

Neuroblastoma was first documented by Dr. Rudolf Virchow in 1864. He described it as a glioma tumor arising in the abdominal cavity in a child (Virchow 1864). However, it was Dr. James Homer Wright in 1910 who conducted detailed examination of its characteristic features and origin. He coined the term “neurocytoma” or “neuroblastoma” after observing that the tumor consisted primarily of undifferentiated nerve cells known as neurocytes or neuroblasts. He proposed that neuroblastoma originates from primitive nerve cells that have migrated during development (Wright 1910). Indeed, it is nowadays well accepted that neuroblastoma arise from the sympatho-adrenal lineage of the neural crest (Nakagawara 2004). During normal embryonic development, the neural crest cell precursors migrate from the dorsal neural tube and differentiate into various lineages, including melanocytic, sensory, enteric and sympathetic neurons. However, a significant number of these developing neurons undergo programmed cell death, mainly via apoptosis, during terminal differentiation (Nakagawara 1998a, Nakagawara 1998b). The remaining neurons successfully differentiate into mature neuronal cells with proper function. Neuroblastoma-initiating cells inappropriately resists these death stimuli and proliferate (Marshall *et al.* 2014). Neuroblastoma exclusively originates from precursor or stem cells of the sympatho-adrenal lineage and does not arise from other neural crest lineages (Matthay *et al.* 2016). This suggests that the oncogenic event leading to neuroblastoma occurs after migrating cells have received the signal to differentiate into sympathetic neurons. Disturbance of neural crest migration, maturation or differentiation considerably contribute to neuroblastoma development (Whittle *et al.* 2017). Several transcriptional regulators, such as MASH1, ID2, dHAND, HIF and PHOX2, are involved in determining the fate of cells within sympathetic lineages. These regulators likely play roles in the pathogenesis of neuroblastoma (Isogai *et al.* 2011, Ichimiya *et al.* 2001, Lasorella *et al.* 2002, Gestblom *et al.* 1999, Pietras *et al.* 2009, Jögi *et al.* 2002, van Limpt *et al.* 2004).

Clinically, neuroblastoma presents with remarkable heterogeneity, ranging from spontaneous regression to aggressive and chemoresistant disease (Nuchtern 2006, Nuchtern *et al.* 2012). Notably, neuroblastoma exhibits the highest rates of spontaneous regression observed in human cancers, which suggests delayed activation of normal apoptotic pathways may contribute to this phenomenon (Brodeur 2018). Neuroblastoma primarily originates either in the adrenal medulla (47%) or the paraspinal sympathetic ganglia of the abdomen (24%), thorax (15%), pelvis (3%) and neck (3%; Vo *et al.* 2014). Tumor arising from the cervical or thoracic regions are more common in infants and typically have a more favorable prognosis than adrenal tumors, which are often associated with advanced

stages and unfavorable genetic characteristics (Vo *et al.* 2014, Whittle *et al.* 2017). Clinical symptoms of neuroblastoma include weight loss, fever, bruising, bone pain, and lumps in the abdomen, neck or chest. At diagnosis, approximately half of patients present with highly aggressive disease characterized by rapid tumor growth and metastasis (DuBois *et al.* 1999, Kholodenko *et al.* 2018). Common metastatic sites include lymph nodes, bone and bone marrow, while metastasis to the lung, central nervous system and skin is less frequent (Vo *et al.* 2014, Thompson *et al.* 2016). Patients with stage 4S tumors, classified by the International Neuroblastoma Staging System, exhibit a distinct metastatic pattern, with higher propensity for liver (80%), bone marrow (35%) and skin (14%) involvement than metastasis in lymph nodes (9%) and adrenals (6%; DuBois *et al.* 1999). Only 50% of patients with distant metastases will achieve long-term survival (Cohn *et al.* 2009). Conversely, patients with low- or intermediate-risk disease have a better prognosis, achieving greater than 95% overall survival (Maris *et al.* 2007, Gatta *et al.* 2014). The age of diagnosis varies, but generally, neuroblastoma is diagnosed around 18 months of age (Castleberry 1997, Matthay *et al.* 2016, Whittle *et al.* 2017). Familial neuroblastoma cases tend to be diagnosed earlier at around 9 months (Kushner *et al.* 1986). Neuroblastoma rarely occurs in adolescents and young adults. About 40% of cases are diagnosed within the first year of life, 75% before the age of 4 and over 95% before the age of 10 (Grovas *et al.* 1997, Pizzo and Poplack 2015). Generally, younger patients have a better prognosis depending on other known risk factors. Neuroblastoma is the most common extracranial tumor in infancy, accounting for 6-10% of childhood cancers and approximately 15% of all cancer-related childhood deaths (Gurney *et al.* 1997, Stiller 2016, Zafar *et al.* 2021). Unfortunately, the etiology of neuroblastoma largely remains unknown and effective prevention strategies are lacking (Cook *et al.* 2004, Menegaux *et al.* 2004, McDermott *et al.* 2015). Boys are slightly more affected by neuroblastoma than girls, however, the reason for this prevalence is unclear (Whittle *et al.* 2017). Despite intensive multimodal therapy, over 50% of high-risk neuroblastoma cases experience relapse, posing significant treatment challenges (Park *et al.* 2010). Furthermore, the enigmatic aspect of neuroblastoma lies in its high rate of spontaneous regression, even without medical intervention (Carvalho 1973).

2.1.2 Diagnosis

The diagnosis of neuroblastoma relies on a comprehensive approach encompassing laboratory tests, radiographic imaging and pathological assessment (Matthay *et al.* 2016). Disease staging constitutes the initial pivotal step, subsequently guiding patient stratification into risk groups based on various clinical and molecular factors, including age at diagnosis, disease stage, histological characteristics, DNA index and genetic anomalies (Cohn *et al.* 2009). Imaging techniques, such as computed tomography or magnetic resonance imaging, play a crucial role in determining primary tumor size, regional invasion, extent of spread and overall disease stage. Additional imaging of the chest, abdomen

and pelvis aids in identifying potential distant metastatic sites (Whittle *et al.* 2017). Radiolabeled [¹³¹I]-*meta*-iodobenzylguanidine (MIBG) scans represent a valuable tool for detecting both primary tumors and metastases, with approximately 90% of patients exhibiting MIBG-avid tumors (DuBois *et al.* 2012). In cases where MIBG scans yield negative results, [¹⁸F]-fluorodeoxyglucose positron emission tomography scans or technetium-99 bone scintigraphy are recommended for the detection of metastatic lesions (Sharp *et al.* 2009, Taggart *et al.* 2009, Bleeker *et al.* 2015, Nakagawara *et al.* 2018). In conjunction with imaging studies, bone marrow aspirates and biopsies obtained from at least two distinct sites are typically collected (Cheung *et al.* 1999). These findings are then combined with histopathological assessments and/or increased levels of urinary or serum catecholamine to establish a definitive diagnosis of neuroblastoma. Historically, the evaluation of urinary catecholamine levels led to the identification of numerous cases of neuroblastoma, often exceeding the number of tumors that clinically manifest later in life (Sawada *et al.* 1982, Hiyama *et al.* 2008). Notably, the implementation of mass screening in the past resulted in nearly doubling the incidence of diagnosed neuroblastoma, with minimal change in overall mortality (Yamamoto *et al.* 2002, Hisashige 2014). A significant proportion of these diagnosed neuroblastoma exhibited a low-risk profile characterized by favorable clinical and biological features, ultimately undergoing complete spontaneous regression (Schilling *et al.* 2002, Woods *et al.* 2002). As far back as 1963, a report indicated the presence of neuroblastoma-like cells in approximately 1 out of every 40 individuals, although the majority of these cells naturally disappeared before birth (Beckwith and Perrin 1963). This suggests the existence of a greater number of occult neuroblastoma that do not progress to overt clinical disease. In addition to catecholamine levels, various biochemical parameters are assessable, including serum ferritin, neuronal-specific enolase (NSE), lactate dehydrogenase (LDH) and dopamine levels. Elevated ferritin levels have been associated with advanced stage, *MYCN* amplification, and reduced survival rates (Hann *et al.* 1985, Tonini *et al.* 1997, Cangemi *et al.* 2012). Similarly, high levels of NSE or LDH correlate with *MYCN* amplification and poorer clinical outcomes (Zeltzer *et al.* 1986, Joshi *et al.* 1993, Cangemi *et al.* 2012). Nevertheless, it is important to note that increased serum levels of these markers lack specificity for neuroblastoma and none are currently utilized to predict outcomes or guide therapeutic decisions (DuBois *et al.* 2012). The staging of neuroblastoma involves procedures such as tumor excision, biopsy and bone marrow aspiration, which collectively contribute to a comprehensive evaluation of the disease. Immunohistochemistry studies are employed to affirm the neural origin of tumors, relying on the examination of cell morphology and tissue architecture. According to the International Neuroblastoma Pathology Committee, histopathologically, neuroblastoma fall into two main categories: favorable and unfavorable histology (Shimada *et al.* 1999, Shimada *et al.* 2001, Peuchmaur *et al.* 2003). The majority of neuroblastoma are characterized by undifferentiated features, comprising small, round cells with dense hyperchromatic nuclei (neuroblasts) and limited evidence of neural

differentiation (Brodeur 2003). To distinguish neuroblastoma from other tumor types exhibiting similar morphological characteristics, protein markers such as vimentin, NSE, S100 and ELAVL3/4 can be employed (Takemoto *et al.* 2019).

2.1.3 Staging

The clinical stage assigned to a neuroblastoma patient at the time of diagnosis plays a pivotal role in prognostication and dictates the therapeutic approach to be undertaken. As our understanding of neuroblastoma has deepened over time, various classification systems have evolved to refine the categorization of this complex disease. One of the earliest staging systems, introduced by Evans in 1971, emphasized the tumor's position relative to the patient's midline, delineating stage II from stage III, and acknowledged the presence of metastatic disease as key determinant, separating stage IV and IV-S from other stages (Evans *et al.* 1971). Shimada's system, proposed in 1984, introduced age at diagnosis and histological tumor morphology as additional factors for classification (Shimada *et al.* 1984). To establish a standardized framework for improved comparability across research studies and clinical protocols, the International Neuroblastoma Staging System (INSS) was established in 1986, with subsequent revisions in 1993 (Brodeur *et al.* 1988, Brodeur *et al.* 1993). This system is predicated on a comprehensive evaluation of neuroblastoma patients, incorporating clinical, radiographic and surgical assessments. The INSS classifies neuroblastoma into five stages: 1, 2 (further divided into 2A and 2B), 3, 4 and 4S. Stage 1 designates localized tumors without lymph nodes involvement, typically amenable to complete surgical resection, though these cases are relatively rare. Stage 2 encompasses tumors that are largely localized but not amenable to complete surgical removal. Subdivision 2B accounts for lymph node involvement without distant metastasis. Stage 3 aggregates unresectable intermediate- to high-risk tumors coupled with lymph node metastases. Stage 4 represents the most aggressive stage, characterized by distant metastases to lymph nodes, bone marrow, liver, skin or other organs. Stage 4S is unique, specifically affecting children under one year of age. These tumors exhibit primary characteristics akin to stage 1 or 2 tumors but share distant metastatic features with stage 4, excluding lymph nodes. Remarkably, these particular tumors frequently undergo spontaneous regression for reasons that remain enigmatic. While the INSS was a substantial advancement in neuroblastoma management, it predominantly functioned as a postsurgical staging system. This limitation was significant, given that a portion of neuroblastoma patients does not undergo surgical interventions. Consequently, in 2009, the International Neuroblastoma Risk Group (INRG) staging system was introduced (Monclair *et al.* 2009). The INRG systems relies on clinical criteria and image-defined risk factors (IDRFs), facilitating its use prior to surgery. It categorizes neuroblastoma into four risk stages. Stage L1 comprises low-risk, localized tumors, characterized by the absence of IDRFs and confined to a single body compartment. Stage L2 designates locoregional tumors with one or more IDRFs,

representing an intermediate-risk stage. Stage M identifies high-risk tumors with distant metastases, notably affecting lymph nodes. Stage MS, applicable to patients under 18 months, designates tumors with metastases restricted to the skin, liver and/or bone marrow, aligning closely with stage 4S of the INSS. These tumors, akin to stage 4S, exhibit a propensity for spontaneous regression. The INRG system refrains from dictating treatment recommendations, allowing for a comprehensive evaluation and global comparison of treatment regimens. Crucial prognostic risk factors in neuroblastoma encompass tumor stage, age at diagnosis, histology, differentiation grade, DNA ploidy and genetic aberrations such as *MYCN* amplification, 11q loss, 17q gain or the presence/absence of segmental genomic alterations (Table 1).

Table 1: Risk stratification with the INRG staging system.

INRG stage	age at diagnosis (months)	tumor histology	tumor differentiation	MYCN amplification	11q loss	DNA ploidy	pre-treatment risk group
L1/L2	any	GN maturing, GNB intermixed	any	any	any	any	very low
L1	any	any*	any	no	any	any	very low
MS	< 18	any	any	no	no	any	very low
L2	< 18	any*	any	no	no	any	low
L2	≥ 18	GNB nodular, NB	differentiating	no	no	any	low
M	< 18	any	any	no	any	hyper-diploid	low
L2	< 18	any*	any	no	yes	any	intermediate
L2	≥ 18	GNB nodular, NB	differentiating	no	yes	any	intermediate
L2	≥ 18	GNB nodular, NB	poorly differentiated/undifferentiated	no	any	any	intermediate
M	< 18	any	any	no	any	diploid	intermediate
L1	any	any*	any	yes	any	any	high
L2	any	any	any	yes	any	any	high
M	< 18	any	any	yes	any	any	high
M	≥ 18	any	any	any	any	any	high
MS	< 18	any	any	yes	any	any	high
MS	< 18	any	any	any	yes	any	high

*except GN maturing and GNB intermixed; GN - ganglioneuroma, GNB - ganglioneuroblastoma, NB - neuroblastoma; Table derived from (Whittle *et al.* 2017) Table 6.

2.1.4 Genetic susceptibility

Neuroblastoma, although predominantly sporadic in origin (Bunin *et al.* 1990), exhibit rare instances of heritability, accounting for approximately 1-2% of neuroblastoma cases. Familial neuroblastoma

typically follows an autosomal dominant inheritance pattern, often with incomplete penetrance at around 65% akin to the classic two-hit model (Knudson Jr and Strong 1972, Shojaei-Brosseau *et al.* 2004). This familial form is characterized by multifocal primary tumors that manifest early in life (Knudson Jr and Strong 1972, Kushner *et al.* 1986, Maris *et al.* 1997).

In 2004, the first neuroblastoma predisposition gene, paired-like homeobox 2B gene (PHOX2B), was identified (Trochet *et al.* 2004, Bourdeaut *et al.* 2005). Located on chromosome 4p12, PHOX2B plays a pivotal role in the regulation of autonomic nervous system development and differentiation (Pattyn *et al.* 1999, Raabe *et al.* 2008). Two prominent germline mutations, R100L and R141G, result in a loss of PHOX2B function with approximately 6-10% of familial neuroblastoma cases exhibit PHOX2B mutations (van Limpt *et al.* 2004, Mosse *et al.* 2004). Mutated PHOX2B may contribute to the initiation of neuroblastoma by disrupting normal developmental processes, possibly affecting the differentiation or proliferation of neural crest cells, which give rise to neuroblastoma tumors. Notably, PHOX2B mutations are recurrently found in neural crest-derived disorders such as congenital central hypoventilation syndrome and Hirschsprung disease (Amiel *et al.* 2003, Trochet *et al.* 2004). Additionally, these mutations occur in about 2% of sporadic neuroblastoma cases (Serra *et al.* 2008). In contrast, PHOX2B is considered a core regulatory circuit (CRC) factor and is generally highly expressed in non-familial neuroblastoma, in which PHOX2B may contribute to the maintenance of tumor cell identity, survival or other oncogenic processes. This dual role underscores the complexity of genetic factors in cancer predisposition and progression.

Another pivotal predisposition gene, the anaplastic lymphoma kinase (ALK), was identified in 2008 (Mossé *et al.* 2008, Janoueix-Lerosey *et al.* 2008). ALK, located at 2p23, is typically expressed during embryonic and neonatal brain development. Formation of ALK fusion proteins due to chromosomal translocations, resulting in constitutive activation of ALK is observed in various human malignancies (Nakagawara *et al.* 2018). Germline ALK mutations, being the most prevalent genetic mutations, serve as the principal cause of familial neuroblastoma (Mossé *et al.* 2008, Janoueix-Lerosey *et al.* 2008). Within the tyrosine kinase domain of ALK, three germline missense mutations (R1192P, R1275Q and G1128A) were identified in the majority of familial neuroblastoma cases studied. Importantly, germline ALK mutations exhibit incomplete phenotypic penetrance, implying that not all afflicted individuals will develop neuroblastoma. Of these mutations, R1275Q is encountered in both familial and sporadic tumors and demonstrates higher penetrance compared to the weaker activating mutation, G1128A (Mossé *et al.* 2008, Tolbert *et al.* 2017). Intriguingly, mutations in ALK are observed in 7-12% of sporadic neuroblastoma cases (George *et al.* 2008b, Chen *et al.* 2008). Furthermore, due to its genomic proximity to *MYCN*, *ALK* can be co-amplified in *MYCN*-amplified tumors, with ALK serving as direct target gene of *MYCN* (Hasan *et al.* 2013). In neuroblastoma, the constitutive activation of the tyrosine

kinase domain of ALK, resulting from enhanced autophosphorylation via multiple genetic mechanisms, enhance its oncogenic potential. The heightened kinase activity subsequently amplifies several downstream signaling pathways, including PI3K, RAS-MAPK and the RET pathway, culminating in increased survival, migration, cell proliferation and oncogenic transformation (Carpenter and Mosse 2012, Gonzalez Malagon and Liu 2018, Park and Cheung 2020; Figure 1). Moreover, mutations in ALK exhibit an elevated frequency in relapsed neuroblastoma cases (Schleiermacher *et al.* 2014, Eleveld *et al.* 2015, Padovan-Merhar *et al.* 2016).

In addition to PHOX2B and ALK, several other predisposition syndromes for neuroblastoma have been identified, including Li-Fraumeni and Costello syndrome (Barr and Applebaum 2018). Furthermore, other genes (such as NF1) or genomic regions (12p, 16p12-13) have been implicated in neuroblastoma predisposition (Clausen *et al.* 1989, Maris *et al.* 2002, Longo *et al.* 2007).

2.1.5 Mutations and altered gene expression

Only a small fraction of tumors exhibit identifiable oncogenic driver mutations (Vogan *et al.* 1993, Hosoi *et al.* 1994; Figure 2). Unlike some adult cancers, pediatric malignancies like neuroblastoma are often characterized by genomic aberrations rather than somatic mutations (Grobner *et al.* 2018). Recent genome-wide association studies (GWAS) have unveiled an expanding repertoire of mutations and genetic variations linked to neuroblastoma development (Barr and Applebaum 2018). In primary tumors, ALK and PHOX2B mutations are prevalent, driving most cases of familial neuroblastoma as previously described. Other notable mutations will be described briefly below.

TP53 and MDM2

Somatic mutations in the p53 pathway are rare in primary neuroblastoma (Vogan *et al.* 1993, Hosoi *et al.* 1994). Nevertheless, certain germline variants have been associated with neuroblastoma susceptibility and/or high-risk disease (Pugh *et al.* 2013, Diskin *et al.* 2014). The loss of p53 typically occurs in relapsed, treatment-resistant tumors and is more common in cell lines derived from relapsed patients (Keshelava *et al.* 2001, Tweddle *et al.* 2001). Mouse double minute 2 homolog (MDM2), an antagonist of p53, binds to its transactivation domain, promoting ubiquitination and degradation (Haupt *et al.* 1997, Kubbutat *et al.* 1997, Honda *et al.* 1997). Elevated MDM2 levels, often due to gene amplification or a single nucleotide polymorphisms (SNPs) in the promoter (Corvi *et al.* 1995a, Cattelani *et al.* 2008), are linked to poor prognosis, metastasis and advanced stage (Rayburn *et al.* 2005). This elevated MDM2 activity attenuates p53 function, facilitating increased tumor formation. Additionally, MDM2 can directly bind to the MYCN mRNA, enhancing its stability and translation, which could contribute to multidrug resistance in neuroblastoma (Keshelava *et al.* 2001, Gu *et al.* 2012; Figure 1).

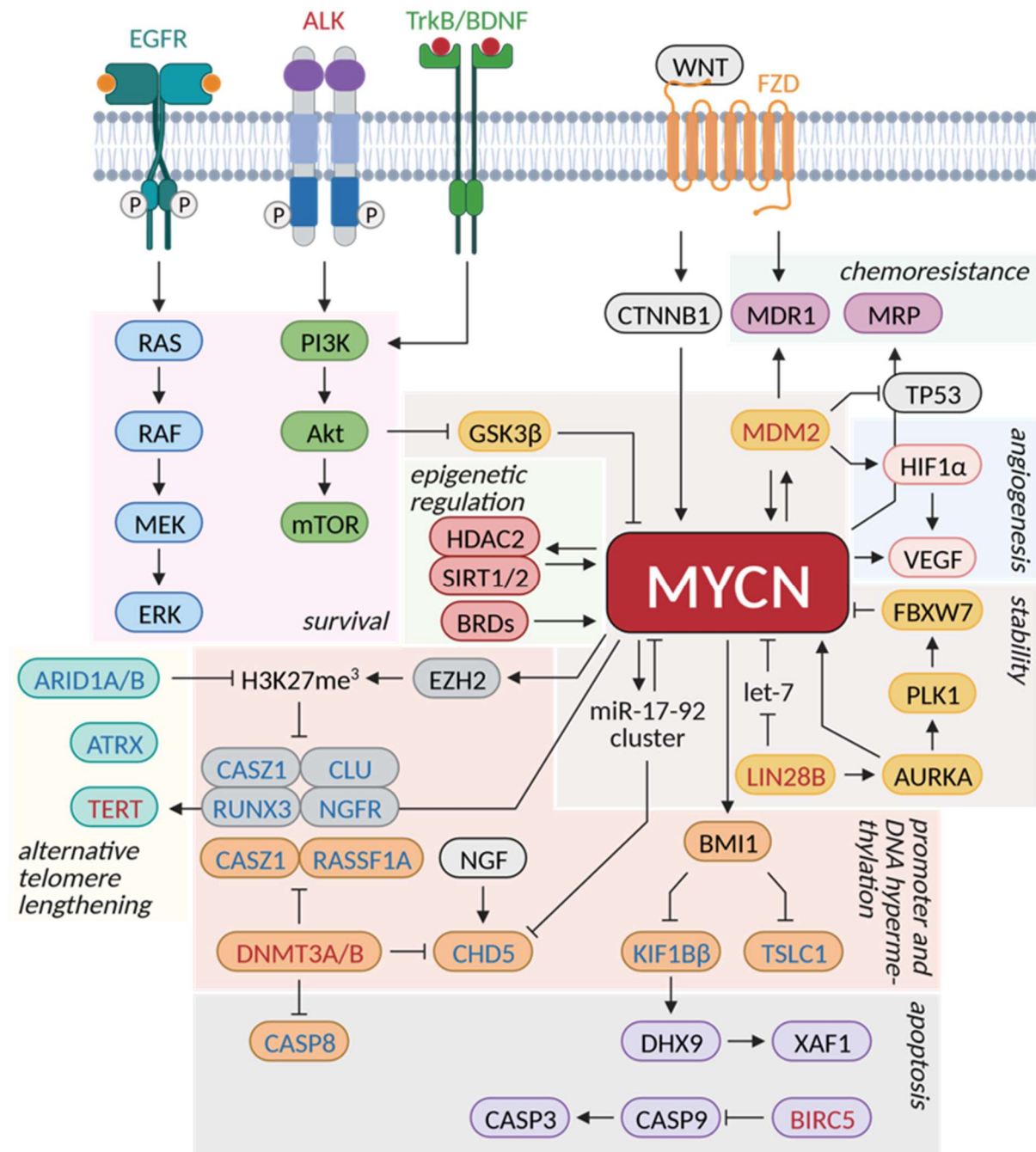


Figure 1: Overview of signaling and regulation pathways in high-risk neuroblastoma. Signaling pathways implicated in neuroblastoma are the RAS-MAPK pathway, the PI3K/Akt/mTOR pathway, ALK signaling, Trk signaling, WNT signaling and the p53-MDM2 pathway. Other regulation pathways promoting high-risk neuroblastoma include the modulation of MYCN transcription and stability, DNA/promoter hypermethylation, deregulation of apoptosis and alternative telomere lengthening. Constitutive active ALK due to mutation or amplification activates both the RAS-MAPK and the PI3K/Akt/mTOR pathway. In addition, ALK enhances the expression of MYCN. The RAS-MAPK and PI3K/Akt/mTOR pathway promote the survival of neuroblastoma cells. TrkB/BDNF signaling activates the PI3K/Akt/mTOR pathway, whereas TrkA/C signaling, which would promote apoptosis or differentiation, is absent in high-risk neuroblastoma. The WNT signaling is involved in chemoresistance, stemness and enhanced MYCN expression. MDM2 inhibits p53 activity, promotes angiogenesis, increases chemoresistance and elevates MYCN expression. Activated p53 is involved in apoptosis and growth arrest. The expression of MYCN is highly regulated at the transcriptional (BRDs/HDACs), mRNA (miRNAs, RBPs) and protein (AURKA, FBXW7, GSK3 β) level. MYCN also promote hypermethylation and subsequent downregulation of tumor suppressor genes as well as altered telomere lengthening through upregulation of TERT. Apoptotic pathways are inhibited through multiple mechanisms. Blue genes are frequently lost (chromosomal aberrations), inactivated (hypermethylation) or mutated in high-risk neuroblastoma. Red genes are overexpressed due to genetic rearrangements or amplifications. Modified from (Zafar *et al.* 2021) Figure 1.

RAS family

Although activating mutations in RAS are infrequent (Ireland 1989, Moley *et al.* 1991), RAS protein activation often results from activating tyrosine kinase receptors, such as the tropomyosin receptor kinase A (TrkA), associated with neural differentiation (Brodeur 2003). High HRAS expression is correlated with lower stage disease and improved outcomes (Tanaka *et al.* 1988). Conversely, missense mutations in NRAS, leading to gain-of-function alterations, are associated with aggressive neuroblastoma (Pugh *et al.* 2013, Li *et al.* 2017b). Similar to TP53, ALK or other RAS-MAPK pathway genes, mutations in the RAS family are more common in relapsed neuroblastoma (Eleveld *et al.* 2015, Schramm *et al.* 2015).

ATRX

Alpha thalassemia/mental retardation syndrome X-linked (ATRX), an SWI/SNF (SWItch/Sucrose Non-Fermentable)-like chromatin remodeler implicated in telomere homeostasis, displays somatic mutations, particularly in older patients, including adolescent and young adults, where roughly 40% harbor ATRX mutations (Cheung *et al.* 2012b). These mutations, spanning missense, nonsense, frameshift and in-frame deletions, are mutually exclusive of *MYCN* amplification (Molenaar *et al.* 2012c, Valentijn *et al.* 2015, Zeineldin *et al.* 2020). They result in the loss of nuclear ATRX protein, alternative telomere lengthening and are linked to overall poor survival with limited treatment options (Cheung *et al.* 2012b, Kurihara *et al.* 2014; Figure 1).

ARID1A/ARID1B

AT-rich interaction domain 1A/B (ARID1A/B), components of the SWI/SNF complex, are among the most frequently mutated genes across all human cancers (Hodges *et al.* 2016). Chromosomal deletions and sequence alterations are associated with early treatment failure, reduced patient survival and increased cell invasion *in vitro* (Sausen *et al.* 2013, Lee *et al.* 2017, Li *et al.* 2017a). Patient data indicate an inverse correlation between ARID1A and TERT (telomerase reverse transcriptase), implying a tumor-suppressive role for ARID1A (Bui *et al.* 2019).

Additionally, GWAS have uncovered other genomic susceptibility loci, including 11p15.4 (LMO1), 1q21.1 (NBPF23), 2p35 (BARD1), 6p22 (CASC15) and several SNPs in LIN28B (6q16.3-q21; Wang *et al.* 2011, Diskin *et al.* 2009, Capasso *et al.* 2009, Russell *et al.* 2015, Diskin *et al.* 2012). Although deletions or mutations in NF1 have been reported in cell lines, there are no documented occurrences in primary tumors (Johnson *et al.* 1993, The *et al.* 1993).

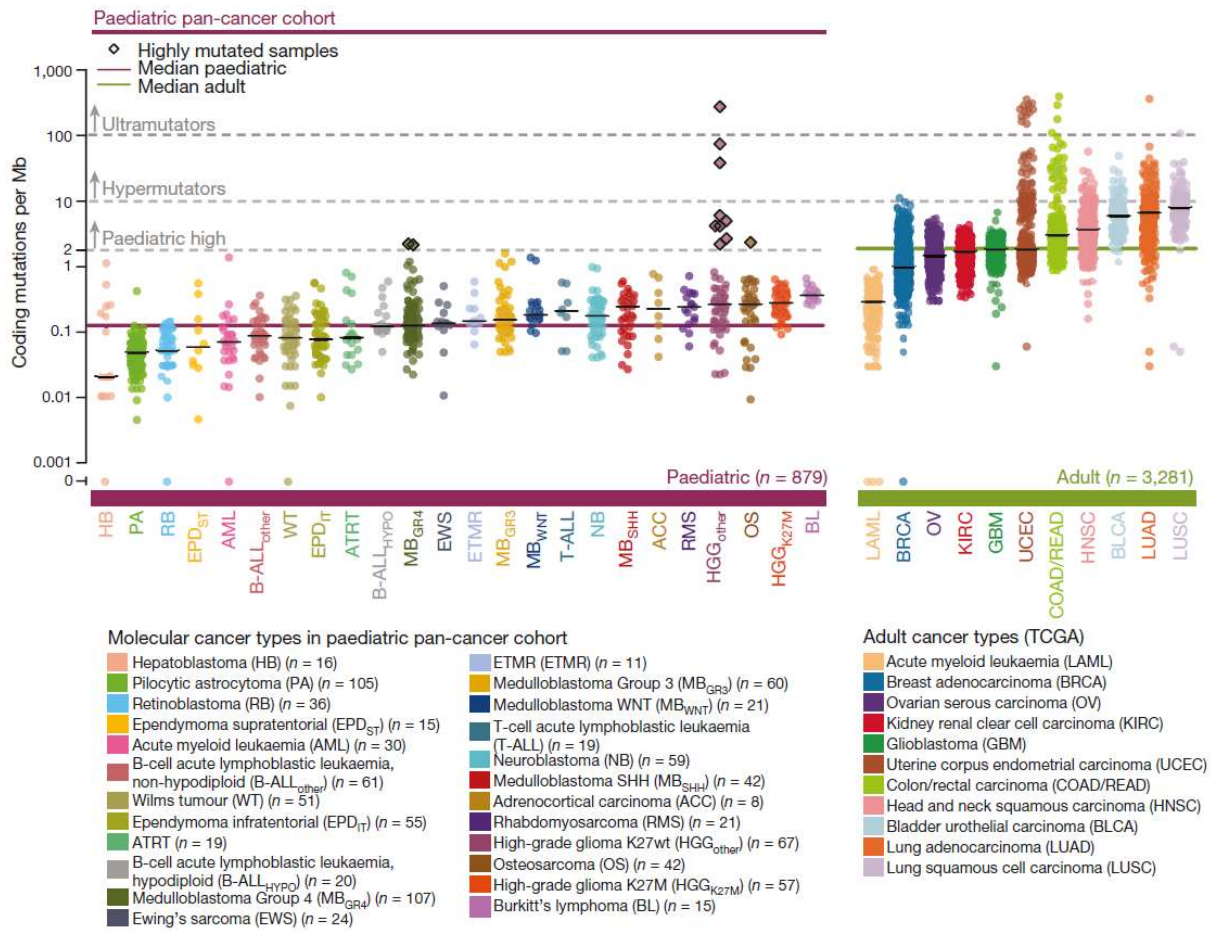


Figure 2: Somatic mutations in pediatric cancer. Somatic coding mutation frequencies in 24 pediatric (n = 879) and 11 adult (n = 3281) cancer types (TCGA). Hypermutated and highly mutated samples are separated by dashed grey lines and highlighted with black squares. Median mutation loads are shown as solid lines (black - cancer types; purple - all pediatric; green - all adult). Derived from (Grobner *et al.* 2018) Figure 1.

The initiation and progression of neuroblastoma are profoundly influenced by altered gene expression in addition to mutations or SNPs. Especially the loss of tumor suppressor genes due to genomic aberrations and the overexpression of oncogenes are key drivers of malignant transformations in this enigmatic malignancy. Cell type-specific developmental gene programs are intricately governed by core regulatory circuitries (CRCs) that meticulously control cell fate and identity by orchestrating the expression of a specific set of genes. These CRCs typically feature super enhancer elements within their promoters to regulate transcription mutually (Saint-Andre *et al.* 2016). Neuroblastoma exhibit two distinct CRCs: An adrenergic cell state managed by ASCL1, EYA1, PHOX2B, HAND1/2, GATA3, SIX3 and AP1-1 and a neural crest/mesenchymal cell-like state promoted by MEOX1/2, SIX1/4, SOX9, SMAD3, WWTR1 and PRRX1 (van Groningen *et al.* 2017, Boeva *et al.* 2017). Additionally, a separate set of CRCs was identified in MYCN-amplified neuroblastoma, involving MYCN, HAND2, ISL1, PHOX2B, GATA3 and TBX2 likely representing an adrenergic cell type (Durbin *et al.* 2018, Decaesteker *et al.* 2018).

MYCN

MYCN belongs to the MYC family of proto-oncogenes, discovered in 1983 as a homolog to C-MYC in neuroblastoma (Schwab *et al.* 1983). Its expression is normally restricted to the nervous system and specific embryonic stages, playing an especial role in normal brain development (Zimmerman *et al.* 1986, Stanton *et al.* 1992). MYCN and C-MYC share functional redundancy due to structural and sequence homology. MYCN regulates diverse cellular functions, including growth, proliferation, metabolism, angiogenesis, apoptosis and differentiation (Beltran 2014). Located on chromosome 2p24, MYCN is frequently amplified in neuroblastoma, leading to aggressive, high-stage disease with poor prognosis and treatment resistance, making MYCN the most important poor prognostic factor in neuroblastoma (Seeger *et al.* 1985). The transcriptional activity of MYCN is mediated by dimerization with MAX, forming MYCN/MAX heterodimers that activate transcription by binding to E-box elements (CANNTG) in the DNA. At steady state, MAX expression is high and favors the formation of MAX/MAX homodimers that repress transcription. However, elevated MYCN levels, resulting from amplification or deregulation, lead to increased MYCN/MAX heterodimers and transcriptional activation (Wenzel *et al.* 1991). In addition, MYCN expression and mRNA stability are tightly regulated (Figure 1). AURKA stabilizes MYCN protein, whereas GSK3 β drives MYCN degradation (Otto *et al.* 2009, Matthay *et al.* 2016). In neuroblastoma, AURKA is generally overexpressed to increase MYCN protein stability. Furthermore, MYCN indirectly upregulates AURKA (Otto *et al.* 2009), leading to a positive feedback loop. The MYCN mRNA is stabilized by MDM2 and ELAVL4 (Gu *et al.* 2012, Samaraweera *et al.* 2017) and negatively regulated by several miRNAs, including the miR-17-92 cluster, the let-7 family as well as miR-34a (Samaraweera *et al.* 2017, Molenaar *et al.* 2012b, Wei *et al.* 2008). Besides protein-coding genes, MYCN also modulates various miRNAs, such as upregulation of the miR-17-92 cluster or miR-9 (Schulte *et al.* 2008, Fuziwara and Kimura 2015, Ma *et al.* 2010) and downregulation of miR-184 or miR-542-5p (Foley *et al.* 2010, Schulte *et al.* 2010), further contributing to tumor progression. Additionally, neural crest-specific MYCN expression triggers neuroblastoma development (Weiss *et al.* 1997, Althoff *et al.* 2015).

Trk family

Neurotrophin signaling, predominantly mediated through the Trk family of tyrosine kinases, plays a pivotal role in normal neuronal development (Barbacid 1995). Transformation of neuroblasts is incompletely understood but likely involves one or more neurotrophin receptor pathways dictating cell differentiation (Brodeur 2003). The extent of differentiation at the time of neoplastic transformation determines the neurotrophin receptor expression pattern, influencing whether neuroblastoma is favorable or unfavorable (Maris and Matthay 1999). The Trk family comprises three members: TrkA, TrkB and TrkC. TrkA activity is mediated by the ligand NGF (nerve growth factor; Yano

and Chao 2000, Patapoutian and Reichardt 2001). NGF withdrawal signals apoptosis in the developing neurons, ensuring elimination of redundant cells. Thus, in the absence of NGF, TrkA-expressing tumor cells undergo programmed cell death pathway, whereas the presence of NGF promote terminal differentiation (Nakagawara 1998b, Brodeur *et al.* 2009). TrkA-expressing tumors generally are hyperdiploid with whole chromosomal gains due to a fundamental defect in mitosis disjunction, whereas structural rearrangements are rarely observed (Maris and Matthay 1999; Figure 3). Thus, TrkA expression is inversely correlating with disease stage and *MYCN* amplification and high expression is a marker of favorable neuroblastoma and good survival probability (Nakagawara *et al.* 1992, Nakagawara *et al.* 1993, Combaret *et al.* 1997). The TrkA/NGF pathway might have an important role in the propensity of some neuroblastoma to differentiate or regress, particularly in TrkA-expressing infants, due to delayed activation of developmentally programmed cell death (Brodeur 2003).

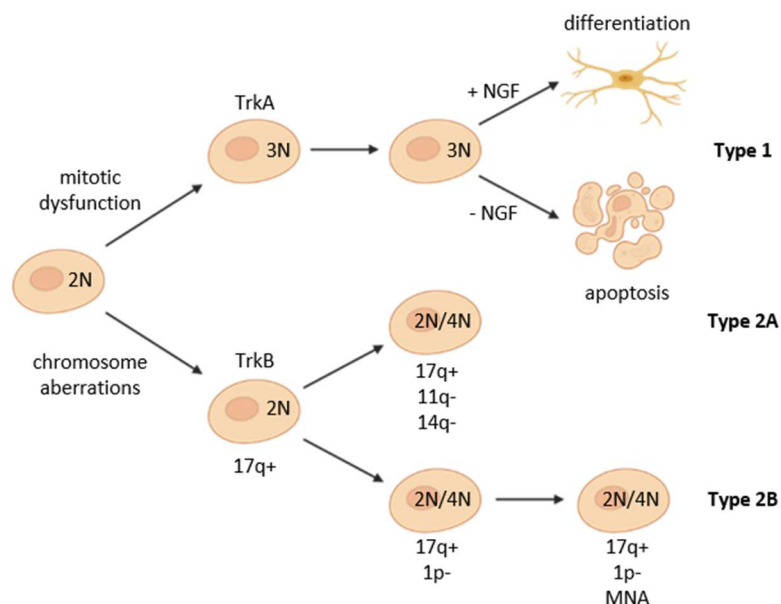


Figure 3: Genetic model of neuroblastoma development. There are at least two genetic subsets of neuroblastoma that are highly predictive of clinical behavior. The degree of differentiation at time of malignant transformation determines the neurotrophin expression pattern. The first type has high levels of TrkA expression and is characterized by mitotic dysfunction leading to whole chromosomal gains. These cells (type 1) are often hyperdiploid or near-triploid (3N) and lack specific genetic changes. They are prone to differentiate in the presence of NGF or to undergo apoptosis when NGF is limited. Patients with type 1 neuroblastoma are generally younger (< 1 year) with localized disease and a good prognosis. The second type is characterized by genomic aberrations and a high TrkB expression, resulting in a near-diploid (2N) or near-tetraploid (4N) karyotype. These tumors (type 2) often have a chromosome 17q gain. Two subtypes can be distinguished depending on further chromosomal aberrations. Type 2A frequently acquire chromosome 11q and/or 14q loss, but rarely develop *MYCN* amplification or chromosome 1p loss. Type 2B often loses distal parts of chromosome 1p and subsequently acquire *MYCN* amplification. These patients are generally older with advanced stage disease and normally a poor outcome. Modified from (Brodeur 2003) Figure 5.

Full-length TrkB and its ligand BDNF (brain derived neurotrophic factor) are predominantly expressed in advanced-stage, *MYCN*-amplified tumors linked to poor prognosis. In favorable neuroblastoma, TrkB expression is low or as a truncated isoform (Nakagawara *et al.* 1994, Yano and Chao 2000, Patapoutian and Reichardt 2001, Brodeur and Bagatell 2014). TrkB-expressing cells rely on autocrine or paracrine

production of BDNF, supporting growth-promoting signals (Nakagawara *et al.* 1994, Matsumoto *et al.* 1995, Acheson *et al.* 1995). TrkB/BDNF also contributes to angiogenesis, drug resistance, migration and invasion (Eggert *et al.* 2000, Ho *et al.* 2002, Hua *et al.* 2016). Tumors that express TrkB are characterized by genomic instability, mostly with gain at chromosome 17q and additional aberrations in 11q/14q or 1p/2p (Maris and Matthay 1999; Figure 3). BDNF itself is located at chromosome 11p14.1 (Yates *et al.* 2017) and gain of 11p occurs more frequently in 11q-deleted neuroblastoma with the smallest region of overlap of 11p gain between 11p11.2 and 11p14, suggesting that 11p gain leads to overexpression of BDNF and therefore contributes to the malignant phenotype (Stallings *et al.* 2003). TrkC and its ligand NT3 (neurotrophin 3) are co-expressed with TrkA in lower-stage, *MYCN* non-amplified tumors with a favorable prognosis (Yano and Chao 2000, Patapoutian and Reichardt 2001, Ryden *et al.* 1996, Yamashiro *et al.* 1996). Its function mirrors that of TrkA, with NT3 promoting cell survival and differentiation, whereas in absence of NT3 TrkC-expressing cells enter apoptosis (Bouzas-Rodriguez *et al.* 2010).

MDR1 and MRP

Acquired drug resistance is a significant cause of neuroblastoma treatment failure, possibly mediated by enhanced drug efflux through the multidrug resistance protein 1 (MDR1) and/or the multidrug resistance-related protein (MRP; Kuroda *et al.* 1991, Keshelava *et al.* 1997). MDR1 expression increases after chemotherapy exposure but is inversely correlated with *MYCN* expression, suggesting it's rarely a cause of *de novo* drug resistance (Bourhis *et al.* 1989, Goldstein *et al.* 1990, Nakagawara *et al.* 1991). In contrast, MRP expression strongly correlates with *MYCN* expression and patient survival, conferring a drug-resistant phenotype (Norris *et al.* 1996). E-box elements in the MRP promoter region suggesting MRP as a direct transcriptional *MYCN* target gene, promoting chemoresistance and treatment failure (Zhu and Center 1994, Norris *et al.* 1997). In addition, high MRP expression is a significant prognostic indicator independent on *MYCN* status (Norris *et al.* 1996).

TERT

In normal cells, TERT plays a pivotal role in maintaining telomere length, stabilizing chromosomes' protective ends. Progressive telomere shortening is implicated in cell senescence and apoptosis, which is overwritten by high telomerase activity (Hiyama *et al.* 1997). Elevated telomerase activity is typical in cancer cells, resulting in telomere stabilization and cell immortalization. Increased telomerase activity seems to be a prerequisite for malignant transformation and is associated with poor survival, *MYCN* amplification, genomic instability and an increased likelihood of additional mutations (Kim *et al.* 1994, Hiyama *et al.* 1995, Brinkschmidt *et al.* 1998). In stage 4S compared to stage 4 tumors, the promoter of *TERT* is hypermethylated, causing lower TERT expression, indicating that telomere shortening may counteract tumor cell immortalization and contribute to spontaneous regression (Binz

et al. 2005, Decock *et al.* 2016). *TERT* is located at chromosome 5p15.33 and genomic rearrangements that affect this region, resulting in an enhanced telomerase activity, occur in approximately 25% of high-risk neuroblastoma, predominantly without *MYCN* amplification and *ATRX* mutations, and are associated with unfavorable outcome (Peifer *et al.* 2015, Valentijn *et al.* 2015). Furthermore, *TERT* is a direct *MYCN* target gene, resulting in increased expression of *TERT* in *MYCN*-amplified tumors without the need of genomic rearrangements (Mac *et al.* 2000).

LIN28B

LIN28B represses the let-7 family of miRNAs, potent tumor suppressors, leading to increased *MYCN* expression in neuroblastoma (Viswanathan *et al.* 2008, Piskounova *et al.* 2011, Molenaar *et al.* 2012b). LIN28B overexpression is common in high-risk disease and is an independent risk factor for poor outcomes (Molenaar *et al.* 2012b). Several SNPs within LIN28B are reported and are associated with high LIN28B expression and adverse disease. In addition, Lin28b transgenic mice develop neuroblastoma with pathological characteristics similar to human disease (Molenaar *et al.* 2012b). A potential signaling pathway involving LIN28B in the promotion of tumorigenesis operates in conjunction with RAN and AURKA (Schnepp *et al.* 2015; Figure 4). In this network, LIN28B indirectly upregulates RAN expression by diminishing levels of let-7 miRNAs, thereby facilitating increased expression of RANBP2, which subsequently stabilizes RAN protein (Patil *et al.* 2014). Furthermore, LIN28B is speculated to directly interact with RAN mRNA, potentially promoting its translation, a mechanism previously proposed for other LIN28B target genes (Peng *et al.* 2011, Wilbert *et al.* 2012). Both, LIN28B and RAN, have been shown to enhance the expression or activity of AURKA (Trieselmann *et al.* 2003, Tsai *et al.* 2003), leading to cell cycle progression and stabilization of *MYCN* oncogene (Otto *et al.* 2009).

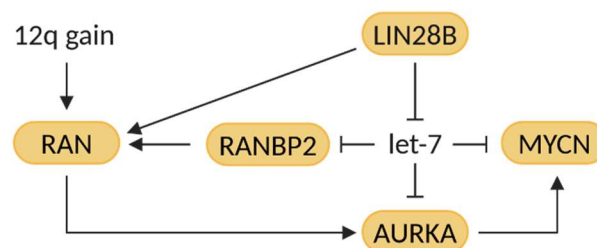


Figure 4: LIN28B-RAN-AURKA-MYCN signaling network in neuroblastoma. This signaling network is operative in both, *MYCN*-amplified and high-risk *MYCN*-non-amplified tumors. In *MYCN*-amplified tumors, LIN28B is frequently upregulated due to *MYCN* amplification, while in *MYCN*-non-amplified tumors, RAN is often overexpressed as a result of genomic aberrations on chromosome 12q. LIN28B inhibits the biogenesis of let-7 miRNAs, leading to elevated levels of RANBP2, AURKA and MYCN. Additionally, RANBP2 serves to stabilize RAN protein, which subsequently phosphorylates and activates AURKA. AURKA then facilitates cell cycle progression and stabilizes MYCN protein. Moreover, LIN28B directly promotes RAN expression through a mechanism independent of let-7 miRNAs. Modified from (Schnepp *et al.* 2015) Figure 6.

Potential chromosome 1p tumor suppressor genes

Chromosome 1p loss is prevalent in neuroblastoma, suggesting the involvement of tumor suppressor genes. One potential tumor suppressor is the kinesin family member 1B (KIF1B β), located at 1p36.22. KIF1B β interacts with DExH-box helicase 9 (DHX9), leading to its nuclear accumulation in the absence of NGF. DHX9 accumulation stimulates the pro-apoptotic XIAP associated factor 1 (XAF1), resulting in apoptosis (Figure 1). In neuroblastoma harboring loss of 1p36, KIF1B β expression is absent or lowered hindering nuclear localization of DHX9, subsequently protecting the cell from apoptosis (Chen *et al.* 2014). Low expression of KIF1B β is therefore associated with poor outcome. In addition, germline loss-of-function missense mutations in KIF1B β exist (Schlisio *et al.* 2008), indicating that it might be a critical pathogenic target of neuroblastoma. Another candidate tumor suppressor is the chromodomain helicase DNA binding protein 5 (CHD5), located at 1p36.31. CHD5 is absent or very low expressed in neuroblastoma (Fujita *et al.* 2008). High expression is strongly associated with younger age, lower stage, no *MYCN* amplification, hyperdiploidy, favorable histopathology and better survival probability, indicating that inactivation of CHD5 drives malignancy (Fujita *et al.* 2008, Koyama *et al.* 2012). Expression of CHD5 is regulated at several stages, including epigenetics and post-transcriptional regulation. Chromosome 1p deletions can lead to hemizygous loss of CHD5. In addition, the promoter of CHD5 is highly methylated, resulting in decreased expression (Koyama *et al.* 2012). Somatic mutations in CHD5 are rare, but recurrently occur in relapsed patients (Schramm *et al.* 2015). Furthermore, CHD5 mRNA can be regulated through *MYCN*-driven miRNAs such as the miR-17-92 cluster, resulting in downregulation of expression, indicating the cross-talk between *MYCN* and a potential chromosome 1p36 tumor suppressor gene (Naraparaju *et al.* 2016). Lastly, NGF upregulates CHD5 in TrkA-expressing cells, resulting in neuronal differentiation (Higashi *et al.* 2015). Calmodulin binding transcription activator 1 (CAMTA1) is another potential tumor suppressor gene, located at chromosome 1p36. Low expression of CAMTA1 is associated with *MYCN* amplification, advanced stage and poor prognosis by slowing cell proliferation, suppressing tumor growth *in vivo* as well as inducing neurite-like processes and markers of neuronal differentiation (Henrich *et al.* 2006, Henrich *et al.* 2011, Henrich *et al.* 2012). A non-coding tumor suppressor on chromosome 1p is the miRNA miR-34a, located at 1p36.22 (Yates *et al.* 2017). Expression of miR-34a is frequently lost in neuroblastoma due to 1p deletions, which is associated with poor prognosis. Thus, miR-34a is a potent tumor suppressor *in vivo* by inducing apoptosis (Welch *et al.* 2007, Tivnan *et al.* 2011). Furthermore, *MYCN* mRNA is directly targeted and degraded by miR-34a (Wei *et al.* 2008). Other potential tumor suppressor gene on chromosome 1p include Castor zinc finger 1 (CASZ1) and RUNX family transcription factor 3 (RUNX3; Wang *et al.* 2012).

Other genes of potential interest

Besides the mentioned genes above, many more are currently under investigation or have been shown to contribute to neuroblastoma formation or progression. These include tumor-suppressive genes positively associated with survival like CD44, HOXC9, TSLC1, miR-337-3p, RASSF1A, CASP8 or DCC (Christiansen *et al.* 1995, Kocak *et al.* 2013, Ando *et al.* 2008, Xiang *et al.* 2015, Astuti *et al.* 2001, Kong *et al.* 1997) and oncogenic genes that contribute to adverse outcome such as PES1, NME1, BIRC5 or ncRAN (Nakaguro *et al.* 2015, Valentijn *et al.* 2005, Islam *et al.* 2000, Yu *et al.* 2009). This also includes oncogenic miRNAs such as the miR-17-92 cluster, miR-18a, miR-128 or miR-380-5p as well as tumor-suppressive miRNAs like miR-9 or miR-184, which up- or downregulation, respectively, promotes cell proliferation and inhibits neuronal differentiation (Zhi *et al.* 2014).

2.1.6 Genetics

Prognostic evaluation in neuroblastoma involves a multifaceted assessment of various clinical and biological parameters to provide insights into the disease's course and patient outcomes. These parameters include the degree of differentiation, presence or absence of stroma, mitosis-karyorrhexis index, age at diagnosis, clinical stage, histological category, DNA ploidy and *MYCN* amplification (Shimada *et al.* 1984, Cotterill *et al.* 2000; Figure 5). Advanced tumors exhibit either a near-diploid or near-tetraploid DNA content with segmental chromosomal rearrangements, including amplifications, deletions and unbalanced translocations demonstrating generalized genomic instability. These tumors are associated with patients older than 18 months, a higher risk of relapse and a decreased overall survival (Brodeur *et al.* 1997, Schleiermacher *et al.* 2012). In favorable neuroblastoma cases, characterized by a hyperdiploid or near-triploid DNA index with whole chromosomal gains, there is a fundamental defect in mitosis and chromosomal segregation. These patients typically have a good prognosis and respond well to therapy (Brodeur *et al.* 1997, Kinzler 1998, Bogen *et al.* 2016). Therefore, DNA ploidy serves as a valuable predictive tool for survival probability, particularly in infants. However, ploidy loses its predictive value for patients older than 1-2 years of age (Look *et al.* 1984, Look *et al.* 1991). Thus, age-specific considerations are crucial when assessing neuroblastoma prognosis based on DNA ploidy.

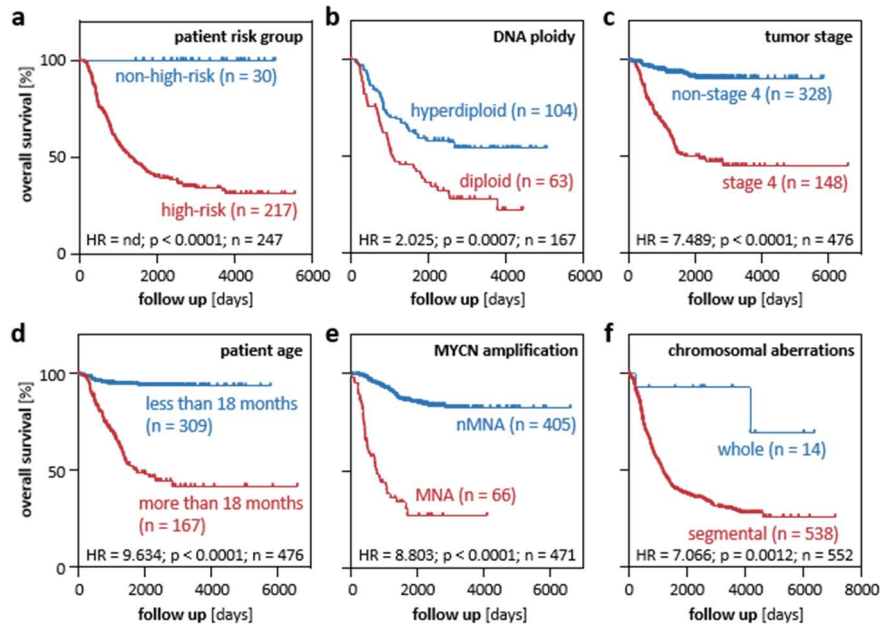


Figure 5: Prognostic factors and their contribution to survival probability. Kaplan-Meier survival analyses by different prognostic factors: patient risk group (a), DNA ploidy (b), tumor stage (c), patient age (d), *MYCN* amplification (e) and chromosomal aberrations (f). Data are derived from neuroblastoma datasets from Asghardazeh (a, b), Kocak (c-e) or de Preter (f) via the R2 database. Statistical significance was determined by log-rank test.

Besides segmental or whole chromosomal aberrations, chromothripsis occur in approximately 20% of primary neuroblastoma with stage 3 or 4 (Molenaar *et al.* 2012c). This phenomenon is also detected in around 2-3% of malignancies across diverse cancer types (Stephens *et al.* 2011). Chromothripsis is characterized by a massive genomic rearrangement, unfolding within a single catastrophic event. In the context of neuroblastoma, its occurrence is notably associated with two key genetic alterations: *MYCN* amplification and chromosome 1p loss. This connection suggests that chromothripsis plays a role in restraining the differentiation of neuroblastoma cells, primarily via the allelic loss of putative tumor suppressor genes located in the 1p36 region. Moreover, chromothripsis leads to structural rearrangements within the *TERT* gene (Valentijn *et al.* 2015). This disruption results in a significant extension of telomere length, particularly in high-stage neuroblastoma cases, suggesting that chromothripsis is contributing to the immortalization of cells, endowing them with the capacity for limitless proliferation. Chromothripsis emerges as a potent indicator of a poor prognosis in neuroblastoma. It underscores the highly intricate relationship between genomic instability, telomere dynamics and neuroblastoma progression.

Beyond chromothripsis, other prominent chromosomal aberrations exert substantial influence on patient risk stratification and survival prognostication, namely *MYCN* amplification, gain of chromosome 17q and losses at chromosome 1p and 11q (Figure 6).

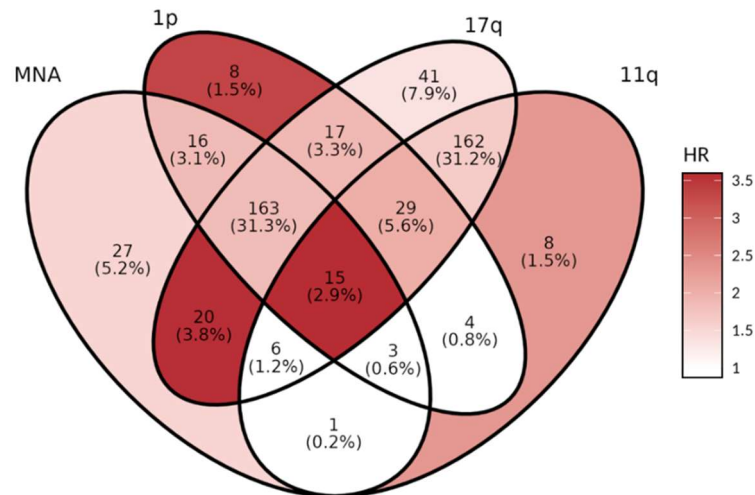


Figure 6: Association of chromosomal aberrations in high-risk neuroblastoma. Association of MYCN amplification, chromosome 17q gain and losses at chromosomes 1p and 11q in 525 neuroblastoma primary tumors. Data are derived from a public R2 dataset (de Preter, cgh_avgpres_nhr556_gent005). Most tumors (87%) harbor a chromosome 17q gain. Co-occurrence of 17q gain with MYCN amplification and 1p loss or with chromosome 11q loss present the two most abundant subtypes. Single chromosomal aberrations occur seldom as well as combination of MYCN amplification and chromosome 11q loss. Subgroups (with $n \geq 8$) are color-coded according to their hazard ratio compared to tumors without these four genomic aberrations.

MYCN amplification

MYCN amplification stands as a pivotal genetic event within the neuroblastoma landscape, occurring with a prevalence ranging from approximately 18% to 38% (Brodeur *et al.* 1984, Seeger *et al.* 1985, Look *et al.* 1991, Edsjö *et al.* 2004, Altungoz *et al.* 2007). Notably, it serves as the sole genetic feature used for treatment stratification in neuroblastoma (Schmidt *et al.* 2000). Elevated *MYCN* expression emerges as a strong indicator of an unfavorable prognosis, aligning with advanced disease stage, diagnosis at an age exceeding 18 months, tumor localization in the adrenal glands or non-thoracic regions, unfavorable histopathological features, diploidy and undifferentiated or poorly differentiated tumor grades (Brodeur *et al.* 1984, Seeger *et al.* 1985, Thompson *et al.* 2016). Furthermore, the amplification of *MYCN* exhibits intricate associations with other genomic alterations. It is closely correlated with chromosome 1p loss and 17q gain, while inversely related to chromosome 11q loss. This indicates that *MYCN* amplification typically occurs concomitantly with 1p loss, 17q gain or both (Figure 6). Thus, *MYCN* amplification is a subsequent event within the sequence of genetic aberrations, often characterizing more advanced stages of neuroblastoma (Fong *et al.* 1989, Caron 1995, Meddeb *et al.* 1996, Guo *et al.* 1999). *MYCN* amplification is also strongly linked to specific metastatic patterns, notably lung metastases, followed by involvement of the bone marrow, bone and skin (Thompson *et al.* 2016). Additionally, it is associated with a higher likelihood of treatment failure (Seeger *et al.* 1985). The amplicon generated by *MYCN* amplification exhibits heterogeneity, with sizes ranging from 100 kb to 1 Mb. However, it consistently features a core domain spanning around 100-200 kb (Amler and Schwab 1989, Reiter and Brodeur 1996). This amplicon may be present in tandem repeats at its

resident site at 2p24 or manifest as homogeneously stained region at other chromosomes or appear as extrachromosomal double minute chromosomes (Schwab *et al.* 1984, Emanuel *et al.* 1985, Corvi *et al.* 1994, Aygun 2017). The mechanisms underlying *MYCN* amplification are intricate and remain incompletely elucidated. A suggested model of gene amplification is the episome model, wherein a submicroscopic chromosomal region, including a replication origin and adjacent genes, undergo deletion via recombination events. These autonomously replicating precursors are termed episomes and subsequently give rise to larger double minute chromosomes. Over time, these may integrate into new chromosomal sites, forming homogeneously stained regions (Carroll *et al.* 1988, Amler *et al.* 1992, Corvi *et al.* 1994). Amplifications as double minute chromosomes are more common in tumors, because acentric structures tend to be lost during mitosis or to be unequally divided between daughter cells allowing high amplifications as observed for *MYCN* in neuroblastoma (Kanda *et al.* 1998). *MYCN* homogeneously stained regions are frequently flanked by segments of 17q material, suggesting that chromosome 17q may be a preferential recombination site for *MYCN* (O'Neill *et al.* 2001). It is noteworthy that the copy number of *MYCN* remains consistent across different regions within individual tumors, between primary tumors and their corresponding metastases, and even between matched samples at initial presentation and relapse (Brodeur *et al.* 1987). In some instances, duplications of the *MYCN* locus at 2p24 may exist, potentially serving as a precursor to full-blown amplification (Corvi *et al.* 1995b). While *MYCN* amplifications often coincides with amplification of other genes, such as *DDX1* or *ALK*, *MYCN* consistently emerges as the primary gene amplified from the 2p region. Intriguingly, no amplification of *ALK* or *DDX1* is reported in the absence of *MYCN* amplification, suggesting a secondary role for these genes in the context of *MYCN* amplification (Reiter and Brodeur 1996, 1998, George and Squire 2000, George *et al.* 2008a).

Chromosome 17q gain

Chromosome 17q gain emerges as the most frequently observed chromosomal aberration in neuroblastoma, occurring in over 50% of cases (Van Roy *et al.* 1994, Caron 1995, Bown *et al.* 1999). This genetic event can take two distinct forms: unbalanced 17q gain and gain of the whole chromosome 17, each carrying distinct clinical implications. Unbalanced 17q gain, characterized by an imbalance between two or more genes flanking the translocation breakpoint, is closely associated with advanced disease stages, patient age exceeding one year at diagnosis, *MYCN* amplification and the presence of diploidy or tetraploidy. Importantly, it correlates with an unfavorable clinical outcome (Caron 1995, Bown *et al.* 1999, Carén *et al.* 2010). Conversely, the gain of the entire chromosome 17 is linked to a more favorable clinical prognosis and genetic profile (Bown *et al.* 1999). Chromosome 17q gain provides vital prognostic information within both, the groups characterized by the absence of 1p deletion and the absence of *MYCN* amplification (Bown *et al.* 1999). The breakpoints on chromosome 17q exhibit heterogeneity but are frequently situated in the 17q11-21 region (Mlakar *et*

al. 2024; Figure 7). The presence of multiple breakpoints implies a gene dosage effect on chromosome 17q, providing a selective growth advantage (Savelyeva *et al.* 1994, Van Roy *et al.* 1994, Van Roy *et al.* 1995, Łastowska *et al.* 2001, Łastowska *et al.* 2002). The smallest region of overlap for 17q gain spans approximately 25 Mb, located at 17q23.1-qter (Meddeb *et al.* 1996). This genetic alteration can manifest independently but is often observed in conjunction with unbalanced translocations between chromosomes 1 and 17. Such translocations result in simultaneous distal 1p loss and gain of 17q. Chromosome 11q represents the second most common partner site for these translocations. Analogous translocations have been documented on chromosomes 3p, 4p, 9p and 14q, underscoring the biological significance of 17q involvement as a predominant mechanism leading to loss of heterogeneity (Van Roy *et al.* 1994, Van Roy *et al.* 1997, Bown 2001). Within the frequently gained region of chromosome 17q, numerous candidate genes have been proposed. These genes are implicated in critical cellular processes such as apoptosis, cell cycle control or neuronal differentiation. Notable examples include *NME1*, *BIRC5*, *TBX2*, *PPM1D*, *TOP2A* or *ALYREF* (Hailat *et al.* 1991, Islam *et al.* 2000, Decaestecker *et al.* 2018, Saito-Ohara *et al.* 2003, Yoon *et al.* 2006, Nagy *et al.* 2021). Another gene within this region, *IGF2BP1*, warrants particular attention and will be explored in greater detail below. Furthermore, it's worth noting that 17q gain is a recurrent event in other cancer types, where it often arises due to the formation of isochromosome 17q. In these cases, it is accompanied by allelic loss at 17p and mutations in the *TP53* gene. However, in neuroblastoma, isochromosome 17q and TP53 mutations are rare, suggesting distinct underlying mechanisms for 17q abnormalities in this specific cancer context (Bown 2001).

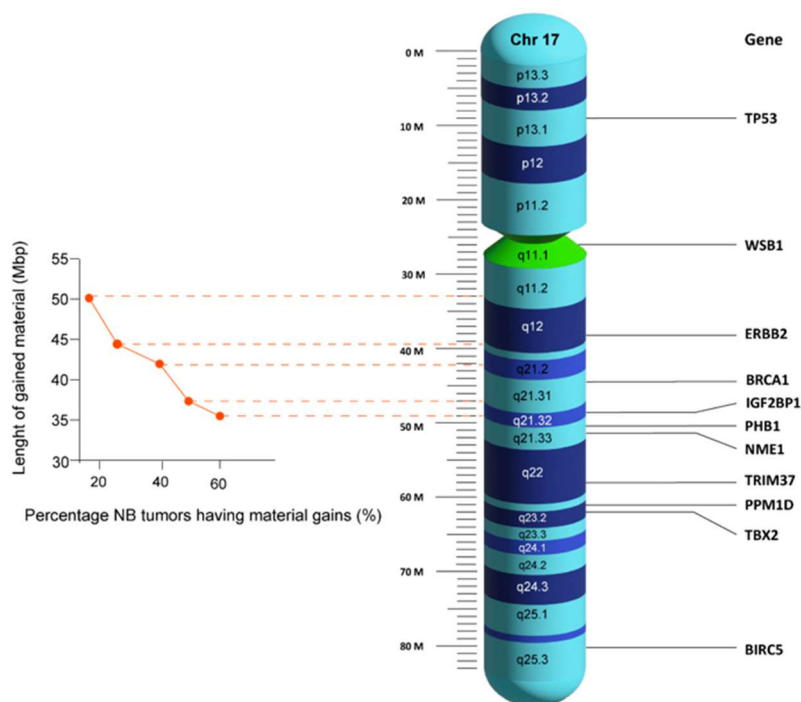


Figure 7: Chromosome 17q breakpoints in neuroblastoma tumors. Location and frequency of chromosome 17q breakpoints. Modified from (Mlakar *et al.* 2024).

Chromosome 1p loss

Chromosomal deletion events involving chromosome 1p are observed in a substantial portion of neuroblastoma cases, ranging from 19% to 36% (Fong *et al.* 1989, White *et al.* 2001, Attiyeh *et al.* 2005). These deletions typically align with unfavorable clinical characteristics, such as unresectable and metastatic disease, advanced stages, the presence of *MYCN* amplification and a poor overall prognosis (Franke *et al.* 1986, Fong *et al.* 1989, Attiyeh *et al.* 2005). The spectrum of breakpoints on chromosome 1p is notably broad, spanning from 1p22 to 1p36. Importantly, there are at least two distinct chromosomal aberrations within this region, each associated with specific clinical outcomes. One of these deletions, a smaller interstitial deletion located in 1p35-36, is more frequently detected in tumors harboring a single copy of *MYCN* and generally linked to a favorable clinical course (Takeda *et al.* 1994, Cheng *et al.* 1995). The second, larger deletion extends proximally into chromosome band 1p21. This deletion is more commonly associated with *MYCN* amplification, advanced disease stages and a diminished likelihood of survival (Takeda *et al.* 1994, Cheng *et al.* 1995, Attiyeh *et al.* 2005). Thus, it appears that at least two distinct tumor suppressor genes reside on chromosome 1p. The tumor suppressor gene located in distal 1p36.2-3 exhibits genomic imprinting, often with a maternal origin preference, and is frequently lost in neuroblastoma cases lacking *MYCN* amplification (Caron *et al.* 1993, Schleiermacher *et al.* 1994). Conversely, the tumor suppressor gene in proximal 1p35-36.1 does not display a preferential allelic loss origin and is closely linked to *MYCN* amplification (Bown 2001). This intriguing relationship suggests that proximal 1p deletion may be a prerequisite for *MYCN* amplification or there could exist an underlying genetic abnormality that predisposes to both 1p loss and *MYCN* amplification. In either scenario, it seems essential to delete a gene that regulates *MYCN* expression or one that mediates programmed cell death in response to elevated *MYCN* gene expression for amplification to occur (Brodeur *et al.* 1997, Kinzler 1998). Notably, the ectopic expression of MYC family members induces apoptosis in the absence of survival signals. Therefore, cancer cells must provide an adequate level of anti-apoptotic signals to tolerate high levels of MYC/N (Pelengaris *et al.* 2002). Chromosome 1p loss actively contributes to tumorigenesis. Experiments involving the transfer of chromosome 1p material into neuroblastoma cells *in vitro* have resulted in morphological differentiation and the suppression of tumorigenicity (Bader *et al.* 1991). The most common event for chromosome 1p loss is the unbalanced translocation $\text{der}(1)\text{t}(1\text{p};17\text{q})$, which entails the loss of distal 1p and the gain of distal 17q. This particular translocation accounts for approximately 42% of 1p loss cases. Simple 1p deletions represent 32% of instances, while unbalanced translocation between 1p and other chromosomes makes up the remaining 26% (Bown 2001).

Chromosome 11q loss

A predominant deletion event observed in neuroblastoma is the loss of chromosome 11q, documented in a substantial percentage of cases ranging from 15% to 44% (Srivatsan *et al.* 1993, Guo *et al.* 1999, Attiyeh *et al.* 2005). The loss of 11q is associated with specific clinical parameters, including patient age exceeding one year at time of diagnosis, advanced disease stages, an unfavorable histological profile and ultimately poorer survival outcomes. Notably, this loss is strongly inversely correlated with *MYCN* amplification, rendering it a valuable prognostic indicator for predicting outcomes in high-risk patients who do not exhibit *MYCN* amplification (Guo *et al.* 1999, Guo *et al.* 2000, Attiyeh *et al.* 2005). The region of chromosomal loss on 11q is notably conserved and mapped to 11q23.3, suggesting the presence of a critical tumor suppressor gene in this genomic region (Guo *et al.* 1999, Tomioka *et al.* 2008). Moreover, 11q loss is frequently concurrent with other chromosomal aberrations, including 17q gain and loss of 1p, 3p, 4p and/or 14q (Breen *et al.* 2000, Luttikhuis *et al.* 2001, Vandesompele *et al.* 2005).

Other chromosomal aberrations

In addition to aforementioned primary chromosomal anomalies, several other genetic aberrations have been identified in neuroblastoma. Generally, the gain of chromosomal segments, aside from 17q gain and *MYCN* amplification, appears to be a less prominent than genetic loss in the context of cancer (Bown 2001). One such gain is observed in chromosome segment 1q21-25, with the smallest region of overlap identified at 1q23. This gain is associated with a progressive disease course, resistance to chemotherapy and an unfavorable clinical outcome (Hirai *et al.* 1999). On the other hand, the loss of chromosome 14q32 is detected in a significant proportion of neuroblastoma cases, ranging from 22% to 27% (Fong *et al.* 1992, Thompson *et al.* 2001). Intriguingly, this loss exhibits a strong correlation with 11q loss and therefore inversely correlates with *MYCN* amplification. This genetic alteration transcends clinical risk groups, suggesting its potential occurrence in early stages of tumor development (Thompson *et al.* 2001). Losses involving chromosomes 3p, 4p, 5q, 9p and 18q appear to manifest at lower frequencies than 1p loss (Ejeskär *et al.* 1998, Caron *et al.* 1996, Meltzer *et al.* 1996, Takita *et al.* 1997, Reale *et al.* 1996). The consensus region for 3p loss spans a substantial area, encompassing the region between 3p14.3 and 3p25.3 (Ejeskär *et al.* 1998). Allelic loss within chromosome 2q occurs in roughly 32% of neuroblastoma cases and encompass the 2q33 region (Takita *et al.* 2000). In both deleted regions, the presence of tumor suppressor genes is suspected, further emphasizing their significance in neuroblastoma pathogenesis.

2.1.7 Epigenetics

Epigenetic mechanisms play pivotal roles in the regulation of growth and development. Any disruption in this finely tuned regulation can lead to the onset and progression of disease. Notably, perturbations in epigenetic regulation leading to altered gene expression are frequent occurrences in cancer, including neuroblastoma (Baylin and Jones 2011, 2016).

DNA methylation

One of the primary epigenetic modifications involves DNA methylation, which primarily affects cytosines within CpG islands, generally correlating with transcriptional repression (Bird 2002, Cedar and Bergman 2009). DNA methylation is done by DNA methyltransferases such as DNMT3A/B, which are responsible for *de novo* methylations. Aberrant DNA methylation patterns are a hallmark of cancer and neuroblastoma is no exception (Alaminos *et al.* 2004). This alteration involves not only the global loss of DNA methylation but also gains in methylation at specific promoters. These changes are associated with clinical features and poor prognosis. Some well-known genes with hypermethylated promoters, leading to decreased expression, include CHD5, CASZ1, RASSF1A and CASP8, all of which are considered candidate tumor suppressor genes in neuroblastoma (Koyama *et al.* 2012, Wang *et al.* 2012, Astuti *et al.* 2001, Teitz *et al.* 2000). Therapies targeting DNA methylation, resulting in DNA hypomethylation, have already gained FDA approval for certain malignancies (Fetahu and Taschner-Mandl 2021).

Histone modifications

Covalent histone modifications, including acetylation, methylation and phosphorylation, constitute another layer of epigenetic regulation. Histone acetylation typically marks active gene expression, while histone methylation can lead to either gene activation or repression, contingent on factors such as the degree of methylation (mono-, di- or tri-methylation), type of amino acid residue affected and their location in the histone tails (Esteller 2008, Bannister and Kouzarides 2011). Changes in histone methylation are facilitated by histone methyltransferases, such as EZH2, and histone demethylases. Chromatin homeostasis depends largely on the interplay between various protein complexes, such as the polycomb repressive complexes 1 and 2 (PRC), trithorax-group proteins (e.g. SWI/SNF) and nucleosome remodelers (Piunti and Shilatifard 2016). Notably, the PRC2 complex is responsible for introducing the repressive mark H3K27me₃, while the SWI/SNF complex opposes its effects (Baylin and Jones 2016). ARID1A/B, key components of the SWI/SNF complex, are frequently mutated in cancer, including neuroblastoma, which is associated with poor survival (Sausen *et al.* 2013, Hodges *et al.* 2016). EZH2, a member of the PRC2 complex, is overexpressed in neuroblastoma and MYCN directly drives EZH2 expression (Cohen *et al.* 2013, Corvetta *et al.* 2013). In addition, regional gains encompassing the EZH2 gene are reported in some neuroblastoma patients (Bate-Eya *et al.* 2017). It

plays a crucial role in maintaining the undifferentiated phenotype by epigenetically repressing multiple tumor suppressor genes, including CASZ1, CLU, RUNX3 and NGFR, and is associated with poor outcomes (Wang *et al.* 2012, Li *et al.* 2018). Additionally, BMI1, another polycomb complex protein, is highly expressed in the majority of primary tumors, directly promoted by MYCN and represses tumor suppressors KIF1B β and TSLC1 (Cui *et al.* 2007, Ochiai *et al.* 2010). Other potentially important histone methyltransferases include EHMT2 and DOT1L (Lu *et al.* 2013, Wong *et al.* 2017). Some histone demethylases, like KDM1A or KDM5B, are overexpressed in neuroblastoma and associated with gene silencing, poorly differentiated cells and a poor prognosis (Amente *et al.* 2015, Kuo *et al.* 2015), while other, such as KDM3A or KDM4B, are upregulated and correlated with poor outcomes, but are associated with gene activation (Tee *et al.* 2014, Yang *et al.* 2015). The role of histone acetyltransferases in neuroblastoma progression is not yet fully elucidated (Fetahu and Taschner-Mandl 2021), while histone deacetylases (HDACs) have garnered substantial attention. A positive feedback loop has been identified between MYCN and HDAC2, SIRT1, and SIRT2, with MYCN directly upregulating these HDACs, thereby promoting its own stability and expression (Kim and Carroll 2004, Marshall *et al.* 2011). HDAC8 and HDAC10 are correlated with poor overall survival and resistance to doxorubicin treatment (Oehme *et al.* 2009, Oehme *et al.* 2013). The precise mechanisms by which the loss or gain of expression of these enzymes contributes to oncogenesis are yet to be fully investigated, especially since the inhibition of enzymes that promote permissive or repressive chromatin states both appear to contribute to reduced tumorigenic features of neuroblastoma cells.

Chromatin readers

Epigenetic regulation also involves chromatin reader proteins that recognize histone modifications and recruit other proteins to the modification site to modulate transcription. These readers include bromodomain-, tudor domain-, and chromodomain-containing proteins. Bromodomain (BRD)-containing proteins can induce chromatin remodeling, histone activation and transcriptional enhancement. This activity is observed in several oncogenes, including MYCN, which experiences enhanced transcription due to increased BRD activity, leading to elevated proliferation and tumor progression (Puissant *et al.* 2013, Henssen *et al.* 2016). Consequently, inhibiting BRD activity is emerging as a potential therapeutic strategy.

2.1.8 Immunological microenvironment of neuroblastoma

Neuroblastoma is presumed to exhibit distinctive immune responses, prompting extensive research into tumor-specific antigens. Among these, disialoganglioside (GD2) has garnered significant attention due to its high expression in the majority of neuroblastoma cells, rendering it a promising target for monoclonal antibody-based therapies (Mujoo *et al.* 1987). Immune responses in neuroblastoma involve a critical role for M2 macrophages, specifically characterized by the expression of CD163. High-

risk neuroblastoma displays elevated levels of CD163+ M2 macrophages and metastatic tumors exhibit greater infiltration of tumor-associated macrophages compared to localized neuroblastoma (Asgharzadeh *et al.* 2012). Both T cells and natural killer cells contribute substantially to the immune response against neuroblastoma cells and are pivotal players in immune-based therapeutic strategies. Ordinarily, cytotoxic T cells exert their cytotoxic effects upon recognition of major histocompatibility complex (MHC) class I. However, neuroblastoma patients, especially those at high risk with *MYCN* amplification, often display markedly reduced MHC class I expression, impairing this recognition process (Sugio *et al.* 1991). In addition, high-risk neuroblastoma patients exhibit elevated expression of programmed death-ligand 1 (PD-L1), which correlates with *MYCN* expression, *MYCN* amplification and a poor prognosis. The co-occurrence of high PD-L1 expression and low MHC class I expression allows neuroblastoma cells to evade immune surveillance, creating an immune-evasive microenvironment (Dondero *et al.* 2016, Melaiu *et al.* 2017, Majzner *et al.* 2017). Therefore, targeting the PD-1/PD-L1 axis emerges as a promising therapeutic strategy against high-risk neuroblastoma. Blocking this immune checkpoint could help restore the immune system's ability to recognize and combat neuroblastoma cells, potentially improving treatment outcomes.

2.1.9 Treatment and therapy

In general, the overall survival rate of non-high-risk neuroblastoma patients is very good with over 95% with limited treatment. In contrast, long-term survival for high-risk patients remains under 50% despite multimodal, aggressive treatment (Gatta *et al.* 2014, Tonini and Capasso 2020). Additionally, high-risk neuroblastoma frequently relapse, which then often acquire chemoresistance (Irwin and Park 2015). Treatment regimens are closely linked to the risk group and stage of the tumor.

Treatment of low-risk patients

The prognosis for low-risk neuroblastoma patients, accounting for approximately 50% of patients, is notably favorable, with a 5-year overall survival rate of 99% for stage 1 and 93-96% for stage 2 (De Bernardi *et al.* 2008, Strother *et al.* 2012). Treatment strategies encompass observation alone, surgical resection or the application of moderate chemotherapy doses coupled with surgery (Baker *et al.* 2010, Strother *et al.* 2012). Infants younger than 6 months often undergo observation (81%), with surgery excluding chemotherapy being the most-used option for the remaining 19%. Remarkably, this surgical approach yields a 3-year overall survival rate of 100% due to a high proportion of spontaneous tumor regression (Nuchtern *et al.* 2012). Surgical intervention alone is generally curative for patients with localized disease, with chemotherapy reserved for cases requiring post-resection management or relapse (Perez *et al.* 2000, De Bernardi *et al.* 2008). Low-stage tumors with favorable biological characteristics tend not to metastasize, even following incomplete resection. This minimizes the necessity for extensive chemotherapy in low-risk patients.

Treatment of intermediate-risk patients

Intermediate-risk neuroblastoma patients achieve a commendable 3-year overall survival rate of 96%. Treatment strategies for this group entail moderate chemotherapy regimens coupled with surgical resection. Intermediate-risk patients can be further categorized into two subgroups based on their biological features: those with favorable biology (characterized by favorable histology and DNA index > 1) and those with unfavorable biology (marked by unfavorable histology and DNA index ≤ 1). Typically, the former group undergoes 4 cycles of chemotherapy, while the latter group requires a more extensive treatment regimen of at least 8 cycles (Baker *et al.* 2010).

Treatment of high-risk patients

About half of patients are diagnosed with high-risk neuroblastoma and treatment remains challenging. The standard regimen for high-risk patients includes four main components: induction chemotherapy, local control, consolidation and maintenance. Crucial for high-risk patients, induction therapy aims to reduce tumor size and mitigate metastatic risk through chemotherapy and surgery (Coughlan *et al.* 2017, Smith and Foster 2018). Response to induction therapy is a key prognostic indicator (Yanik *et al.* 2013). Remission is typically achieved in most patients. However, many patients relapse and approximately 20% of patients experience disease progression or inadequate response during induction therapy (Irwin and Park 2015). Adolescents and adults, often bearing chemoresistant tumors, exhibit lower tumor response rates than younger children (Sorrentino *et al.* 2014, Mosse *et al.* 2014). Patients who do not respond to induction therapy represent an especially challenging subgroup with long-term survival rates below 20% (Whittle *et al.* 2017). Current induction regimens incorporate a combination of anthracyclines, topoisomerase II inhibitors, platinum-containing compounds and alkylating agents such as doxorubicin, topotecan, etoposide, cisplatin, carboplatin, cyclophosphamide and vincristine (Pearson *et al.* 2008). To prevent local recurrence, local control measures include surgical resection, typically after 4-6 cycles of induction therapy, and external beam radiation therapy, targeted at the primary site and sites of residual disease (Whittle *et al.* 2017). Radiation is typically administered to MIBG-avid sites (Mazloom *et al.* 2014). Proton beam radiation therapy, while promising in minimizing radiation exposure to surrounding healthy tissue, currently faces limitations in terms of cost and accessibility (Doyen *et al.* 2016). Early studies using proton beam radiation show promising results and further studies are ongoing (NCT02112617). High-risk neuroblastoma consolidation frequently involves myeloablative chemotherapy and autologous stem cell rescue (ASCR). Peripheral blood is the preferred source for stem cell harvesting, typically after 2-3 induction therapy cycles (Whittle *et al.* 2017). Myeloablative therapy includes regimens such as carboplatin, etoposide and melphalan (CEM) or busulfan and melphalan (Bu-Mel; Ladenstein *et al.* 2011). Repeated cycles of myeloablative chemotherapy with ASCR demonstrate improved outcomes with manageable

toxicity. When using tandem transplant, the first chemotherapy cycle is done with thiopeta alone or in combination with cyclophosphamide, whereas the second cycle includes CEM or Bu-Mel (Seif *et al.* 2013, Park *et al.* 2016). Immunotherapy presents a notable consolidation option. Utilizing anti-GD2 monoclonal antibodies, such as 3F8, in conjunction with granulocyte-macrophage colony-stimulating factor (GM-CSF), isotretinoin and local radiotherapy demonstrates comparable overall survival rates to myeloablative therapy and ASCR (Cheung *et al.* 2012a). Despite the achievement of complete remission in many patients, relapse remains common, emphasizing the significance of minimal residual disease in neuroblastoma relapse (Whittle *et al.* 2017). To address minimal residual disease, various maintenance therapy options have been explored over the past years. Isotretinoin treatment, when administered after chemotherapy or stem cell rescue, has improved survival rates. Isotretinoin is a synthetic retinoid that hinders proliferation and induces differentiation (Matthay *et al.* 1999). Combining the anti-GD2 monoclonal antibody ch14.18 (dinutuximab) with GM-CSF and interleukin-2 alongside isotretinoin has significantly enhanced short-term survival, leading to FDA approval of dinutuximab for high-risk neuroblastoma treatment in 2015 (Dhillon 2015). Immunotherapy with dinutuximab, while effective, entails side effects like allergic reactions, fever, hypotension, capillary leak syndrome and pain (Yu *et al.* 2010). Another anti-GD2 monoclonal antibody, 3F8, has demonstrated improved event-free survival rates, though side effects parallel those of dinutuximab (Cheung *et al.* 1998). Utilizing the anti-protozoal drug difluoromethylornithine (DFMO, nifurtimox) for maintenance therapy shows promise. DFMO, an irreversible inhibitor of MYCN-driven ornithine decarboxylase (ODC1), the rate-limiting enzyme in the synthesis of polyamines, was well tolerated, improved event-free survival rates and reduced MYCN expression (Hogarty *et al.* 2008, Saulnier Sholler *et al.* 2009, Cabanillas Stanchi *et al.* 2015). Nifurtimox, long employed for treatment of Chagas disease, a parasitic disease caused by *Trypanocoma cruzi*, exhibits most likely limited adverse side effects in children (Carrillo *et al.* 2007). It is currently investigated in combination with topotecan and cyclophosphamide (Moore *et al.* 2014). Combination therapy of anti-GD2 immunotherapy and DFMO further elevates survival rates (Sholler *et al.* 2018). Overall, the outcome of high-risk neuroblastoma patients improved over the past years with the incorporation of immunotherapy into maintenance therapy regimens. Ongoing research aims to refine the treatment landscape for high-risk neuroblastoma, with molecularly targeted therapies offering hope for continued improvements in patient survival rates.

Treatment of relapsed and refractory neuroblastoma

Despite recent advancements, a considerable proportion of high-risk neuroblastoma patients experience relapse or exhibit refractory disease, showing poor responsiveness to therapy. Unfortunately, established curative treatments remain elusive for most of these patients. The 5-year survival rate for patients with relapsed neuroblastoma stands at just 20% and those with refractory

disease face similarly poor prognosis (London *et al.* 2011). While some patients experienced isolated relapses may benefit from curative approaches involving surgery and/or localized radiation therapy, the majority present with metastatic, chemoresistant disease often characterized by acquired mutations induced by prior chemotherapy. Commonly employed drugs in this context include topotecan, alone or in combination with cyclophosphamide, vincristine and/or doxorubicin, irinotecan, primarily in combination with temozolomide, and the combination of ifosfamide, carboplatin and etoposide (Kushner *et al.* 2006, Kushner *et al.* 2010, Kushner *et al.* 2013). Emerging strategies also center on targeting specific cell surface markers, such as the norepinephrine transporter, or utilized targeted radiation through [¹³¹I]-MIBG (Matthay *et al.* 2007). However, additional relapse and disease progression frequently leaves these children with limited further treatment options.

Novel therapeutic approaches

Over the past decade, neuroblastoma research has unveiled novel therapeutic targets, with several agents showing promise in preclinical studies and clinical trials. Clinical trials increasingly emphasize therapies guided by genomic alterations and personalized treatment approaches. Among these emerging targets is ALK, with ongoing investigations into ALK inhibitors like crizotinib, ceritinib and lorlatinib. Crizotinib exhibits limited activity against various ALK mutants, while ceritinib shows efficacy against the F1174L mutant (Mossé *et al.* 2013, Balis *et al.* 2017). Lorlatinib, also demonstrating potent antitumor activity, stands out as effective against crizotinib-resistant cells (Infarinato *et al.* 2016). Given the association of *MYCN* amplification with high-risk disease, *MYCN* itself has become an appealing target. Yet, direct inhibition of *MYCN* remains challenging, with no current approved compounds. Instead, current efforts center on the indirect inhibition of *MYCN*, including targeting BRD proteins, HDACs or AURKA. BRD inhibitors downregulate *MYCN* transcription, resulting in apoptosis and cell cycle arrest, with ongoing clinical trials evaluating their safety and efficacy (Puissant *et al.* 2013, Henssen *et al.* 2016). HDAC inhibitors also feature prominently in ongoing research, with vorinostat, for instance, inducing growth arrest and apoptosis, particularly when combined with chemotherapy, like paclitaxel, or radiotherapy (De los Santos *et al.* 2007, Mueller *et al.* 2011, Zhen *et al.* 2017). Panobinostat, another HDAC, enhances survival rates and demonstrates synergistic effects with cisplatin, doxorubicin or etoposide (Wang *et al.* 2013, Waldeck *et al.* 2016). Combining BRD (JQ1) and HDAC (panobinostat) inhibitors synergistically inhibits growth and induces apoptosis, accompanied by reduced levels of *MYCN* and *LIN28B* (Shahbazi *et al.* 2016). AURKA inhibitors, like alisertib or tozasertib, reduce *MYCN* protein stability. Alisertib is applied alone or in combination with irinotecan and temozolomide and show evidences for efficacy in relapsed neuroblastoma (Brockmann *et al.* 2013, Gustafson *et al.* 2014, DuBois *et al.* 2016). Furthermore, immune checkpoint inhibitors targeting PD-1 pathway components, such as atezolizumab or pembrolizumab, are under investigation (Nakagawara *et al.* 2018), along with strategies targeting DNA methylation to inhibit DNA synthesis

and cell proliferation. DNA methylation inhibitors like 5'-aza-2'-deoxycytidine (DAC), when combined with cisplatin, doxorubicin and etoposide, have demonstrated superiority over monotherapy. Multiple clinical studies are underway examining the potential of DAC and other DNA methylation inhibitors (Charlet *et al.* 2012). Lastly, inhibition of TrkB presents another viable approach. Trk inhibitors, including GNF-4256, AZD6918, CEP-751 or Entrectinib, have shown anti-proliferative activity and enhanced effectiveness when combined with chemotherapeutic agents and radiation (Croucher *et al.* 2015, Iyer *et al.* 2016).

2.1.10 Genetically engineered mouse models (GEMMs)

GEMMs of high-risk neuroblastoma are instrumental in unraveling the intricacies of tumor initiation, progression and metastasis, and in validating pivotal tumor drivers and drug targets. Notably, GEMMs have substantiated *MYCN* amplification, *ALK* mutation and *LIN28B* overexpression as key drivers of neuroblastoma tumorigenesis (Table 2).

Table 2: GEMMs of high-risk neuroblastoma.

GEMM	incidence	median survival	mouse strain
Th-<i>MYCN</i>	100% (+/+)	28-48 d	129X1/SvJ
	20-50% (+/-)	39-133 d	129X1/SvJ
	0-10%	> 100 d	C57BL6
LSL-<i>MYCN</i>	76% (+/-)	26-337 d	C57BL6 x 129X1/SvJ
LSL-<i>ALK</i>^{F1174L}	42%	130-351 d	C57BL6
LSL-<i>ALK</i>^{F1174L}/Th-<i>MYCN</i>	100%	22-55 d	C57BL6 x 129X1/SvJ
Th-<i>ALK</i>^{F1174L}	0%	-	C57BL6/J
Th-<i>ALK</i>^{F1174L}/Th-<i>MYCN</i>	100%	40 d	C57BL6/J x 129X1/SvJ
<i>ALK</i>^{R1275Q} knockin	0%	-	C57BL6 x 129X1/SvJ
<i>ALK</i>^{R1275Q} knockin/Th-<i>MYCN</i>	100%	41-177 d	C57BL6 x 129X1/SvJ
LSL-<i>Lin28b</i>	25%	36-56 d	129X1/SvJ

MYCN transgenic models

Among these models, the Th-*MYCN* transgenic mouse was the first neuroblastoma model developed in 1997 and remains the most widely utilized and extensively characterized (Weiss *et al.* 1997). Thereby, human *MYCN* expression is directed to developing neuroblasts through a rat tyrosine hydroxylase (Th) promoter. Spontaneous tumor development arises from neuronal progenitors within sympathetic ganglia. In normal mice, these neuroblasts undergo hyperplasia followed by regression within two weeks of birth (Hansford *et al.* 2004). The *MYCN* transgene extends hyperplasia, delays regression and permits neuroblast persistence. Tumor incidence varies, contingent upon transgene quantity and mouse genetic background. In general, homozygous mice exhibit higher tumor incidence and shorter latency compared to heterozygous mice, independent of genetic background (Weiss *et al.* 1997, Rasmuson *et al.* 2012). The 129X1/SvJ mouse strain is prone to tumor development, while

C57BL6 strains tend to exhibit lower penetrance. Microscopic metastases may manifest in the lung, liver and ovary, but infrequently in bone or bone marrow (Weiss *et al.* 1997). Tumors arising in Th-*MYCN* models recapitulate human disease histopathologically, with copy number alterations closely resembling those seen in human neuroblastoma. In detail, homozygous tumors typically exhibit no or only few chromosomal aberrations. In contrast, alterations were predominantly observed in heterozygous tumors, where gains were more common than deletions. Chromosomal gains include murine chromosomes 1 (25-30%), 3 (50%), 6 (25%), 11 (20-40%), 14 (20-30%), 17 (15-35%) and 18 (15-35%), whereas *Mycn* amplification occur seldom. Among others, these regions are syntenic to human chromosome 6 and 17, both frequently gained in human neuroblastoma. Lost regions include chromosomes 5 (10-20%), 9 (10-20%) and 16 (15-25%), corresponding to human chromosomes 4, 11 and 3, respectively (Weiss *et al.* 1997, Weiss *et al.* 2000, Hackett *et al.* 2003, Rasmuson *et al.* 2012). In 2015, a new neuroblastoma model, LSL-*MYCN*;Dbh-iCRE, emerged due to limitations associated with the Th-*MYCN* mouse model, such as not well defined transgene integration site, tumor formation predominantly in the abdomen, no intrinsic imaging option and inconsistency between genetic backgrounds (Althoff *et al.* 2015). The LSL-*MYCN* model conditionally expresses human MYCN in dopamine β -hydroxylase (Dbh)-expressing cells. Tumors develop in 76% of mice within sympathetic ganglia and adrenal medulla, regardless of genetic background. However, the latency period for tumor development in this model is more variable and prolonged than in the Th-*MYCN* model. In the LSL-*MYCN* model nearly no deletions were observed, except for loss of chromosome 8 in 15% of cases. Chromosomal gains include murine chromosomes 3 (62%), 6 (38%), 11q (31%) and 12 (23%). Importantly, these aberrations correspond to human chromosomal regions 17q and *MYCN* amplification (Althoff *et al.* 2015).

ALK transgenic mice

Following the identification of ALK as a major predisposition gene in familial neuroblastoma, transgenic mouse models were developed in 2012 and 2016 (Berry *et al.* 2012, Heukamp *et al.* 2012, Ueda *et al.* 2016). These models incorporate two common activating mutations: ALK^{R1275Q} and ALK^{F1174L}. ALK^{F1174L} was investigated by different approaches using the Th and the LSL system. LSL-ALK^{F1174L} mice develop neuroblastoma with an incidence of 42% and exhibit a prolonged latency period, independent whether Dbh or Th was used as driver line for the Cre recombinase. Tumors primarily arise in paravertebral ganglia or the adrenal gland, with 50% of cases developing liver metastases. Unlike MYCN models, ALK models often exhibit more pronounced chromosomal aberrations, including segmental alterations correlated with more aggressive disease. Chromosomal gains comprise murine chromosomes 3 (50%) and 11q (25%), along with *Mycn* amplification (25%), resembling human chromosomal regions 1q and 17q. Chromosomal losses include murine chromosomes 4 and 5 (50%), syntenic to human chromosome 1p36 (Heukamp *et al.* 2012). The relatively long latency, variable time to tumor

development, incomplete penetrance and observed chromosomal aberrations indicate a requirement of a secondary genetic event for neuroblastoma development. In contrast, the Th-*ALK*^{F1174L} mouse model failed to induce tumor formation alone (Berry *et al.* 2012). However, crossing LSL-*ALK*^{F1174L} or Th-*ALK*^{F1174L} with Th-*MYCN* mice results in 100% tumor penetrance with shorter latency period and significantly less chromosomal aberrations compared to Th-*MYCN* or LSL-*ALK*^{F1174L} models (Berry *et al.* 2012, Heukamp *et al.* 2012). Similarly, an *ALK*^{R1275Q} knock-in mouse does not develop tumors within 200 days but had complete tumor penetrance in combination with Th-*MYCN* (Ueda *et al.* 2016).

LIN28B transgenic mice

In 2012, the first neuroblastoma mouse model relying on forced expression of a RNA-binding protein, LIN28B, was established (Molenaar *et al.* 2012b). Conditional overexpression of murine Lin28b with Dbh-driven CRE expression led to spontaneous neuroblastoma formation in 25% of mice with a short latency period. Tumors predominantly developed in ganglia and adrenal glands, with chromosomal aberrations observed at a lower frequency than MYCN GEMMs, but more akin to the *ALK*^{F1174L}/*MYCN* model. Key among these aberrations were gains at murine chromosome 3 (100%) and fewer gains at chromosomes 7 (17%), 10 (17%) and 11q (33%). Deletions, apart from loss of chromosome 14q in 33% of cases, were minimal.

These murine neuroblastoma mouse models closely resemble human disease in terms of localization and gene expression signatures. Furthermore, characteristic chromosomal aberrations are a common feature in most transgenic models, particularly involving gains on murine chromosomes 11q and 12. These regions correspond to human chromosome 17q gain and *MYCN* amplification, respectively, which are well-established genetic anomalies in human neuroblastoma. However, the gain on murine chromosome 3 appears as a prevailing and consistent feature across these models. The centromere region of murine chromosome 3 is syntenic to the human chromosome 1q31.2-1q32.1, which is frequently gained in *MYCN*-amplified neuroblastoma. Moreover, the extent of chromosomal aberration exhibits a direct relationship with the duration of tumor induction, with an escalation in chromosomal anomalies observed in models with extended latency periods (De Wilde *et al.* 2018). Conversely, transgenic models incorporating two genetic hits show a decrease in the frequency of chromosomal changes. This suggests that, in general, at least two genetic events are necessary to initiate neuroblastoma tumor formation. The first genetic hit is provided by transgene overexpression, while the second hit is predominantly acquired through the occurrence of chromosomal aberrations. Importantly, it is worth noting that strong oncogenes, such as *MYCN* or *LIN28B*, induce fewer chromosomal abnormalities than the comparatively weak oncogene *ALK*. The decreasing frequency of chromosomal changes in these models follows the order: LSL-*ALK*^{F1174L} > LSL-*MYCN* > LSL-Lin28b > TH-*MYCN* (heterozygous) > *ALK* and *MYCN* double transgenic models = TH-*MYCN* (homozygous).

2.2 Insulin-like growth factor 2 mRNA binding protein family - IGF2BPs

The insulin-like growth factor 2 mRNA binding protein (IGF2BP) family in humans comprises three canonical members: IGF2BP1, IGF2BP2 and IGF2BP3. Over the years, various synonyms have arisen in the literature, reflecting the diverse research fields investigating IGF2BPs. These alternative designations encompass IMP1-3 in humans, murine CRD-BP (coding region instability determinant binding protein), chicken ZBP1 (zipcode bonding protein 1), KOC (KH domain-containing protein overexpressed in cancer), Vg1RBP/Vera (*Xenopus laevis*) and VICKZ (an acronym formed from the initial letters of these synonyms; Yisraeli 2005). In *Drosophila melanogaster*, a shorter variant of IGF2BPs exist, referred to as dIMP. IGF2BPs were first identified in 1992 by binding to the mRNA of MYC, without detailed analysis of the protein structure (Bernstein *et al.* 1992). Five years later, ZBP1 was characterized in detail as an RNA-binding protein (RBP) that regulates the subcellular localization of β -actin (ACTB) mRNA in fibroblasts derived from chicken embryos (Ross *et al.* 1997). Simultaneously, KOC (now recognized as IGF2BP3) was identified through a screening effort aimed at elucidating overexpressed proteins in pancreatic carcinoma (Mueller-Pillasch *et al.* 1997). One year later, it was demonstrated that MYC is upregulated by human and murine orthologues through their interaction with the coding region instability determinant (CRD; Doyle *et al.* 1998). To avoid any confusion in nomenclature, the official gene symbols, IGF2BP1-3, will be used throughout this study.

2.2.1 Structural features and RNA binding

In mammals, all three IGF2BPs share the same domain organization, possessing two *N*-terminal RNA-recognition motifs (RRMs) and four *C*-terminal hnRNPK homology (KH) domains (Figure 8). These paralogues exhibit an amino acid sequence identity exceeding 56%, particularly within the RRM and KH domains, resulting in calculated molecular weight ranging from 58 to 66 kDa. Notably, IGF2BP1 and IGF2BP3 share a higher sequence identity of approximately 73% (Bell *et al.* 2013). These structural resemblances suggest shared biological functions.

In agreement, all IGF2BP members, across different organisms, have demonstrated strong RNA-binding activity. Early *in vitro* studies suggest that RNA binding is primarily facilitated through the KH domains (Farina *et al.* 2003). The RRM, on the other hand, play a pivotal role in the subcellular localization of bound transcripts (Farina *et al.* 2003) and potentially contribute to stabilizing the IGF2BP-RNA complex (Nielsen *et al.* 2004). The formation of an anti-parallel pseudo-dimer of KH3 and 4 suggests that IGF2BPs induce a specific conformation in associated RNAs (Chao *et al.* 2010). Mutations of the GXXG loop within all four KH domains of IGF2BP1 and IGF2BP2 have confirmed the essentiality of KH domains for proper RNA binding (Wächter *et al.* 2013), although this dependency appears to vary based on the target RNA (Dagil *et al.* 2019). In contrast, it has been shown that all six

protein domains in IGF2BP3 are involved in RNA binding (Wächter *et al.* 2013, Schneider *et al.* 2019). However, given the absence of structural studies including protein-RNA complexes with the full-length protein, a definite elucidation of how IGF2BPs bind RNA remains a subject for future research.

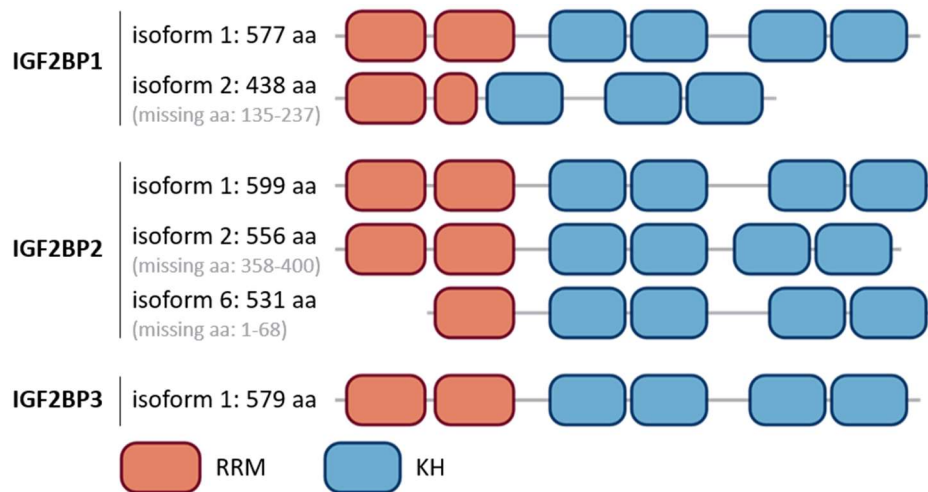


Figure 8: The structure of the IGF2BP family. Domain structure of human IGF2BP isoforms. Isoforms were derived from UniProt (www.uniprot.org). Depicted are IGF2BP1 isoform 1 (Q9NZI8-1) and 2 (Q9NZI8-2); IGF2BP2 isoform 1 (Q9Y6M1-2), 2 (Q9Y6M1-1) and 6 (Q9Y6M1-6); and IGF2BP3 isoform 1 (O00425-1). Isoforms of IGF2BP1 and IGF2BP2 are generated by alternative splicing. Modified from (Bell *et al.* 2013) Figure 1. RRM - RNA recognition motif; KH - hnRNPK homology domain

Additionally, despite various approaches such as CLIP (cross-linking and immunoprecipitation) and SELEX (systematic evolution of ligands by exponential enrichment), a clear binding motif for IGF2BPs has not been identified thus far (Hafner *et al.* 2010, Biswas *et al.* 2019). Because IGF2BPs exhibit six RNA-binding domains, multiple motifs over an elongated sequence could be expected, increasing the difficulty of these experiments. Putative binding motifs could include CAUH (H = A, U, C; Hafner *et al.* 2010), UGGAC (Huang *et al.* 2018a) or a combination of GGC and CA sequences (Schneider *et al.* 2019). Furthermore, recent research has described IGF2BPs as m⁶A-binding proteins (Huang *et al.* 2018a). In terms of RNA-binding, the KH3 and 4 domains have been shown to be essential for m⁶A recognition and binding, while the KH1 and 2 domains play supportive roles. However, the exact mechanism by which IGF2BPs bind m⁶A modifications remains unclear, given the absence of a classical domain for m⁶A binding (like the YTH domain in YTHDF1) in IGF2BPs. The consensus motif for m⁶A modification is RRACH (R = G, A; H = A, U, C), which may potentially overlap with an IGF2BP binding motif, if such a motif exists. Another mode of action, at least proposed for IGF2BP3, could be the “m⁶A switch”. Thereby, the m⁶A modification induces an unfolding of the RNA and enhances the accessibility of the actual binding motif (Sun *et al.* 2019). More research is needed to clarify how IGF2BPs interact with m⁶A modifications.

2.2.2 Subcellular localization and mRNA complexes

IGF2BPs predominantly reside in the cytoplasm, often found within granular-like protein-RNA complexes. Furthermore, there is evidence suggesting that IGF2BPs can bind to their target mRNAs within the nucleus, particularly at their sites of transcription (Oleynikov and Singer 2003, Hüttelmaier *et al.* 2005, Pan *et al.* 2007). This notion aligns with the presence of a nuclear export signal in IGF2BPs and observations of these proteins within the nuclei of spermatogenic cells (Nielsen *et al.* 2003). Additionally, IGF2BPs are primarily associated with “virgin” mRNAs, which include components of the exon junction complex and the nuclear cap-binding protein (NCBP1). Importantly, these mRNAs lack eIF4E and eIF4G, implying that IGF2BP-associated transcripts are translationally inactive (Jonson *et al.* 2007, Weidensdorfer *et al.* 2009). Hence, IGF2BPs form cytoplasmic messenger ribonucleoprotein complexes (mRNP) along with other proteins such as Y-box binding protein 1 (YBX1) and ELAV-like RNA-binding protein 1 (ELAVL1; Jonson *et al.* 2007, Weidensdorfer *et al.* 2009, Wächter *et al.* 2013). These mRNPs are enriched in the peri-nuclear region but are also observed in neurites of developing neurons, supporting the role of IGF2BPs in promoting mRNA localization (Zhang *et al.* 2001, Farina *et al.* 2003). This “caging” effect offers protection to specific target mRNAs, such as CD44, MYC, PTEN or BTRC, by limiting the release of IGF2BP-associated transcripts, thereby preventing premature decay (Vikesaa *et al.* 2006, Lemm and Ross 2002, Köbel *et al.* 2007, Stöhr *et al.* 2012, Noubissi *et al.* 2006, Elcheva *et al.* 2009). Moreover, these stable, “translationally silenced” mRNPs enable the long-distance transport of mRNAs, as demonstrated for ACTB or CFL1 (Zhang *et al.* 2001, Hüttelmaier *et al.* 2005, Maizels *et al.* 2015).

2.2.3 Role of IGF2BPs in RNA regulation

IGF2BPs influences the fate of their target mRNAs by impacting their subcellular localization, turnover and/or translation. Comprehensive CLIP studies have unveiled IGF2BPs’ capacity to interact with a multitude of mRNAs in a pleiotropic manner, implicating over 8000 potential mRNA targets (Hafner *et al.* 2010, Conway *et al.* 2016, Van Nostrand *et al.* 2016). Additionally, IGF2BP1 has been shown also to bind non-coding RNAs (ncRNA), like the Y3 RNA (Köhn *et al.* 2010), the long non-coding RNAs (lncRNA) H19, HULC and THOR (Runge *et al.* 2000, Hammerle *et al.* 2013, Hosono *et al.* 2017) or the circular RNAs circXPO1 and circPTPRA (Huang *et al.* 2020, Xie *et al.* 2021; Figure 9). Most of these ncRNAs serve as temporary scaffolds, thereby facilitating or inhibiting IGF2BP1 binding to mRNAs by forming distinct non-coding RNPs (THOR, circXPO1, circPTPRA). Notably, Y3 and IGF2BP1 form special mRNA-lacking yRNA ribonucleoprotein complexes (Köhn *et al.* 2010). For the lncRNA H19 it is reported that IGF2BP1 participates in localization to lamellipodia and peri-nuclear regions in fibroblasts (Runge *et al.* 2000). Depending on the specific mRNA target, IGF2BPs modulate their localization, stability or translation, consequently leading to alterations in protein expression levels (Figure 9).

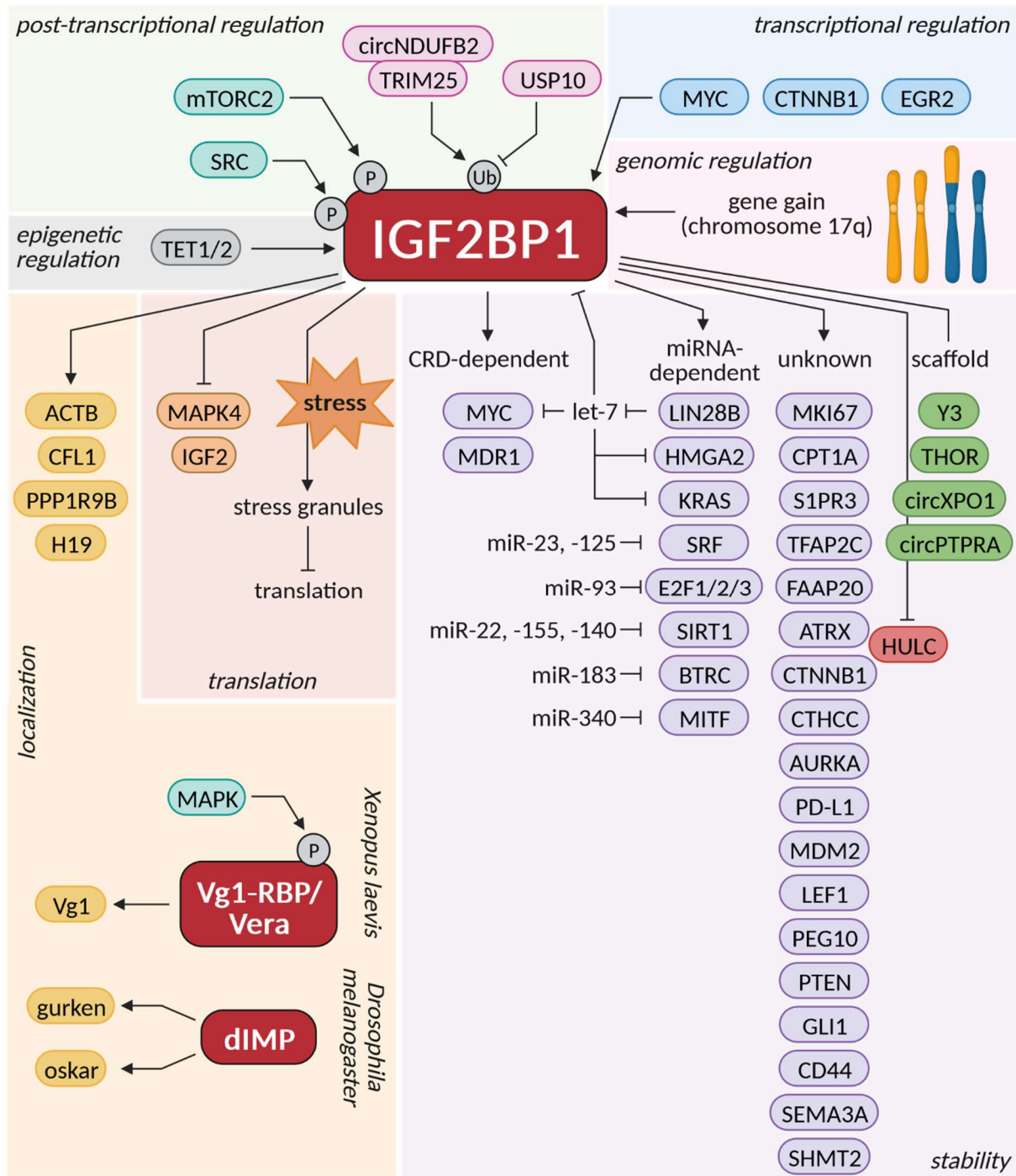


Figure 9: Overview of IGF2BP1 regulation and function. IGF2BP1 is regulated at every level, including epigenetic activation by TET1/2, genomic amplification by unbalanced chromosome 17q gain, especially in neuroblastoma, as well as transcriptional and post-transcriptional regulation. Known transcription factors include MYC, CTNNB1 and EGR2. Post-transcriptional regulation include downregulation by miRNAs, such as let-7, phosphorylation by SRC or mTORC2 that modulates IGF2BP1 function and ubiquitination by TRIM25/circNDUFB2 leading to protein degradation. IGF2BP1 modulates mRNA localization and spatial translation primarily in the embryonic development, for example for the ACTB or CFL1 mRNA. Localized expression is conserved across organisms like *Xenopus laevis* and *Drosophila melanogaster*. Furthermore, IGF2BP1 inhibits translation of certain mRNAs, such as IGF2 and MAPK4, by safeguarding these mRNAs in mRNPs. Translational repression is especially important during cellular stress when IGF2BP1 and the bound transcripts are localized in stress granules. The main function of IGF2BP1 in carcinogenesis is the modulation of mRNA stability. Target transcripts are protected from miRNA-dependent or CRD-dependent endonucleolytic degradation. IGF2BP1 also bind ncRNAs, which mainly function as scaffolds to mediate IGF2BP1 function. The only reported destabilized RNA for IGF2BP1 is the lncRNA HULC.

For instance, IGF2BP1 transiently represses the translation of ACTB mRNA upon binding to the zipcode in its 3'UTR, leading to sequestration in "translationally silent" mRNPs. These mRNPs are transported along the cytoskeleton to the leading edge of fibroblasts or to exploratory growth cones of developing neurons (Zhang *et al.* 2001, Eom *et al.* 2003, Oleynikov and Singer 2003, Perycz *et al.* 2011, Song *et al.* 2015). Other examples are the cofilin-1 (CFL1) mRNA, bound by IGF2BP1 in the 3'UTR and transported to the cell periphery of lung carcinoma cells (Maizels *et al.* 2015) or the spinophilin (PPP1R9B) mRNA, where IGF2BP1 facilitate the dendritic localization in developing hippocampal neurons (Patel *et al.* 2012). IGF2BP1 also modulates translational repression for the name-giving IGF2 mRNA by binding to its 5'UTR (Nielsen *et al.* 1999) as well as for the MAPK4 mRNA upon 3'UTR binding (Stöhr *et al.* 2012). In addition, IGF2BPs stabilize transcripts during cellular stress, when global mRNA translation is reduced, by forming transient stress granules (Stöhr *et al.* 2006). However, in cancer cells, the main role of IGF2BP1 is to regulate RNA stability by shielding specific mRNAs from degradation. For example, it binds to the CRD region in the coding sequence of MYC and MDR1 (multi-drug resistance protein 1) thus safeguarding these mRNAs from endonucleolytic degradation (Doyle *et al.* 1998, Lemm and Ross 2002, Sparanese and Lee 2007). Furthermore, IGF2BP1 predominantly modulate mRNA fate in a CRD-independent manner, preventing miRNA-mediated degradation. The first identified target was β -transducin repeat-containing E3 ubiquitin protein ligase (BTRC/ β TrCP1) by inhibiting miR-183-mediated degradation (Noubissi *et al.* 2006, Elcheva *et al.* 2009). Over the last decade, numerous target mRNAs have been identified, for which IGF2BP1 exerts a protective function against miRNA-induced degradation. These include, among others, KRAS (Mongroo *et al.* 2011), MITF (Goswami *et al.* 2015), LIN28B and HMGA2 (Busch *et al.* 2016), SIRT1 (Müller *et al.* 2018), SRF (Müller *et al.* 2019), E2F1-3 (Müller *et al.* 2020) or AURKA (Glaß *et al.* 2021). By maintaining high expression of LIN28B, a key repressor of let-7 biogenesis, IGF2BP1 significantly influences various let-7 target mRNAs. Given that these miRNAs primarily exhibit tumor-suppressive characteristics, IGF2BP1 contributes to the upregulation of several oncogenes such as MYC or KRAS (Sampson *et al.* 2007, Mongroo *et al.* 2011). Moreover, IGF2BP1 was recently found to enhance SRC activation in an RNA-independent manner, promoting epithelial-to-mesenchymal transition (EMT) in ovarian carcinoma (Bley *et al.* 2020). Additionally, IGF2BP1 modulates the tumor microenvironment by inhibiting immune cell infiltration and enhancing PD-L1 presentation, ultimately resulting in immune escape and tumor progression (Liu *et al.* 2022, Tang *et al.* 2023). Similar mechanisms have been reported for the other IGF2BP paralogues. IGF2BP2 safeguards HMGA1, HMGA2 and CCND1 mRNAs from let-7-mediated degradation (Degrauwe *et al.* 2016), while IGF2BP3 also shields HMGA2 from miRNA attack (Jonson *et al.* 2014). All these instances collectively indicate that IGF2BPs predominantly promote RNA stability and less frequently modulate RNA localization or translation, although other mechanisms of post-transcriptional regulation have been reported. For example, IGF2BP1 destabilizes the HULC lncRNA by recruiting the

CCR4-NOT complex (Hammerle *et al.* 2013) and IGF2BP3 has been shown to destabilize particular mRNAs by recruiting the miRNA-induced silencing complex (Ennajdaoui *et al.* 2016). Additionally, IGF2BPs can also promote the translation of certain target mRNAs like IGF2 and cIAP1 by stimulating the translation initiation through an internal ribosomal entry site (Liao *et al.* 2005, Dai *et al.* 2011, Faye *et al.* 2015).

Recent studies have unveiled a significant involvement of IGF2BPs in the regulation of circular RNAs (circRNAs). CircRNAs are a class of non-coding RNAs that form covalently closed continuous loops and are generated through a back-splicing process where a downstream 5' splice site is joined to an upstream 3' splice site. These circRNAs have been increasingly recognized for their roles in various cellular processes, including gene expression regulation, miRNA sponging and protein interaction modulation (Chen and Shan 2021). IGF2BPs have been shown to interact with specific circRNAs. For example, studies have demonstrated that circRNAs such as circNSUN2, circXPO1 or circPTPRA bind to IGF2BPs, thereby modulating their association with target mRNAs (Chen *et al.* 2019, Huang *et al.* 2020, Xie *et al.* 2021). Additionally, IGF2BP1 has been implicated in facilitating the export of certain circRNAs from the nucleus to the cytoplasm, where they can exert their regulatory functions (Ngo *et al.* 2024). On the other hand, circNDUFB2 enhances the binding of the E3 ubiquitin ligase TRIM25 to IGF2BPs, facilitating their proteasome degradation, suggesting a complex interplay between IGF2BPs and circRNAs (Li *et al.* 2021).

However, the protection of bound mRNAs requires a signaling event to selectively release silenced transcripts for either protein synthesis or mRNA decay. For instance, SRC-directed phosphorylation of IGF2BP1 in the linker region between KH2 and KH3 (Tyr396) triggers the disassembly of IGF2BP1-containing mRNPs, thereby releasing bound mRNAs (Hüttelmaier *et al.* 2005). This mechanism appears to be conserved, as the phosphorylation of Vg1RBP/Vera by mitogen-activated protein kinases (MAPKs) is believed to modulate the release of the Vg1 mRNA from mRNPs (Git *et al.* 2009). In addition, IGF2BP1 was shown to be phosphorylated at serine 181 by the mTORC2 complex, enhancing the binding capability of IGF2BP1 to the IGF2 leader 3' 5'UTR (Dai *et al.* 2013). Thus, post-transcriptional modifications of IGF2BPs have emerged as an essential aspect of their function, especially in the spatiotemporal control of mRNA fate (Figure 9).

2.2.4 Control of IGF2BP expression

The mechanisms governing the transcriptional regulation of IGF2BP expression remain largely unknown. However, some insights have been gained regarding specific factors that influence the transcription of individual IGF2BP paralogues (Figure 9). IGF2BP1 synthesis, for instance, is under the control of β -catenin (CTNNB1) and promoted in a TCF4-dependent manner (Noubissi *et al.* 2006, Gu *et*

et al. 2008). This regulation proposes a positive feedback loop, as IGF2BP1, in turn, stabilizes the CTNNB1 mRNA, thereby enhancing the expression of both IGF2BP1 and CTNNB1 (Gu *et al.* 2008). Another transcription factor known to promote IGF2BP1 expression is MYC (Noubissi *et al.* 2010), which also contributes to a positive feedback mechanism (Lemm and Ross 2002). As MYC and MYCN share structural and functional similarities, MYCN was proposed to enhance the expression of IGF2BP1 (Bell *et al.* 2015). Additionally, early growth response 2 (EGR2) was recently shown to promote IGF2BP1 expression in renal cell cancer (Ying *et al.* 2021). In the case of IGF2BP2, transcriptional activation is attributed to the architectural transcription factors HMGA2 and NFKB1 (Brants *et al.* 2004, Cleyne *et al.* 2007). Unfortunately, factors governing IGF2BP3 expression have not been studied to date.

Beyond transcriptional control, IGF2BPs features multiple miRNA binding sites in their 3'UTR regions, notably let-7 miRNA sites (Boyerinas *et al.* 2008). Consequently, IGF2BP1 can reinforce its own expression by stabilizing LIN28B mRNA, leading to elevated LIN28B protein levels and reduced let-7 miRNA levels (Busch *et al.* 2016). Notably in some cancer cell lines and tumors, IGF2BP1 3'UTR is shortened by alternative cleavage and polyadenylation, increasing its stability, protein expression and oncogenic potential due to the loss of miRNA-mediated repression (Mayr and Bartel 2009). In addition, IGF2BP1's expression can be influenced by genetic gains on chromosome 17, especially in neuroblastoma (Bell *et al.* 2015), and at the epigenetic level by TET1/2 DNA demethylases (Mahaira *et al.* 2014). Recently, IGF2BP1 was proposed to be regulated by ubiquitination. By binding circNDUFB2 in a ternary complex with TRIM25, IGF2BP1 is ubiquitinated and degraded (Li *et al.* 2021). Conversely, USP10 is proposed to stabilize IGF2BP1 due to its deubiquitinase activity (Shi *et al.* 2023).

2.2.5 IGF2BPs in development and cancer

The IGF2BP family members, while structurally similar and sharing functional characteristics, exhibit unique expression patterns during development and carcinogenesis. These distinct expression profiles may underscore their specific roles in various biological contexts. During embryonic development, all IGF2BPs are prominently expressed, reaching a peak around mouse embryonic day E10.5 to E12.5 (Nielsen *et al.* 1999). However, as embryogenesis progresses and birth approaches, their expression levels decline, with IGF2BP1 and IGF2BP3 becoming nearly undetectable in adult mouse organs, except for the reproductive tissues (Hansen *et al.* 2004, Hammer *et al.* 2005). In contrast, IGF2BP2, although decreasing during embryogenesis, remains detectable in several adult mouse tissues (Yaniv and Yisraeli 2002, Yisraeli 2005, Christiansen *et al.* 2009), indicating that it is the sole member engaged in directing mRNA fate in non-transformed adult tissue. This notion aligns with a comprehensive analysis of 1542 RBPs in human hippocampus development (Gerstberger *et al.* 2014; Figure 10).

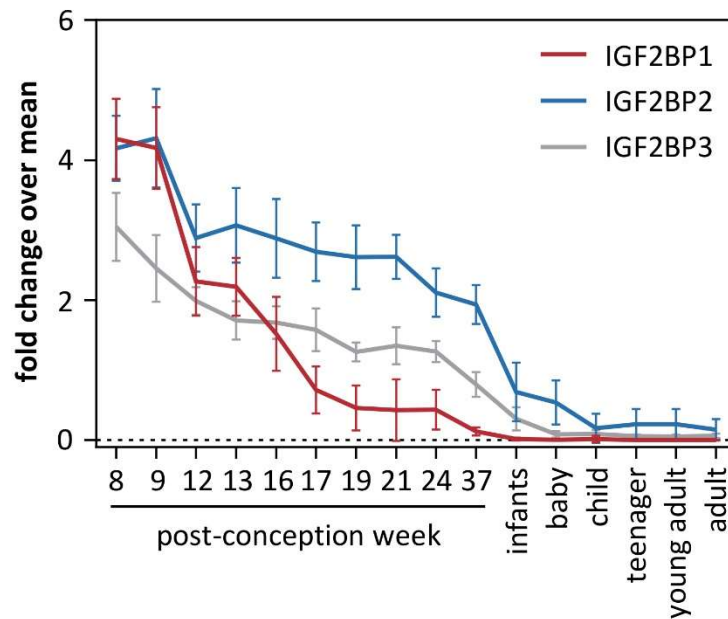


Figure 10: Expression of IGF2BP family members in human hippocampus development. The fold change over mean expression is shown for IGF2BP1-3 across different stages of human hippocampus development. Data after birth was divided into infants (< 1 year), baby (1-4 years), child (5-12 years), teenager (13-17 years), young adults (18-25 years) and adults (> 25 years). Data from post-conception week 25, 26 and 35 were excluded due to low sample number. Expression was profiled by RNA-seq and data were deposited in the BrainSpan database (www.brainspan.org). Picture modified from (Gerstberger *et al.* 2014).

IGF2BP2 is of particular significance as SNPs in the second intron, identified by GWAS, have been associated with an increased risk of type 2 diabetes (Christiansen *et al.* 2009). Moreover, it plays a role in enhancing glucose, lipid and amino acid metabolism by controlling the translation of various mitochondrial components, such as UCP1 mRNA (Dai *et al.* 2015, Dai 2020). Hence, IGF2BP2 knockout mice display smaller size, extended lifespans and have an increased resistance to obesity and tumorigenesis (Dai *et al.* 2015). In comparison, IGF2BP1 gene-trap knockout mice exhibit increased perinatal mortality and surviving mice display a dwarfism phenotype (about 40% smaller) due to hypoplasia (Hansen *et al.* 2004). Additionally, complete knockout of IGF2BP1 is embryonal lethal, whereas IGF2BP3 knockout is viable according to the International Mouse Phenotyping Consortium (www.mousephenotype.org; IGF2BP2 has not been investigated thus far by this consortium). This suggests that IGF2BP1 is a crucial factor in promoting cell growth and differentiation. Furthermore, IGF2BP1 is implicated in promoting the self-renewal of fetal neural stem/progenitor cells, a pivotal function for maintaining stem cell properties necessary for cellular expansion and brain development (Nishino *et al.* 2013). It also contributes to the survival and adhesion of human pluripotent stem cells (Conway *et al.* 2016). The precise spatiotemporal control of mRNA localization is widely recognized as a pivotal factor in the intricate processes governing neuronal development, cytoskeletal remodeling and ultimately synaptic function (Doyle and Kiebler 2011, Jung *et al.* 2012), highlighting IGF2BPs significant roles in these fundamental biological mechanisms. In context of developing neurons,

IGF2BP1 is instrumental not only in the spatially restricted translation of ACTB mRNA but also in the facilitation of neurite outgrowth and branching in hippocampal neurons. Interestingly, it's noteworthy that IGF2BP1's involvement is dispensable for the maintenance of matured dendrites (Perycz *et al.* 2011). This observation is concise with the fact that IGF2BP1 expression is notably diminished in adult tissues (Figure 10). Another study has implicated IGF2BP1 in enhancing the nerve regeneration capacity of adult sensory neurons, suggesting that IGF2BP1 may indeed have roles in mature neurons, particularly in the context of regeneration processes (Donnelly *et al.* 2011). Collectively, these findings underscore IGF2BP1's essential roles in neural development. Studies in *Drosophila* and *Xenopus* support the critical roles of IGF2BPs in nervous system development. In *Drosophila*, only one orthologue is present termed dIMP. Loss-of-function mutations in dIMP are zygotic lethal and the overexpression of dIMP disrupts dorsal/ventral polarity (Boylan *et al.* 2008). Consistently, dIMP direct the fate of localized mRNAs during early development, including *gurken* and *oskar* (Geng and Macdonald 2006, Munro *et al.* 2006), as well as play a role in determining cell fate in testis stem cells (Toledano *et al.* 2012). Additionally, dIMP is responsible for synaptic terminal growth and modulation of protein synthesis at neuromuscular junctions (Boylan *et al.* 2008). Moreover, dIMP is required for chinmo-driven brain tumor initiation in *Drosophila* (Narbonne-Reveau *et al.* 2016). Similarly, in *Xenopus*, Vg1RBP/Vera influences cell migration during neural tube formation of the embryo and is essential for the migration of neural crest cells (Yaniv *et al.* 2003), the proposed origin of neuroblastoma. Hence, IGF2BPs are integral players in cell growth and differentiation during development.

Although IGF2BP1 and IGF2BP3 are nearly absent in adult tissue, both proteins undergo a strong *de novo* synthesis in cancer. Due to this characteristic expression pattern, both proteins are considered oncofetal. In contrast, IGF2BP2 is expressed in adult tissue, but also often upregulated in cancer. Elevated expression of all IGF2BPs is associated to nearly all types of cancer and poor prognosis, including neuroblastoma (Bell *et al.* 2015), ovarian carcinoma (Köbel *et al.* 2007), liver cancer (Gutschner *et al.* 2014) and thyroid carcinoma (Haase *et al.* 2021) to name a few. Notably, IGF2BP1 is intensively studied by multiple research laboratories and has been shown to influence cell proliferation, migration, apoptosis, invasion, chemoresistance and immune response. Stabilized transcripts include MDR1 (Sparanese and Lee 2007), KRAS (Mongroo *et al.* 2011), MKI67 (Gutschner *et al.* 2014), MYC (Gutschner *et al.* 2014, Huang *et al.* 2018a), LIN28B (Busch *et al.* 2016) or E2F1 (Müller *et al.* 2020) among others, indicating a pro-proliferative and oncogenic target spectrum (Figure 9).

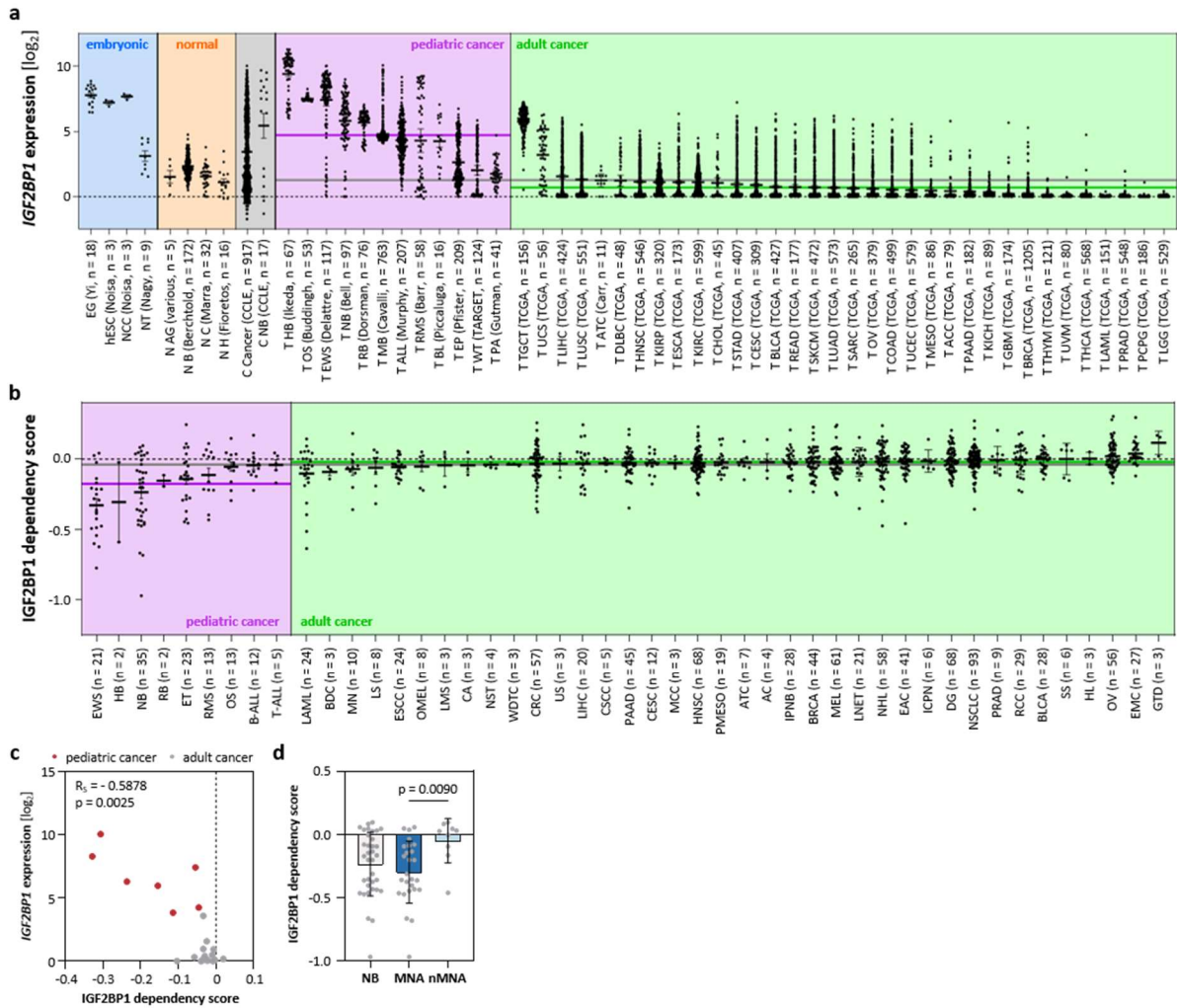


Figure 11: Expression and dependency for IGF2BP1 in human cancer. (a) IGF2BP1 expression in human embryonic (blue) and normal (orange) tissue, cancer-derived cell lines (grey) as well as pediatric (purple) and adult (green) cancer entities. Expression data is derived from the TCGA or the R2 database with indicated authors and cohort size. The lines indicate the average expression across all (grey), pediatric (purple) or adult (green) cancer entities, respectively. **(b)** Dependency scores for IGF2BP1 in pediatric (purple) and adult (green) cancer entities are derived from DepMap. The lines indicate the average dependency score across all (grey), pediatric (purple) or adult (green) cancer entities, respectively. **(c)** Correlation between IGF2BP1 expression score and dependency score in human cancer. Spearman correlation coefficient and p-value is indicated. **(d)** Dependency score for IGF2BP1 in all neuroblastoma samples and subdivided into *MYCN*-amplified (MNA) and non-amplified (nMNA) samples.

Abbreviations Figure 11: AC - ampullary carcinoma; ACC - adenoid cystic carcinoma; ALL - acute lymphocytic leukemia; ATC - anaplastic thyroid carcinoma; B-ALL - B-cell acute lymphocytic leukemia; BDC - breast ductal carcinoma; BL - Burkitt's lymphoma; BLCA - bladder urothelial carcinoma; BRCA - breast cancer; C Cancer - cancer cell lines; C NB - neuroblastoma cell lines; CA - cervical adenocarcinoma; CESC - cervical squamous cell carcinoma and endocervical adenocarcinoma; CHOL - cholangiocarcinoma; COAD - colon adenocarcinoma; CRC - colorectal cancer; CSCC - cutaneous squamous cell carcinoma; DG - diffuse glioma; DLBC - lymphoid neoplasm diffuse large B-cell lymphoma; EAC - esophagogastric adenocarcinoma; EG - embryogenesis; EMC - endometrial carcinoma; EP - ependymoma; ESCA - esophageal carcinoma; ESCC - esophageal squamous cell carcinoma; ET - embryonal tumors; EWS - Ewing's sarcoma; GBM - glioblastoma; GTD - gestational trophoblastic disease; HB - hepatoblastoma; hESC - human embryonic stem cells; HL - Hodgkin lymphoma; HNSC - head and neck squamous cell carcinoma; ICPN - intracholecystic papillary neoplasm; IPNB - intraductal papillary neoplasm of the bile duct; KICH - kidney chromophobe; KIRC - kidney renal clear cell carcinoma; KIRP - kidney renal papillary cell carcinoma; LAML - acute myeloid leukemia; LGG - low-grade glioma; LIHC - liver hepatocellular carcinoma; LMS - leiomyosarcoma; LNET - lung neuroendocrine tumor; LS - liposarcoma; LUAD - lung adenocarcinoma; LUSC - lung squamous cell carcinoma; MB - medulloblastoma; MCC - Merkel cell carcinoma; MEL - melanoma; MESO - mesothelioma; MN - myeloproliferative neoplasms;

2. Introduction

N AG - normal adrenal gland; N B - normal brain; N C - normal colon; N H - normal hematopoietic; NB - neuroblastoma; NCC - neural crest cells; NHL - non-Hodgkin lymphoma; NSCLC - non-small cell lung cancer; NST - nerve sheath tumor; NT - neural tube; OMEL - ocular melanoma; OS - osteosarcoma; OV - ovarian cancer; PA - pilocytic astrocytoma; PAAD - pancreatic adenocarcinoma; PCPG - pheochromocytoma and paraganglioma; PMESO - pleural mesothelioma; PRAD - prostate adenocarcinoma; RB - retinoblastoma; RCC - renal cell carcinoma; READ - rectum adenocarcinoma; RMS - rhabdomyosarcoma; SARC - sarcoma; SKCM - skin cutaneous melanoma; SS - synovial sarcoma; STAD - stomach adenocarcinoma; T-ALL - T-cell acute lymphocytic leukemia; TGCT - testicular germ cell tumor; THCA - thyroid carcinoma; THYM - thymoma; UCEC - uterine corpus endometrial carcinoma; UCS - uterine carcinosarcoma; US - uterine sarcoma/mesenchymal; UVM - uveal melanoma; WDTC - well-differentiated thyroid carcinoma; WT - Wilm's tumor

Expression data from The Cancer Genome Atlas (TCGA) and different R2 datasets of embryonic, normal and tumor tissue as well as cancer-derived cell lines confirm the high expression of IGF2BP1 during embryogenesis, in human embryonic stem cells and neural crest cells (Figure 11a). In contrast, IGF2BP1 is less abundant in neural tube cells and the expression is markedly reduced in adult tissue of the adrenal gland, brain and colon or in cells of hematopoietic origin. This analysis also confirms high expression of IGF2BP1 in all pediatric and some adult tumor entities (Figure 11a). Notably, neuroblastoma presents the entity with the fourth highest expression of IGF2BP1 ($p = 2.8e-20$). In addition, analysis of essentiality data derived from the DepMap portal revealed higher dependency for IGF2BP1 in pediatric cancers (Figure 11b). Among these, neuroblastoma ranked on third place. IGF2BP1 expression and dependency correlate well over all cancer entities, but especially in pediatric malignancies (Figure 11c), indicating a pivotal role of IGF2BP1 in these diseases. Furthermore, investigating neuroblastoma cell lines revealed a significant higher dependency for IGF2BP1 in *MYCN*-amplified cell lines compared to non-amplified ones, suggesting an association of *MYCN* and IGF2BP1 in this malignancy (Figure 11d). In neuroblastoma, IGF2BP1 have reported gene gain by unbalanced translocation of chromosome 17q, suggested *MYCN*-associated roles and is associated with a poor patient outcome, but detailed mechanisms are missing (Bell *et al.* 2015). IGF2BP2's relevance to neuroblastoma remains largely unreported, while IGF2BP3 is linked to undifferentiated histology, advanced stages, *MYCN* amplification and poor outcome in the context of this cancer (Chen *et al.* 2011). Recently, two studies focusing on RBPs in neuroblastoma confirmed upregulation of IGF2BP1. The first study emphasizes the link between IGF2BP1 and *MYCN* amplification (Bell *et al.* 2020). In contrast, the second study reveals a general increase in IGF2BP expression compared to normal tissue, ranking IGF2BP1 as the third most upregulated gene, following *LIN28B* and *TERT* (Yang *et al.* 2021). In the past years, more insights were gained for the function of IGF2BP1 in neuroblastoma related to the results of this thesis. Therefore, these results will be examined in the discussion.

2.2.6 Inhibition of IGF2BP1

IGF2BP1 stands out as a promising therapeutic target for cancer treatment due to its characteristic oncofetal expression pattern and its close association with various oncogenic factors. In 2017, the first inhibitor of IGF2BP1 was identified, a small molecule known as BTYNB. This compound effectively disrupts the interaction between IGF2BP1 and its target mRNA, as exemplified with a MYC RNA fragment via a fluorescence anisotropy-based assay (Mahapatra *et al.* 2017). However, it's worth noting that the precise binding site of BTYNB on IGF2BP1 remains yet to be revealed. BTYNB demonstrated a remarkable ability to significantly reduce the proliferation of cells derived from ovarian carcinoma and melanoma *in vitro*, with a primary mechanism involving the inhibition of MYC expression (Mahapatra *et al.* 2017). Subsequently, BTYNB has exhibited efficacy in diverse cancer types, including leukemia (Jamal *et al.* 2023), esophageal squamous carcinoma (Wang *et al.* 2023) as well as lung, liver and pancreatic carcinoma (Müller *et al.* 2020). These findings collectively suggest that IGF2BP1 is, in principle, an attractive target for pharmacological intervention. Recent developments have introduced two additional inhibitors of IGF2BP1, denoted as 7773 (Wallis *et al.* 2022) and cucurbitacin B (CuB; Liu *et al.* 2022). Compound 7773 functions by interacting with a hydrophobic surface situated at the boundary of IGF2BP1 KH3 and 4 domains, effectively impeding the binding of IGF2BP1 to mRNA targets such as KRAS. Additionally, 7773 exerts inhibitory effects on downstream signaling, wound healing and growth of lung carcinoma cells *in vitro* (Wallis *et al.* 2022). In contrast, CuB covalently targets IGF2BP1 at a unique site (Cys253), located within the KH1-2 domain. This interaction results in a pharmacological allosteric effect, preventing IGF2BP1 from recognizing m⁶A-modified mRNA targets, notably exemplified with MYC. CuB has displayed anti-proliferative properties in hepatocellular carcinoma, both *in vitro* and *in vivo*, by inducing apoptosis and subsequently recruiting immune cells to the tumor microenvironment (Liu *et al.* 2022). These newly identified inhibitors offer promising avenues for the development of therapeutic strategies aimed at targeting IGF2BP1 in cancer treatment.

2.2.7 IGF2BP1 mouse models in cancer

Although there is limited *in vivo* data available for IGF2BP1, insights from xenograft studies have provided valuable information. Xenograft investigations have suggested that IGF2BP1 plays a role in tumorigenesis. Notably, overexpression of IGF2BP1 in a colorectal cancer cell line resulted in increased tumor development and the enhanced spread of cancer cells into the bloodstream. Consistently, IGF2BP1 knockdown in the same cell line reduced the dissemination of tumor cells into the bloodstream, indicating that IGF2BP1 may be implicated in early-stage metastasis (Hamilton *et al.* 2013). Moreover, xenograft studies involving cell lines derived from various cancer types have demonstrated impaired tumor growth following IGF2BP1 depletion (Gutschner *et al.* 2014, Müller *et al.*

al. 2018), providing additional evidence for the oncogenic role of IGF2BP1 in cancer progression. It's worth noting that only one transgenic mouse model for IGF2BP1 has been reported thus far. In this model, murine *Igf2bp1* is overexpressed under the control of the whey acidic protein (WAP) promoter, leading to the induction of mammary carcinoma in lactating mice (Tessier *et al.* 2004). The incidence of tumor formation in this model is 95% in mice with high levels of expression and 65% in mice with low expression, with a relatively long latency period of approximately 53 and 60 weeks, respectively. This indicated that IGF2BP1 has oncogenic potential. In support of this, targeted knockdown of IGF2BP1 specifically within the intestine led to a reduction in the number of tumors in a transgenic model of intestinal tumorigenesis using *Apc*^{Min/+} mice (Hamilton *et al.* 2013). Remarkably, prior to this study, no mouse models existed for investigating the role of IGF2BP1 in the context of neuroblastoma.

2.3 Aims of the thesis

Chromosome 17q gain represents one of the most prevalent genomic aberrations in neuroblastoma and is frequently closely associated with *MYCN* amplification, a hallmark of aggressive disease. This genomic region encompasses a multitude of genes suspected to contribute to tumor progression. Among them, IGF2BP1 exhibits elevated expression in aggressive neuroblastoma and associated roles with *MYCN*. Nonetheless, our current understanding of the precise mechanisms underlying IGF2BP1's involvement in neuroblastoma remains limited, emphasizing the necessity of further investigation. Therefore, the primary objectives of this doctoral thesis are as follows:

- I. **The investigation of the relation between IGF2BP1 and MYCN in neuroblastoma by a potential feedforward loop and subsequent analysis of shared downstream targets.**
- II. **The evaluation of various compounds to target this regulatory network *in vitro*.**
- III. **The assessment of the IGF2BP1 inhibitor BTYNB efficacy in neuroblastoma *in vivo*.**
- IV. **The analysis of IGF2BP1's oncogenic potential in neuroblastoma mouse models.**

To achieve these objectives, a comprehensive analysis of a human neuroblastoma cohort comprising 100 samples has been conducted, involving both transcriptomic and genomic assessments to affirm the association of IGF2BP1 with high-risk neuroblastoma. In depth *in silico* data analysis further substantiated the critical role of chromosome 17q gain and especially the overexpression of IGF2BP1 in neuroblastoma. To unravel the regulatory network between IGF2BP1 and *MYCN*, various *in vitro* models and techniques were employed, following validation through *in vivo* models. In this context, the impact of BTYNB-mediated IGF2BP1 inhibition in neuroblastoma was explored using cell culture systems and mouse models. Furthermore, an array of compounds was assessed *in vitro* through comparative analyses of their potency, efficacy and potential synergistic effects when combined with BTYNB. Ultimately, the oncogenic potential of IGF2BP1 in neuroblastoma has been explored by establishing a transgenic mouse model characterized by IGF2BP1 overexpression in the adrenal glands and peripheral nerves.

3. Material and Methods

3.1 Material

3.1.1 Patient samples

The human neuroblastoma cohort consists of 69 previously published untreated primary samples (Bell *et al.* 2015) extended by 31 additional tumor specimens (Appendix Table 28). Tumors were granted after patient consent and ethical approval from the Cologne tumor bank and the Universitätsklinikum Essen, Germany. The International Neuroblastoma Staging System criteria (INSS) was used for staging.

3.1.2 Animals

Animals (Table 3) were handled according to the guidelines of the Martin Luther University. Permission was granted by the state administration office of Saxony-Anhalt (reference number: 42502-2-1381 MLU, 42502-2-1530 MLU, 42502-2-1625 MLU).

Table 3: Mice strains.

name	genotypes	reference/company
athymic nude mouse	Crl:NU(NCr)- <i>Foxn1</i> ^{nu}	Charles River
<i>Dbh</i> -iCRE	<i>Dbh</i> -iCRE ^{+/-}	Johannes Schulte (Charité Berlin)
LSL- <i>MYCN</i>	LSL- <i>MYCN</i> ^{+/-}	Johannes Schulte (Charité Berlin)
LSL- <i>MYCN</i> ; <i>Dbh</i> -iCRE	LSL- <i>MYCN</i> ^{+/-} ; <i>Dbh</i> -iCRE ^{+/-}	Johannes Schulte (Charité Berlin)
LSL- <i>IGF2BP1</i>	LSL- <i>IGF2BP1</i> ^{+/-} LSL- <i>IGF2BP1</i> ^{+/+}	this study / Taconic Bioscience
LSL- <i>IGF2BP1</i> ; <i>Dbh</i> -iCRE	LSL- <i>IGF2BP1</i> ^{+/-} ; <i>Dbh</i> -iCRE ^{+/-} LSL- <i>IGF2BP1</i> ^{+/+} ; <i>Dbh</i> -iCRE ^{+/-}	this study
LSL- <i>IGF2BP1</i> ;LSL- <i>MYCN</i> ; <i>Dbh</i> -iCRE	LSL- <i>IGF2BP1</i> ^{+/-} ;LSL- <i>MYCN</i> ^{+/-} ; <i>Dbh</i> -iCRE ^{+/-}	this study

3.1.3 Bacteria

For cloning purposes, the bacteria strain *Escherichia coli* TOP10 (genotype: F-mcrA $\Delta(mrr-hsdRMS-mcrBC)$ $\Phi 80lacZ\Delta M15 \Delta lacX74 recA1 deoR araD139 \Delta(ara-leu)7697 galU galK rpsL$ (StrR) *endA1 nupG*) was used. Bacterial culture media (LB, lysogeny broth) contained 1% (w/v) Peptone, 0.5% (w/v) yeast extract and 1% (w/v) NaCl. For the generation of LB-Agar, 1.5% (w/v) Agar-Agar was supplemented. For selection of recombinant clones, 30 μ g/ml Kanamycin or 150 μ g/ml Ampicillin was added to the LB medium, respectively.

3.1.4 Cell lines

Table 4: Parental cell lines.

cell line	ID	origin
BE(2)-C	CRL-2268 (ATCC)	bone marrow metastasis
KELLY	ACC 355 (DSMZ)	neuroblastoma
NBL-S	ACC 656 (DSMZ)	primary adrenal gland tumor (stage 3)
TET21N	obtained from Dr. Schwab (DKFZ)	bone marrow metastasis
KNS42	-	glioblastoma
HEK293T17	CRL-11268 (ATCC)	embryonal kidney
A549	CRM-CCL-185 (ATCC)	lung carcinoma
H522	CRL-5810 (ATCC)	non-small cell lung adenocarcinoma (stage 2)
Huh7	-	adult hepatocellular carcinoma
HepG2	HB-8065	pediatric hepatocellular carcinoma

Cell lines (Table 4) were purchased from ATCC or DSMZ. Neuroblastoma cell lines (BE(2)-C, KELLY, TET21N, NBL-S) were authenticated at Eurofins Genomics by 16 independent PCR systems (D8S1179, D21S11, D7S820, CSF1PO, D3S1358, TH01, D13S317, D16S539, D2S1338, AMEL, D5S818, FGA, D19S433, vWA, TPOX and D18S51) and compared to online databases of the DSMZ and Cellosaurus. KELLY cells had some additional signals but were nevertheless correctly authenticated. TET21N cells were stated as SH-SY-5Y Tet-On SNCA cells because no STR profile exists for TET21N cells in the databases. SH-SY-5Y and TET21N cells have the same parental cell line (SK-N-SH) and show therefore probably similar STR profiles. Within this study, several stable modulated cell lines and clone have been generated (Table 5).

Table 5: Generated cell lines and clones.

cell line / clone	parental cell line	technique
BE(2)-C IGF2BP1 knockout	BE(2)-C	CRISPR/Cas9
KELLY IGF2BP1 knockout	KELLY	CRISPR/Cas9
NBL-S IGF2BP1 knockout	NBL-S	CRISPR/Cas9

3.1.5 Chemicals and reagents

All chemicals used throughout this study were purchased from Thermo Fisher Scientific, Sigma-Aldrich and Carl Roth, unless otherwise stated. Enzymes, including respective reaction buffers, PCR-master mixes, transfection reagents as well as DNA and protein ladders were purchased from Promega, Thermo Fisher Scientific and New England Biolabs. Cell culture dishes and flasks were purchased from TPP (Techno Plastic Products) and cell culture solutions were acquired from Thermo Fisher Scientific (medium, FBS, OptiMEM, GlutaMax, TE and PBS). Small molecule inhibitors are listed in Table 6.

Table 6: Small molecule inhibitors.

compound	target	company
ABBV-075 (Mivebresib)	BRD4	MedChemExpress (HY-100015)
ARV-771	BRD2/3/4 (PROTAC)	MedChemExpress (HY-1000972)
BTYNB	IGF2BP1	Selleckchem (S9871)
CPI-0610	BRD2/3/4, BRDT	Abcam (ab230374)
Doxorubicin	TOP2A	Selleckchem (S1208)
EN-4	MYC	Selleckchem (S9807)
Entinostat	HDAC1/3	Selleckchem (S1053)
FM28	HDAC8/11	synthesized by the group of Wolfgang Sippl
FM35	HDAC11	synthesized by the group of Wolfgang Sippl
HI2.1	HDAC1/2/3	synthesized by the group of Wolfgang Sippl
HI7.3	HDAC1/2	synthesized by the group of Wolfgang Sippl
INCB-057643	BRD2/3/4	MedChemExpress (HY-111485)
KH16	panHDAC	synthesized by the group of Wolfgang Sippl
NI-16	HDAC3	synthesized by the group of Wolfgang Sippl
Panobinostat	panHDAC	Selleckchem (S1030)
PCI-34051	HDAC8	Selleckchem (S2012)
PS59	HDAC8	synthesized by the group of Wolfgang Sippl
PSP50	HDAC1/3/8/11	synthesized by the group of Wolfgang Sippl
SIS17	HDAC11	Selleckchem (S6687)
Vorinostat	panHDAC	Selleckchem (S1047)
YM-155	BIRC5	Selleckchem (S1130)

3.1.6 Buffers

Table 7: Standard buffer.

buffer	ingredients
PBS (phosphate buffered saline), pH 7.4	137 mM NaCl
	2.7 mM KCl
	10 mM Na ₂ HPO ₄
	2 mM KH ₂ PO ₄
PBST (PBS-Tween)	PBS + 1% Tween-20 (v/v)
TAE (Tris/Acetate/EDTA)	40 mM Tris
	20 mM acetic acid
	1 mM EDTA (pH 8.0)
MOPS SDS-running buffer	50 mM MOPS
	50 mM Tris
	0.1% SDS (v/v)
	1 mM EDTA
NuPAGE transfer buffer	50 mM Tris
	40 mM glycerol
	0.04% SDS (v/v)
	10% methanol (v/v)

Ponceau-S	0.1% Ponceau-S (w/v) 5% acetic acid (v/v)
TRIZOL	0.8 mM guanidinium thiocyanate 0.4 mM ammonium thiocyanate 0.1 mM sodium acetat (pH 4.0) 5% glycerol (w/v) 48% Roti-Aqua-Phenol (v/v)
total lysis buffer	50 mM Tris (pH 7.4) 50 mM NaCl 1% SDS (v/v) 2 mM MgCl ₂
RIP buffer	10 mM HEPES (pH 7.4) 150 mM KCl 5 mM MgCl ₂ 0.5% NP-40 (v/v)

3.1.7 Antibodies

Table 8: Primary and secondary antibodies.

primary antibodies	species	company	dilution
AGO2	rabbit	abcam (ab156870)	2 µg / IP
AGO2	rat	Thermo Fisher (14-6519-82)	1:1000 WB
AURKA	mouse	Cell Signaling (12100)	1:1000 WB
phospho-AURKA(T288)	rabbit	Cell Signaling (3875T)	1:1000 WB
AURKB	rabbit	Cell Signaling (3094)	1:1000 WB
BIRC5	rabbit	Novus (nb500-201)	1:1000 WB
CDK1	mouse	Cell Signaling (9116)	1:1000 WB
phospho-CDK1(Y15)	rabbit	Cell Signaling (9111)	1:1000 WB
CDKN1A	rabbit	Cell Signaling (2947)	1:1000 WB
E2F1	mouse	abcam (ab135251)	1:1000 WB
ELAVL1	mouse	Santa Cruz (sc-5261)	1:1000 WB
GAPDH	rabbit	Proteintech (10494-1-AP)	1:5000 WB
GSK3B	mouse	Thermo Fisher (MA5-15597)	1:1000 WB
phospho-GSK3B(S9)	rabbit	Cell Signaling (5558)	1:1000 WB
H3K9ac	rabbit	abcam (ab10812)	1:2500 WB
IGF2BP1	rabbit	Mobitec (RN007P)	2 µg / IP 1:1000 WB
IGF2BP1	mouse	Biozol (RN001M)	1:1000 WB
METTL14	rabbit	Sigma Aldrich (HPA038002)	1:1000 WB
METTL3	rabbit	Proteintech (15073-1-AP)	1:1000 WB
MS2-BP	mouse	Cell Signaling (E8032)	1:1000 WB
MYC	rabbit	Cell Signaling (18583S)	1:1000 WB
MYCN	mouse	Santa Cruz (sc-53993)	1:1000 WB
MYCN	rabbit	Cell Signaling (51705T)	1:1000 WB
MYCN-AF790	mouse	Santa Cruz (sc-53993 AF790)	1:1000 WB

phospho-MYCN(T58)	rabbit	Cell Signaling (46650T)	1:1000 WB
PHOX2B	rabbit	Cell Signaling (83811)	1:1000 WB
PHOX2B	rabbit	Cell Marque (EP312)	IHC
PLK1	mouse	abcam (ab17056)	1:1000 WB
phospho-PLK1(T210)	rabbit	Cell Signaling (5472)	1:1000 WB
PYCR1	rabbit	Proteintech (13108-1-ap)	1:1000 WB
TK1	rabbit	Cell Signaling (8960)	1:1000 WB
TOP2A	rabbit	Cell Signaling (12286)	1:1000 WB
TP53	mouse	Santa Cruz (sc-126)	1:1000 WB
VCL	mouse	Sigma Aldrich (V9131)	1:5000 WB
WEE1	rabbit	Call Signaling (13084)	1:1000 WB
secondary antibodies	species	company	dilution
IRDye [®] 680RD anti-Mouse IgG (H+L)	donkey	Li-Cor (926-68072)	1:10000 WB
IRDye [®] 680RD anti-Rabbit IgG (H+L)	donkey	Li-Cor (926-68073)	1:10000 WB
IRDye [®] 800CW anti-Mouse IgG (H + L)	donkey	Li-Cor (926-32212)	1:10000 WB
IRDye [®] 800CW anti-Rabbit IgG (H + L)	donkey	Li-Cor (926-32213)	1:10000 WB
IRDye [®] 800CW anti-Rat IgG (H+L)	goat	Li-Cor (926-32219)	1:10000 WB

3.1.8 Plasmids

Table 9: Cloning vectors and plasmids.

plasmid	resistance	reference
pcDNA-Cas9-T2A-GFP	Ampicillin	(Müller <i>et al.</i> 2018)
psg-RFP-IGF2BP1 Exon6	Ampicillin	(Müller <i>et al.</i> 2018)
psg-RFP-IGF2BP1 Exon7	Ampicillin	(Müller <i>et al.</i> 2018)
pmirGLO-MCS	Ampicillin	(Busch <i>et al.</i> 2016)
pmirGLO-MYCN 3'UTR WT	Ampicillin	this study
pmirGLO-MYCN 3'UTR mut	Ampicillin	this study
pmirGLO-AURKA 3'UTR	Ampicillin	this study
pmirGLO-AURKB 3'UTR	Ampicillin	Jacob Haase (AG Hüttelmaier)
pmirGLO-BIRC5 3'UTR	Ampicillin	this study
pmirGLO-CDK1 3'UTR	Ampicillin	this study
pmirGLO-NME1 3'UTR	Ampicillin	this study
pmirGLO-PKMYT1 3'UTR	Ampicillin	this study
pmirGLO-PLK1 3'UTR	Ampicillin	this study
pmirGLO-PYCR1 3'UTR	Ampicillin	this study
pmirGLO-TK1 3'UTR	Ampicillin	this study
pmirGLO-TOP2A 3'UTR	Ampicillin	this study
pmirGLO-WEE1 3'UTR	Ampicillin	this study
pcDNA3.1-2xMS2 loops	Ampicillin	(Busch <i>et al.</i> 2016)
pcDNA3.1-MYCN 3'UTR WT-2xMS2 loops	Ampicillin	this study
pcDNA3.1-GFP-stop	Ampicillin	this study
pcDNA3.1-GFP-stop-MYCN 3'UTR WT	Ampicillin	this study
pcDNA3.1-GFP-stop-MYCN 3'UTR mut	Ampicillin	this study
pcDNA3.1-iRFP	Ampicillin	this study

pcDNA3.1-iRFP-IGF2BP1 WT	Ampicillin	this study
pcDNA3.1-iRFP-IGF2BP1 mut	Ampicillin	this study
pcDNA3.1-iRFP-ELAVL4	Ampicillin	this study
pcDNA3.1-iRFP-stop	Ampicillin	this study
pcDNA3.1-iRFP-stop-2x perfect miR-17	Ampicillin	this study
pcDNA3.1-iRFP-stop-2x perfect let-7a	Ampicillin	this study
pcDNA3.1-FFL	Ampicillin	Marcell Lederer (AG Hüttelmaier)
pNL3.1 [Nluc/minP]	Ampicillin	Promega (N1031)
pNL3.1 [Nluc/minP] E-Box	Ampicillin	this study
pLVX-shC-PGK-puro-T2A-iRFP	Ampicillin	(Gutschner <i>et al.</i> 2014)
psPAX2	Ampicillin	Addgene (12260)
pMD2.G	Ampicillin	Addgene (12259)
pcR® blunt	Kanamycin	Thermo Fisher (K270040)

3.1.9 Oligonucleotides

Oligonucleotides for cloning (Table 10), RT-qPCR (Table 11) and genotyping (Table 12) were purchased from Eurofins Genomics GmbH. Primer pairs for RT-qPCR were selected using Primer Blast (<https://www.ncbi.nlm.nih.gov/tools/primer-blast/>).

Table 10: Oligonucleotides and restriction sites for cloning.

oligonucleotide	sequence (5' - 3')	restriction site
MYCN_3'UTR_s	gggGAATTCacgcttctcaaaactggacagtactgcc	EcoRI
MYCN_3'UTR_as	gggCTCGAGcatgaggtatttcaaagtctataagatgcagc	XhoI
MYCN_3'UTR_mut	Synthesized by GenScript Biotech, then sub-cloned.	EcoRI / XhoI
AURKA_3'UTR_s	ggGAATTCgaatcgtgcaggggagaaatcc	EcoRI
AURKA_3'UTR_as	ggCTCGAGgcatatttaaagtttacacacatgctatgactcc	XhoI
BIRC5_3'UTR_s	gggGAATTCgaaaggagatcaacatttcaaattagatg	EcoRI
BIRC5_3'UTR_as	gggCTCGAGccacatgagactttattggcaattg	XhoI
CDK1_3'UTR_s	ggGAATTCctaattttattaatatttgcactgtggatataaaggac	EcoRI
CDK1_3'UTR_as	ggCTCGAGggaaaaagataaagcagaatctgtatccc	XhoI
NME1_3'UTR_s	gggGAATTCcaggaggcagaccacattg	EcoRI
NME1_3'UTR_as	gggCTCGAGagaaggaaaaaaagcaatgcaacaatag	XhoI
PKMYT1_3'UTR_s	ggGAATTCgccccagactctgcctct	EcoRI
PKMYT1_3'UTR_as	ggCTCGAGgggtgctccaaggttcaaatac	XhoI
PLK1_3'UTR_s	gggCTTAAGtagctgccctcccctcc	AflIII
PLK1_3'UTR_as	gggCTCGAGgtgcataaagccaag	XhoI
PYCR1_3'UTR_s	gggGAATTCcacgtcctgctgaccacc	EcoRI
PYCR1_3'UTR_as	gggCTCGAGgattacattgacattttaatcagtaaggcagatgcc	XhoI
TK1_3'UTR_s	gggGAATTCgggacctgagggccg	EcoRI
TK1_3'UTR_as	gggCTCGAGcaattagtttaattcataagctacagcagaggcgtgg	XhoI
TOP2A_3'UTR_s	gggGAATTCaatgtgaggcgattattttaagtaattatc	EcoRI
TOP2A_3'UTR_as	gggCTCGAGgtttagaacattttattaaagtacaaaattgttg	XhoI
WEE1_3'UTR_s	ggGAATTCgctactccttcccactccc	EcoRI
WEE1_3'UTR_as	ggCTCGAGcatcatgctacatttctagcaagtcacatg	XhoI

GFP_s	gggGCTAGCcatggtgagcaagggcgaggagctg	NheI
GFP_stop_as	gcgGAATTCttactgtacagctcgtccatgccgagagtgatcccg	EcoRI
iRFP_s	ggGCTAGCatggctgaaggctccctgc	NheI
iRFP_as	ggGAATTCctcttccatcacgccgatctgc	EcoRI
IGF2BP1 WT	Sub-cloned from previous vector.	EcoRI / XhoI
IGF2BP1 mut	Sub-cloned from previous vector.	EcoRI / XhoI
ELAVL4_s	ggGAATTCatggttatgataattagcacatggag	EcoRI
ELAVL4_as	ggCTCGAGTcaggacttggggcttggttg	XhoI
iRFP_stop_as	ggGAATTCtactcttccatcacgccgatct	EcoRI
2x perfect let-7a_s	ggGAATTCctagaAACTATACAACCTACTACCTCAacgcgtAAC TATACAACCTACTACCTCAgccCTCGAGcc	oligo annealing (EcoRI / XhoI)
2x perfect let-7a_as	ggCTCGAGggcTGAGGTAGTAGGTTGTATAGTTacgcgtTGA GGTAGTAGGTTGTATAGTTttagGAATTCcc	(EcoRI / XhoI)
2x perfect miR-17_s	ggGAATTCctagaCTACCTGCACTGTAAGCACTTTGacgcgtCT ACCTGCACTGTAAGCACTTTGgccCTCGAGcc	oligo annealing (EcoRI / XhoI)
2x perfect miR-17_as	ggCTCGAGggcCAAAGTGCTTACAGTGCAGGTAGacgcgtCA AAGTGCTTACAGTGCAGGTAGttagGAATTCcc	(EcoRI / XhoI)
6x E-Box_s	CTAGCggccacgtgaatcgacgtgtgcacgtggacacgtgtggccacgt gactagccacgtgaccA	oligo annealing
6x E-Box_as	AGCTTggtcacgtggctagtcacgtggccacacgtgtccacgtgcacacg tgcgattcacgtggccG	(NheI / HindIII)

Table 11: RT-qPCR primer.

human gene	sense (5' - 3')	antisense (5' - 3')
AURKA	CAGGCAACCAGTGTACCTCA	CCCAGAGGGCGACCAATTC
AURKB	GGGAACCCACCCTTTGAGAG	GGGGTTATGCCTGAGCAGTT
BIRC5	GGACCACCGCATCTCTACAT	GTCTGGCTCGTTCTCAGTGG
CDK1	GCGGAATAATAAGCCGGGATCT	CATGGCTACCACTTGACCTGT
E2F1	AAGAGCAAACAAGCCCGAT	ACAACAGCGGTTCTTGCTCC
EEF2	CCTTGTGGAGATCCAGTGTCC	TTGACCACAAACATGGGGGT
GAPDH	CATCAAGAAGGTGGTGAAGCAG	TGTCATACCAGGAAATGAGCTT
HIST1H2AC	TTTCTCGTGAGCTTAGGCCG	CCTTGCTTACCACGTCCAGA
HIST2H3A	CTACCAGAAGTCCACGGAGC	AAGCGCAGGTCCGTCTTAAA
IGF2BP1	TAGTACCAAGAGACCAGACCC	GATTTCTGCCCGTTGTTGTC
IGF2BP1 (transgene)	GGGCCATCGAGAATTGTTGC	CGGGAGCCTGCATAAAGGAG
IRF1	CCTGTGCACCGTAGCAGGGC	TCTTCCCAGGAGGCAGGGCC
MDM2	TGCCAAGCTTCTCTGTGAAA	GTCCGATGATTCCTGCTGAT
METTL14	GGGGTTGGACCTTGAAGAG	CCCATGAGGCAGTGTTCCTT
METTL3	TATCCAGGCCCAAGAAGC	GAAGTCTGAAGCTGTGCTG
MYCN	CACAAGGCCCTCAGTACCTC	ACCACGTCGATTTCTTCTC
NME1	GGACCGTCCATTCTTTGCCG	CGATCTCCTTCTCTGCACTCT
PKMYT1	CAGGGACACCCTGGATTAC	AAGTAGGCTGGGACTGGGAT
PLK1	AAGAGGAGGAAAGCCCTGAC	TTCTTCTCTCCCCGTCATA
PYCR1	TTGGCTGCCCAAGATAAT	GTCTCCTTGTGGGGTGT
RPLP0	CCTCGTGGAAGTGACATCGT	ATCTGCTTGGAGCCACATT

TK1	GTAATTGTGGCTGCACTGGA	GTCAGCTTCACCACGCTCTC
TOP2A	CAAACAAAGGGACCCAAAAA	CAACTTTGTGTTCAACAACAGGA
WEE1	CACACGCCCAAGAGTTTGC	CACTTGAGGAGTCTGTCGCA
mouse gene	sense (5' - 3')	antisense (5' - 3')
Eef2	GTGGTGGACTGTGTGTCTGG	CGCTGGAAGGTCTGGTAGAG
Gapdh	TCTTCCAGGAGCGAGACCCCA	TTCAAGTGGGCCCCGGCCTT
Igf2bp1	GACGTGGCCGCCATGAGCTT	AGCCTGGGCGGGGATGAACA
Mycn	GGAGAGGATACCTTGAGCGA	AGTGGTTACCGCCTTGTTGT
Rplp0	CAGGTGTTTGACAACGGCAG	GAAGGCCTTGACCTTTTCAGT

Table 12: Primers for genotyping.

genotyping PCR primers	sequence
A1 (<i>Rosa26_s</i>)	CTCTCCCTCGTGATCTGCAACTCC
A2 (knockin_s)	TTGGGTCCACTCAGTAGATGC
A3 (<i>Rosa26_as</i>)	CATGTCTTTAATCTACCTCGATGG
I1 (IGF2BP1_transgene_s)	GAAGGTCTCCTACATCCCCGATGAGCAG
I2 (IGF2BP1_transgene_as)	CCTTCCTTGCCAATGAGACGCCCTAC
M1 (MYCN_transgene_s)	ACCACAAGGCCCTCAGTACC
M2 (MYCN_transgene_as)	TGGGACGCACAGTGATGG
iCRE_s	GAACCTGATGGACATGTTCAGGGACAGGC
iCRE_as	GGTGTGTAGGCAATGCCCAGGAAGGC

3.1.10 siRNAs

All siRNAs (Table 13) used in this study were synthesized by Eurofins Genomics GmbH.

Table 13: siRNAs.

siRNAs	sequence
siC (<i>cel-miR-239b-5p</i>)	UUUGUACUACACAAAAGUACUG
siIGF2BP1 pool	CCGGGAGCAGACCAGGCAA
	UGAAUGGCCACCAGUUGGA
	CCAGGCAAGCCAUCAUGAAGCUGAA
	GGCUGCUCCCUAUAGCUCCUUUAUG
	GGGAAGAGCUGGAGGCCUA
	CCAUCCGCAACAUCACAAA
	AAGCUGAAUGGCCACCAGUUG
	AACACCUAGACUCCAAAGUUCG
	GUAUGGUACAGUAGAGAAC
	CCUGAAGAAGGUAGAGCAA
GUUCGUAUGGUUAUCAUCA	
GUGAACACCGAGAGUGAGA	
siMETTL3 pool	GCAAGUAUGUUCACUAUGAAA
	GUAUGAACGGGUAGAUGAAAU
	CUACAGAUCUGAGUUAGAGA

siMETTL14 pool	CUUACAAGCCGAUUAUAGAAGC GGCUAAAGGAUGAGUUAAUAG GAGAGAAUUGCUGAAACAAG
siMYC pool	CGUUAGCUUCACCAACAGG CCAGAGGAGGAACGAGCUAAA ACUGAAAGAUUUAGCCAUAAU
siMYCN pool	CCCGGACGAAGAUGACUUCUA CGUGCCGGAGUUGGUAAAGAA AAAUUGAACACGCUCGGACU UGAUCUGCAAGAACCCAGA CAUACCUAAGUACUGUAAUAA

3.1.11 Kits and systems

Table 14: Standard systems and kits.

name	company
AllPrep [®] DNA/RNA/Protein Mini Kit	Qiagen
Caspase-Glo [®] 3/7 Assay System	Promega
CellTiter-Glo [®] Luminescent Cell Viability Assay	Promega
Click-iT [™] Nascent RNA Capture Kit	Invitrogen Life Technologies
DC Protein Assay	Bio-Rad
Dual-Glo [®] Luciferase Assay System	Promega
KAPA mouse genotyping kit	Sigma Aldrich
Monarch [®] RNA Cleanup Kit (50 µg)	New England Biolabs
Nano-Glo [®] Dual-Luciferase Assay System	Promega
NuPAGE [®] Bis-Tris Electrophoresis System	Invitrogen Life Technologies
ORA [™] qPCR Green ROX L Mix	HighQu
Phusion High-Fidelity PCR-Kit	New England Biolabs
PureLink [™] Quick Gel Extraction Kit	Invitrogen Life Technologies
Q5 [®] High-Fidelity 2X Master Mix	New England Biolabs
QIAGEN Plasmid Midi Kit	Qiagen
QIAprep Spin Miniprep Kit	Qiagen
RiboMAX [™] Large Scale RNA Production Systems - T7	Promega
Zero Blunt [™] PCR Cloning Kit	Invitrogen Life Technologies

3.1.12 Instruments

Table 15: Instruments.

application	device (company)
Block heater	QBD2 and QBA1 (Grant) Thermo-Shaker PHMT (Grant-bio)
Cell Counter	TC20™ Automated Cell Counter (Bio-Rad)
Cell culture bench	Scanlaf Mars 1200 (Labogene)
Centrifuges	Biofuge® Stratos (Heraeus) Fresco™ 17 (Heraeus) miniSpin (Eppendorf) Megafuge 1.0R (Heraeus) Sprout® Plus (Heathrow Scientific)
Flow Cytometry	FACS Melody (BD) MACSQuant Analyzer 9® (Miltenyi BioTech)
Gel documentation	E-Box VX5 (VILBER)
Gel electrophoresis	XCell SureLock™ Mini-Cell (Invitrogen) XCell II™ Blot Modul (Invitrogen) Mini-Sub® Cell GT (Bio-Rad)
Homogenizer	Precellys 24 (berting technologies)
Incubator	CO2 incubator CB150 (Binder) shaking incubator 3032 (GFL) Unitron (INFORS HT)
Infrared scanner	Odyssey Infrared Scanner (Li-Cor) Pearl® Small Animal Imaging System (Li-Cor)
Luminescence / Absorption	GloMax® Discover 96 Well Microplate Reader (Promega)
Microscopy	Eclipse TS2 (Nikon) Eclipse TS100 (Nikon) Eclipse TE2000-E IncuCyte S3® (Sartorius)
Microtome	RM2235 (Leica)
pH meter	Lab875 (SI Analytics)
Power supplier	PowerPac 200 and basic (Bio-Rad)
Rotator	i Roll RnR 10 (neuation) rotator SB2 (stuart)
RT-qPCR	Light Cycler® 480 II (Roche)
Scales	Pioneer™ PA2202C and PA224C (Ohaus)
Shaker	Rocker-Shaker PMR-100 (grant-bio)
Spectroscopy	Spark (Tecan)
Stirrer	RCT basic (IKA)
Thermocycler	Mastercycler Nexus II (Eppendorf)
Vortexer	VortexGenie®2 (Scientific Industries)
Water bath	ecoline RE104 (LAUDA)

3.2 Animal work

3.2.1 Mouse xenograft studies

Female immunodeficient athymic nude mice were obtained from Charles River, Germany. For subcutaneous xenograft assays 1×10^6 iRFP-labeled BE(2)-C or 2×10^6 iRFP-labeled NBL-S cells (stably transduced using iRFP encoding lentiviruses) were harvested in PBS, afterwards supplemented with 50% (v/v) matrigel (Sigma Aldrich) and injected into the left flank of six-week old mice. Prior injection, cells were counted using a TC20 Cell Counter (Bio-Rad). Mice were held with access to chlorophyll-free food to avoid background noise in iRFP image acquisition. Subcutaneous tumor growth and volume were measured and monitored by non-invasive near-infrared imaging using a Pearl Impulse Imaging System (Li-Cor) and isoflurane as anesthetic (2.5 - 5%). Tumor volume was calculated using the formula $\pi/6 \times L1 \times L2 \times L3$. The mice were sacrificed, once the first tumor reached a diameter of 1 - 1.5 cm. For testing BTYNB *in vivo* BE(2)-C cells were treated for 24 h with BTYNB or DMSO prior to harvesting. For intra-tumoral application of BTYNB 5×10^5 iRFP-labeled BE(2)-C cells were injected into nude mice and grown for two weeks. Afterwards treatment was started by injecting 50 mg/kg body weight BTYNB in 100 μ l 35% cyclodextrin solution in PBS with a final DMSO concentration of 7%. Treatment was performed in two cycles with five days of treatment and two days break. Tumor volume and mouse weight was documented over time.

3.2.2 Patient-derived xenograft study

Patient-derived xenografts (PDX) were performed by the EPO company in Berlin, Germany. The neuroblastoma tumor 14647 harboring *MYCN* amplification and 17q gain was implemented in NOG mice to generate PDX. Treatment was performed by intra-peritoneal application of DMSO, 100 mg/kg body weight BTYNB, 2.5 mg/kg body weight YM-155 and the combination of BTYNB and YM-155 in 100 μ l 30% cyclodextrin solution in PBS with a final DMSO concentration of 7%. Compound application was done in three cycles with five days of treatment and two days break. Tumor volume and mouse weight was documented over time. Mice initially lost weight due to compound application but recover from that loss after 3 days.

3.2.3 Transgenic mouse studies

Transgenic mice were generated by Taconic Bioscience (LSL-*IGF2BP1*) or were obtained from Johannes Schulte (Charité Berlin). For getting a homogenous background, mice were backcrossed to C57BL6/NCrl mice and afterwards crossbred to generate transgenic lines. Mouse genotyping was confirmed by gPCR. Mice were palpated weekly for abdominal tumors and are summarized in Appendix Table 29. Primer sequences are provided in Table 12.

3.2.4 Immunohistochemistry

Transgenic tumor samples were fixated with Roti-Histofix (Roth) and embedded in paraffin. Paraffin blocks were sliced at 4 μm thickness using RM2235 (Leica) and transferred to a specimen slide. Slides were heated for 15 min at 65°C and then incubated twice in xylene (4 min), washed twice in 96% ethanol (1 min) and for 1 min in distilled water. Afterwards slides were stained with hematoxylin for 10 min, washed 10 min under tap water, stained for 3 min with eosin and again washed 1 min under tap water. Prior to adding the clover slip, slides were washed twice in 96% ethanol and xylene. Staining of Phox2b was done with the Cell Marque antibody EP312. Images were acquired using a Nikon Eclipse TE2000-E microscope with a 20x objective and 1.5 manual magnification.

3.3 Cell biological methods

3.3.1 Cell culture

BE(2)-C cells were cultured in a 1:1 mixture of DMEM/F12 (with HEPES, Gibco) and MEM (Gibco). KELLY, TET21N, HEK293T17, KNS42, Panc-1, H522, HepG2 and Huh7 cells were cultured in DMEM (Gibco). NBL-S cells were cultured in IMDM (Gibco). All media were supplemented with 10% FBS and 1% GlutaMAX (Gibco). Cells were grown at 37°C and 5% CO₂. Prior to passaging, the medium was discarded and the cells were washed with PBS. Afterwards, cells were detached adding Trypsin-EDTA, followed by resuspension in complete media to stop the detaching. Subsequently, cells were counted and seeded into cell culture dishes.

3.3.2 Transfection

For siRNA knockdown 4.5 x 10⁵ BE(2)-C, 1.5 x 10⁶ KELLY, 5 x 10⁵ TET21N, Panc-1, H522, HepG2 or Huh7 cells were transfected on a 6-well plate using 7.5 μl Lipofectamine RNAiMAX (Thermo Fisher Scientific) and 50 pmol siRNA according to the manufacturer's instructions. In brief, Lipofectamine was mixed with 100 μl OptiMEM (Gibco). Then 1 μl of siRNA was mixed with 100 μl of OptiMEM and 100 μl of Lipofectamine/OptiMEM was added to the siRNA mixture. After incubation of 5 minutes at room temperature, 200 μl were added to the cells.

3.3.3 CRISPR/Cas9-mediated knockout

For genomic deletion of IGF2BP1 via CRISPR/Cas9 5 x 10⁵ cells were transfected on a 6-well plate using 3.75 μl Lipofectamine 3000 (Thermo Fisher Scientific), 2 μg Cas9- and 1 μg sgRNA-encoding plasmids. Plasmid DNAs were mixed with 2 $\mu\text{l}/\mu\text{g}$ P3000. Subsequent procedure was similar to siRNA transfection (see 3.3.2). 48 h post transfection cells were sorted for single cell clones by seeding one RFP- and GFP-

positive cell per 96-well using a FACS Melody sorter. The deletion of IGF2BP1 was validated by western blotting.

3.3.4 Luciferase reporter assay

For luciferase reporter studies 5×10^4 BE(2)-C or 1.25×10^5 KELLY or NBL-S cells were transfected on a 24-well plate with 1 μ l Lipofectamine 2000 (Thermo Fisher Scientific) and 200 ng pmirGLO vector. The Lipofectamine was mixed with 25 μ l OptiMEM. Plasmid DNA and 25 μ l OptiMEM were mixed, then 25 μ l Lipofectamine/OptiMEM was added to the DNA mixture. After incubation of 5 minutes, 50 μ l were added to the cells. 36 h post transfection, Dual-Glo luciferase reporter analyses were performed according to manufacturer's protocol. In brief, cells were lysed in 220 μ l of a 1:1 mixture of PBS and Dual-Glo substrate 1. After 10 minutes incubation, duplicates (100 μ l each) were pipetted in a white 96-well plate and Firefly luciferase activity was measured with a GloMAX Discover. Afterwards, 50 μ l of substrate 2 (1:100 dilution in stop and glow buffer) was added to measure after 10 minutes the Renilla Luciferase activity. Ratios of Firefly to Renilla activity were calculated and the activity of the 3'UTR reporters were normalized to the respective controls. For luciferase assays with BTYNB, medium was changed 6 h post transfection and DMSO or BTYNB was added at EC₅₀ concentration. Reporter containing a minimal vector-encoded 3'UTR served as normalization control. For measuring the transcriptional activity of MYCN, cells were handled similarly, but transfected with 200 ng Firefly control and 20 ng Nano luciferase vector. After 36 h, Nano luciferase assay was performed, essentially as the Dual-Glo luciferase assay.

3.3.5 Fluorescence reporter assay

For the fluorescence reporter assay 3.5×10^5 BE(2)-C cells were seeded in a 6-well plate and after 6 h transiently transfected with 2.5 μ g GFP reporter and 7 μ g iRFP vector using 14.5 μ l Lipofectamine 3000 reagent. Plasmid DNAs were mixed with 2 μ l/ μ g P3000. Subsequent procedure was similar to siRNA transfection (see 3.3.2). Medium was changed after 24 h and cells were harvested and analyzed by flow cytometry 48 h post transfection.

3.3.6 Lentiviral transduction

For the production of lentiviral particles, 3.6×10^6 HEK293T17 cells were transfected on a 6-well plate with 7 μ l Lipofectamine 3000, the packaging plasmids psPax2 (3 μ g) and pMD2.G (1.5 μ g) as well as the lentiviral expression vector pLVX (4 μ g) encoding iRFP. 2 μ l P3000 per μ g DNA was added. Lentiviral particle-containing supernatant was collected 24 and 48 h post transfection and stored at -80°C. Titers were analyzed 72 h post infection of 5×10^4 HEK293T17 cells and determined by flow cytometry (iRFP)

using a MACS Quant Analyzer 9. Lentiviral transduction for downstream experiments was accomplished at 5 MOI (multiplicity of infection).

3.3.7 Inhibition of RNA and protein synthesis

For mRNA or protein decay analyses, 5×10^5 BE(2)-C or TET21N cells were seeded one day before the experiment in a 6-well plate. Cells were treated with Actinomycin D (5 μ M, Sigma Aldrich) or Emetine (100 μ M, Sigma Aldrich), respectively, for indicated time points. Abundance at these time points were analyzed by RT-qPCR or Western blot, respectively.

3.3.8 2D growth assay

To analyze 2D proliferation, cells were seeded in a 6-well plate at low density and tracked through the IncuCyte S3. Confluence was determined over time with the internal IncuCyte software.

3.3.9 3D spheroid formation assay

For spheroid growth assay 2×10^3 cells were seeded in a 96-well round-bottom ultra-low attachment plate (Corning) with 10% FBS. Spheroid formation was induced by centrifugation for 5 minutes at 2000 rpm. Images were acquired over five days using the IncuCyte S3.

3.3.10 Anoikis resistance assay

For anoikis assay 5×10^3 cells were seeded in a 96-well flat-bottom ultra-low attachment plate (Corning) with 1% FBS. Five days post seeding cells were transferred to a round-bottom plate, centrifuged for 5 minutes at 2000 rpm and then images were acquired using an IncuCyte S3.

3.3.11 Cell viability measurement

Cell viability was measured with CellTiter-Glo 72 h after drug exposure or after five days of 3D or anoikis resistance assay according to the manufacturer's protocol. In brief, for drug assays the medium was discarded and 70 μ l of a 1:1 mixture of PBS and CellTiter-Glo was added to the cells. For 3D and anoikis resistance assays, 50 μ l CellTiter-Glo was directly added to the medium. After incubation for 10 minutes, the cell lysates were transferred to a white 96-well plate and luminescence was measured using a GloMAX Discover. Inputs were measured accordingly when seeding the cells at the start of the experiment.

3.3.12 Apoptosis measurement

Apoptosis was measured with the Caspase-Glo 3/7 assay after five days of 3D or anoikis resistance assay according to the manufacturer's protocol. In brief, 50 μ l Caspase-Glo was added to each 96-well.

After incubation for 30 minutes, the cell lysates were transferred to a white 96-well plate and luminescence was measured using a GloMAX Discover. Inputs were measured accordingly.

3.3.13 Compound testing

For determining the EC₅₀ values 5 x 10³ BE(2)-C, 1 x 10⁴ NBL-S, 1.25 x 10⁴ KELLY or 2 x 10⁴ Panc-1, H522, HepG2 or Huh7 cells were seeded per well of a 96-well plate. A serial dilution of the drugs was performed and added to the cells at the indicated concentrations. DMSO served as control condition. After 72 h of treatment, an image was acquired using IncuCyte S3. Confluence was determined using the IncuCyte software. Confluence values were normalized to DMSO control. For the analysis of synergy between two drugs, the cell viability was determined 72 h upon drug exposure using CellTiter-Glo in a drug matrix screen at indicated concentrations. Synergy relief maps were generated using the SynergyFinder web application (<https://synergyfinder.fimm.fi>; version 2.0) and the ZIP (Zero interaction potency) method (Ianevski *et al.* 2020). For BTYNB recovery experiment DMSO or 5 µM BTYNB were added to the cells and grown for 72 h. Afterwards one third of the BTYNB-treated cells were harvested (referred to as '3 days BTYNB') while the rest was treated further with DMSO ('BTYNB+DMSO 6 days' = recovery) or 5 µM BTYNB ('6 days BTYNB'), respectively.

3.4 Biochemical methods

3.4.1 Cloning

All generated and used plasmids, oligonucleotides and restriction sites are summarized in Table 9 and Table 10. All constructs were validated by Sanger sequencing at Eurofins Genomics GmbH.

Plasmid digestion

For restriction cloning, 2 µg plasmid DNA was digested with 0.5 µl of the respective restriction enzymes and its buffer (NEB) for 4 h at 37°C. Digested plasmids were separated on an agarose gel.

DNA amplification by polymerase-chain reaction (PCR)

To generate luciferase reporter comprising different 3'UTRs, the respective DNA was amplified from human genomic DNA (Promega) using the Q5 polymerase. For cloning purposes, DNA amplification from plasmids were performed with the Q5 polymerase. To fuse multiple fragments in a Fusion-PCR, the Phusion High-Fidelity DNA Polymerase (Thermo Fisher Scientific) was used (Table 16, Table 17).

Table 16: PCR reaction setup.

	PCR from gDNA	PCR from plasmids	Fusion-PCR
template	200 ng	10 ng	50 ng
10 μ M oligonucleotide mix	0.5 μ l	0.5 μ l	1 μ l
10 mM dNTPs			0.5 μ l
buffer	5 μ l Q5 2x mix	5 μ l Q5 2x mix	5 μ l
polymerase			0.5 μ l
nuclease-free water	add to 10 μ l	add to 10 μ l	add to 25 μ l

Table 17: PCR program.

steps	temperature	time	
initial denaturation	98°C	30 s	
denaturation	98°C	10 s	37 cycles
primer annealing	50-72°C	20 s	
elongation	72°C	15 s / kb (Q5) 30 s / kb (Phusion)	
final elongation	72°C	1 min	
	4°C	hold	

Oligonucleotide annealing

For the annealing of oligonucleotides, 15 μ l sense and 15 μ l antisense oligonucleotide (100 μ M each) were mixed with 15 μ l nuclease-free water, incubated for 3 minutes at 95°C, 65°C and 37°C and then cooled to room temperature. Annealed oligonucleotides were used for ligation in linearized vectors.

Agarose gel electrophoresis

Amplified PCR products and digested plasmids were separated on a 1% TAE agarose gel containing ethidium bromide at 140 V. Therefore, DNA samples were mixed with 6x Gel Loading Dye (NEB). The Quick-Load 2-log DNA ladder (NEB) served as size marker. Signals were detected with an UV imager and respective bands were cut out of the gel.

DNA extraction from agarose gels

DNA extraction from agarose gels was performed with the PureLink Quick Gel Extraction Kit according to the manufacturer's instructions. In brief, the gel was solubilized in Gel Extraction Buffer, incubated at 65°C for 5 minutes and spun through the DNA column. The column was washed with Washing Buffer and the DNA was eluted with nuclease-free water.

Ligation

The ligation of linearized DNA fragments (= insert) and vectors was performed according to Table 18. The reaction mix was incubated at room temperature for at least 1 h.

Table 18: Ligation.

	pcR blunt vector	final vector
10x Ligation Buffer (Roche)	1.2 μ l	1.2 μ l
T4 Ligase (Roche)	0.8 μ l	0.8 μ l
insert	9.5 μ l	7.5 μ l
vector	0.5 μ l	2.5 μ l

Transformation

Chemo-competent *E. coli* TOP10 were thawed on ice for 15 minutes. Subsequently, 200 μ l bacteria were added to the ligation mix and incubated for another 20 minutes on ice. Afterwards, heat shock was performed for 45 s at 42°C in a water bath. Tubes were cooled for 3 minutes on ice, then 500 μ l LB medium without antibiotics were added to the transformation batch and incubated for 1 h at 37°C on a thermal shaker. Finally, bacteria were plated on LB-agar plates containing the respective antibiotic and incubated over night at 37°C in an incubator.

Colony PCR

Colonies were picked from the agar plates and analyzed by PCR using the OneTaq 2x Master Mix (NEB) according to manufacturer's protocol.

Plasmid DNA preparation from *E. coli*

For positive clones a 4-ml overnight culture was inoculated and plasmid DNA extraction was performed using the QIAprep Spin Miniprep Kit, according to the manufacturer's instructions. If necessary, the QIAGEN Plasmid Midi Kit was used for DNA extraction of 100-ml overnight cultures.

3.4.2 RNA isolation

Total RNA from cell culture samples was isolated using phenol-chloroform extraction. Cells were harvested, washed with PBS, lysed in 1 ml TRIZOL and shock frozen in liquid nitrogen. After thawing of the samples, 200 μ l chloroform were added, mixed thoroughly and samples were centrifuged for 10 minutes at 13.000 rpm and 4°C to separate phases. The RNA-containing upper phase was transferred to a new reaction tube and mixed with 1 volume of isopropanol. Subsequently, samples were mixed thoroughly and centrifuged for 30 minutes at 13.000 rpm and 4°C. The RNA pellet was washed twice with 80% ethanol and centrifuged for 10 minutes at 13.000 rpm and 4°C. The ethanol was removed completely. The pellet was dried at 65°C and resolved in RNase-free water. RNA concentration and purity was assessed by nanodrop.

3.4.3 Reverse transcription

Table 19: RT program.

steps	temperature	time
	20°C	5 min
annealing	25°C	5 min
	30°C	5 min
	42°C	1 h
reverse transcription	72°C	15 min
inactivation	4°C	hold

For cDNA synthesis, 2 µg total RNA served as a template using M-MLV Reverse Transcriptase (Promega) and random hexamer (R6) primers following manufacturer's protocol. In brief, RNA in 13.5 µl RNase-free water was mixed with 1 µl R6 primer (5 µM). Samples were heated for 5 minutes at 65°C to obstruct any secondary structures. Afterwards, 5.5 µl reaction mix (4 µl 5x RT buffer (Promega), 1 µl dNTPs, 0.5 µl M-MLV Reverse Transcriptase) was added and the RT program was initiated (Table 19). For RNA decay analyses oligo-dT primers were used instead of random hexamer primers. Final cDNA was diluted 1:10 and stored at -20°C.

3.4.4 Quantitative real-time PCR

RT-qPCR analyses were performed on a LightCycler 480 II (Roche) with 2.5 µl ORA™ qPCR Green ROX L Mix (highQu), 2.5 µl diluted cDNA and 0.02 µl primer mix. The PCR conditions are shown in Table 20. In general, RPLP0, EEF2 and GAPDH served as housekeeping genes (normalization controls). For RNA decay analyses RPLP0 served as normalization control. For IGF2BP1 RIP assays RNA data are input normalized and HIST1 served as normalization control. For AGO2 RIP assays RNA data are input normalized and IGF2BP1-KO cells were normalized against control cells. Relative RNA abundance was determined by the $\Delta\Delta C_t$ method, as previously described (Livak and Schmittgen 2001).

Table 20: RT-qPCR program.

steps	temperature	time
activation of DNA polymerase	95°C	5 min
denaturation	95°C	10 s
primer annealing	60°C	10 s
elongation	72°C	20 s
melting curve	55-95°C	-
	4°C	hold

3.4.5 Protein extraction

For protein extraction of cell culture samples, cells were harvested, washed with PBS and lysed in total lysis buffer supplemented with 0.5 µl Benzodase (Merck Millipore) per 100 µl. For phosphoprotein

analyses protease and phosphatase inhibitor (Sigma Aldrich) were added during lysis. Protein concentrations were determined using the *DC* Protein Assay, according to manufacturer's instructions, and the GloMAX Discover at 600 nm. A BSA standard curve (0 to 10 mg/ml) served as quantification control.

3.4.6 SDS-PAGE and Western blot analysis

For SDS-PAGE, 4x NuPAGE LDS Sample Buffer (Invitrogen) supplemented with 100 mM DTT was added to the protein lysates and incubated for 3 minutes at 95°C. Separation of proteins was accomplished on a NuPAGE Novex 4-12% Bis-Tris protein gel (Invitrogen) with MOPS SDS-running buffer. The SeeBlue Plus2 Pre-Stained Protein Standard (Thermo Fisher) served as marker for size detection. Subsequently, proteins were transferred using NuPAGE transfer buffer by wet blotting onto a nitrocellulose membrane (GE Healthcare). Finally, membranes were blocked with 5% (w/v) milk or 5% (w/v) BSA for detection of proteins or phosphoproteins, respectively. Protein expression was analyzed by Western blotting with indicated primary antibodies by using fluorescence-coupled secondary antibodies and an infrared scanner (Li-Cor). Vinculin (VCL/Vcl) served as a loading and normalization control. For RIP analyses VCL served as negative control. For the miTRAP study VCL served as negative control and MS2-BP as control for equal loading of the resin.

3.4.7 Mouse tissue preparation

Transgenic tumors and murine organs were dissected and shock-frozen on dry ice. For preparation of DNA, RNA and protein the Qiagen AllPrep DNA/RNA/Protein Kit was used. Approximately 30 mg of frozen tissue was lysed in 600 μ l RLT lysis buffer containing β -mercaptoethanol. Tumors were homogenized with Zirconium Oxide beads and Precellys 24 homogenizer (berting technologies). Lysates were subjected to the Qiagen AllPrep DNA/RNA/Protein Kit protocol, with the exception, that precipitated protein was solubilized in 5% SDS solution. For preparation of genomic DNA from mouse tail tip biopsies, the KAPA Mouse Genotyping Kit was used, according to manufacturer's protocol.

3.4.8 RNA immunoprecipitation

Cell extracts (3.5×10^6 BE(2)-C or 12.5×10^6 KELLY and NBL-S) for RNA immunoprecipitation (RIP) were prepared on ice using RIP buffer. Cleared lysates were incubated with anti-IGF2BP1 or anti-AGO2 antibody and Protein G Dynabeads (Life Technologies) for 30 min at room temperature. After three washing steps with RIP buffer, protein-RNA complexes were eluted by addition of 1% SDS and 65°C for 5 minutes. Protein enrichment was analyzed by western blotting. Co-purified RNAs were extracted using TRIZOL and analyzed by RT-qPCR. If indicated, DMSO or 5 μ M BTYNB was added 6 h before RIP was performed.

3.4.9 Nascent mRNA capture

For analyzing the newly synthesized RNA the Click-iT™ nascent RNA capture kit was used according to manufacturer's instructions. In brief, cells were transfected with siC and siMYCN, after 72 h labeled with 0.2 mM ethylenuridine (EU) for 4 h, harvested and RNA was extracted using TRIZOL. 10 µg total RNA served as input for biotinylation of the EU-labeled RNA by click reaction using 1 mM biotin azide. 1 µg of biotinylated RNA served as input for the purification of nascent RNAs using Streptavidin T1 magnetic beads. Total RNA and purified nascent RNA served as templates for cDNA-synthesis and qPCR analysis.

3.4.10 miTRAP

Plasmid preparation

20 µg plasmid DNA were digested with 10 µl enzyme (PspOMI or ApaI) in 100 µl overnight. Linearization was confirmed on an agarose gel. DNA was purified using the PureLink Quick Gel extraction kit as described in 3.4.1. DNA was eluted in 40 µl TE buffer and concentration was determined.

In vitro transcription

In vitro transcription was performed using the RiboMax Large Scale RNA Production Systems - T7 kit (Promega). The reaction mix (Table 21) was incubated for 4 h at 37°C. RNA size was confirmed on an agarose gel. Afterwards, 1 µl DNase I (Promega) per µg DNA was added and incubated for 30 minutes at 37°C. *In vitro* transcribed RNA was stored at -20°C.

Table 21: *In vitro* transcription reaction mix.

	control (MS2)	target (MYCN 3'UTR)
5x T7 transcription buffer	10 µl	20 µl
rNTPs	15 µl	30 µl
DNA	5 µg	10 µg
T7 enzyme mix	5 µl	10 µl
nuclease-free water	add 50 µl	add 100 µl

RNA purification

In vitro transcribed RNA was purified using the Monarch RNA Cleanup Kit (NEB). Therefore, RNA was thawed on ice and filled up to 100 µl. Then 200 µl RNA Cleanup Binding Buffer and 300 µl 100% ethanol was added and mixed by pipetting. The samples were centrifuged through a filter cartridge (13.000 rpm, 30 s). The flow-through was discarded and the bound RNA was washed twice with 500 µl RNA Cleanup Wash Buffer. Finally, the RNA was centrifuged for 5 minutes to remove residual wash solution. For elution, 35 µl RNase-free water were added, incubated for 3 minutes at 65°C and then

centrifuged for 1 minute at room temperature. To determine the RNA concentration by nanodrop, 1 μ l RNA was diluted with 10 μ l RNase-free water. RNA size was again confirmed on an agarose gel.

RNA pulldown

miRNA trapping by RNA *in vitro* affinity purification (miTRAP) experiments using the 3'UTR of MYCN or MS2 control RNA were essentially performed as described recently (Braun *et al.* 2014). Thirty microliters amylose resin (NEB) was washed four times with binding buffer (BB: 20 mM Tris, pH 7.5, 150 mM NaCl, 1.5 mM MgCl₂, 8.6% glycerol and 0.05% NP40) and incubated with 100 pmol recombinant MBP-MS2BP in 1 ml BB for 30 min. On blocking with bovine serum albumin (25 μ g/ml) and yeast tRNA (20 μ g/ml) for 30 min in 1 ml BB buffer, resin was washed three times with BB. Afterward, *in vitro* transcribed bait RNA was immobilized to the resin by 1 h incubation of 20 pmol RNA with the resin in 1 ml BB supplemented with 11 μ g/ml heparin (Sigma Aldrich). In the meanwhile, 2×10^7 cells were lysed on ice for 10 min with 1 ml BB supplemented with protease inhibitor cocktail (1:200; Sigma Aldrich) and cleared by centrifugation (10 min, 12000 g). Resin with immobilized bait RNA was washed one time with BB supplemented with 11 μ g/ml heparin. Next, the resin was incubated with 500 μ l cell extract supplemented with 500 μ l BB, 11 μ g/ml heparin, 1 mM DTT and 400 U/ml RNasin (Promega) for 30 min. After incubation, the amylose resin was washed four times with heparin-supplemented BB. All steps, except cell lysis, were performed at room temperature under constant agitation. For protein analysis, amylose resins were incubated with 25 μ l of SDS-sample buffer supplemented with 10% β -mercaptoethanol. For miRNA isolation, protein-RNA complexes were eluted twice in 150 μ l BB supplemented with 15 mM maltose.

RNA preparation

miRNAs were purified from maltose solution by phenol-chloroform extraction. 80 μ l nuclease-free water and 3 μ l proteinase K (NEB, only inputs) was added to 280 μ l eluate and incubated for 15 minutes at 50°C. Afterwards, 80 μ l NH₄-acetat and 400 μ l phenol/chloroform/isoamyl alcohol was added and the samples were centrifuged for 15 minutes at 4°C. The upper phase was transferred to a new tube and precipitated with 1 ml 100% ethanol containing 1 μ l glycogen for 10 minutes at -20°C followed by 10 minutes centrifugation at 4°C. The supernatant was removed and the pellet washed once with 80% ethanol. The pellet was resolved in 32 μ l (input) or 8 μ l (pulldown) nuclease-free water.

3.4.11 Flow cytometry

GFP and iRFP fluorescence was measured with a MACSQuant Analyzer 9. Transfected cells were harvested, washed once with PBS and then resuspended in 1% BSA in PBST. To exclude dead cells DAPI was added to the sample automatically by the machine. Cells were gated to analyze a homogenous and single cell population. Mean fluorescence of GFP and iRFP double positive cells was analyzed. The

mean GFP fluorescence of empty GFP, GFP-MYCN 3'UTR wt and GFP-MYCN 3'UTR mut transfection was first normalized to respective empty iRFP vector co-transfection and then normalized to empty GFP with respective iRFP vector transfection.

3.5 Bioinformatic methods

3.5.1 RNA sequencing and differential expression analysis

RNA-seq library preparation and sequencing

Library preparation of human neuroblastoma tumor samples was performed on fragmented RNA, subsequently reverse transcribed using random hexamer and Superscript III (Life Technologies). Second strand synthesis was achieved using the TargetAmp kit (Epicentre) according to the instructions of the manufacturer. Final steps of library preparation, e.g. blunt end repair, adapter ligation, adapter fill-in and amplification were done as previously described (Meyer and Kircher 2010). Barcoded libraries were purified and quantified using the Library Quantification Kit - Illumina/Universal (KAPA Biosystems) according to the instructions of the manufacturer. A pool of up to 10 libraries was used for cluster generation at a concentration of 10 nM using an Illumina cBot. High-throughput sequencing of 100 bp long unstranded paired-end reads was performed with an Illumina HiScanSQ sequencer at the sequencing core facility of the IZKF (Leipzig) using version 3 chemistry and flowcell according to the instructions of the manufacturer. This resulted in around 17 million reads per sample.

For RNA-seq library preparation of transgenic mouse tumor samples, 2 µg of total RNA served as input for polyA(+)-RNA enriched and strand-specific library preparation, performed by Novogene (Hongkong). Sequencing was accomplished with an Illumina NovaSeq 6000 machine, resulting in 150 bp long stranded paired-end reads with an average of 55 million reads per sample.

Transfected BE(2)-C and KELLY cells were harvested after 72 h. RNA extraction was performed using TRIZOL according to manufacturer's protocol. polyA(+)-RNA was enriched using oligo-dT beads. RNAs are fragmented randomly by adding fragmentation buffer. Synthesis of cDNA using random hexamers primer was accomplished followed by second strand synthesis. Strand-specific double-stranded cDNA libraries were completed by size selection (250-300 bp) and PCR enrichment. Paired-end sequencing (150 bp) of three biological replicates per condition was performed on an Illumina NovaSeq 6000 platform at Novogene (Hongkong).

miRNA-seq library preparation and sequencing

Total RNA of neuroblastoma tumor samples was extracted from 30 mg of primary tumor tissue using the Qiagen AllPrep tumor protocol with miRNeasy kits (Qiagen). 500 ng of total RNA was used in the small RNA protocol with the TruSeq™ Small RNA sample prekit v2 (Illumina) according to the

instructions of the manufacturer. The barcoded libraries were size restricted between 140 and 165 bp, purified and quantified using the Library Quantification Kit - Illumina/Universal (KAPA Biosystems) according to the instructions of the manufacturer. A pool of 10 libraries was used for cluster generation at a concentration of 10 nM using an Illumina cBot. Sequencing of 51 bp was performed with an IlluminaHighScan-SQ sequencer at the sequencing core facility of the IZKF (Leipzig) using version 3 chemistry and flowcell according to the instructions of the manufacturer.

SmallRNA-seq libraries of transgenic mouse tumor samples was performed with small RNA library preparation kit after TRIZOL extraction of approximately 30 mg of tissue. Sequencing was accomplished with an Illumina NovaSeq 6000 machine, resulting in 50 bp long unstranded single-end reads with an average of 26 million reads.

Analysis of high-throughput RNA sequencing data

Demultiplexing of raw reads, adapter trimming and quality filtering were done as previously described (Stokowy *et al.* 2014). Low quality read ends as well as remaining parts of sequencing adapters were clipped off from RNA-seq, smallRNA-seq and sWGS reads using Cutadapt (human: v1.18, mouse: v2.8). Subsequently, the processed sequencing reads were aligned by HiSat2 (Kim *et al.* 2015) to the human (UCSC hg38) or mouse genome (UCSC mm39). SmallRNA-seq reads were aligned by Bowtie2 (Langmead and Salzberg 2012) to the human (UCSC hg38) or mouse genome (UCSC mm10). For sequencing reads, FeatureCounts (Liao *et al.* 2014) was used for summarizing gene-mapped reads. Ensembl GRCh38.96 (Cunningham *et al.* 2019) or GRCm39.105 (Cunningham *et al.* 2022) and miRbase 22 (Kozomara *et al.* 2019) was used as annotation basis for human and mouse samples. RNA-seq reads of transgenic mouse tumor samples was corrected for a determined batch effect using ComBat-seq from R package sva (Leek *et al.* 2012) with default parameters in full mode. Differential gene expression was determined using the R package edgeR (Robinson *et al.* 2010) utilizing trimmed mean of M-values (Robinson and Oshlack 2010) normalization. A false discovery rate (FDR) value below 0.05 was considered as threshold for the determination of differential gene expression.

Principal component analysis (PCA) on normalized fragments per kilobase of transcript per million fragments mapped (FPKM) and filtered genes with zero expression was performed by the prcomp function within the R environment. R package factoextra (<https://rpkgs.datanovia.com/factoextra/>; v1.0.7) was used for visualization of PCA results on centered and scaled data.

Copy number (CN) variations from sWGS data was determined using the R package cn.Mops (Klambauer *et al.* 2012) utilizing poisson based genome normalization followed with circular binary segmentation performed by the DNACopy algorithm (Venkatraman and Olshen 2007). The window length of the initial segmentation of the genome was set to 20 kb to allow a proper CN detection based

on the low coverage of sWGS and enable detection of small regions of CN alterations, e.g. the *MYCN* locus with around 6.46 kb.

3.5.2 Gene set enrichment analysis

Gene set enrichment analysis (Subramanian *et al.* 2005) was performed using the R package clusterProfiler (Yu *et al.* 2012) and MSigDB (Liberzon *et al.* 2011) gene sets utilizing the fgsea algorithm and setting the exponent parameter to 0 for unweighted analyses of log₂ fold-change ranked protein-coding genes from RNA-seq data. The hallmark (Liberzon *et al.* 2015), curated human (C2) and mouse (M2) gene set collection was applied with a minimum set size of 10 and no upper size restriction. To analyze the human C2 collection on mouse tissue, mouse gene symbols were homology converted to human symbols by using the R package biomaRt (Durinck *et al.* 2009).

3.5.3 Shallow whole genome sequencing

A total amount of 50 ng - 1 µg DNA per sample was used as input material for DNA sample preparation of human neuroblastoma and transgenic mouse tumor samples. Shallow whole genome sequencing (sWGS) libraries were generated using NEBNext DNA Library Prep Kit following manufacturer's recommendations and indices were added to each sample. The genomic DNA was randomly fragmented to a size of 350 bp by shearing, then DNA fragments were end polished, A-tailed, and ligated with NEBNext adapter for Illumina sequencing and further PCR enriched by P5 and indexed P7 oligonucleotides. The PCR products were purified (AMPure XP system) and resulting libraries were analyzed for size distribution by Agilent 2100 Bioanalyzer and quantified using real-time PCR. sWGS of all samples was performed on an Illumina NovaSeq 6000 at Novogene (Hongkong), resulting in 150 bp unstranded paired-end reads with a low coverage of around 0.7x comprising approximately 15 million reads per sample for mouse and human samples, respectively.

Quantitative analysis of copy number data

For copy number analysis, threshold values were set to known log₂ ratios of -0.4 and +0.3 associated with losses and gains, respectively (Gardina *et al.* 2008). Percentage plot of gains and losses was calculated on the determined fraction across all samples based on the gains and losses thus defined. Each chromosome was divided into equal bins of 1000 kb and centromere regions were excluded.

Identification of balanced and unbalanced 17q samples is based on median copy number fold-change comparing the whole 17p region (17p) with the 17q region from *IGF2BP1* locus to the terminal end (IMP1-ter). A balance value (bv) is determined on linear regression model, separating each sample into balanced or unbalanced 17q. Linear regression is defined as $bv = (-IMP1-ter + 17p + 0.2)$, resulting in unbalanced if $bv \leq 0$ and balanced if $bv > 0$. Identification of *MYCN*-amplified samples is based on

CN of the *MYCN* locus (CN > 4 as MNA). Visualization of CN changes and comparison of gain and loss regions was performed with the R package karyoploteR (Gel and Serra 2017). Genome conversion of coordinates and annotations between mouse (Jun. 2020 (GRCm39/mm39)) and human (Dec. 2013 (GRCh38/hg38)) assemblies was performed using USCS Lift Genome Annotations (<https://genome.ucsc.edu/cgi-bin/hgLiftOver>) with default parameters.

3.5.4 Kaplan-Meier survival analysis

Survival analysis were performed using TMM normalized expression data. mRNAs were expression filtered (at least 1 FPKM in sum across all samples), log₂ transformed and associated with available clinical data of the tumor cohort. Mantel-Cox log-rank test was performed with the R package survival (v3.2-11, <https://CRAN.R-project.org/package=survival>). High and low expression groups were separated by the respective median of log₂-transformed normalized expression values to investigate the influence of an altered mRNA/miRNA expression on survival. Survival analysis for IGF2BP1 expression was determined by best cut-off method. Hazardous ratios (HR) were determined by differences of Kaplan-Meier survival curves for both respective groups with p values indicate difference of survival curves. For determining the overall HR of oncogenic and tumor suppressive miRNA signatures, respectively, the log₂-transformed expression values of all oncogenic or tumor suppressive miRNAs were first median-centered, then combined and afterwards divided into high and low expression group (median cut-off). In addition, proportional Cox hazard ratios were established to assess the general effect of the expression of the observed mRNAs on survival. Multi-variate cox regression was performed using the coxph function of the R package survival (v3.4.0) via an in-house R script. Survival analysis upon *MYCN* amplification and/or 17q unbalancing was performed based on determined CN. Of 100 tumors one was lacking survival data and for three samples RNA sequencing failed, resulting in different amount of total samples depending on analysis. Survival analysis of LUAD, PAAD and LIHC TCGA datasets was performed with GEPIA2 (Tang *et al.* 2019).

3.5.5 Public data analysis

Pan-cancer loss-of-function analysis

To identify essential genes in MNA neuroblastoma, pan-cancer loss-of-function CRISPR screens of 620 cancer cell lines from different primary diseases were utilized for dependency analysis, using the Broad Institute Cancer Dependency Map (DepMap) portal (Meyers *et al.* 2017). Genetic dependency of CRISPR-Cas9 gene knockout, CCLE RNA-seq expression as well as gene level CN data were retrieved from DepMap (Hart *et al.* 2014, Blomen *et al.* 2015). 13 MNA cell lines (*MYCN* CN > 4) were selected from 46 available neuroblastoma cell lines and compared against 607 non-neuroblastoma cell lines (referred to as others). Subsequently, all available genes were filter by minimum expression (log₂

TPM > 2) in at least 11 of 13 MNA cell lines. Median dependency was calculated for remaining genes across MNA and others, filtering for essential genes in both groups by a median below -0.2 and above -0.3 for MNA and others, respectively. Following, genes not present in both groups or to be considered as common essential genes, retrieved by DepMap, were removed. For the final identification of MNA essential genes in neuroblastoma, significance in dependency changes between MNA and other cell lines were determined, performing a two-group comparison across the remaining genes by parametric empirical Bayes method provided by the Limma R package (Ritchie *et al.* 2015). A FDR value below 0.05 was considered as threshold for the determination of statistically significant essential genes in MNA neuroblastoma compared to other cancer cell lines. Genes were ranked by significance.

IGF2BP1 CLIP studies

IGF2BP1 eCLIP (enhanced crosslinking and immunoprecipitation) peak data of Hep-G2 and K-562 cells were obtained from the ENCODE portal (www.encodeproject.org; ENCODE Project Consortium, 2012; identifiers ENCF486BXN, ENCF976DBP and ENCF435MEM, ENCF701YCW, respectively). IGF2BP1 eCLIP data of human embryonic stem cells (hESCs) were obtained from the Gene Expression Omnibus (GEO; sample IDs GSM2071742 and GSM2071745). Overlap between CLIP-peaks and candidate genes was determined via an in-house R script using the annotatr package (Cavalcante and Sartor 2017). Gene annotations for hg19 are derived from the TxDb (Carlson and Maintainer 2015) and org.db (Carlson 2019) packages.

RNA modification analysis

N⁶-Methyladenosine (m⁶A) modification sites were identified using the RNA Modification Database, RMBase (Xuan *et al.* 2018). The database integrates public high-throughput modification sequencing data retrieved from the Gene Expression Omnibus (GEO), covering 13 species. Positions of m⁶A modification sites were predicted from m⁶A- or MeRIP-seq via the RMBase workflow, resulting in 477.452 human m⁶A-sites, matched to transcripts of known human RefSeq genes (UCSC hg19).

MYCN ChIP-seq analysis

MYCN ChIP-seq (chromatin immunoprecipitation sequencing) data was obtained from ChIP-Atlas database (Oki *et al.* 2018), integrating public available data from different sources, e.g. the SRA (Sequence Read Archives) in NCBI. Peak locations of MYCN ChIP sites (+/- 5 kb distance to TSS, HG38) were retrieved from peak-calling data records from 9 untreated neuroblastoma-derived cell lines (BE(2)-C, CHP-134, COG-N-415, KELLY, LA-N-5, NB-1643, NB69, NGP, SK-N-BE(2)), comprising 15 experiments (SRX1690205, SRX5662024, SRX5662025, SRX5662026, SRX6935370, SRX1690210, SRX2550934, SRX3542258, SRX6935374, SRX2550935, SRX6935376, SRX6935379, SRX1690213, SRX2550933, SRX1178181). The stated MYCN ChIP values refer to the number of experiments, indicating a peak at the observed position. Binding information of MYCN incorporated in the

IGF2BP1/MYCN-dependent regulation and diseases relevance score is based on the average MYCN binding values obtained from each of the experiments used.

Locations of E-Box sequences were determined via an in-house R script using pattern matching of the MYC/N E-Box motif (CANNTG) at investigated sequences (Murphy *et al.* 2009).

miRNA target prediction

Predicted and validated miRNA-MYCN bindings were obtained by utilizing the R-package multiMiR (Ru *et al.* 2014). Eight databases containing predicted and two databases including validated binding information were queried (prediction cutoff 20%) for targeting MYCN mRNA. If a certain miRNA-mRNA pair was obtained by at least two (predicted) and one (validated) database, it was considered as a putative interacting pair.

ADRN/MES signature

For determination of the ADRN/MES signature for mouse tissues, previously published gene sets were used (van Groningen *et al.* 2017). Human ADRN/MES gene symbols were homology converted to mouse gene symbols by using the R package biomaRt (Durinck *et al.* 2009) resulting in 471 mouse MES and 378 mouse ADRN genes instead of 485 human MES and 369 human ADRN genes, respectively.

3.6 Statistics and presentation

All experiments were performed at least in biological triplicates unless otherwise noted. For transgenic mouse experiments biological replicates are individual mice. Statistical significance was tested by parametric two-sided Student's *t*-test on equally distributed data (errors defined as standard deviation of the mean). This includes all lab-based analyses. Otherwise, a non-parametric two-sided Mann-Whitney-test was performed (error defined as standard error of the mean). This includes all tumor-related analyses. For box plots, horizontal lines demonstrate the median with upper and lower box boundaries demonstrating the 25th-75th centiles. Error bars represent the maximum and minimum. For Kaplan-Meier survival analyses, statistical significance was determined by log-ranked test. No testing for outliers was performed. Data were visualized with GraphPad Prism (v8.0.1). Heatmaps were generated with Flourish web application (<https://flourish.studio/>). Graphical figures were generated with BioRender (<https://www.biorender.com/>).

n.s., non-significant; *, $p < 0.05$; **, $p < 0.01$; ***, $p < 0.001$; ****, $p < 0.0001$.

4. Results

4.1 Genome analyses of primary neuroblastoma

The existing cohort of human neuroblastoma (Bell *et al.* 2015) was expanded to include 100 samples and subsequently re-evaluated regarding gene expression, survival outcomes and copy number gains. The assessment of chromosomal aberrations was performed using shallow whole genome sequencing (sWGS), which is a more accurate and comprehensive technique compared to the previous used PCR method. This approach confirmed the presence of common chromosomal changes, including amplification of the *MYCN* gene (MNA) and gains at chromosome 2p, 7 and 17q, as well as losses at chromosome 1p, 3, 4 and 11q (Figure 12a). In general, chromosomal gains were observed more frequently than deletions. Notably, the most prevalent aberration was the gain of chromosome 17q, detected in approximately 80% of cases, followed by complete chromosome 7 gain in 45% of cases. *MYCN* amplification was identified in roughly 20% of patients. Among the deletions, loss of chromosome 11q was the most common, occurring in approximately 25% of cases, followed by losses on chromosome 3p and 14q. Deletion within the chromosomal region 1p was less frequent, observed in only around 10% of patients. In summary, the frequencies of these gains and losses were consistent with those reported in previously published neuroblastoma cohorts (Table 22; Maris and Matthay 1999, Bown *et al.* 1999, Bown *et al.* 2001, Spitz *et al.* 2003, Stallings *et al.* 2003, Park *et al.* 2010, Kuzyk *et al.* 2015).

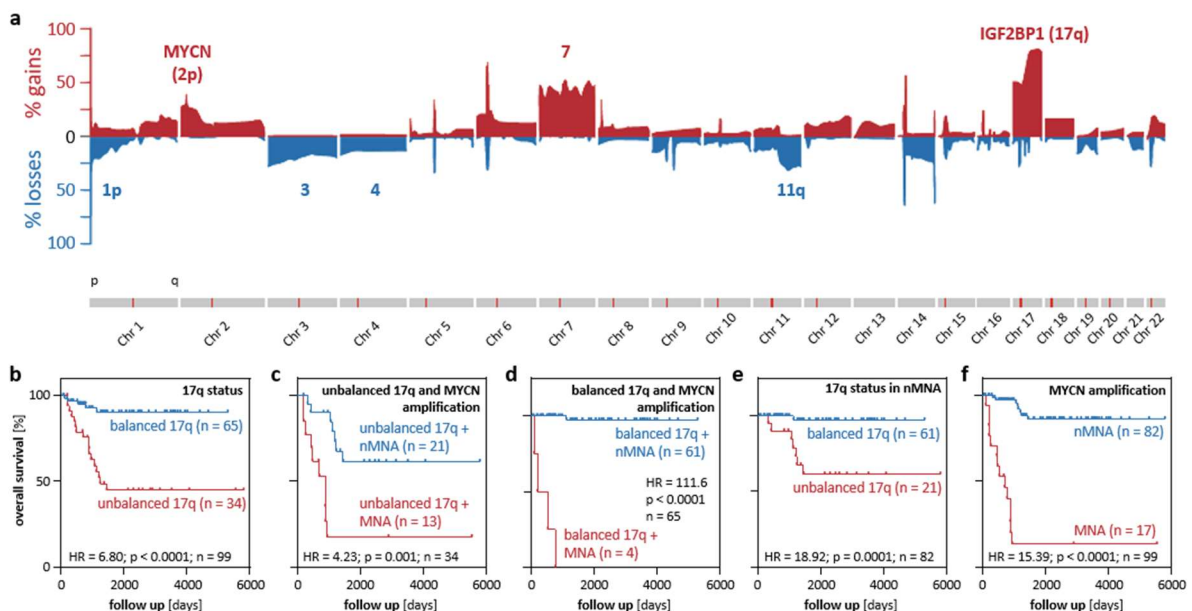


Figure 12: The genomic landscape of neuroblastoma is predictive for patient outcome. (a) Frequency (in %) of DNA copy number gains (red) and losses (blue) for chromosome 1 to 22 in 100 primary human neuroblastoma samples. **(b-f)** Kaplan-Meier survival analyses by chromosome 17q balance status (b), *MYCN* amplification status in chromosome 17q unbalanced (c) or balanced (d) tumors, chromosome 17q status in nMNA tumors (e) and *MYCN* amplification status (f). Statistical significance was determined by log-rank test.

Table 22: Frequency of chromosomal aberrations in neuroblastoma.

chromosomal region	genomic aberration	frequency	frequency literature
1p	loss	10%	30-40%
2p	gain	23%	20-35%
3p	loss	24%	18%
4p	loss	14%	20%
7	gain	44%	40%
11q	loss	27%	29-44%
14q	loss	20%	22-25%
17q	gain	79%	> 50%
unbalanced 17q	gain	35%	44-66%

Since segmental chromosomal changes are associated with more aggressive forms of neuroblastoma (Maris 2010), the most frequently observed aberration, gain of chromosome 17q, was further classified into unbalanced and balanced samples. Unbalanced 17q tumors exhibited an uneven distribution of DNA quantities from the region encompassing IGF2BP1 to the terminal end (IMP1-ter) of chromosome 17q relative to the 17p arm. The balance score was calculated as follows: $bv = (-IMP1-ter + 17p + 0.2)$ and tumors were classified as unbalanced if $bv < 0$ or balanced if $bv \geq 0$. Balanced chromosome 17 refers to the state where there is either gain of the entire chromosome or maintenance of the normal chromosomal status (Figure 13). Conversely, unbalanced chromosome 17 may arise due to loss of the short arm (17p) or gain of the long arm (17q).

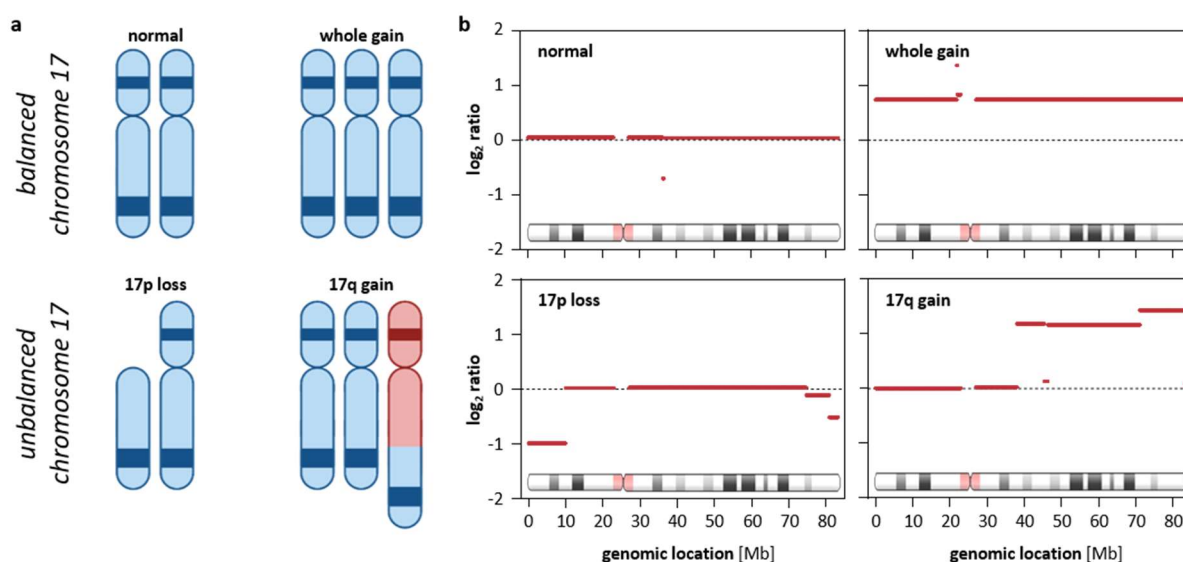


Figure 13: Unbalancing of chromosome 17. (a) Scheme of balanced and unbalanced chromosome 17 variants. **(b)** Examples of CN gain for different chromosome 17 states in neuroblastoma specimens.

Subsequent analysis revealed that patients with unbalanced 17q tumors had a lower overall survival probability compared to patients with balanced chromosome 17 (Figure 12b), confirming previous findings (Bown *et al.* 1999). The adverse prognosis of 17q unbalanced patients was further exacerbated by concurrent *MYCN* amplification, indicating a pro-oncogenic association between chromosomes 2p

and 17q (Figure 12c). Only few tumors with balanced 17q and *MYCN* amplification were observed, limiting conclusive analyses (Figure 12d). Additionally, unbalancing of chromosome 17q was also found to have prognostic value in patients without *MYCN* amplification (nMNA; Figure 12e). As expected, *MYCN* amplification had a significant impact on patient survival (Figure 12f). Furthermore, Cox multivariate analysis confirmed that both MNA (HR = 20.4, $p = 5.05e-10$) and unbalanced 17q gain (HR = 8.2, $p = 1.56e-4$) were independent predictors of poor outcome. In summary, this suggests that the analyzed tumor cohort represents the clinical and genomic characteristics of neuroblastoma and therefore, it was selected for further analyses.

4.2 Identification of essential candidate genes on chromosome 17q in neuroblastoma

To identify crucial candidate genes in neuroblastoma, publicly available pan-cancer loss-of-function CRISPR screen data were analyzed for 13 MNA neuroblastoma and 607 non-neuroblastoma cell lines using the DepMap portal (Meyers *et al.* 2017). This analysis aimed to determine the essentiality of protein-coding genes for proliferation and survival, as indicated by cell model-specific dependency scores. This revealed 177 genes (175 autosomal, 2 gonosomal) with increased essentiality in MNA neuroblastoma (Figure 14a). Among these genes were several known neuroblastoma-related genes, like *MYCN*, *PHOX2B* or *LIN28B* (Schnepf and Diskin 2016, Durbin *et al.* 2018). Notably, *MYCN*, *ISL1* and *HAND2* were the top-ranked candidates in terms of significance (Table 23). Further investigating the genomic distribution of these genes using hypergeometric testing showed that only chromosome 17 had a significantly higher number of enriched candidates than expected (Table 24). All identified chromosome 17 candidate genes, except *CHD3*, were located on the q-arm of chromosome 17, with *IGF2BP1*, *GJC1* and *MSI2* being the top-ranking genes (Table 23).

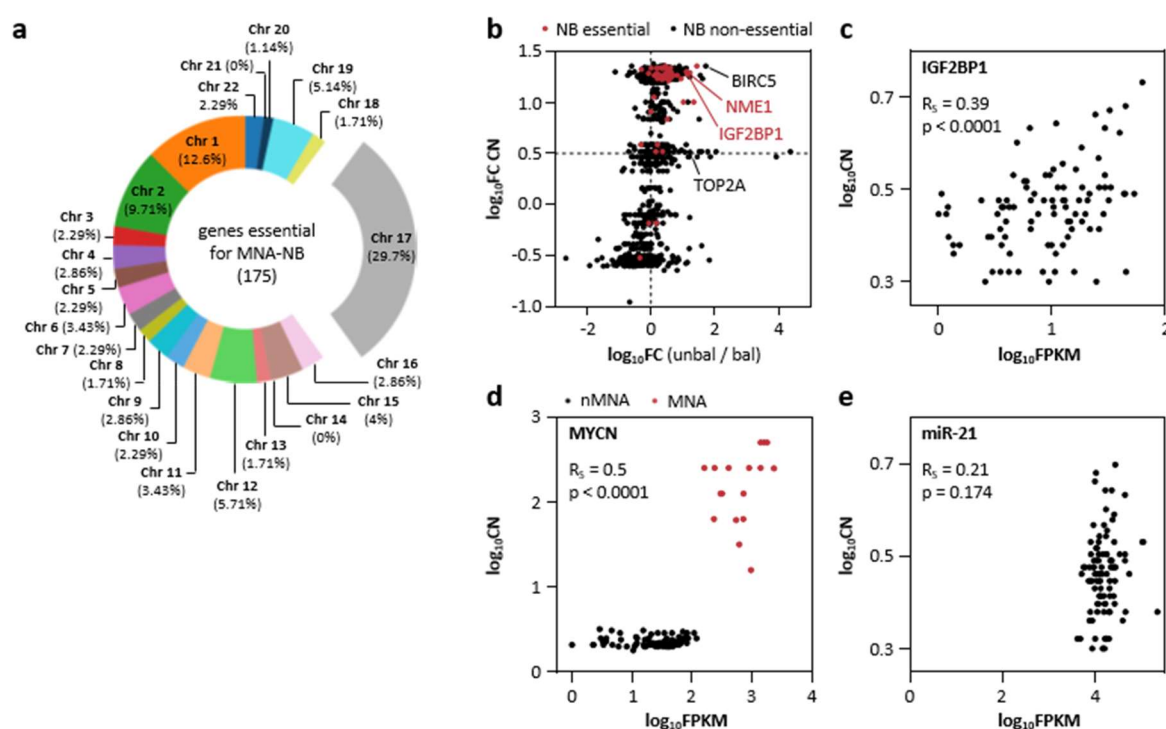


Figure 14: Chromosome 17q harbors most neuroblastoma essential genes. (a) Genomic distribution of 175 autosomal essential genes in MNA neuroblastoma. (b) Correlation of fold-changes of copy number gain (CN) and mRNA expression of chromosome 17 genes between unbalanced and balanced 17q tumors. Neuroblastoma (NB) essential genes are highlighted in red. (c-e) Correlation of copy number and mRNA expression (FPKM) of *IGF2BP1* (c), *MYCN* (d) and *miR-21* (e) in 100 primary neuroblastoma tumors. Spearman correlation coefficient and p-values are indicated.

Table 23: Top 10 essential gene candidates by significance.

MNA-NB essential genes		chromosome 17 essential genes	
gene	p-value	gene	p-value
MYCN	2.14e-36	IGF2BP1	1.78e-13
ISL1	2.25e-35	GJC1	1.20e-11
HAND2	4.66e-32	MSI2	1.24e-11
PDK1	5.91e-32	PCTP	3.92e-8
PHOX2A	6.52e-23	LIMD2	2.79e-6
PHOX2B	3.02e-20	TOM1L1	2.96e-6
SOX11	1.57e-17	AFMID	6.16e-6
LIN28B	1.04e-14	PRKCA	8.49e-6
HDAC2	1.12e-13	NT5C	3.46e-5
IGF2BP1	1.78e-13	MFSD11	3.70e-5

Table 24: Hypergeometric testing for distribution of MNA neuroblastoma essential genes.

chromosome	protein coding genes	NB essential genes	% distribution	p-value
1	2048	22	12.6%	0.2497
2	1247	17	9.7%	0.0668
3	1075	4	2.3%	0.9905
4	751	5	2.9%	0.8245
5	886	4	2.3%	0.9652
6	1047	6	3.4%	0.9239
7	917	4	2.3%	0.9716
8	683	3	1.7%	0.9528
9	781	5	2.9%	0.8493
10	731	4	2.3%	0.9076
11	1311	6	3.4%	0.9835
12	1035	10	5.7%	0.4816
13	321	3	1.7%	0.5682
14	612	0	0.0%	1
15	599	7	4.0%	0.3129
16	853	5	2.9%	0.8971
17	1188	52	29.7%	5.05E-22
18	268	3	1.7%	0.4479
19	1471	9	5.1%	0.9305
20	546	2	1.1%	0.9626
21	232	0	0.0%	1
22	444	4	2.3%	0.5853

To gain a closer understanding of chromosome 17, the fold-change in mRNA expression between unbalanced and balanced 17q tumor samples was correlated with DNA copy number gain (Figure 14b). A positive correlation was observed ($R_s = 0.6257$, $p < 0.0001$), indicating that increased DNA copy number was associated with higher mRNA expression. However, not all genes that gained DNA copies showed a corresponding increase in mRNA expression in unbalanced 17q tumors (Figure 14b). Most of

the neuroblastoma essential genes exhibited enrichment at both, the DNA and mRNA levels. Specifically, IGF2BP1 and MYCN showed a strong correlation between mRNA and copy number (Figure 14c, d). However, miR-21, a potent oncogenic miRNA that shared DNA gains with IGF2BP1, did not show an association between DNA and RNA levels (Figure 14e). This suggests that copy number gain of a single gene does not always translate to increased expression. These findings indicate that multiple processes are involved in the up- or downregulation of genes in cancer. Most importantly, however, these findings highlight the potential significance of gained genes on chromosome 17q in neuroblastoma progression, with IGF2BP1 emerging as a top candidate.

4.3 IGF2BP1 expression and prognostic significance in neuroblastoma

IGF2BP1 (17q21.32), located within the frequently gained region on chromosome 17q, has been identified as one of the most essential genes in *MYCN*-amplified neuroblastoma. Consistently, IGF2BP1 expression is an independent prognostic factor confirmed by Kaplan-Meier and Cox multi-variate analysis (Figure 15a; Cox: HR = 1.4, $p = 0.0213$). Furthermore, although often not statistically significant, IGF2BP1 exhibit prognostic value in various low- and high-risk neuroblastoma subgroups, including nMNA, unbalanced or balanced 17q gain and higher stages (Figure 15b-e). Prognostic results for low-risk subgroups such as stage 1, 2 or 4S are not available due to non-decreasing patients. Notably, IGF2BP1 lacks prognostic potential in MNA tumors, as *MYCN* alone serves as a strong predictor of patient survival (Figure 15f).

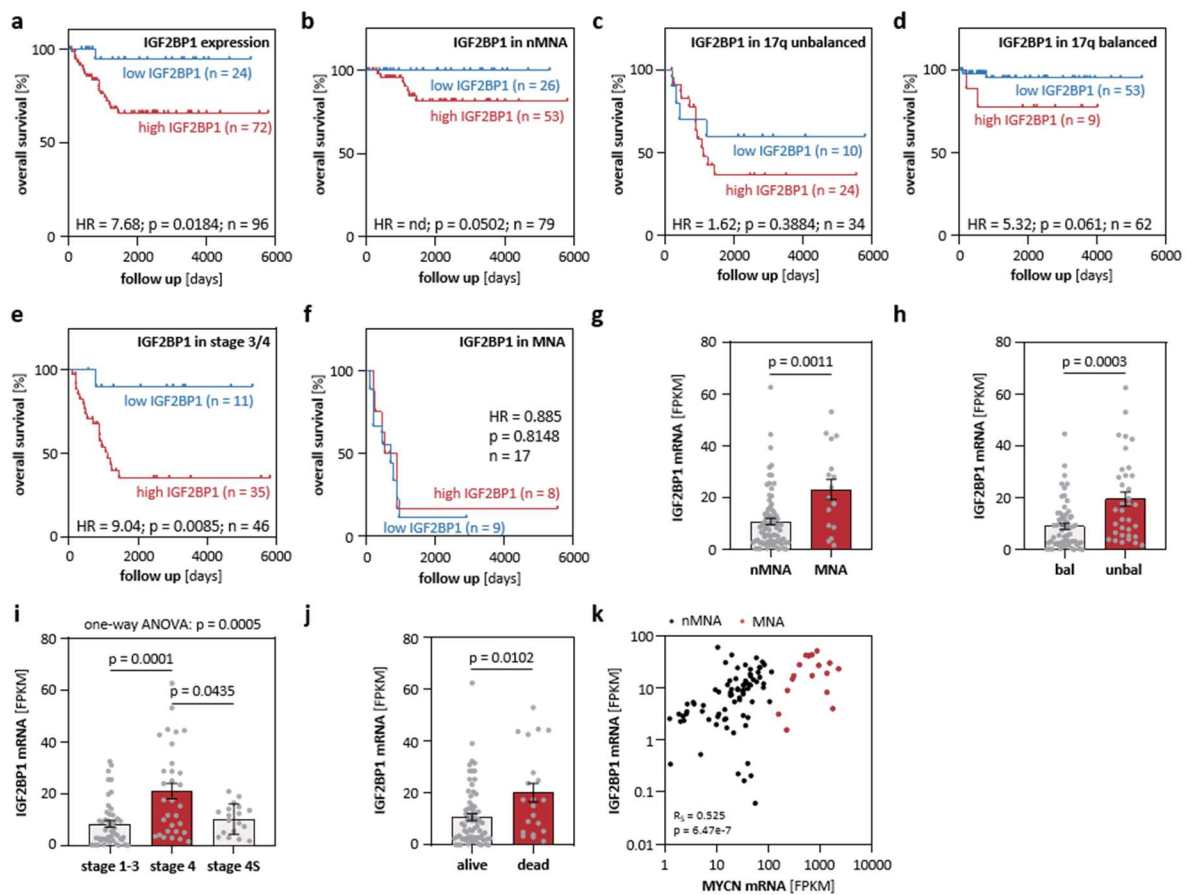


Figure 15: IGF2BP1 has prognostic relevance in different neuroblastoma subgroups, is highly expressed in aggressive neuroblastoma and correlates with MYCN abundance. (a-f) Kaplan-Meier survival analyses of IGF2BP1 expression overall (a), in nMNA (b), unbalanced (c) or balanced (d) 17q, stage 3/4 (e) and MNA (f) tumors (best cut-off). Statistical significance was determined by log-rank test. **(g-j)** IGF2BP1 mRNA expression separated by MYCN amplification status (g), chromosome 17q balance status (h), INSS stage (i) and survival (j). Statistical significance was determined by Mann-Whitney test (errors defined as SEM). Non-parametric one-way ANOVA and Kruskal-Wallis test was performed to compare all stages. **(k)** Correlation of IGF2BP1 and MYCN mRNA expression in neuroblastoma tumors. MNA samples are indicated in red. Spearman correlation coefficient and p-value is indicated.

Additionally, IGF2BP1 expression is significantly increased in MNA, unbalanced 17q, INSS-4 and deceased patients (Figure 15g-j). Furthermore, IGF2BP1 exhibits a strong correlation with MYCN at the RNA level (Figure 15k), suggesting a potential interconnected disease-driving role of both proteins in high-risk neuroblastoma. To explore this further, IGF2BP1-driven gene expression was correlated with that of all transcription factors. Best associated transcription factors were MYBL2, E2F1 and FOXM1 (Table 25). High-risk neuroblastoma is often driven by the core-regulatory circuit (CRC) of transcriptional regulators (Ciaccio *et al.* 2021). Among CRC transcription factors, MYCN was identified as the top candidate at position 35. Notably, PRRX1, a driver of mesenchymal neuroblastoma lineage identity, did not show an obvious positive correlation, supporting the notion that IGF2BP1 promotes adrenergic and aggressive neuroblastoma lineage identities. This is further supported by the negative correlation observed with the tumor-suppressive transcription factor TCF21 (Ao *et al.* 2020). In conclusion, IGF2BP1 exhibits high expression in aggressive neuroblastoma and correlates strongly with MYCN expression. Moreover, it demonstrates prognostic potential for patient stratification, even in lower risk subgroups such as nMNA or patients with balanced 17q. These findings emphasize the significance of IGF2BP1 in neuroblastoma disease progression and highlight its potential as biomarker for risk stratification, as previously shown in anaplastic thyroid carcinoma (Haase *et al.* 2021), as well as for targeted therapies.

Table 25: Selected IGF2BP1-associated transcription factors.

rank	transcription factor	R _s
1	MYBL2	0.9702
2	E2F1	0.9613
3	FOXM1	0.9586
27	TOP2A	0.9330
33	ALK	0.9282
35	MYCN*	0.9260
53	TBX2*	0.9165
609	PHOX2B*	0.8433
664	ISL1*	0.8394
929	HAND2*	0.8160
1075	GATA3*	0.8013
1675	ASCL1*	0.6498
1725	TFAP2B	0.6014
1885	PRRX1	0.0936
2520	TCF21	- 0.7902
2747	KLF5	- 0.9170

CRC transcription factors are indicated by an asterisk (*). The p value for all selected genes is < 2.2e-16.

R_s - Spearman correlation coefficient

4.4 IGF2BP1 and MYCN form a self-promoting feedforward loop

4.4.1 MYCN as a transcriptional regulator of IGF2BP1 in neuroblastoma

MYC family members play crucial roles in tumorigenesis by functioning as transcription factors that activate various oncogenes through direct binding to E-Box elements in the promoter regions. Previously studies have demonstrated that MYC promotes the synthesis of IGF2BP1 (Noubissi *et al.* 2010). Considering the similarities between MYC and MYCN (Huang and Weiss 2013), the strong association of IGF2BP1 and MYCN expression in neuroblastoma (Figure 15k) as well as the co-occurrence of chromosome 2p and 17q aberrations in neuroblastoma (Bown 2001), it was hypothesized that MYCN might also contribute to the transcriptional activation of IGF2BP1. To investigate this hypothesis, publicly available MYCN ChIP-seq data (Oki *et al.* 2018) performed in neuroblastoma cell lines were analyzed. These studies confirmed the presence of MYCN binding at the *IGF2BP1* promoter region, which encompasses several E-Box motifs (Figure 16a). Consistently, transient depletion of MYCN using siRNAs resulted in a significant reduction in both, IGF2BP1 mRNA and protein levels in two different MNA neuroblastoma cell lines (Figure 16b). Additionally, analysis of nascent transcript synthesis validated the decrease of IGF2BP1 upon MYCN depletion in BE(2)-C (Figure 16c).

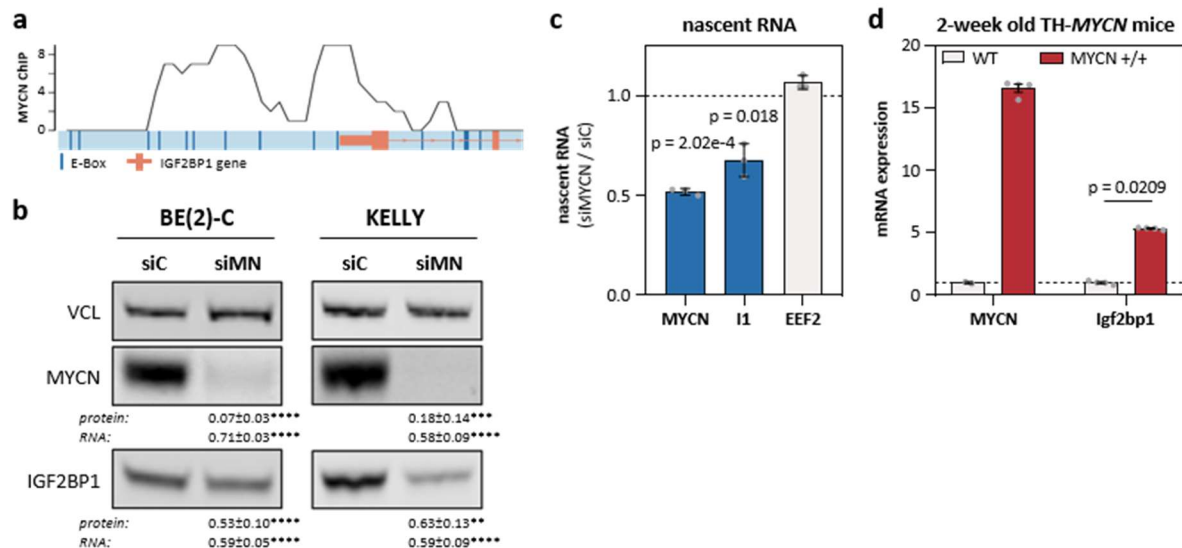


Figure 16: MYCN directly promotes IGF2BP1 transcription. (a) MYCN ChIP-seq profile of the *IGF2BP1* promoter region. E-Boxes, putative MYC/N binding sites, are indicated in dark blue. The *IGF2BP1* gene is depicted schematically in orange up to the beginning of the second intron. (b) Western blot (n = 3) and RT-qPCR (n = 3) analysis of IGF2BP1 expression upon MYCN (siMN) compared to control knockdown (siC) in two MNA neuroblastoma cell lines. (c) RT-qPCR (n = 3) analysis of indicated nascent mRNAs upon MYCN compared to control knockdown in BE(2)-C. (d) Relative expression of transgenic MYCN and endogenous *Igf2bp1* mRNA in two-week old pre-cancerous ganglia from TH-MYCN (n = 4) compared to wildtype mice. Statistical significance was determined by parametric two-sided Student's *t*-test (errors defined as SD). **, $p < 0.01$; ***, $p < 0.001$; ****, $p < 0.0001$.

Furthermore, examination of pre-cancerous ganglia derived from 2-week old TH-MYCN mice showed a significant increase in endogenous Igf2bp1 expression in comparison to wildtype mice (Figure 16d; unpublished data from Daniel Carter, Children's Cancer Institute, University of New South Wales, Sydney, Australia). Importantly, this early period is considered as the time of neuroblastoma initiation in this mouse model (Hansford *et al.* 2004). Collectively, these findings provide evidence that MYCN is a potent driver of IGF2BP1 transcription in neuroblastoma, supporting recent findings in breast cancer (Shi *et al.* 2022).

4.4.2 Deregulated miRNAs distinguishes MYCN-amplified neuroblastoma

Aiming to reveal the MYCN-dependent microRNA transcriptome, miRNA expression was evaluated in 17 MYCN-amplified versus 80 non-amplified primary neuroblastoma tumors. Differential expression analysis between these two groups identified 52 significantly up- and 66 significantly downregulated miRNAs in MNA neuroblastoma samples (FDR < 0.05; Table 30, Figure 17a). Remarkably, all upregulated miRNAs exhibited an oncogenic character, as indicated by a HR > 1, whereas all downregulated miRNAs displayed tumor-suppressive properties, with HR < 1. Kaplan-Meier survival analysis of these oncogenic and tumor-suppressive miRNA signatures confirmed that high expression of oncomiRs was associated with substantial reduction in overall survival probability, as expected (Figure 17b). Conversely, low expression of tumor suppressor miRs was correlated with a poor prognosis (Figure 17c).

Consistent with these findings, examination of miRNA expression in individual tumor samples clearly demonstrated the ability of these two miRNA signatures to distinguish between MNA and nMNA neuroblastoma (Figure 17d). Former studies indicated that MYCN-regulatory miRNAs are predominantly downregulated in MNA neuroblastoma (Beckers *et al.* 2015b). In support of this, the reported miR-542 (Schulte *et al.* 2010) and the predicted miR-488 were confirmed among tumor-suppressive miRNAs. However, contrary to expectations, the majority of previously reported MYCN-regulating miRNAs were found to be upregulated in MNA tumors. This included miR-17 (Lazarova *et al.* 1999, Samaraweera *et al.* 2017), miR-19a (Buechner and Einvik 2012), miR-15b and miR-16 (Chava *et al.* 2020). Furthermore, miR-20a and miR-93, which share the same seed sequence as miR-17, as well as members of the let-7 family (Molenaar *et al.* 2012a, Powers *et al.* 2016), which are known or expected to target MYCN mRNA, were among the upregulated miRNAs in MNA tumors. Additionally, other miRNAs from the miR-17-92 cluster family, namely miR-18a, miR-25, miR-92a and miR-92b, were significantly upregulated. This observation is consistent with the role of MYC transcription factors in promoting the expression of this miRNA cluster through direct binding to E-Box elements in the promoter (Schulte *et al.* 2008, Fuziwara and Kimura 2015). Consistent with various previous studies, upregulation of miR-9 (Ma *et al.* 2010) and miR-181a/b (Schulte *et al.* 2008) as well as downregulation

of miR-628-5p (Mestdagh *et al.* 2010, Megiorni *et al.* 2017) and miR-137-3p (Inomistova *et al.* 2016) was observed in MNA neuroblastoma. Additionally, several previously unreported miRNAs were identified (Table 30). Surprisingly, miR-34c expression was elevated in MNA tumors, despite previous studies claiming that the miR-34 family is downregulated in high-risk neuroblastoma (Wei *et al.* 2008, Mei *et al.* 2014, Galardi *et al.* 2018). In summary, these findings suggest that a variety of MYCN-targeting miRNAs, particularly the miR-17-92 cluster, are upregulated in MNA neuroblastoma. This suggests a mechanism that limit MYCN downregulation through these miRNAs.

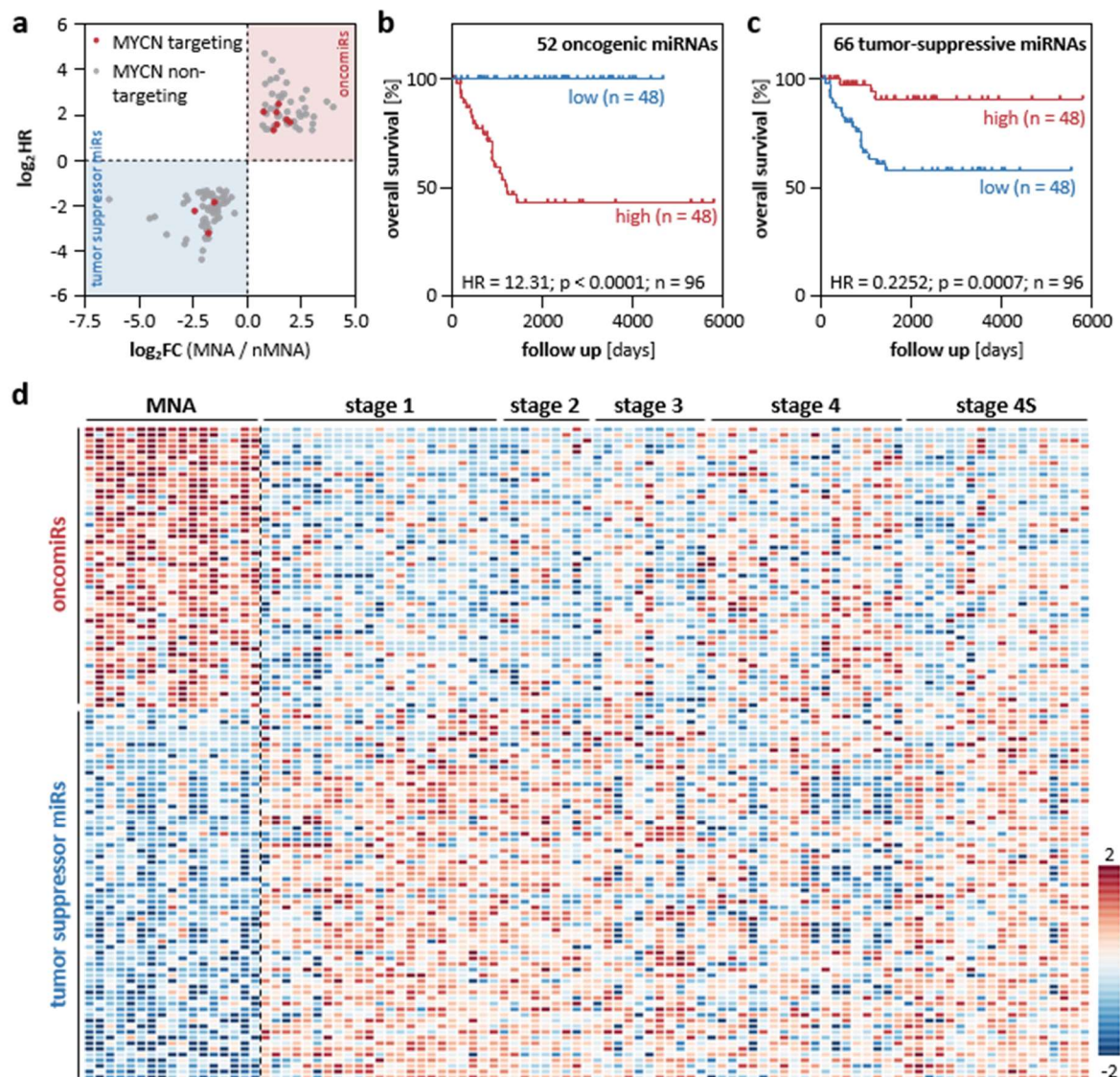


Figure 17: miRNA expression can distinguish between MNA and nMNA tumors. (a) Differential miRNA expression analysis in 17 MNA and 80 nMNA neuroblastoma tumors and subsequent determination of hazardous ratio (HR) of these miRNAs revealed 52 oncogenic and 66 tumor suppressive miRNAs. MYCN-targeting miRNAs are indicated red. (b, c) Kaplan-Meier survival analysis of upregulated (b) or downregulated (c) miRNA signatures in primary neuroblastoma tumors. Statistical significance was determined by log-rank test. (d) The 118 differential expressed miRNAs distinguish MNA and nMNA tumors. Expression values are scaled for individual miRNAs (rows in heatmap). MYCN-amplified tumors (MNA) as well as clinical staging of nMNA tumors are indicated above the heatmap.

4.4.3 Evaluation of directly associated miRNAs with MYCN using miTRAP

Contrasting results regarding the expression of MYCN-targeting miRNAs in MNA tumors as well as the need to investigate direct association of miRNAs with the MYCN mRNA prompted an evaluation of bound miRNAs by miTRAP. For pulldown of associated miRNAs, an *in vitro* transcribed MYCN 3'UTR fused to MS2 loops was used as bait in MYCN-amplified BE(2)-C neuroblastoma and MYCN-driven KNS42 glioblastoma cell lines. For conserved miRNA binding, KNS42 cells were included, as they express MYCN and high levels of let-7 miRNAs. The association of miRNAs was assessed by determining miRNA abundance through small RNA sequencing of MYCN 3'UTR and MS2 control pulldowns. Enrichment of miRNAs was calculated based on the fold-change between MYCN 3'UTR and MS2 pulldown samples. Notably, miRNA enrichment was largely independent of miRNA abundance as indicated by Spearman correlation coefficients of 0.04142 and 0.06627 for BE(2)-C and KNS42, respectively (Figure 18a). Among the top 10 enriched miRNAs in both cell lines, more than half belonged to the miR-17-92 cluster, with miR-17 being one of the most highly enriched miRNA (Table 31).

Additionally, other previously published MYCN-targeting miRNAs could be validated using miTRAP, including miR-29 (Sun *et al.* 2017) and miR-16 (Chava *et al.* 2020). Surprisingly, despite their substantial abundance in both cell lines and their reported role in regulating MYCN expression (Molenaar *et al.* 2012a, Powers *et al.* 2016), members of the let-7 family exhibited only modest enrichment with the MYCN 3'UTR compared to miRNAs of the miR-17-92 cluster (Figure 18b). Similarly, although known to regulate MYCN expression, miR-34a was not enriched with the MYCN 3'UTR, probably due to its low abundance. Furthermore, novel miRNAs potentially targeting MYCN mRNA were identified based on their substantial enrichment with the MYCN 3'UTR, including miR-193-3p and the miR-302 family, both predicted as MYCN-regulatory miRNAs, as well as miR-6782-5p and miR-1248. Comparing miRNA enrichment between the two cell lines revealed a remarkable conservation of MYCN-targeting miRNAs (Figure 18c). Furthermore, analysis of MYCN-enriched miRNAs and their altered expression in MNA neuroblastoma indicated that miRNAs of the miR-17-92 cluster stood out due to substantially increased expression in MNA neuroblastoma and enrichment in both analyzed cell lines (Figure 18d). In summary, these findings provided further evidence that MYCN-regulatory miRNAs are enriched in MNA neuroblastoma and support the idea of an alternative escape mechanism.

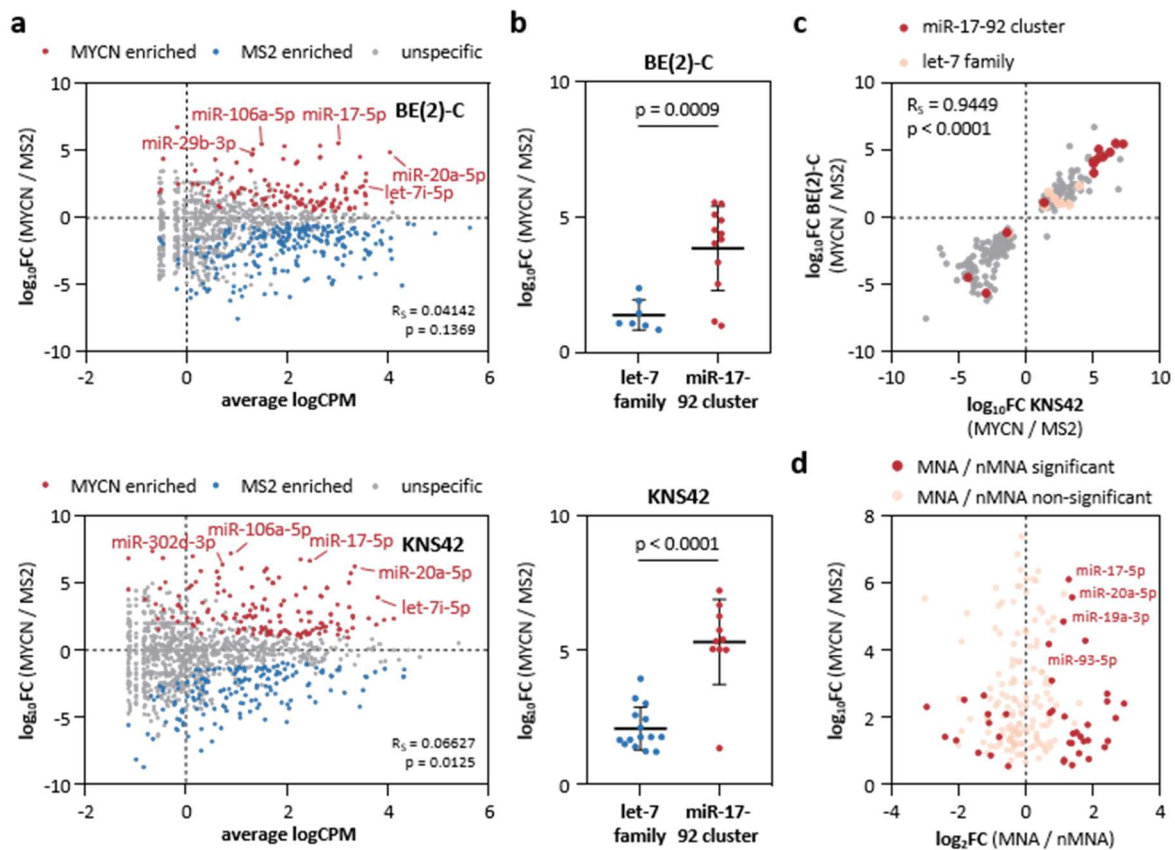


Figure 18: miTRAP identified selective co-purified miRNAs with *in vitro* transcribed bait RNA. (a) Correlation analysis of average miRNA abundances in the input and the fold-change of enrichment of miRNAs between MYCN 3' UTR and MS2 control pulldown in BE(2)-C (top) and KNS42 (bottom). Spearman correlation coefficient and p-values are indicated. (b) Enrichment of members of the let-7 family and the miR-17-92 cluster at the MYCN 3' UTR in BE(2)-C (top) and KNS42 (bottom). Statistical significance was determined by parametric two-sided Student's *t*-test (errors defined as SD). (c) Correlation of significantly enriched miRNAs in BE(2)-C and KNS42. Members of the miR-17-92 cluster and let-7 family are highlighted in dark or light red, respectively. Spearman correlation coefficient and p-value are indicated. (d) Comparison of average miRNA enrichment in both cell lines with the fold-change of these miRNAs in MNA versus nMNA neuroblastoma. miRNAs with significant deregulated expression in MNA tumors are depicted in darker color.

4.4.4 IGF2BP1 is a potent regulator of MYCN mRNA expression

To investigate the potential mechanism of uncoupling MYCN-driven expression of the miR-17-92 cluster from the inhibition of MYCN mRNA by these miRNAs in a feedback loop, a dual fluorescent reporter assay was established. This enabled the rapid assessment of altered protein expression by flow cytometry (Figure 19a, b). The assay involved GFP (green fluorescence protein) reporters comprising a control vector (= GFP, 1) and vectors in which GFP was fused to the wildtype (= wt, 2) or mutant (= mut, 3) MYCN 3' UTR. In the latter, over 90% of predicted/validated miRNA seed sequences, including those from the miR-17-92 cluster and let-7 family, among others, were mutated (Table 32). Additionally, two different iRFP reporter systems were employed: one involving the infra-red fluorescence protein (= iRFP, 1) or iRFP-fusion proteins with wildtype IGF2BP1 (= I1 wt, 2), mutant IGF2BP1 (= I1 mut, 3) or ELAVL4 (= HuD, 4) and another utilizing an iRFP-antisense reporter without a 3' UTR (5), with two miR-17 (6) or let-7a (7) binding sites. ELAVL4 was reported to interfere with a

miR-17 binding site in the MYCN 3'UTR (Lazarova *et al.* 1999, Manohar *et al.* 2002, Samaraweera *et al.* 2017). However, ELAVL4 mRNA expression is significantly downregulated in MNA and deceased patients, with a similar trend observed in stage 4 tumors and low expression is associated with poor overall survival probability (Figure 20). On the other hand, IGF2BP1 is associated with high-risk neuroblastoma and MYCN expression (Bell *et al.* 2015, Bell *et al.* 2020). Moreover, the main and conserved role of IGF2BP1 in cancer cells is the impairment of miRNA-directed mRNA degradation (Bell *et al.* 2013, Busch *et al.* 2016, Müller *et al.* 2018, Glaß *et al.* 2021), highlighting IGF2BP1 as a promising candidate for regulating MYCN expression at the post-transcriptional level. Investigation of GFP-tagged MYCN 3'UTR demonstrated significant downregulation of the wt 3'UTR reporter compared to the GFP control (Figure 19c), indicating the pivotal role of the MYCN 3'UTR in controlling MYCN expression. Notably, inactivation of eight miRNA seed regions resulted in a significant increase in GFP expression but failed to restore the expression to control levels. This suggests that miRNA-dependent regulation contributes to the 3'UTR-dependent regulation of MYCN expression. However, other regulatory elements (AU/GU-rich elements, other miRNAs), translation initiation or secondary structures also have an effect on mRNA expression, possibly affected by the introduced mutations.

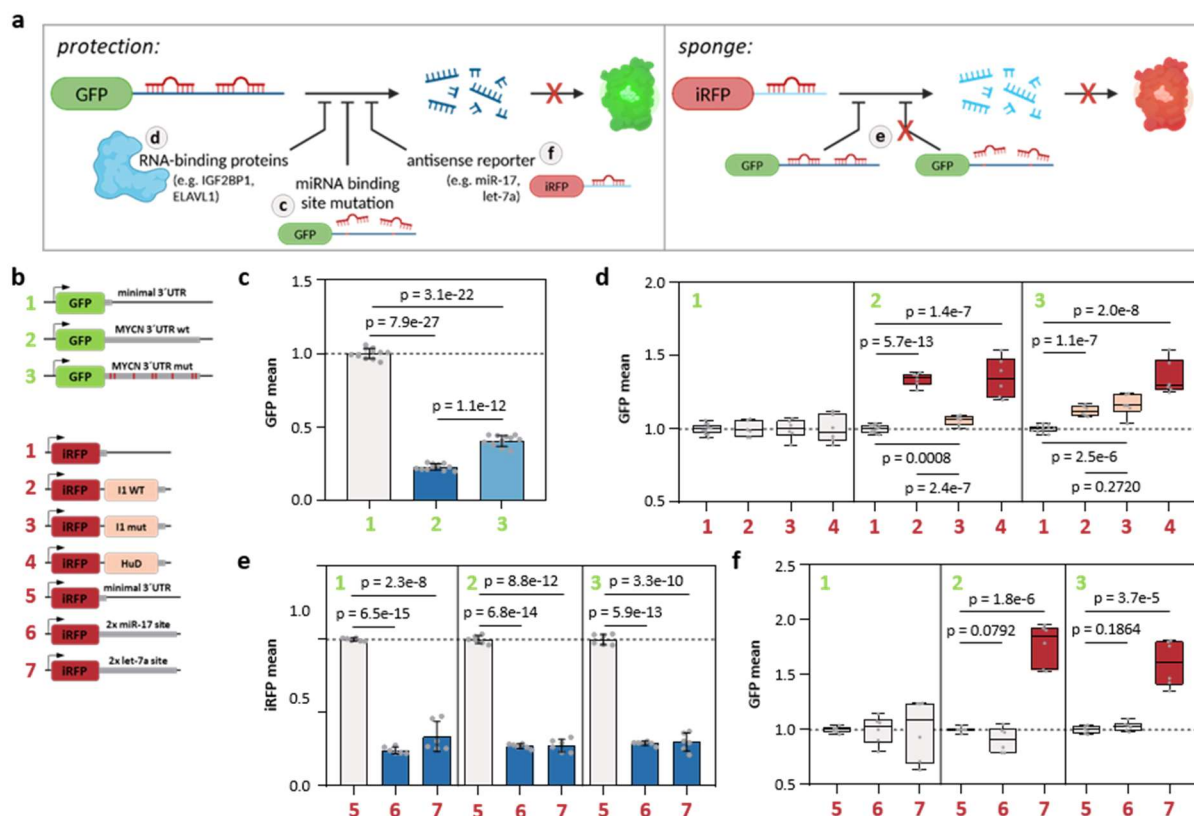


Figure 19: IGF2BP1 and ELAVL4 are potent regulators of MYCN expression. (a, b) Scheme of the assay (a) and used GFP and iRFP reporters (b). Control (1, 5) and iRFP-fusion (1-4) reporter contained only a minimal, vector-encoded 3'UTR. (c) Normalized mean GFP fluorescence in BE(2)-C cells transiently transfected with GFP reporter (n = 3). (d-f) Normalized mean GFP (d, f) or iRFP (e) fluorescence after co-transfection of indicated GFP and iRFP reporter in BE(2)-C cells (n = 3). Statistical significance was determined by parametric two-sided Student's *t*-test (errors defined as SD).

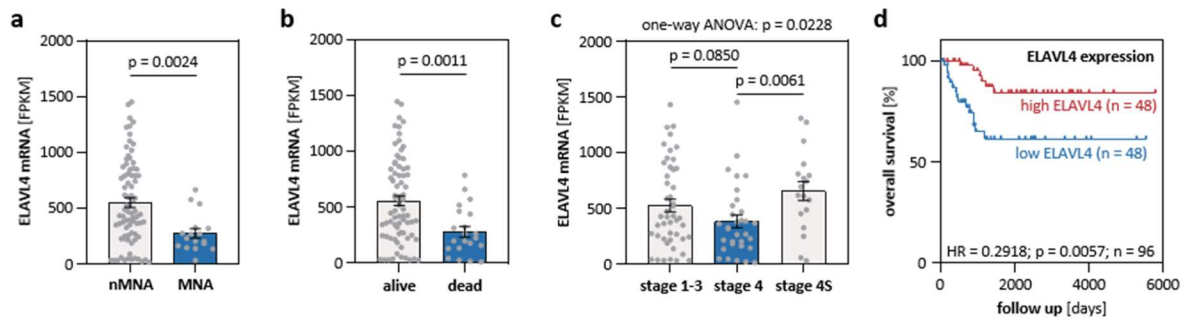


Figure 20: ELAVL4 is downregulated in aggressive neuroblastoma subtypes. (a-c) ELAVL4 mRNA expression separated by MYCN amplification status (a), survival (b) and INSS stage (c). Statistical significance was determined by Mann-Whitney test (errors defined as SEM). Non-parametric one-way ANOVA and Kruskal-Wallis test was performed to compare all stages. (d) Kaplan-Meier survival analysis of ELAVL4 expression (median cut-off). Statistical significance was determined by log-rank test.

When co-expressing iRFP-fused RNA-binding proteins with the GFP control reporter, the mean GFP fluorescence was largely unaffected (Figure 19d, left panel). In contrast, GFP fluorescence was markedly increased when co-expressing wildtype IGF2BP1 or ELAVL4 with the GFP-tagged MYCN 3'UTR. Interestingly, only a modest increase was observed with the RNA-binding mutant of IGF2BP1 (Figure 19d, middle panel), indicating that both, IGF2BP1 and ELAVL4, promote MYCN expression, as previously proposed, and that this regulation largely relies on the MYCN 3'UTR. Analysis of the mutant GFP-tagged MYCN 3'UTR showed that both IGF2BP1 proteins modestly elevated the GFP fluorescence (Figure 19d, right panel). More importantly, no difference was observed between wildtype and mutant IGF2BP1, suggesting secondary, RNA-binding independent regulation. Surprisingly, co-expression of ELAVL4 still resulted in an increase in GFP fluorescence, indicating that ELAVL4 potentially regulate MYCN mRNA either by impairing other miRNAs or through largely miRNA-independent mechanisms, such as stimulation of translation. In conclusion, IGF2BP1 emerges as a potent miRNA-dependent regulator of MYCN expression, which could contribute to the uncoupling of elevated miRNA and MYCN expression. Furthermore, the miTRAP analysis revealed a strong effect of miR-17-92 miRNAs and potential involvement of the let-7 family in the regulation of MYCN mRNA in neuroblastoma. To investigate the proposed function of the MYCN 3'UTR as a miRNA sponge (Powers *et al.* 2016), iRFP-fused miR-17 and let-7a antisense reporters were analyzed. Evaluation of iRFP fluorescence demonstrated substantial activity of miR-17 and let-7a in BE(2)-C cells (Figure 19e, left panel). Notably, when co-expressing wt or mut GFP-tagged MYCN 3'UTR, the activity of the antisense reporter remained largely unaffected (Figure 19e, middle and right panel), strongly arguing against a miRNA sponge effect of the MYCN 3'UTR. Next, GFP fluorescence was assessed in the presence of the iRFP-antisense reporter. The activity of the control GFP reporter remained largely unaffected by antisense reporter (Figure 19f, left panel). Analysis of the wt and mut GFP-tagged MYCN 3'UTR revealed differences between miR-17 and let-7a antisense reporters. While the GFP reporters were unaffected by miR-17 antisense reporter, both, the wt and mut GFP-tagged MYCN 3'UTR, showed significantly

elevated expression upon co-expression of the let-7a antisense reporter, despite all reported let-7 binding sites being mutated (Figure 19f, middle and right panel). This suggests that let-7 dependent regulation of MYCN expression is largely secondary. An explanation could be the upregulation of let-7 target genes, e.g. IGF2BP1 and ELAVL1 among others, due to the transfected antisense reporter, which would lead to an increased mRNA stability.

4.4.5 IGF2BP1 directly binds MYCN mRNA in a 3'UTR- and miRNA-dependent manner

To investigate whether IGF2BP1 directly binds to the MYCN mRNA, two different analyses were conducted. Firstly, the miTRAP experiment was employed to examine co-purified proteins on the MS2-fused MYCN 3'UTR. Robust co-purification of the RISC protein AGO2, supporting the miRNA-dependent regulation of MYCN, and IGF2BP1 was observed in both cell lines analyzed, while VCL was not co-purified. No co-purification of these proteins occurred using the MS2 bait control 3'UTR (Figure 21a).

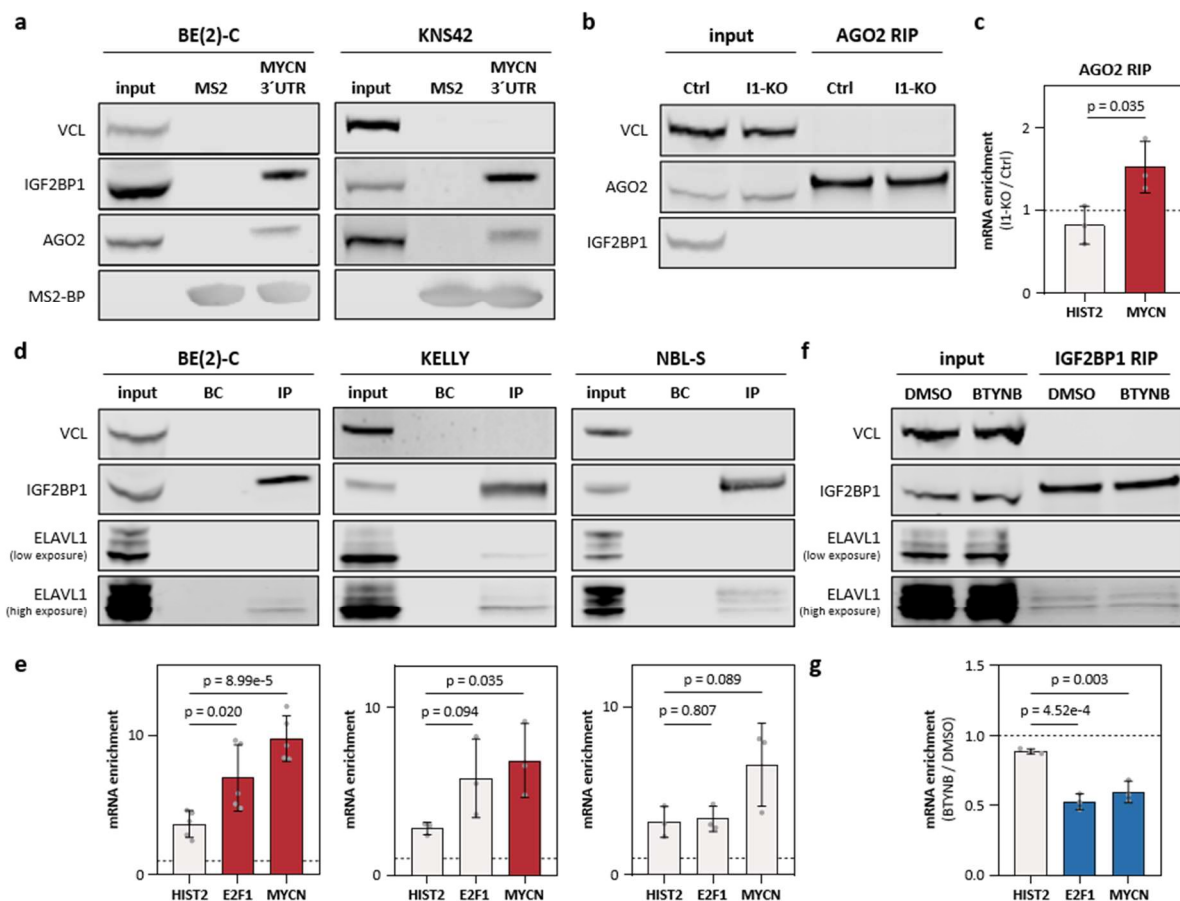


Figure 21: IGF2BP1 directly binds the MYCN mRNA. (a) Western blot analysis (n = 1) after miTRAP of indicated proteins isolated from BE(2)-C and KNS42 lysate co-purified with MS2 control transcript or the MS2-fused MYCN 3'UTR, respectively. VCL served as negative control for unspecific binding, whereas MS2-BP indicates equal loading of the resin. (b) Western blot analysis (n = 3) of indicated proteins after AGO2 RIP in control (Ctrl) and IGF2BP1 knockout (I1-KO) BE(2)-C cells. (c) RT-qPCR analysis after AGO2 RIP in IGF2BP1 knockout versus control BE(2)-C cells (n = 3). (d, e) Western blot (d) and RT-qPCR (e) analysis after IGF2BP1 RIP in indicated parental neuroblastoma cell lines (n = 3-5). (f, g) Western blot (f) and RT-qPCR (g) analysis after IGF2BP1 RIP in BE(2)-C treated with DMSO or 5 μ M BTYNB for 6 h (n = 3). Statistical significance was determined by parametric two-sided Student's *t*-test (errors defined as SD).

Additionally, to determine if the potential IGF2BP1-dependent regulation of MYCN mRNA is miRNA-dependent, AGO2-RIP was performed. IGF2BP1 knockout significantly increased the association of AGO2 with the MYCN mRNA (Figure 21b, c). Secondly, IGF2BP1-RIP was conducted in three different neuroblastoma cell lines (Figure 21d). These experiments confirmed a pronounced association of IGF2BP1 with the validated target mRNA E2F1 and the MYCN transcript (Figure 21e). Co-purification of ELAVL1 confirmed the isolation of intact mRNPs. Significance was observed for MYCN mRNA in the MNA cell lines BE(2)-C and KELLY as well as for E2F1 in BE(2)-C cells. Other enrichments did not reach statistical significance, but showed trends as expected, except for E2F1 in NBL-S cells. HIST2 served as negative control of unspecific binding. To further investigate the potential of IGF2BP1 to bind the MYCN mRNA, the small molecule inhibitor BTYNB was used, which can disrupt the association of IGF2BP1 with its target mRNAs. IGF2BP1-RIP under BTYNB treatment in BE(2)-C cells showed significant less enrichment of E2F1 and MYCN mRNA with IGF2BP1 (Figure 21f, g). Therefore, exposure of BTYNB effectively disturbed the association of MYCN mRNA with IGF2BP1, supporting previous findings that IGF2BP1 can directly bind the MYCN mRNA. To further analyze these findings, luciferase reporters lacking a native 3'UTR (control) and containing the wildtype (wt) or mutated (mut) MYCN 3'UTR were utilized. In the latter, several miRNA binding sites were inactivated by mutation (Table 32). The activity of the wt reporter was consistently reduced, confirming the conserved miRNA-dependent regulation of the MYCN 3'UTR (Figure 22a). Mutation of several miRNA binding sites led to a significant, although incomplete, increase in luciferase activity in all cell models (Figure 22a-c). Both, IGF2BP1 knockout and BTYNB treatment, further decreased the activity of the wt reporter in three different neuroblastoma cell lines, while the mut reporter remained unaffected (Figure 22a, b, d, e). These findings indicate that IGF2BP1 regulates the MYCN mRNA in a 3'UTR- and miRNA-dependent manner and that BTYNB can selectively disrupt this miRNA-dependent regulation of MYCN by IGF2BP1.

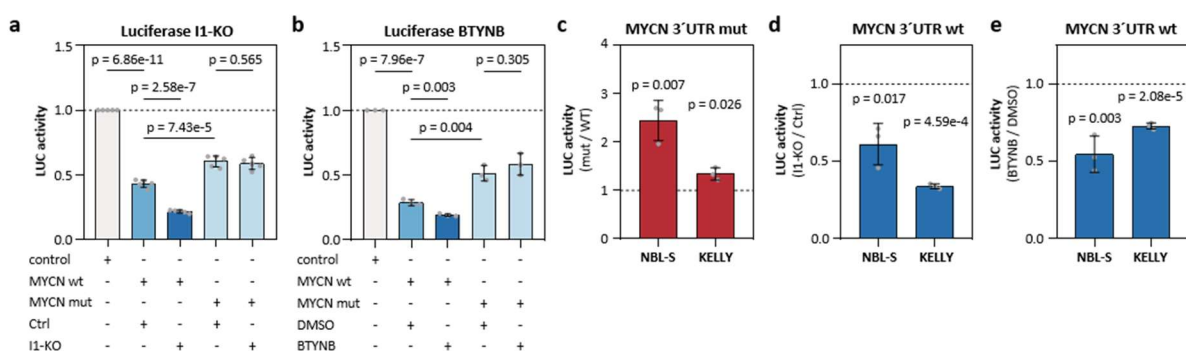


Figure 22: IGF2BP1 stimulated MYCN expression is miRNA-dependent. (a) Expression of miRNAs in BE(2)-C and mutated fraction of MYCN-targeting miRNA-binding sites (left). A scheme of the luciferase reporter constructs is shown on the right site. (b, c) Activity of indicated luciferase reporter in control and IGF2BP1 knockout (b, n = 5) or DMSO- and BTYNB-treated (c, n = 3) BE(2)-C. (d-f) Activity of MYCN 3'UTR luciferase reporter in NBL-S and KELLY determined between mutant and wildtype MYCN 3'UTR (d), IGF2BP1 knockout and control cells (e) or BTYNB- and DMSO-treated (f) cells (n = 3). Statistical significance was determined by parametric two-sided Student's *t*-test (errors defined as SD).

4.4.6 IGF2BP1 stabilizes the MYCN mRNA, which is targetable by BTYNB

Previous studies have reported the involvement of IGF2BP1 in modulating MYCN expression in neuroblastoma (Bell *et al.* 2015), but the underlying mechanisms remain unclear. CLIP studies in hESCs indicated the association of IGF2BP1 with the MYCN 3'UTR as well as the last exon (Figure 23a), which was confirmed in this study through pulldown and luciferase assays (Figure 21, Figure 22). Deletion or depletion of IGF2BP1 consistently reduced MYCN protein and mRNA levels in three neuroblastoma cell lines (Figure 23b, c). It should be noted that in KELLY cells, the IGF2BP1 knockout was incomplete due to an alternative start codon producing a smaller variant of IGF2BP1. Nevertheless, IGF2BP1 expression was significantly decreased and MYCN levels were affected similarly to other knockout cell lines. The main role of IGF2BP1 in cancer is to impair miRNA-directed downregulation of mostly oncogenic mRNAs. Consistent with this, IGF2BP1 knockout in BE(2)-C cells significantly decreased MYCN mRNA half-life (Figure 23d).

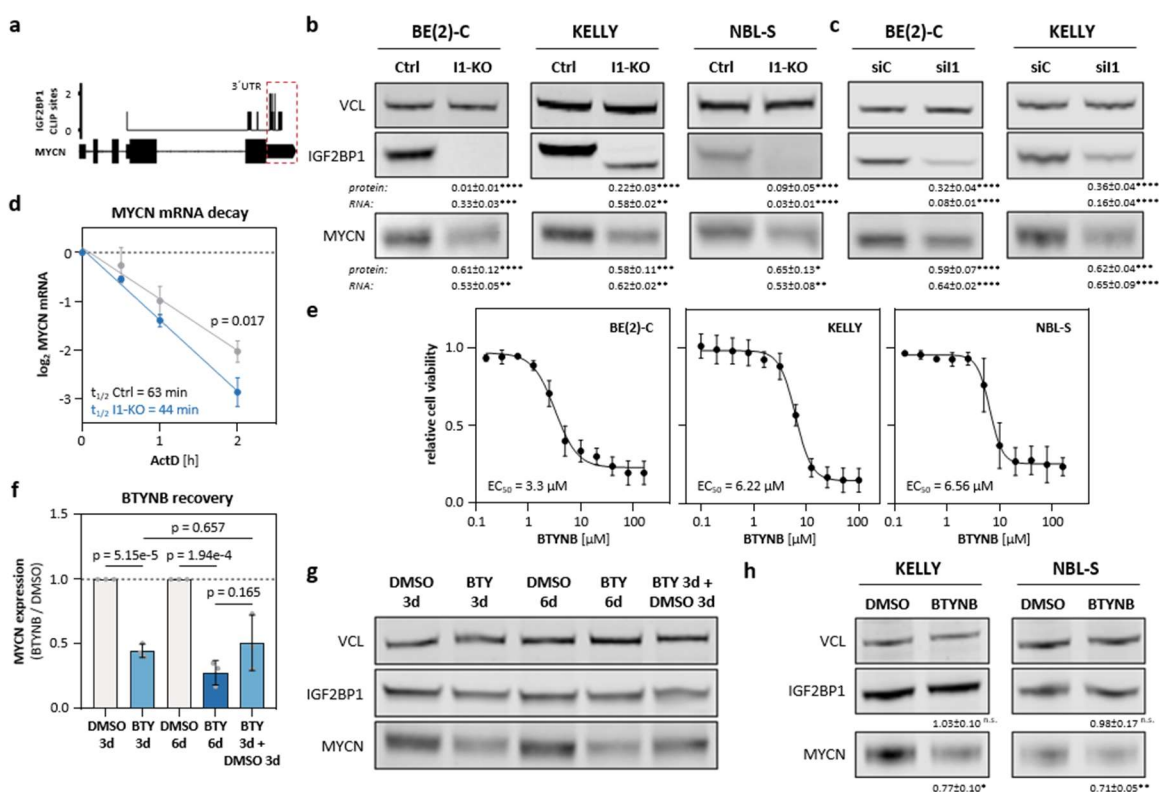


Figure 23: BTYNB disrupts IGF2BP1 stabilization of MYCN mRNA. (a) IGF2BP1 CLIP hits in the MYCN mRNA derived from two studies in hESCs. (b, c) Western blot and RT-qPCR analysis of MYCN expression upon IGF2BP1 knockout (b) or depletion (c) in indicated cell lines ($n = 3$). (d) MYCN mRNA decay monitored by RT-qPCR in control (grey) and IGF2BP1-deleted (blue) BE(2)-C cells upon indicated time of Actinomycin D (ActD) treatment ($n = 3$). (e) BTYNB response curve in indicated cell lines ($n = 3$). (f, g) Western blot analysis (g) and quantification (f) of MYCN expression in BE(2)-C treated with 3 μ M BTYNB (BTY, $n = 3$) for 3 and 6 days or replacement of BTYNB by DMSO after 3 day treatment. Quantification and significance are blotted in panel f. (h) Western blot analysis of MYCN expression upon treatment with 5 μ M BTYNB in indicated cell lines ($n = 3$). Statistical significance was determined by parametric two-sided Student's t -test (errors defined as SD).

Recently, different small molecule inhibitors were published for IGF2BP1, which disturb the association with its target mRNAs. To test the effect of BTYNB, the first identified IGF2BP1 inhibitor (Mahapatra et al. 2017), EC₅₀ values were evaluated in three neuroblastoma cell lines (Figure 23e). The EC₅₀ values ranged from approximately 3 to 6 μ M, which is within the expected range observed in other carcinoma-derived cell lines. Treatment with BTYNB not only reduced cell viability, but also decreased MYCN protein expression in all three cell lines without causing dramatic changes in IGF2BP1 levels (Figure 23f-h). Prolonged treatment for six days further decreased MYCN expression (Figure 23f, g). Importantly, upon compound withdrawal and subsequent incubation without treatment, MYCN protein levels recovered, indicating the reversible impairment of IGF2BP1-stimulated expression of MYCN by BTYNB (Figure 23f, g).

4.4.7 Regulation of MYCN by IGF2BP1 is rather m⁶A-independent

The stabilization of certain target mRNAs, such as MYC or E2F1 (Müller *et al.* 2020), by IGF2BP1 is known to be enhanced by m⁶A-modification mediated by the METTL3/METTL14 methyltransferase complex. Analysis of RMBase data revealed strong m⁶A-modification of the MYCN mRNA (Xuan *et al.* 2018). Aiming to reveal the role of METTL3 and METTL14 in modulating MYCN expression, co-depletion of these mRNAs was performed in two neuroblastoma cell lines. The co-depletion of METTL3 and METTL14 resulted in a significant reduction of E2F1 protein and mRNA levels, whereas the abundance of IGF2BP1 remained unchanged, as previously reported (Müller *et al.* 2020). However, MYCN protein and mRNA expression remained largely unaffected by METTL3/14 depletion, suggesting that IGF2BP1 promotes MYCN expression in an m⁶A-independent manner (Figure 24b).

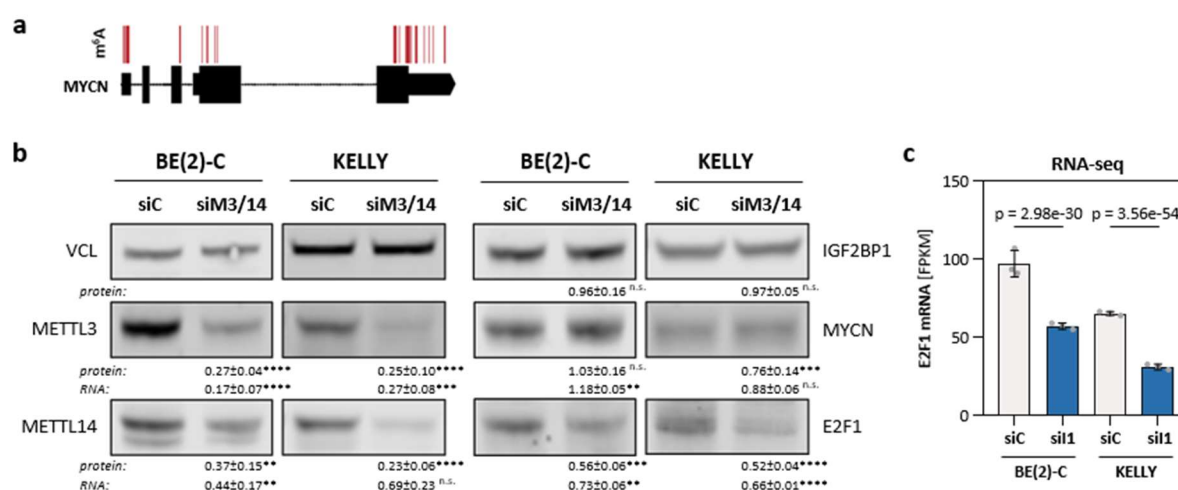


Figure 24: Regulation of MYCN by IGF2BP1 is largely m⁶A-independent. (a) N⁶-Methyladenosine (m⁶A) modification profile of MYCN mRNA derived from RMBase. (b) Western blot and RT-qPCR analyses of MYCN expression upon co-depletion of the key mRNA m⁶A-methyltransferase complex METTL3/14 (siM3/14) compared to control knockdown (siC; n = 3-4). Statistical significance was determined by parametric two-sided Student's *t*-test (errors defined as SD). n. s., non-significant; **, p < 0.01; ***, p < 0.001; ****, p < 0.0001 (c) RNA-seq data of E2F1 expression in BE(2)-C and KELLY cells upon transient control (siC) and IGF2BP1 (sil1) knockdown (n = 3).

All these findings indicate that IGF2BP1 and MYCN exhibit a self-promoting feedforward loop in tumorigenesis. As MYCN-targeting miRNAs are upregulated in high-risk neuroblastoma, tumor cells require mechanisms to evade miRNA-mediated downregulation of MYCN. RNA-binding proteins serve as protective shields, safeguarding oncogenic mRNAs from degradation. In cancer, IGF2BP1 plays a pivotal role by inhibiting miRNA-dependent mRNA degradation. The findings of this study indicate that IGF2BP1 directly bind to the MYCN mRNA, thereby enhancing its stability and leading to increased MYCN protein expression. Notably, this regulation is susceptible to targeting by the small molecular inhibitor BTYNB, which disrupts the binding of IGF2BP1 to its mRNA targets. Unlike some other reported IGF2BP1 targets, MYCN appears to be regulated in an m⁶A-independent manner. Furthermore, MYCN can directly stimulate the expression of IGF2BP1 at the transcriptional level by binding to E-Box elements in the promoter region. This establishes a transcriptional/post-transcriptional regulatory loop between IGF2BP1 and MYCN, uncoupling MYCN expression from miRNA-dependent degradation. Consequently, this regulatory loop has the potential to drive more aggressive disease phenotypes.

4.5 Impairment of IGF2BP1 expression reduces neuroblastoma growth *in vitro* and *in vivo*

4.5.1 IGF2BP1 enhances cell proliferation, viability and self-renewal capacity

The emerging role of IGF2BP1 as a key regulator of MYCN expression in neuroblastoma prompted further investigation of its impact on neuroblastoma growth. Various 2D and 3D cell culture assays were conducted to assess the effects of IGF2BP1 on neuroblastoma cell behavior. IGF2BP1 knockout in BE(2)-C significantly reduced 2D growth, as evidenced by a decreased cell proliferation rate and increased doubling time (dt; Figure 25a). Furthermore, spheroid formation was impaired upon IGF2BP1 deletion in two neuroblastoma cell lines (Figure 25b). Notably, IGF2BP1 deletion resulted in decreased spheroid viability and a slightly increase in caspase 3/7 activity (Figure 25c). Growth curve analysis of IGF2BP1 knockout spheroids compared to control cells revealed no striking difference, possibly due to larger and more diffuse spheroids under depletion condition (Figure 25d). Moreover, both knockout cell lines, BE(2)-C and NBL-S, exhibited reduced viability and slightly increased apoptosis under conditions of nutrient deprivation and anchorage independent growth (Figure 25e, f). Remarkably, the findings obtained with IGF2BP1 depletion were consistent with the effects observed upon treatment with the IGF2BP1 inhibitor BTYNB. Spheroid treated with BTYNB displayed reduced size, decreased viability and slower growth compared to control cells treated with DMSO (Figure 25g-i).

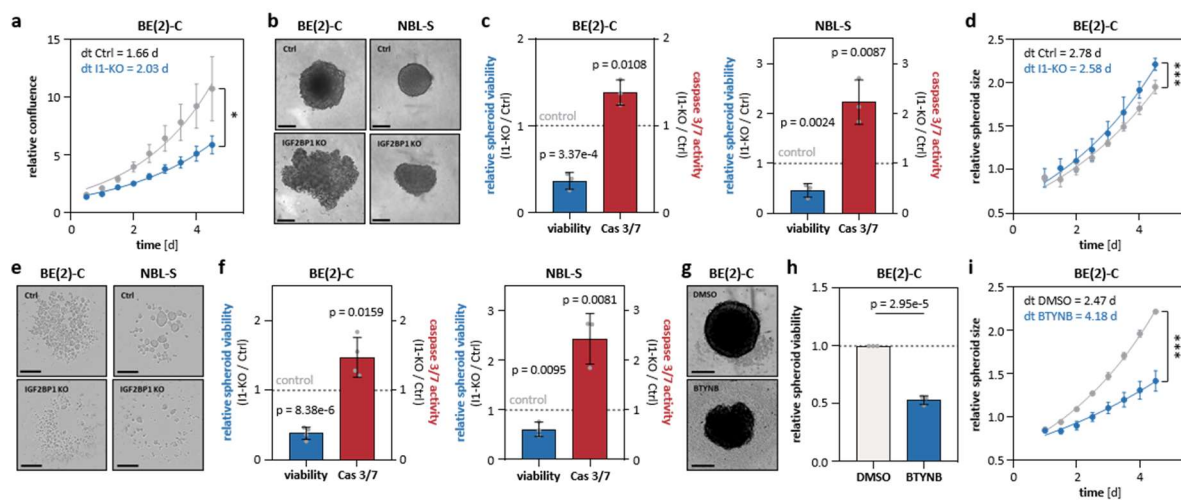


Figure 25: Impairment of IGF2BP1 reduced neuroblastoma growth *in vitro*. (a) Growth curve analysis of control (grey) and IGF2BP1 knockout (blue) BE(2)-C under 2D cell culture conditions (n = 3). (b-d) Representative spheroid pictures (b, bars 200 μm), analysis of viability and caspase 3/7 activity (c, n = 3) and growth curve analysis (d, n = 6) of control (grey) and IGF2BP1 knockout (blue) spheroids. (e, f) Representative pictures (e, bars 400 μm) and analysis of viability and caspase 3/7 activity after anoikis resistance assay in IGF2BP1 knockout compared to control cells (f, n = 3-4). (g-i) Representative spheroid pictures (g, bars 200 μm), analysis of viability (h, n = 6) and growth curve analysis (i, n = 6) of DMSO- (grey) and BTYNB-treated (blue) spheroids. Statistical significance was determined by parametric two-sided Student's *t*-test (errors defined as SD).

4.5.2 IGF2BP1 promotes neuroblastoma xenograft growth

To evaluate the oncogenic capacity of IGF2BP1 in neuroblastoma, xenograft models were employed using IGF2BP1 knockout BE(2)-C or NBL-S cells injected into immunocompromised athymic nude mice. Tumor growth was monitored using non-invasive infra-red imaging and measurement of tumor volume (Figure 26a). IGF2BP1 knockout resulted in impaired tumor cell engraftment and a significant delay in tumor growth by approximately 5 to 7 days (Figure 26b). Moreover, IGF2BP1-deleted tumors exhibited reduced tumor mass and MYCN expression (Figure 26c, d), providing further evidence of IGF2BP1's role in neuroblastoma progression *in vivo*.

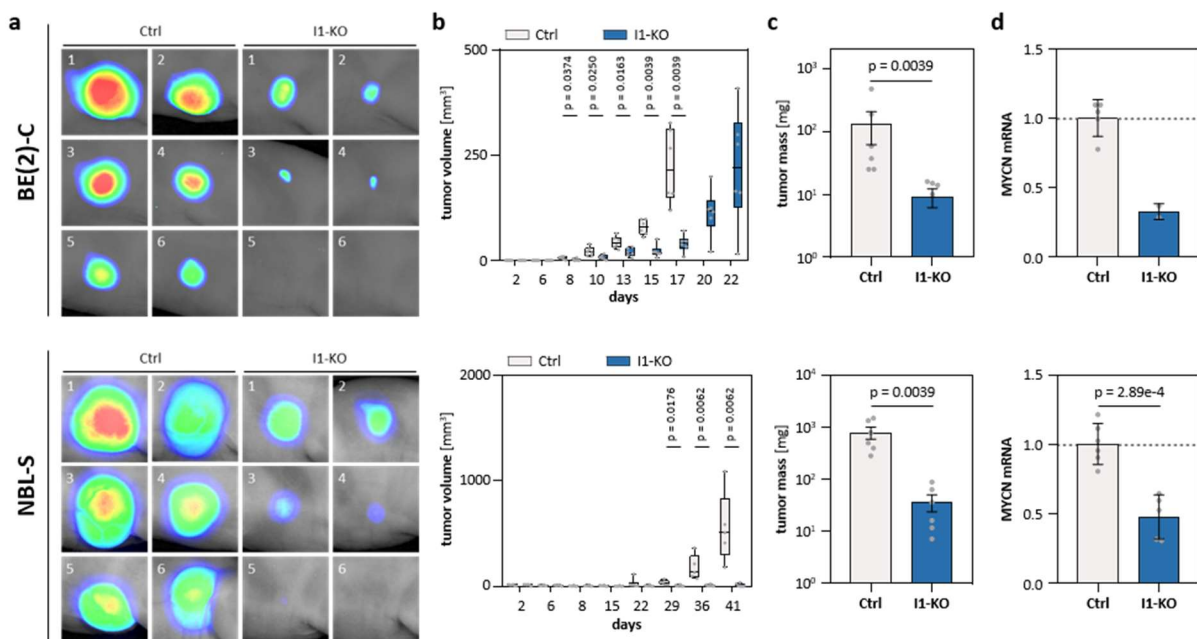


Figure 26: IGF2BP1 knockout impaired neuroblastoma xenograft growth. (a-c) Tumor growth (n = 6) of control (grey) and IGF2BP1 knockout (blue) subcutaneous xenografts was monitored by non-invasive infra-red imaging (a), tumor volume over time (b) and final tumor mass (c). (d) RT-qPCR analysis of MYCN mRNA levels in excised xenograft tumors and non-palpable tumor cell mass (control, n = 6; IGF2BP1 knockout, n = 2-5). Statistical significance was determined by non-parametric two-sided Mann-Whitney test (errors defined as SEM).

To assess the *in vivo* activity of the IGF2BP1 inhibitor BTYNB, BE(2)-C cells were pre-treated with BTYNB prior to xenograft tumor formation. This pre-treatment resulted in similar delayed growth of xenograft tumors (Figure 27a). Additionally, a patient-derived xenograft (PDX) neuroblastoma model (EPO company Berlin; PDX 14647) with MYCN amplification and unbalanced 17q gain was utilized to evaluate the efficacy of BTYNB treatment in high-risk neuroblastoma. PDX tumors were administered subcutaneously in NOG mice. Mice harboring PDX tumors were treated with intra-peritoneal injections of 100 mg/kg body weight BTYNB for three cycles. The treatment showed no apparent toxicity based on the unaltered mouse weight (Figure 27b) and examination of animals revealed no obvious signs of side effects (e.g. behavior). However, BTYNB treatment did not significantly impact tumor growth (Figure 27c). Although significance was not reached due to high variation in the control population,

systemic application of BTYNB tended to slow down tumor growth. This finding suggested weak *in vivo* potency of the lead compound BTYNB.

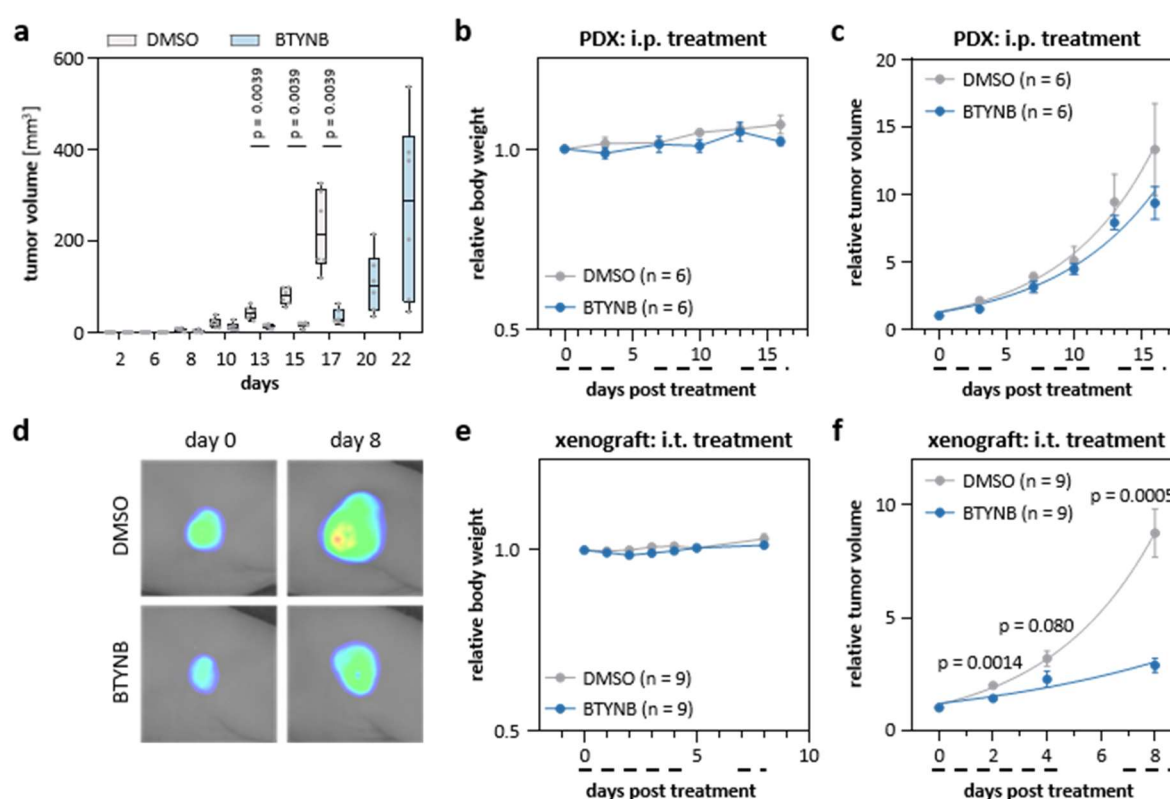


Figure 27: BTYNB impaired neuroblastoma xenograft growth. (a) Tumor growth (n = 6) of DMSO- (grey) and BTYNB-pretreated (blue) subcutaneous BE(2)-C xenografts was monitored by tumor volume over time. (b, c) Subcutaneous PDX tumors were treated intra-peritoneal with DMSO (grey) or BTYNB (blue). Daily treatment is indicated by dashed lines below the x-axis. Total mouse weight (b) and relative tumor growth (c) were monitored (n = 6). (d-f) Subcutaneous BE(2)-C xenograft tumors were treated intra-tumoral with DMSO (grey) or BTYNB (blue). Daily treatment is indicated by dashed lines below the x-axis. Representative pictures of the tumors at treatment start (day 0) and end (day 8) were obtained by non-invasive infrared imaging (d). Total mouse weight (e) and relative tumor growth (f) were monitored (n = 9). Statistical significance was determined by non-parametric two-sided Mann-Whitney test (errors defined as SEM).

To analyze this further, BTYNB stability was assessed in collaboration with the group of Wolfgang Sippl (Institute of Pharmacy). BTYNB demonstrated good stability in cell culture conditions, as it remained stable for at least 72 hours in DMEM media (Table 26). However, in simulated acidic conditions (10% v/v trifluoroacetic acid), the stability of BTYNB slightly decreased after 48 hours to approximately 85%. In addition, BTYNB showed high binding to plasma proteins (FBS or HSA), suggesting limited stability and bioavailability of the lead compound BTYNB *in vivo*. This is in line with observed results in the PDX model. To overcome these limitations and to test if BTYNB shows higher efficiency when applied directly to the tumor, subcutaneous BE(2)-C xenograft tumors were treated with intra-tumoral injections of 50 mg/kg body weight BTYNB for two cycles. As for intra-peritoneal treatment, no obvious signs of toxicity were observed (Figure 27e). Remarkably, intra-tumoral treatment substantially impaired tumor growth compared to control tumors (Figure 27d, f).

Table 26: BTYNB stability.

condition	0h	6h	12h	24h	48h	72h
BTYNB in DMEM	100%	100.4 %	101.2 %	103.1 %	105.3 %	107.7 %
BTYNB in DMEM under acidic condition	100%	98.3 %	97.4 %	95.1 %	85.8 %	84.3 %

In summary, targeting IGF2BP1 by depletion, knockout or inhibiting its RNA-binding impedes both neuroblastoma cell growth *in vitro* and tumor growth *in vivo*. These findings emphasize the potential of IGF2BP1 as a therapeutic target for cancer therapy, in particular for the treatment of neuroblastoma. However, BTYNB remains a lead compound with obviously limited pharmacokinetics. Thus, further development of more potent and specific IGF2BP1 inhibitors holds promise for the treatment of neuroblastoma by downregulating MYCN-driven gene expression.

4.6 IGF2BP1 and MYCN share oncogenic downstream targets

4.6.1 IGF2BP1 and MYCN enhances expression of chromosome 17q genes

The feedforward regulation of IGF2BP1 and MYCN likely impacts many effectors due to the broad target range on the transcriptional (MYCN) and post-transcriptional level (IGF2BP1; Huang and Weiss 2013, Huang *et al.* 2018b). This suggests that IGF2BP1 and/or MYCN also synergize with other oncogenic genes located on chromosome 17q. To investigate the influence of the IGF2BP1/MYCN feedforward loop on downstream targets, a comprehensive analysis was conducted on selected oncogenes, tumor-suppressors, common essential genes on chromosome 17q and the 52 previously identified neuroblastoma essential genes on chromosome 17 (Figure 14). Multiple criteria were used to establish a scoring system to distinguish potential target genes regulated by IGF2BP1 and MYCN. These criteria included median gene dependency score in MNA neuroblastoma cell lines, mRNA expression changes in neuroblastoma subgroups (MNA, unbalanced 17q, stage 4), gene hazard ratio, correlation with IGF2BP1 and MYCN expression, fold-change in mRNA expression upon IGF2BP1 or MYCN depletion, MYCN ChIP-seq data and IGF2BP1 3'UTR CLIP data (Figure 28). Analysis of these criteria revealed a strong association of IGF2BP1/MYCN-driven gene expression with common essential genes located on chromosome 17, with the top-ranking candidates *BIRC5* (survivin) and *TOP2A*. Among the neuroblastoma essential genes, *NME1*, *PYCR1* and *TK1* emerged as top candidates in addition to *IGF2BP1* itself.

The top candidates were further validated by depleting IGF2BP1 or MYCN and evaluating protein abundance. Consistent reduction in TK1 and PYCR1 expression was observed in both neuroblastoma cell lines upon IGF2BP1 or MYCN depletion (Figure 29a). *BIRC5* and *TOP2A* also showed decreased expression, except in KELLY cells with MYCN knockdown where the results were not significant. Further examination of *BIRC5* revealed potential E-Box elements and binding of both, MYCN and IGF2BP1, to the promoter or 3'UTR, respectively, as indicated by MYCN ChIP and IGF2BP1 CLIP profiles (Figure 29b, c).

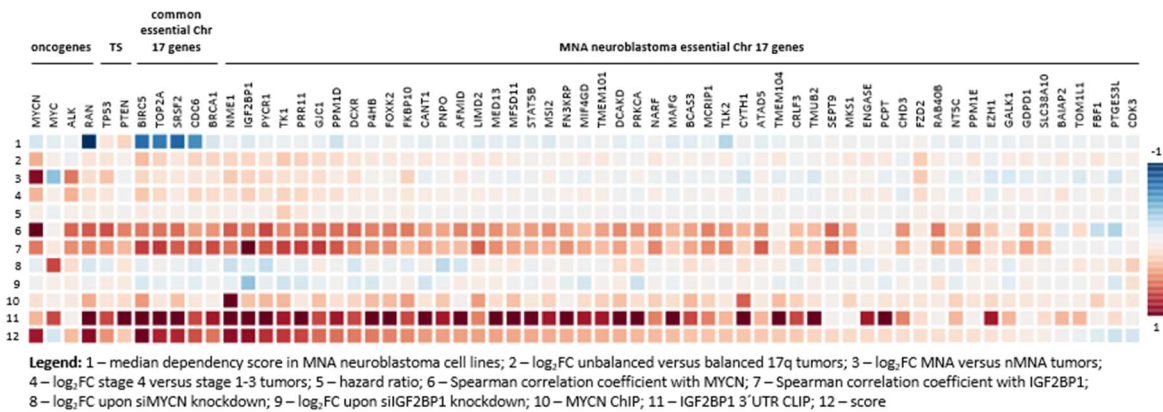


Figure 28: Identification of potential chromosome 17 downstream targets. Heatmap representing the identification of potential IGF2BP1 and MYCN downstream effectors in neuroblastoma progression. Analysis was performed on selected oncogenes, tumor-suppressors, five common and 52 neuroblastoma essential genes on chromosome 17q. Data over all annotated genes were scaled within each row to range 0 and 1 (ChIP and CLIP) or -1 and 1 (all other).

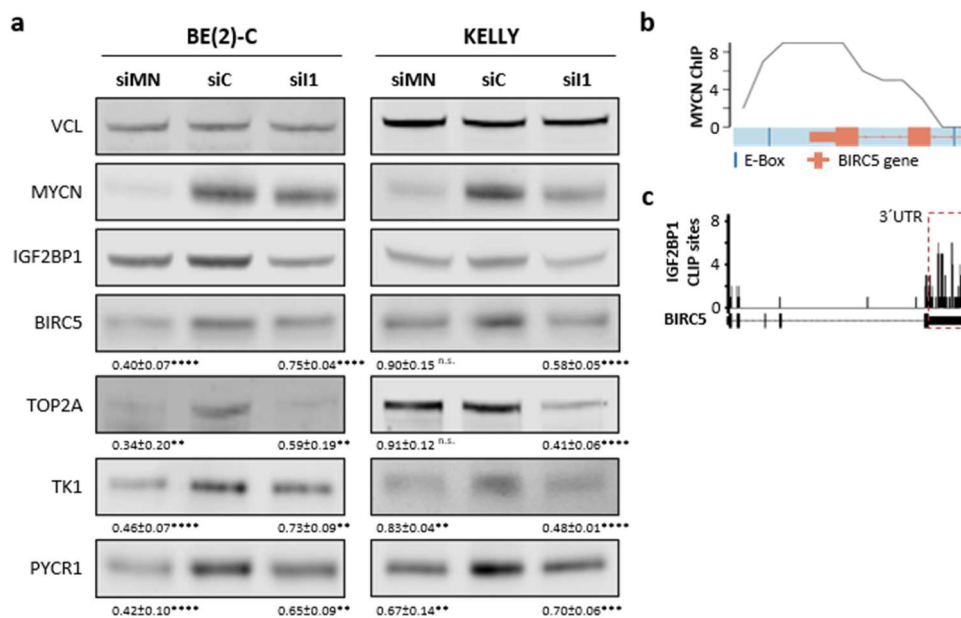


Figure 29: IGF2BP1 and MYCN promote oncogenic genes located on chromosome 17q. (a) Western blot analysis (n = 3) of indicated proteins upon MYCN (siMN) or IGF2BP1 (siI1) compared to control (siC) knockdown in two neuroblastoma cell lines. (b) MYCN ChIP-seq profile of the *BIRC5* promoter region. E-Boxes, putative MYC/N binding sites, are indicated in dark blue. The *BIRC5* gene is depicted schematically in orange up to the beginning of the second intron. (c) IGF2BP1 CLIP profile for the *BIRC5* mRNA derived from eight experiments from different cell lines. Statistical significance was determined by parametric two-sided Student's *t*-test (errors defined as SD). n. s., non-significant; **, $p < 0.01$; ***, $p < 0.001$; ****, $p < 0.0001$

Analysis of clinical data derived from the analyzed cohort revealed hazard ratios above one for these top candidate genes, with *BIRC5* and *TK1* reaching statistical significance (Figure 30a). Furthermore, all analyzed candidates were significantly enriched in aggressive neuroblastoma subgroups, including those with *MYCN* amplification, unbalanced 17q gain and stage 4 tumors (Figure 30b). Consistent with previous findings, these candidates showed a high correlation with *MYCN* and especially *IGF2BP1* expression (Figure 30c).

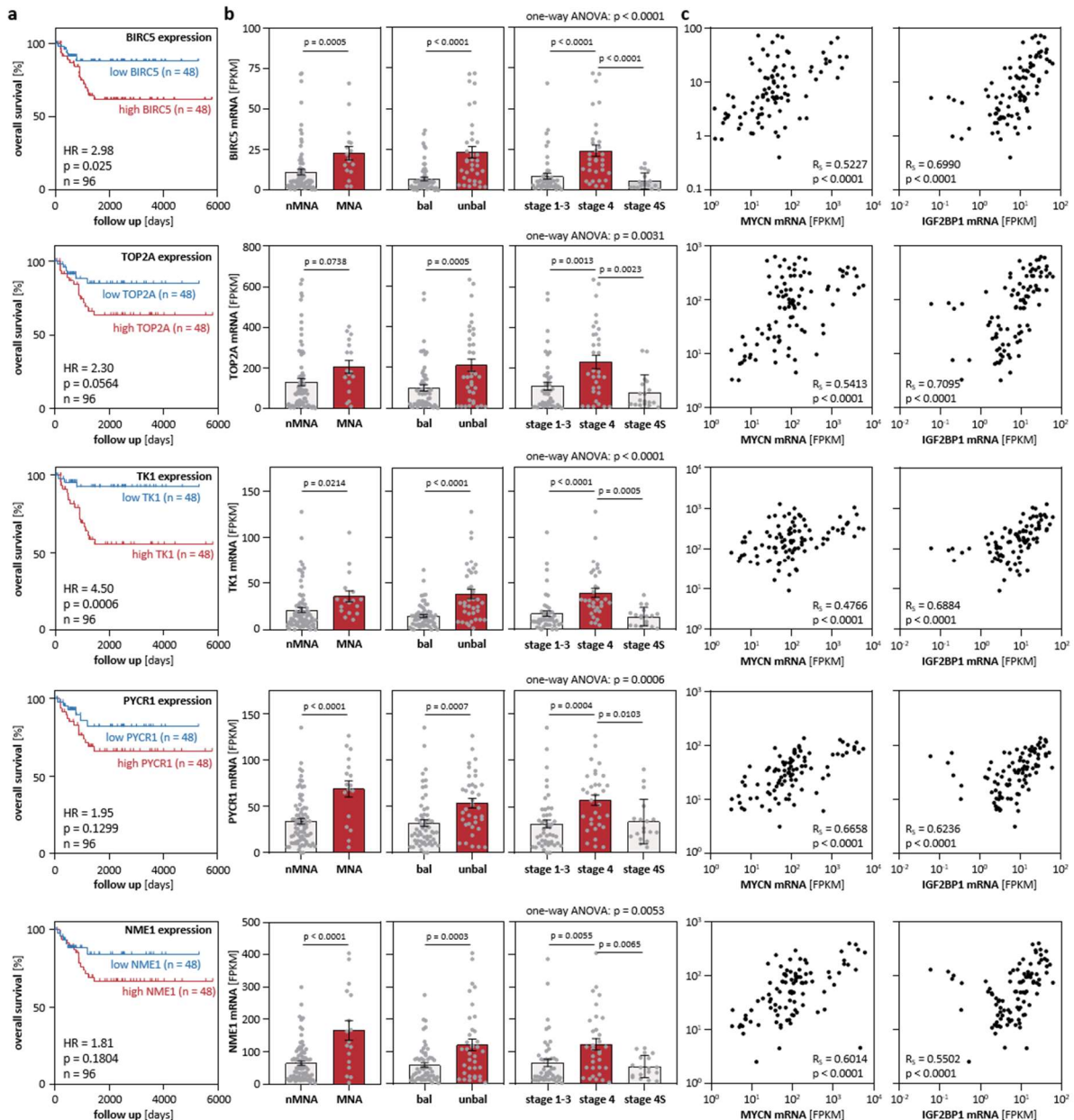


Figure 30: Top 17q IGF2BP1/MYCN target genes are highly expressed in aggressive neuroblastoma. (a) Kaplan-Meier survival analyses of indicated gene expression (median cut-off). Statistical significance was determined by log-rank test. **(b)** The mRNA expression of indicated genes was separated by MYCN amplification status (left), chromosome 17q balance status (middle) and INSS stage (right). Statistical significance was determined by Mann-Whitney test (errors defined as SEM). Non-parametric one-way ANOVA and Kruskal-Wallis test were performed to compare all stages. **(c)** Correlation of mRNA expression of indicated genes with MYCN (left) or IGF2BP1 (right) mRNA expression in neuroblastoma tumors. Spearman correlation coefficients and p-values are indicated.

To further validate the interaction between these target genes and IGF2BP1, RNA immunoprecipitations were performed in three neuroblastoma cell lines. Consistent enrichment of TOP2A and PYCR1 mRNA with IGF2BP1 was observed, although TOP2A in NBL-S cells did not reach statistical significance due to high variance (Figure 31a-c). BIRC5, TK1 and NME1 were not enriched in any cell line in comparison to negative controls HIST2 and IRF1, although these genes exhibit a strong association according to CLIP data (Figure 28). Possible explanations could be the experimental setup

(cross-linking versus transient interaction), the sensitivity of the detection (high-throughput sequencing versus RT-qPCR) or RNA accessibility. MDM2 served as positive control (Mu *et al.* 2022). Additionally, luciferase reporter assays were conducted using the 3' UTRs of the potential target genes. Treatment with BTYNB resulted in reduced activity of the BIRC5 and TOP2A reporters in BE(2)-C and KELLY cells (Figure 31d, e). A similar trend, albeit weaker, was observed for other potential target genes TK1, PYCR1 and NME1. The significance of these findings could not be determined due to limited experimental data. Additionally, IGF2BP1 knockout in both cell lines showed similar results for BIRC5 and TOP2A, except for TOP2A in KELLY cells, which was surprisingly unaffected (Figure 31f, g). Taken together, these analyses suggest that several chromosome 17q genes are influenced by MYCN and IGF2BP1, contributing to tumorigenesis. Furthermore, this indicates a strong synergy between gained regions and enhanced expression of certain genes in neuroblastoma.

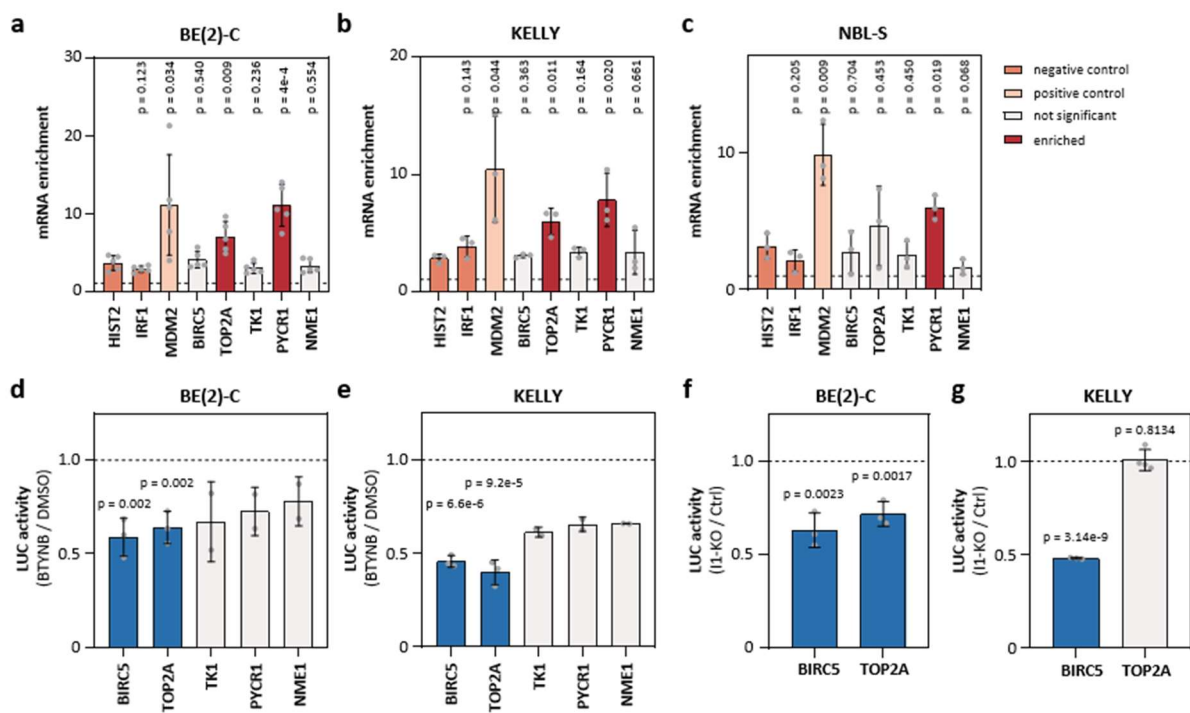


Figure 31: IGF2BP1 regulate 17q essential neuroblastoma genes in a 3' UTR-dependent manner. (a-c) RT-qPCR analysis after IGF2BP1 RIP in indicated parental neuroblastoma cell lines (n = 3-5). **(d-g)** Relative activity of indicated luciferase reporter in BTYNB-treated (d-e, n = 2-3) or IGF2BP1 knockout (f-g, n = 3) cell lines. Statistical significance was determined by parametric two-sided Student's *t*-test (errors defined as SD).

4.6.2 Modulation of BIRC5 by IGF2BP1 and MYC/N is conserved across cancer types

To investigate the conservation of this regulatory network in other cancer entities, the expression of IGF2BP1, MYC and BIRC5 were examined in four carcinoma cell lines from pancreas (Panc-1), lung (H522) and liver (Huh7 and HepG2). Notably, HepG2 cells are derived from a hepatoblastoma patient, representing a pediatric liver disease, in contrast to Huh7 cells. These cell lines predominantly express MYC rather than MYCN, thereby extending the IGF2BP1/MYCN network to another member of the

MYC family. IGF2BP1 knockdown consistently reduced MYC protein levels in all analyzed cell lines (Figure 32a). Conversely, transient MYC depletion resulted in a moderate reduction in IGF2BP1 expression, with non-significant results in Panc-1 and Huh7 cells. Nevertheless, in all four cell lines, knockdown of IGF2BP1 or MYC consistently led to reduced expression of BIRC5, corroborating the previous findings in neuroblastoma cell lines. To evaluate the clinical relevance of this regulatory network, a three gene signature, comprising IGF2BP1, MYC and BIRC5 was applied to the respective cancer entities, including pancreatic ductal adenocarcinoma (PAAD), lung adenocarcinoma (LUAD) and liver hepatocellular carcinoma (LIHC), using the GEPIA2 survival tool (Tang *et al.* 2019). The analysis revealed significantly reduced overall survival for high expression of the three genes, except for LIHC alone (Figure 32b). This highlights the importance of BIRC5, in addition to IGF2BP1 and MYC/N, as a key oncogenic factor in these cancer entities.

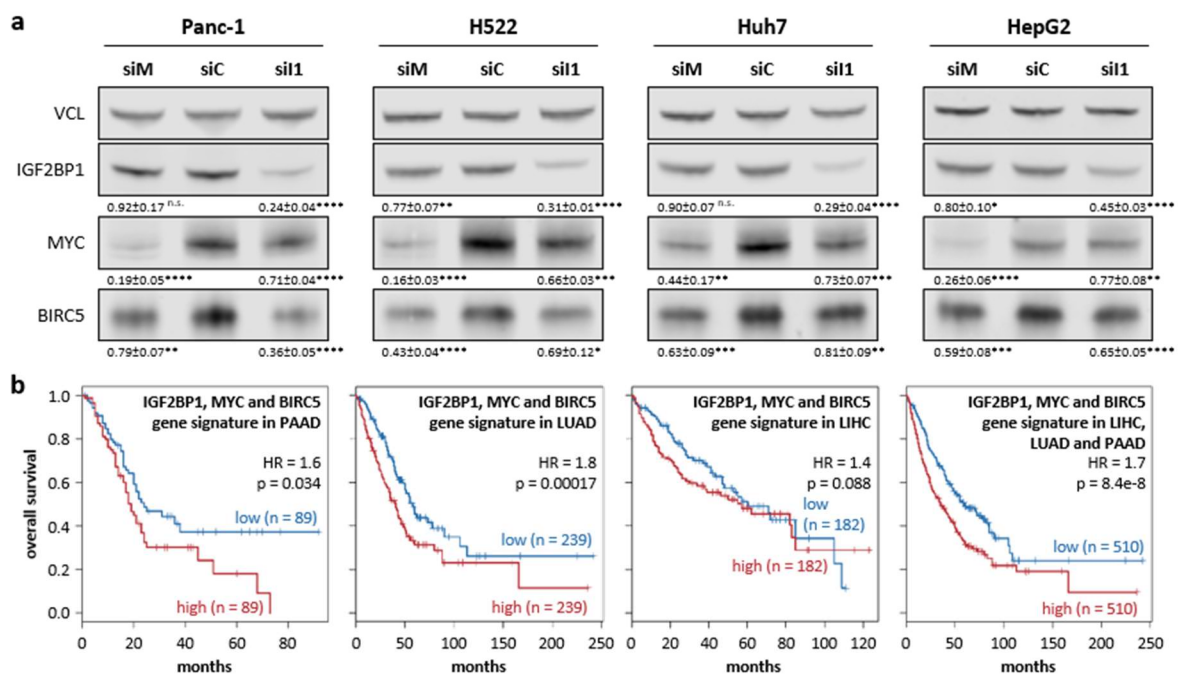


Figure 32: IGF2BP1- and MYC/N-dependent regulation is conserved across cancer. (a) Western blot analysis (n = 3) of indicated proteins upon MYC (siM) or IGF2BP1 (siI1) compared to control (siC) knockdown in indicated cell lines. Statistical significance was determined by parametric two-sided Student's *t*-test (errors defined as SD). n. s., non-significant; *, p < 0.05; **, p < 0.01; ***, p < 0.001; ****, p < 0.0001 **(b)** Kaplan-Meier survival analysis of the three gene signature using the GEPIA2 website. Statistical significance was determined by log-rank test.

Taken together, these findings suggest that IGF2BP1 and MYC/N act synergistically to upregulate oncogenic target genes on chromosome 17q, particularly BIRC5. This regulatory network appears to be conserved in different carcinoma cell lines, highlighting its potential as therapeutic target across multiple cancer types.

4.6.3 Cell cycle kinases as potential targets of the IGF2BP1/MYCN-driven network

To assess the involvement of IGF2BP1 and MYCN in the regulation of protein kinases, a comprehensive analysis was conducted considering hazard ratios, median dependency scores in MNA neuroblastoma cell lines, correlation with IGF2BP1 or MYCN in tumors, IGF2BP1 CLIP or MYCN ChIP data and the fold-change of mRNA expression upon transient IGF2BP1 or MYCN depletion, as previously done for chromosome 17q genes (Figure 33a). The analysis revealed several cell cycle-related protein kinases as top-ranking candidates, including PLK1, AURKA, CHEK1, WEE1, PKMYT1, BUB1B, AURKB and CDK1. Additionally, two kinases associated with pyrimidine biosynthesis (CAD) and neuronal processes (CAMKK2) were also highly correlated. Further investigation focusing on kinases within the cell cycle showed a strong association with the G2/M phase (Figure 33b). Previously findings highlighted the role of IGF2BP1 as a regulator of E2F transcription factors, primarily influencing the G1/S transition (Müller *et al.* 2020). The observed correlation in this study suggests that IGF2BP1 also has a significant impact on the G2/M checkpoint by regulating the abundance of protein kinases. This is supported by the identification of MYBL2 and FOXM1 as top-correlated transcription factors besides E2F1 (Table 25), as some of these kinases are MMB-FOXM1 target genes induced by MYBL2 and/or FOXM1 (PLK1, AURKA, WEE1, BUB1B, AURKB, CDK1).

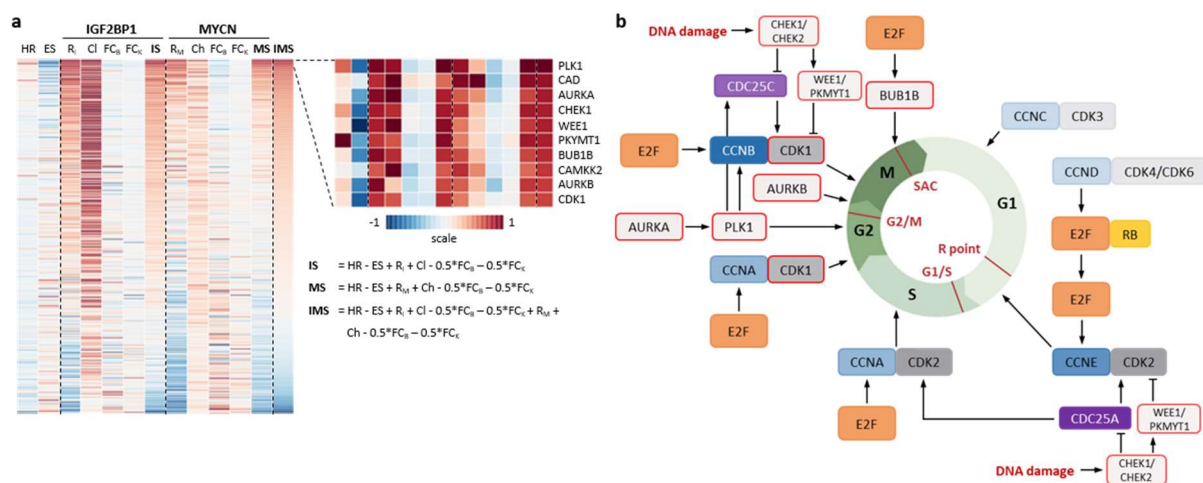


Figure 33: Determination of potential IGF2BP1 and MYCN target kinases. (a) Heatmap representing the identification of potential IGF2BP1 and MYCN downstream targets. Analysis was performed on all protein kinases. Data of each column were scaled to range 0 and 1 (ChIP and CLIP) or -1 and 1 (all other). Top ten kinases were depicted in the enlargement on the right. ES - essentiality score in MNA neuroblastoma; R_i/R_M - correlation coefficient with IGF2BP1/MYCN in neuroblastoma; CI - CLIP score IGF2BP1; Ch - ChIP score MYCN; FC_B/FC_K - log₂ FC BE(2)-C/KELLY (IGF2BP1 or MYCN depletion) **(b)** Scheme of cell cycle and contributing kinases. The red encircled kinases are potential IGF2BP1/MYCN targets identified in this study. R point - restriction point; G1/S - G1/S checkpoint; G2/M - G2/M checkpoint; SAC - spindle assembly checkpoint

To further investigate the regulation of these kinases by IGF2BP1 and MYCN, knockdown analyses were performed in two neuroblastoma cell lines. Overall, MYCN knockdown exhibited a stronger effect on kinase abundance, but IGF2BP1 consistently reduced the levels of all analyzed kinases (Figure 34a).

Only CDK1 and AURKB in KELLY cells showed non-significant results due to high experimental variation, however, both kinases tended to be downregulated upon IGF2BP1 or MYCN depletion in this cell line.

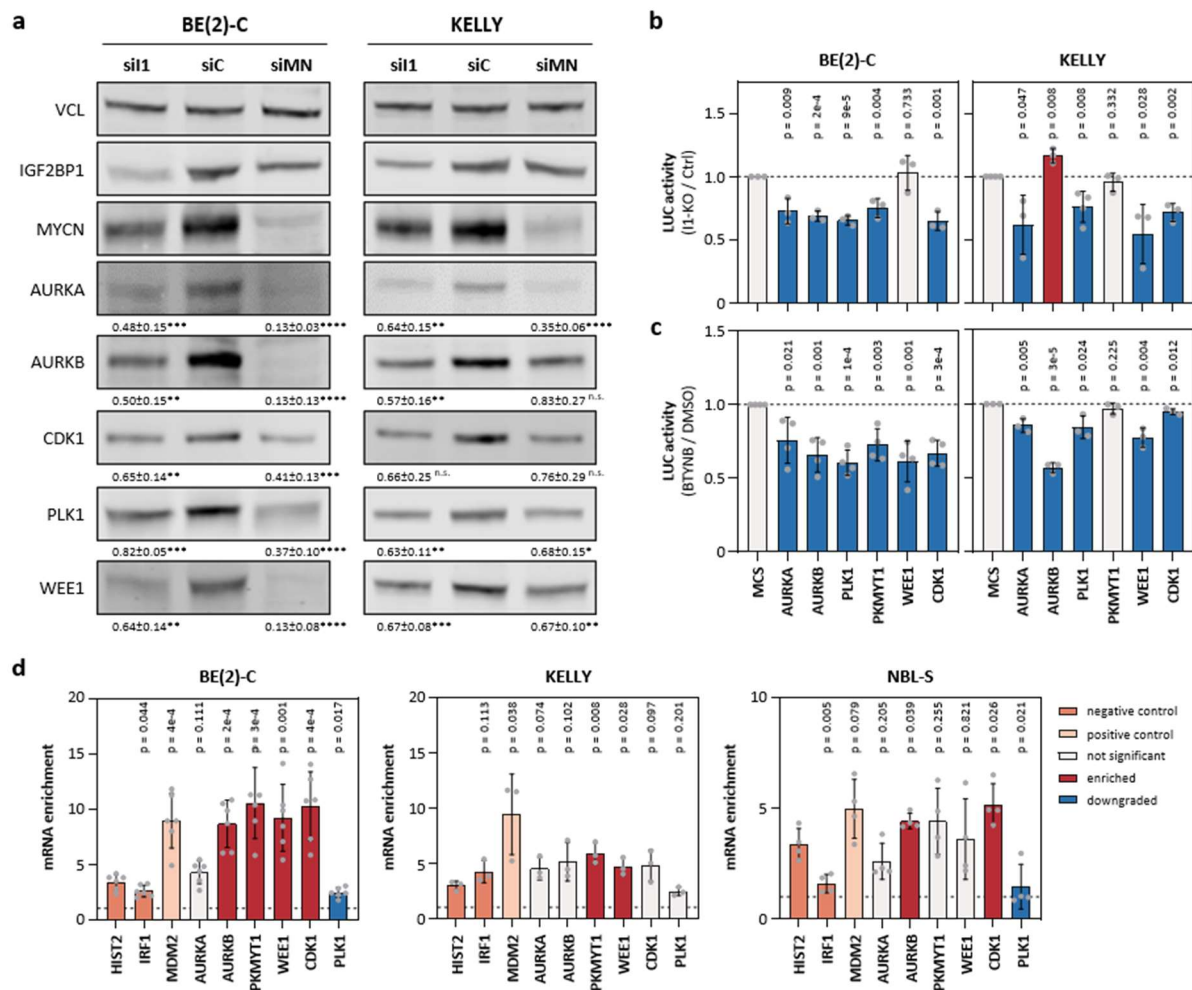


Figure 34: IGF2BP1 regulates G2/M checkpoint kinases in a 3'UTR-dependent manner. (a) Western blot analysis (n = 3) of indicated proteins upon MYCN (siMN) or IGF2BP1 (sil1) compared to control (siC) knockdown in indicated cell lines. (b, c) Relative activity of indicated luciferase reporter in IGF2BP1 knockout (b, n = 3) or BTYNB-treated (c, n = 3-4) cell lines. (d) RT-qPCR analysis after IGF2BP1 RIP in indicated parental neuroblastoma cell lines (n = 3-6). Statistical significance was determined by parametric two-sided Student's *t*-test (errors defined as SD). n. s., non-significant; *, *p* < 0.05; **, *p* < 0.01; ***, *p* < 0.001; ****, *p* < 0.0001

Subsequently, the potential regulation of these kinases by IGF2BP1 was assessed using 3'UTR luciferase reporter under IGF2BP1 knockout condition and BTYNB treatment. Moderate overall downregulation of luciferase activity was observed, with consistent reduction of AURKA, PLK1 and CDK1 in both cell lines (Figure 34b, c). AURKB and PKMYT1 luciferase activity was reduced in BE(2)-C cells, while PKMYT1 remained unaffected and AURKB exhibited opposing effects under IGF2BP1 knockout and BTYNB treatment in KELLY cells. WEE1 was consistently downregulated in KELLY cells, but only reduced in BE(2)-C cells upon BTYNB treatment. Furthermore, RNA immunoprecipitation analysis was conducted to investigate the direct binding of IGF2BP1 to the mRNAs of these kinases. In BE(2)-C, all analyzed kinases, except PLK1, showed significant enrichment compared to negative

controls (Figure 34d left panel). However, PLK1 was indeed significantly downgraded. Enrichment in KELLY cells was overall weaker than in BE(2)-C, but PKMYT1 and WEE1 were still significantly enriched (Figure 34d middle panel). AURKA, AURKB and CDK1 also exhibited enrichment, although not reaching significance due to low overall enrichment and high variance. Once again, PLK1 was not enriched. As also observed during analysis of 17q target genes, immunoprecipitation in NBL-S cells demonstrated inconsistent results (Figure 34d right panel), with enrichment of AURKB and CDK1, and downgrading of PLK1, showing overlap with the findings from the other cell lines. AURKA, PKMYT1 and WEE1 did not exhibit enrichment above the negative controls. Even the positive control MDM2 failed to reach significance, suggesting caution in interpreting the results from this cell line. Possible explanations could be differences in cellular context or in the signal-to-noise ratio in these cell lines. BE(2)-C cells exhibited the highest ratio, therefore being the most reliable cell line, whereas NBL-S had the worst ratio. In summary, IGF2BP1 exerts a strong influence on the abundance of several protein kinases involved in cell cycle progression, highlighting its target potential.

4.6.4 IGF2BP1 indirectly influences MYCN protein turnover

During analysis of protein kinases, some of them were considered to be involved in MYCN protein turnover, namely CDK1, PLK1 and AURKA (Liu *et al.* 2020; Figure 35a). To investigate the impact of IGF2BP1 on MYCN protein turnover, an IGF2BP1 depletion experiment was conducted in TET21N cells, which express exogenous MYCN without its native 3'UTR to exclude post-transcriptional regulation through it (Lutz *et al.* 1996). IGF2BP1 depletion substantially reduced MYCN protein level (Figure 35b), indicating the presence of additional regulatory mechanisms affecting MYCN protein stability or mRNA stabilization through the coding sequence. Furthermore, RNA-seq data revealed significant downregulation of AURKA, CDK1 and PLK1 mRNA upon IGF2BP1 knockdown in two neuroblastoma cell lines (Figure 35c), consistent with the findings at the protein level (Figure 34a). In contrast, the expression of GSK3B and FBXW7 remained unchanged or even increased, suggesting that IGF2BP1 predominantly stabilizes rather than destabilizes MYCN protein. To further investigate the role of IGF2BP1 in MYCN protein degradation, protein decay analysis was performed in TET21N cells. This cell line expresses exogenous MYCN without its 3'UTR. Therefore, it was used to avoid the 3'UTR-dependent effects of IGF2BP1 and maybe increase the signal-to-noise ratio. Analysis revealed a halved protein half-life after IGF2BP1 depletion, while IGF2BP1 abundance remained unaffected during this time period (Figure 35d, e). Subsequently, the activity of the respective kinases was analyzed by investigating their phosphorylation status upon IGF2BP1 depletion. Overall, changes in kinase abundance and activity were similar, providing no evidence to support the notion that IGF2BP1 directly modulates kinases activity, but rather destabilizes MYCN protein through the reduction of kinase abundance (Figure 35f).

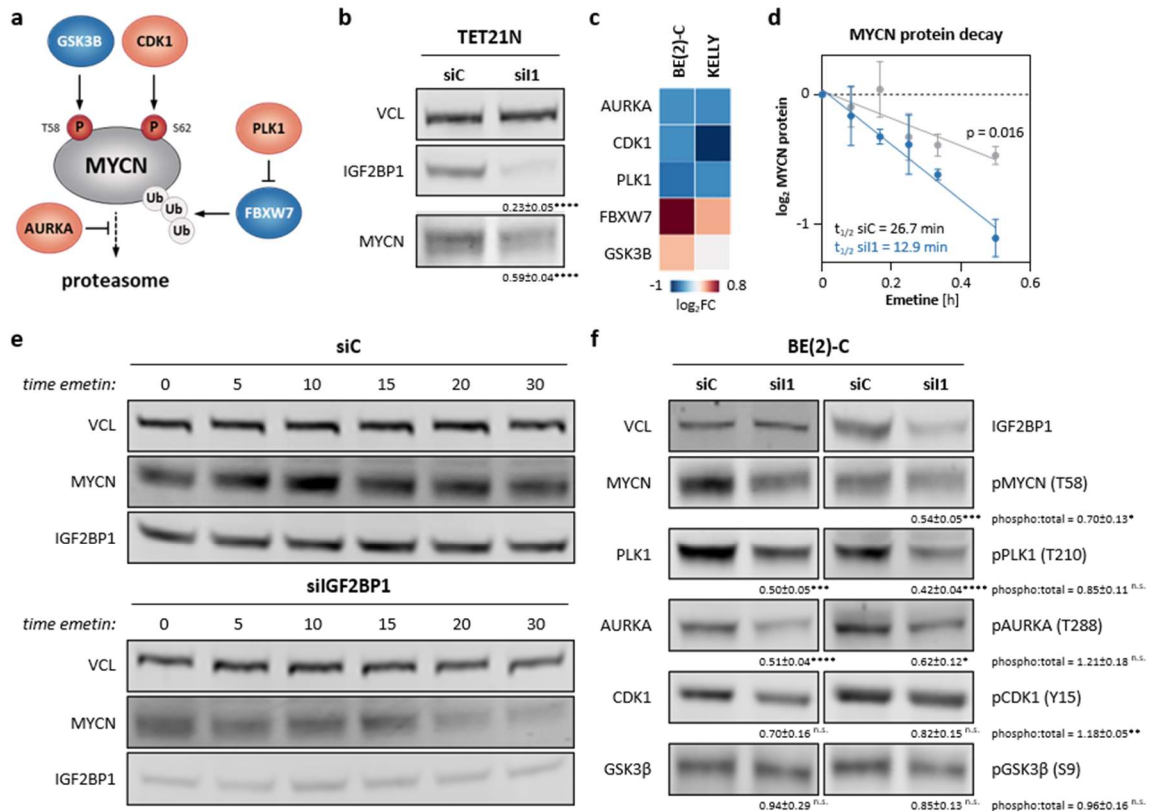


Figure 35: IGF2BP1 enhances MYCN protein stability. (a) Scheme of MYCN protein regulation. Stabilizing and destabilizing proteins are indicated in red or blue, respectively. (b) Western blot analysis of MYCN expression after transient IGF2BP1 knockdown in TET21N cells (n = 5). (c) RNA-seq analysis of indicated mRNAs upon IGF2BP1 knockdown in indicated cell lines. (d, e) MYCN protein decay (d) was monitored by Western blot analysis (e) in control (grey) and IGF2BP1 knockdown (blue) TET21N cells upon indicated time of Emetine treatment (n = 3). MYCN half-life is indicated. (f) Western blot analysis of indicated proteins and phosphoproteins upon IGF2BP1 knockdown in BE(2)-C. Relative changes of phosphorylation signals to total protein level are indicated. Statistical significance was determined by parametric two-sided Student's *t*-test (errors defined as SD). n. s., non-significant; *, *p* < 0.05; **, *p* < 0.01; ***, *p* < 0.001; ****, *p* < 0.0001

These findings highlight the broad target spectrum of IGF2BP1 and support the proposed feedforward loop between IGF2BP1 and MYCN. Additionally, IGF2BP1 and MYCN share downstream targets, resulting in transcriptional and post-transcriptional dysregulation of oncogenic factors, as demonstrated here for chromosome 17q genes and cell cycle kinases. The extensive deregulation observed contributes to tumor progression, underscoring the potential of targeting the IGF2BP1/MYCN-axis for the development of novel therapeutic strategies.

4.7 Inhibition of the IGF2BP1/MYCN-driven network

4.7.1 EN4 impairs MYCN transcriptional activity and neuroblastoma cell growth

The direct targeting of MYC/N has been a challenging endeavor thus far (Liu *et al.* 2020), but a recent publication identified EN4 as a covalent ligand that binds to MYC (Boike *et al.* 2021). EN4 reduces MYC/MAX thermal stability and MYC activity, downregulates MYC targets and impairs tumorigenesis. However, the interaction between EN4 and MYCN has not been investigated yet. Although C171, the targeted residue by EN4 in MYC, is not conserved in MYCN (Figure 36a), it possesses seven other cysteines that could potentially be targeted. To evaluate the accessibility of cysteine residues in MYCN for regio-selective chemical modification, HEK293T cells transfected with SBP-tagged MYCN were treated with varying amounts of 2,5-dibromohexamide. The conversion of free cysteines to dehydroalanines, which blocks the binding of cysteine-directed compounds was analyzed through affinity purification and LC-MS/MS analysis in collaboration with the group of Andrea Sinz (Institute of Pharmacy). This revealed conserved modification of C186 in MYCN, while two cysteines (C115, C464) were not covered by the analysis and the remaining four cysteines exhibited inconsistent or no modifications. Notably, C186 is also conserved in MYC within MYC box III (Figure 36a), which has been reported to play essential roles in the transformation potential of MYC/N (Conacci-Sorrell *et al.* 2014). Thus, C186 is identified as targetable residue in MYCN.

Aiming to evaluate the impact of the MYC-directed inhibitor EN4 on MYCN-expressing neuroblastoma cell lines, the MNA BE(2)-C and nMNA NBL-S cell line, were exposed to the compound. The determined EC₅₀ value for both cell lines was approximately 25 μ M and thus roughly twice as high as reported by previous studies for the MYC-expressing HEK293T cell model (Boike *et al.* 2021). Treatment with EN4 at EC₅₀ concentration reduced neuroblastoma 2D growth and cell viability in both cell lines (Figure 36d, e). Similar results were observed in 3D spheroids (Figure 36f, g), indicating that EN4 has the potential to target MYCN-expressing cells. Furthermore, the transcriptional activity of MYCN was assessed using a luciferase reporter system. Integration of six E-Box elements upstream of a Nano-luciferase resulted in approximately 60-fold increase in activity, indicating that the reporter is suitable for monitoring MYC/N transcriptional activity. Treatment with EN4 or transient MYCN depletion significantly reduced luciferase activity in BE(2)-C cells (Figure 36h left). Notably, depletion or knockout of IGF2BP1 also decreased MYCN transcriptional activity, but to a lesser extent and with variable effects among knockout clones (Figure 36h right). Therefore, EN4 demonstrates potent inhibitory effects on neuroblastoma cell growth *in vitro*. Further studies, like analysis of EN4 binding to MYCN by mass spectrometry are needed. Also, modification of EN4 could be helpful to increase its specificity and reactivity for MYCN.

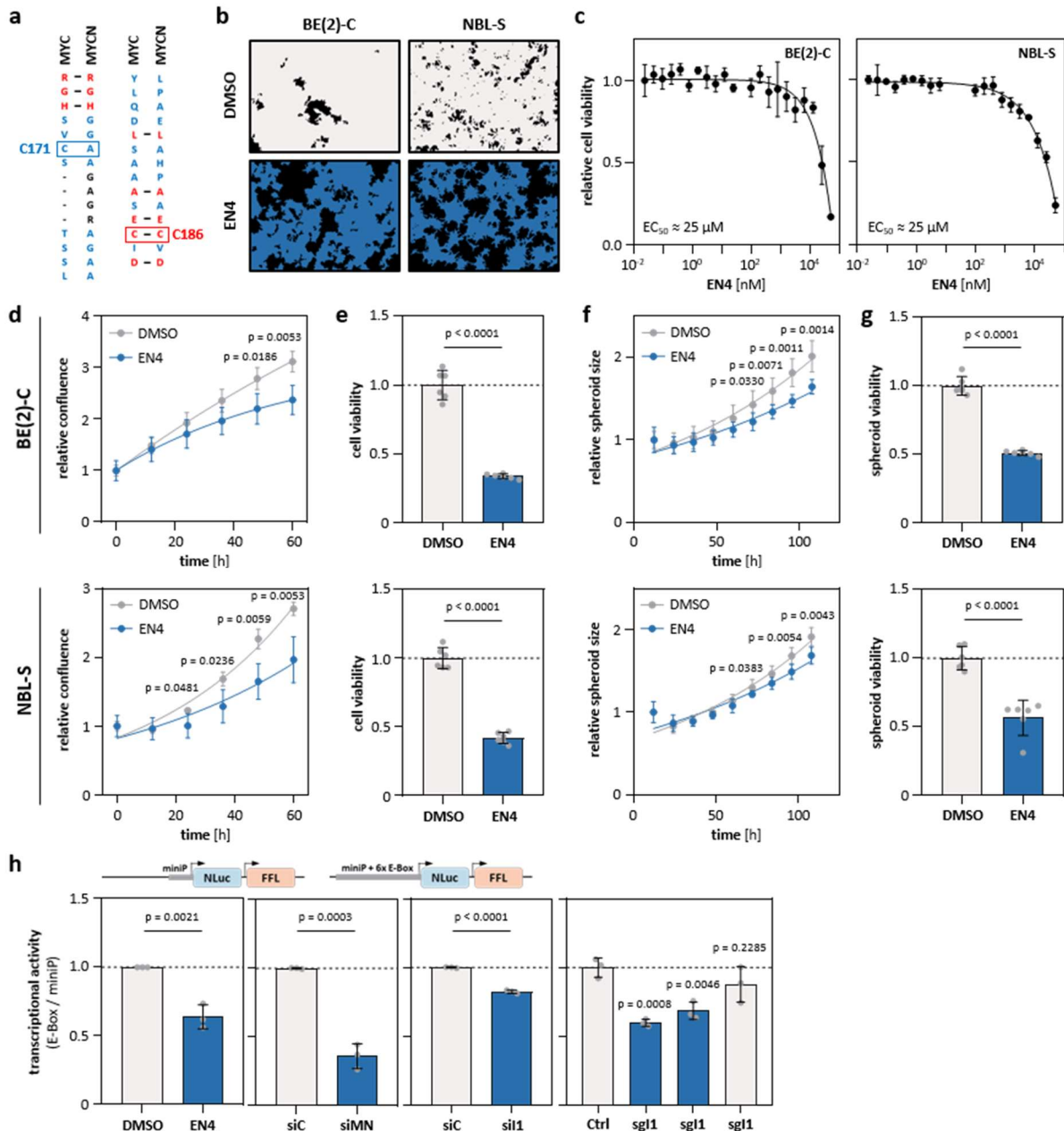


Figure 36: EN4 inhibits neuroblastoma growth and reduces MYCN transcriptional activity. (a) Pairwise protein homology analysis of human MYC and MYCN for the indicated region using NCBI:COBALT (https://www.ncbi.nlm.nih.gov/tools/cobalt/re_cobalt.cgi). Conserved and non-conserved amino acids are depicted in red and blue, respectively. Black amino acids are only present in one protein. C171 and C186 are indicated. (b) Confluence pictures of BE(2)-C and NBL-S cells treated with DMSO or EN4 at EC₅₀ concentration. (c) Response curve analysis for EN4 in indicated cell lines. The approximately EC₅₀ values are indicated. (d-g) Growth curve analysis (d, f) and viability measurement (e, g) of two neuroblastoma cell lines treated with DMSO (grey) or EN4 (blue) in 2D (d, e) and 3D (f, g) cell culture assays. (h) Relative transcriptional activity of a luciferase reporter harbouring six E-Box elements. Transcriptional activity was assessed upon EN4 treatment, MYCN or IGF2BP1 knockdown and IGF2BP1 deletion (from left to right). Statistical significance was determined by parametric two-sided Student's *t*-test (errors defined as SD).

4.7.2 Combined treatment of BRD inhibitors and BTYNB is beneficial

Inhibition of MYCN often occurs indirectly, such as through bromodomain inhibitors (BRDi). To assess the impact of BRDi on neuroblastoma cell lines, four BRDi that were previously reported to impair

MYCN abundance and transcriptional activity were selected (Puissant *et al.* 2013, Henssen *et al.* 2016). All four BRDi demonstrated high potency in the analyzed cell lines, as indicated by EC_{50} values below 5 μ M (Figure 37a). Among them, Mivebresib was one of the most potent inhibitors. Notably, IGF2BP1 knockout sensitized MNA neuroblastoma cell lines to BRDi treatment (Figure 37b), supporting the concept of a cooperative network between IGF2BP1 and MYCN. The EC_{50} values were reduced nearly 7-fold in BE(2)-C and 4.5-fold in KELLY by IGF2BP1 knockout.

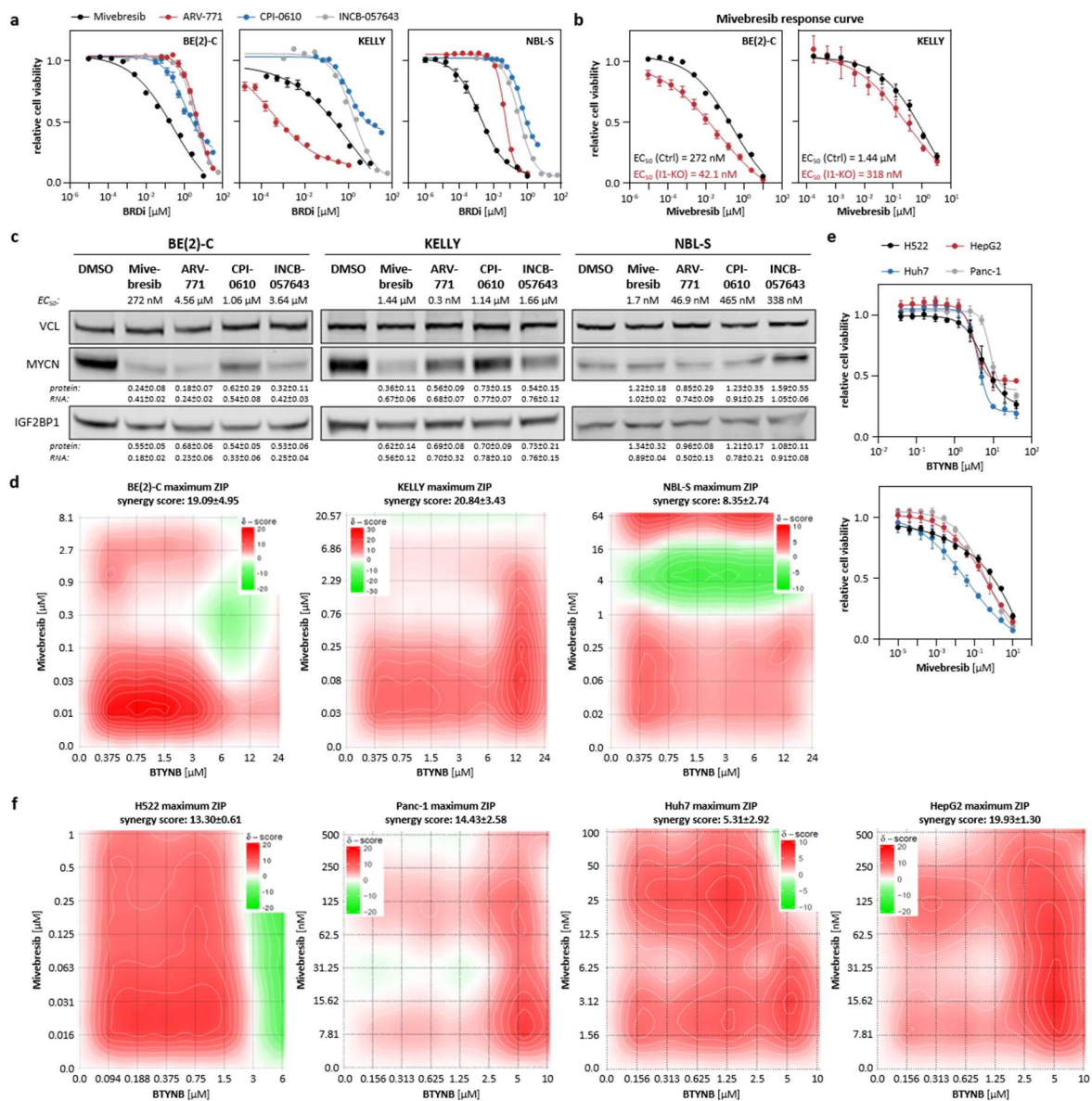


Figure 37: Combined BTYNB and BRD inhibition is beneficial. (a) Response curve analysis for indicated BRD inhibitors in three neuroblastoma cell lines ($n = 4$). (b) Mivebresib response curve in control (black) and IGF2BP1 knockout (red) cells ($n = 4$). EC_{50} values are indicated. (c) Western blot and RT-qPCR analysis of MYCN and IGF2BP1 expression upon treatment with BRD inhibitors at indicated EC_{50} concentrations in neuroblastoma cell lines ($n = 3$). (d) Relief plot depicting the ZIP synergy score for combined treatment of BTYNB and Mivebresib in neuroblastoma cell lines ($n = 3$). (e) BTYNB (top) and Mivebresib (bottom) response curve analysis in indicated carcinoma-derived cell lines ($n = 3$). (f) Relief plot depicting the ZIP synergy score for combined treatment of BTYNB and Mivebresib in carcinoma-derived cell lines ($n = 3$). Statistical significance was determined by parametric two-sided Student's t -test (errors defined as SD).

In MNA cell lines, BRDi consistently decreased MYCN and IGF2BP1 protein and mRNA abundance, with Mivebresib showing the most robust downregulation (Figure 37c). In contrast, MYCN and IGF2BP1 expression remained largely unaffected by BRDi in the nMNA cell line NBL-S. This cell line has a genomic translocation upstream of *MYCN* with a region from chromosome 4, implicating *FBXO8/HAND2* enhancer hijacking as the cause of elevated MYCN synthesis (Zimmerman *et al.* 2018). Hence, MYCN expression in NBL-S cells could be largely BRD-independent. Moreover, drug matrix screens with BTYNB and Mivebresib confirmed substantial benefit of combined treatment exclusively in MNA cell lines, as indicated by maximum synergy scores of 19-21 (Figure 37d). In general, a score above ten is considered as synergy, while additive effects are observed with a score between zero and ten. In translocated NBL-S cells, additive effects were still visible, with a maximum synergy score of approximately eight. Additionally, the synergy between BTYNB and Mivebresib was evaluated in other non-neuroblastoma entities. Additive to synergistic effects were recapitulated in four cell lines, as indicated by maximum synergy scores of 5-20 (Figure 37e, f). These findings suggest effective targeting of MYC/N and IGF2BP1 through combined treatment with BRDi and IGF2BP1 inhibitors in MNA neuroblastoma as well as in other MYC-driven carcinomas as long as the BRD-dependent regulation of MYC/N is not disturbed.

4.7.3 HDAC1-3 inhibition is sufficient to reduce IGF2BP1 and MYCN

It has been previously reported that HDAC inhibition reduces MYCN expression levels in neuroblastoma (Witt *et al.* 2009). In this study, the effects of several commercial and newly developed HDAC inhibitors (HDACi) on neuroblastoma cell growth and the expression of oncogenic factors were investigated to evaluate their contribution to the IGF2BP1/MYCN network inhibition. Firstly, four commercially available HDACi were tested: Panobinostat and Vorinostat, both panHDAC inhibitors, Entinostat, a potent HDAC1/3 inhibitor, and PCI-34051, a HDAC8 inhibitor. All inhibitors showed inhibition of BE(2)-C cell growth, with Panobinostat being the most potent (EC_{50} value around 30 nM) and PCI-34051 the least potent (EC_{50} value approximately 4 μ M; Figure 38a). Protein level analysis confirmed downregulation of MYCN with all four HDACi tested (Figure 38b, c), with Panobinostat and Vorinostat showing the most significant reduction and PCI-34051 having the weakest effect. Additionally, IGF2BP1 and PHOX2B were strongly downregulated except for PCI-34051 treatment, suggesting a loss of neuronal characteristics. CDKN1A was drastically upregulated upon HDACi treatment despite a reduction in p53 expression. Overall acetylation levels of histone H3K9 showed contradictory results, with downregulation observed with Panobinostat and PCI-34051, but upregulation with Vorinostat and Entinostat.

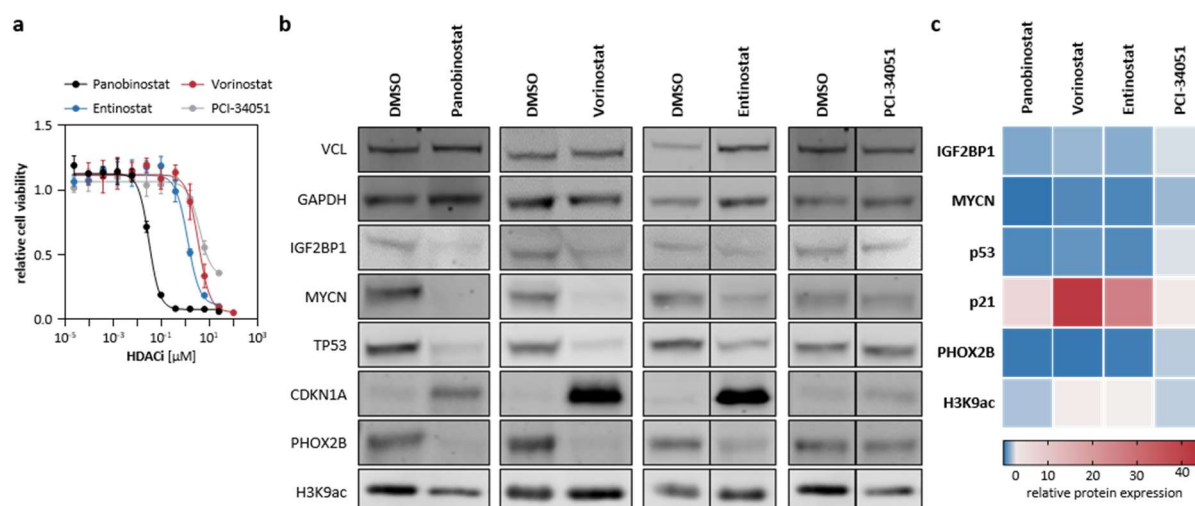


Figure 38: HDAC inhibitors are efficient in reducing MYCN levels. (a) Response curve analysis of indicated HDAC inhibitors in BE(2)-C ($n = 4$). **(b, c)** Western blot analysis (b) and quantification (c) of indicated proteins upon treatment with HDAC inhibitors at EC_{50} concentrations ($n = 3$). Statistical significance was determined by parametric two-sided Student's t -test (errors defined as SD).

Further analysis included several self-made HDAC inhibitors synthesized by the group of Wolfgang Sippl (Institute of Pharmacy). The analyzed inhibitors and respective EC_{50} and K_D values are summarized in Table 27. EC_{50} values ranged from around 100 nM to over 20 μM (Figure 39a). Like the commercial inhibitors, HDACi targeting HDAC1/2/3 or all three of them led to significant downregulation of MYCN, IGF2BP1, PHOX2B and p53 proteins, along with an increase in p21 expression (Figure 39b, c). Histone H3K9 acetylation levels were overall decreased rather than increased.

Table 27: Tested HDAC inhibitors.

inhibitor	target	EC_{50} in BE(2)-C	IC_{50} <i>in vitro</i> [μM]			
			HDAC1	HDAC3	HDAC8	HDAC11
Panobinostat	panHDAC	31.2 nM				
Vorinostat	panHDAC	3.52 μM				
Entinostat	HDAC1/3	1.26 μM				
PCI-34051	HDAC8	3.87 μM				
SIS17	HDAC11	> 20 μM				0.17
FM35	HDAC11	2.03 μM	> 10	> 10	> 10	0.022
FM28	HDAC8/11	416 nM	> 10	> 10	0.03	0.073
PS59	HDAC8	3.04 μM	n. d.	n. d.	0.144	
PSP50	HDAC1/3/8/11	269 nM	0.011	0.037	0.028	0.093
KH16	panHDAC	93 nM	0.013	0.006	0.021	0.8
HI2.1	HDAC1/2/3	598 nM	0.13	0.3	> 10	12
NI-16	HDAC3	5.81 μM	> 1	0.5	> 1	> 10
HI7.3	HDAC1/2	> 10 μM	0.255	> 20	> 10	4.7

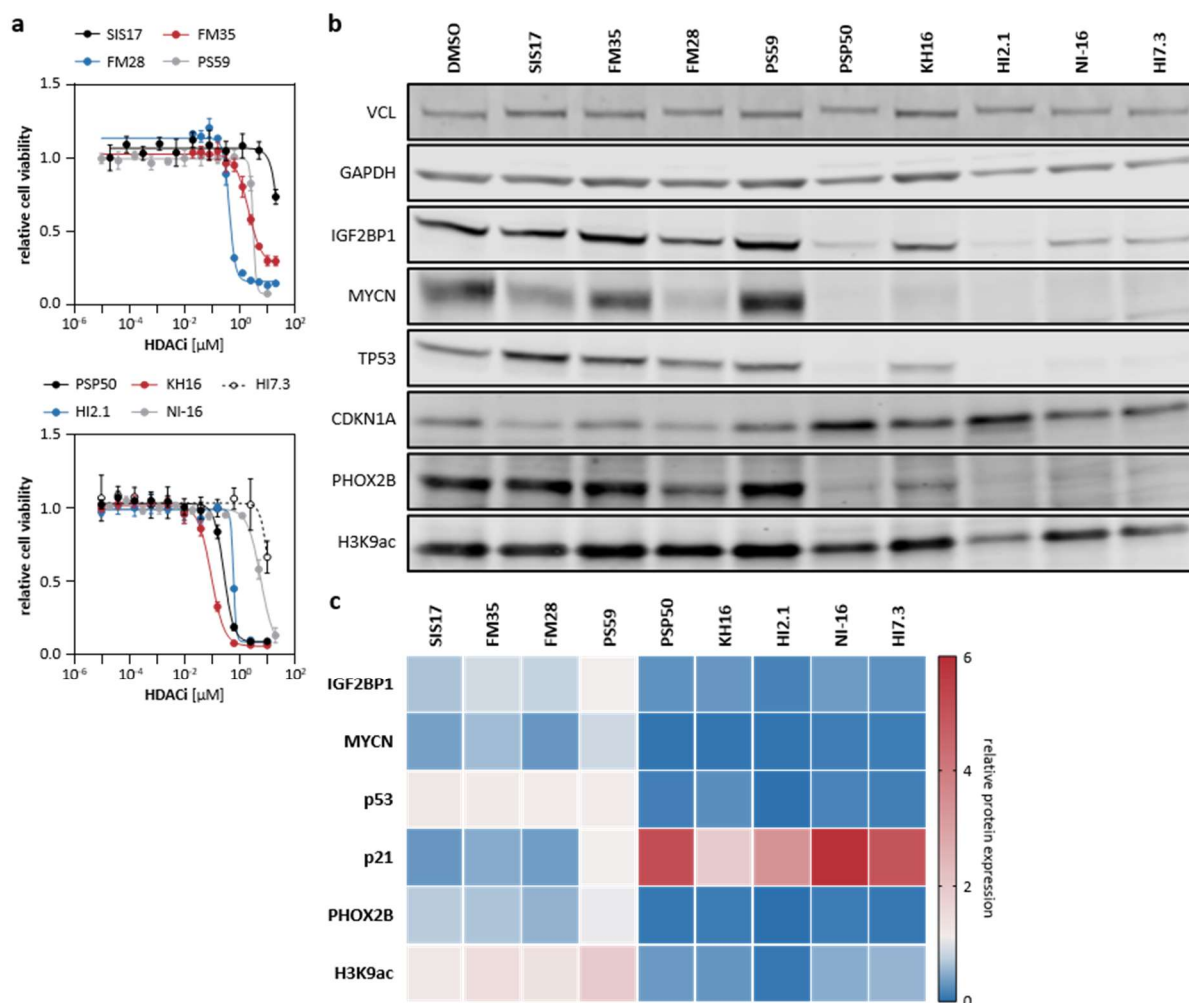


Figure 39: HDAC1-3 inhibitors are sufficient and necessary to impair MYCN expression. (a) Response curve analysis of indicated HDAC inhibitors in BE(2)-C (n = 4). (b, c) Western blot analysis (b) and quantification (c) of indicated proteins upon treatment with HDAC inhibitors at EC₅₀ concentrations (n = 3). Statistical significance was determined by parametric two-sided Student's *t*-test (errors defined as SD).

However, specific HDAC8 inhibition with PS59 failed to reduce MYCN, IGF2BP1 and PHOX2B expression, like the commercial HDAC8 inhibitor PCI-34051 (Figure 39b, c). Interestingly, specific HDAC11 inhibition with SIS17 and combined HDAC8/11 inhibition with FM28 reduced MYCN levels without affecting IGF2BP1, PHOX2B, p53 expression or inducing p21. Histone acetylation levels remained largely unchanged with these treatments. Another HDAC11 inhibitor, FM35, did not show promising effects on MYCN or other targets, providing contradictory results to SIS17 and FM28. In conclusion, inhibition of HDAC1-3 is sufficient to reduce MYCN levels, thereby also reducing IGF2BP1 and PHOX2B expression and inducing p21. HDAC11 may have some influence on MYCN, but its mechanism of action appears to be different, as other genes were not or mildly affected. HDAC8 inhibition alone is not sufficient to reduce MYCN levels.

4.7.4 Combined inhibition of chromosome 17q target genes and IGF2BP1 is beneficial

The IGF2BP1/MYCN network has been shown to influence various chromosome 17q MNA essential genes (Figure 29). Given that IGF2BP1 knockout sensitized neuroblastoma cells to BRDi (Figure 37), the effect of IGF2BP1 deletion on the BIRC5 inhibitor YM-155 was investigated. YM-155 has demonstrated good tolerance in clinical trials and exhibited anti-tumor activity in combination therapy (Tolcher *et al.* 2008, Satoh *et al.* 2009, Rauch *et al.* 2014, Papadopoulos *et al.* 2016).

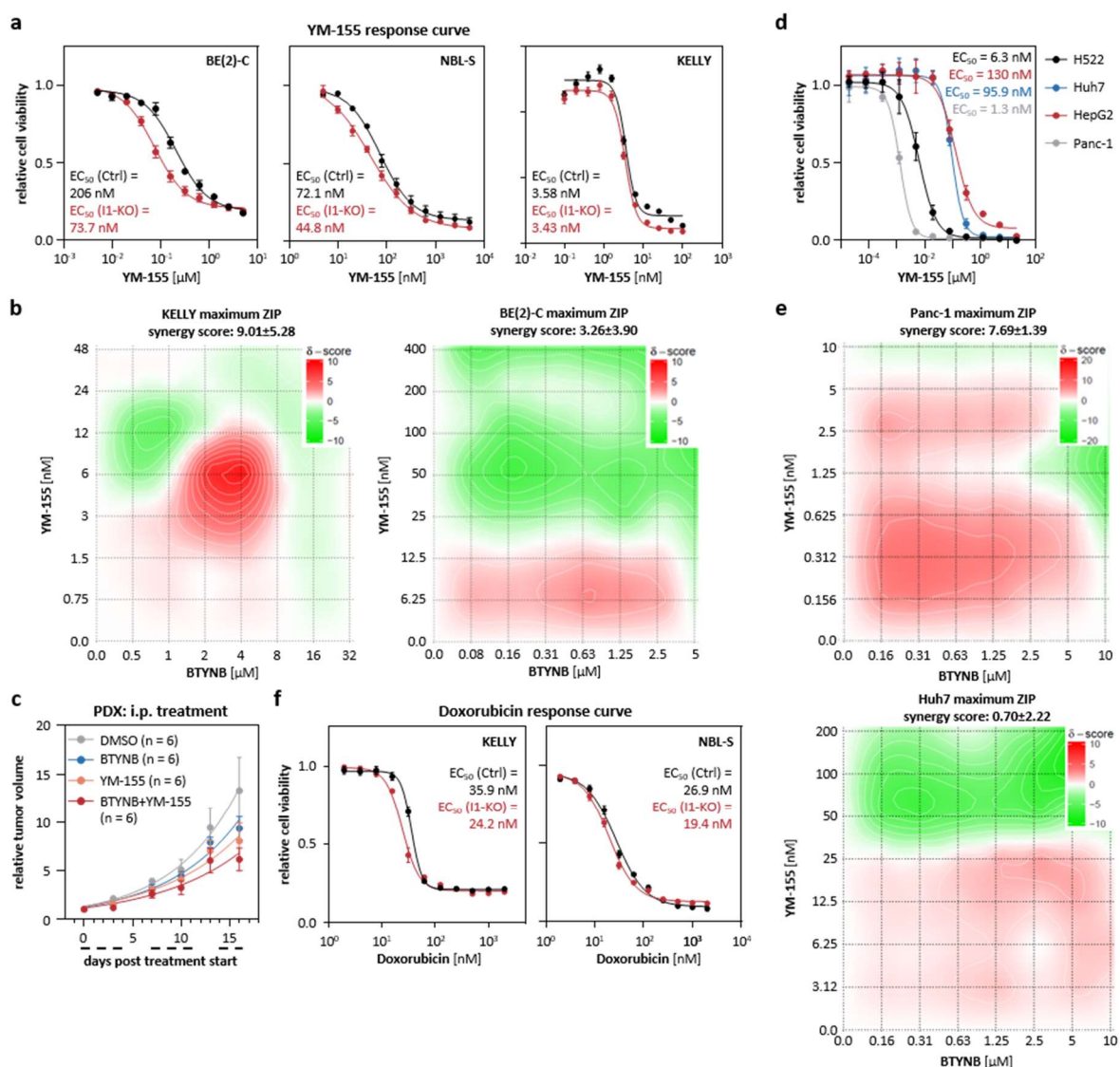


Figure 40: BIRC5 and IGF2BP1 inhibition are beneficial in combination treatment. (a) YM-155 response curve in control (black) and IGF2BP1 knockout (red) cells (n = 4). EC₅₀ values are indicated. (b) Relief plot depicting the ZIP synergy score for combined treatment of BTYNB and YM-155 in neuroblastoma cell lines (n = 3). (c) Subcutaneous PDX tumors were treated intra-peritoneal with DMSO (grey), BTYNB (blue), YM-155 (orange) or in combination of BTYNB and YM-155 (red). Daily treatment is indicated by dashed lines below the x-axis. Relative tumor growth was monitored (n = 6). (d) YM-155 response curve analysis in indicated carcinoma-derived cell lines (n = 3). EC₅₀ values are indicated. (e) Relief plot depicting the ZIP synergy score for combined treatment of BTYNB and YM-155 in carcinoma-derived cell lines (n = 3). (f) Doxorubicin response curve in control (black) and IGF2BP1 knockout (red) cells (n = 4). Statistical significance was determined by parametric two-sided Student's *t*-test (errors defined as SD).

IGF2BP1 knockout reduced the EC_{50} value for YM-155 approximately 2.8-fold in BE(2)-C and 1.6-fold in NBL-S (Figure 40a). However, the extremely sensitive response of KELLY cells to YM-155 (EC_{50} value of 4 nM) rendered IGF2BP1 knockout ineffective in this cell line. Drug matrix analyses in BE(2)-C and KELLY cells supported a moderate benefit of combined BTYNB and YM-155 treatment, indicated by a maximum synergy score of three or nine, respectively (Figure 40b). Further *in vivo* experiments were conducted using the PDX model previously used for BTYNB treatment (Figure 27). The PDX tumors were treated with 2.5 mg/kg body weight YM-155 alone or in combination with 100 mg/kg body weight BTYNB. While the results remained non-significant, the moderate reduction of tumor growth by YM-155 was slightly enhanced by BTYNB in combined treatment (Figure 40c). The limited effect of additional BTYNB application can be attributed to the poor pharmacokinetics of BTYNB. The effect of YM-155 on cell viability and the additive benefit of combined treatment with BTYNB and YM-155 was validated in carcinoma-derived cell lines (Figure 40d, e). In addition, the impact of IGF2BP1 knockout on the sensitivity to Doxorubicin treatment, a TOP2A inhibitor, was assessed. Both tested IGF2BP1 knockout cell lines showed a higher sensitivity to Doxorubicin compared to control cells, with slight changes observed in KELLY (1.5-fold) or NBL-S (1.4-fold) cells, respectively (Figure 40f). These findings are consistent with previous publications in neuroblastoma and colorectal cancer, which have reported altered drug sensitivity after IGF2BP1 inhibition or knockdown (Bell *et al.* 2015, Biegel *et al.* 2021, Betson *et al.* 2022). It has been published that IGF2BP1 influences MDR1 mRNA stability by binding to the CRD and inhibiting endonucleolytic digestion of the mRNA (Sparanese and Lee 2007), thereby modulating drug efflux via MDR1, which could explain the shift towards higher sensitivity.

4.8 Establishment of a new neuroblastoma transgenic mouse model

4.8.1 LSL-IGF2BP1 transgenic mice induces neuroblastoma in synergy with MYCN

To investigate the oncogenic potential of IGF2BP1 in a sympatho-adrenal, non-immune compromised neuroblastoma model, transgenic mice expressing LSL-IGF2BP1-IRES-iRFP were established in a C57BL6/NCrl background, essentially as previously described for MYCN and Lin28b (Molenaar *et al.* 2012a, Althoff *et al.* 2015; Figure 41a). The model was designed to simulate enhanced expression of IGF2BP1 in neuroblastoma. Notably, the approximately 9 kb long IGF2BP1 3'UTR was discarded to enhance expression by preventing miRNA-directed downregulation, primarily by let-7 miRNAs (Busch *et al.* 2016). The system utilized a stop cassette to block transcription, which could be excluded upon co-expression of a CRE recombinase, inducing transcription of the transgene under a synthetic CAG promoter (CMV early enhancer element, first exon and intron of the chicken β -actin gene, splice acceptor of the rabbit β -globin gene). Additionally, iRFP is co-expressed to track transgenic cells. To assess the synergy with MYCN *in vivo*, the LSL-MYCN mouse model was obtained from Johannes Schulte (Charité Berlin), expressing a luciferase instead of an iRFP (Figure 41b). Specific transcription in peripheral nerves and adrenal gland tissue was achieved by using a *Dbh*-driven CRE for directing recombination to sympatho-adrenal cell lineages. Validation of heterozygous or homozygous transgene integration at the *Rosa26* locus was performed using gDNA-PCR (Figure 41c). LSL-IGF2BP1 mice were fertile and offspring were born according to Mendelian ratio.

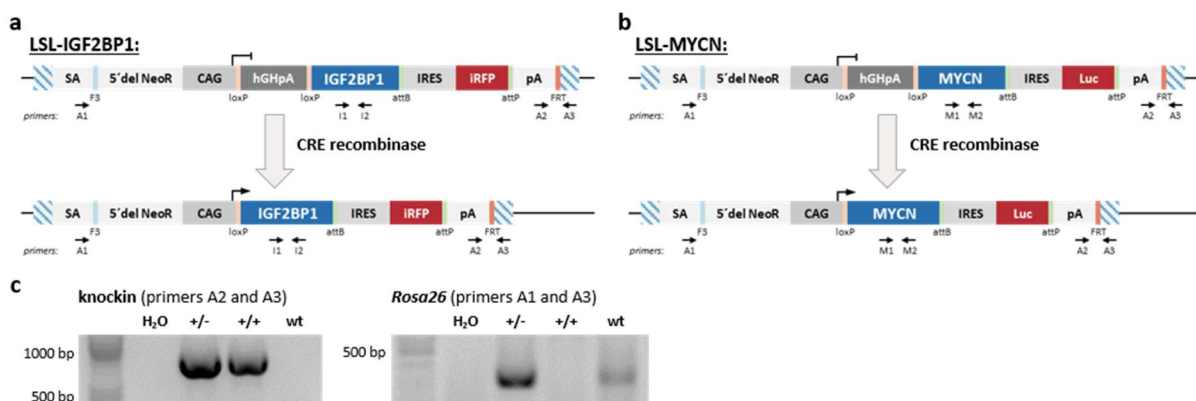


Figure 41: Scheme of transgenic mouse system. (a, b) Schematic overview of the LSL-transgene expression of IGF2BP1 and iRFP (a) or MYCN and luciferase (b), respectively, from the *Rosa26* locus. Location of primers used for genotyping (A1, A2, A3, I1, I2, M1, M2) are indicated. Splice acceptor site (SA), neomycin resistance (5'del NeoR), the synthetic promoter (CAG), transcriptional stop cassette made of the human growth hormone polyadenylation signal (hGHpA), transgene open reading frame (blue), internal ribosomal entry site (IRES), iRFP or luciferase open reading frame (red), polyadenylation signal (pA), recombination sites of the bacteriophage (loxP), λ integrase (attP, attB) and *Saccharomyces cerevisiae* (F3, FRT). (c) Representative genotyping PCR validating the transgene knockin (left, primers A2 and A3) and the wildtype *Rosa26* locus (right, primers A1 and A3) in heterozygous (+/-), homozygous (+/+) and wildtype (wt) mice.

No tumor formation was observed in the controls LSL-*IGF2BP1*, LSL-*MYCN* or *Dbh-iCRE* mice. Heterozygous LSL-*IGF2BP1*;*Dbh-iCRE*^{+/-} ($R26^{IGF2BP1/-}$) mice displayed a low tumor burden, with only one out of eight mice developing tumors within one year (Figure 42a). In contrast, mice with homozygous LSL-*IGF2BP1*;*Dbh-iCRE*^{+/-} ($R26^{IGF2BP1/IGF2BP1}$) developed tumors with 100% incidence (7 out of 7 mice) and ethical culling was required after 169 to 305 days (median survival 234 days), indicating a strong dose-dependent role of IGF2BP1 in neuroblastoma initiation. Surprisingly, no tumor formation (0 out of 6 mice) was observed in heterozygous LSL-*MYCN*;*Dbh-iCRE*^{+/-} ($R26^{MYCN/-}$) mice, contrary to previously published data (Althoff *et al.* 2015). Strikingly, however, when the IGF2BP1 and MYCN transgenes were co-expressed in double transgenic mice ($R26^{IGF2BP1/MYCN}$), tumor incidence was 100% (8 out of 8 mice) and median survival was reduced to 107 days (65 to 159 days), validating a strong synergy between IGF2BP1 and MYCN in promoting neuroblastoma. Most IGF2BP1-induced tumors ($R26^{IGF2BP1}$, 7 out of 8) were located in the lower abdomen, potentially arising from sympathetic nerves, while only one tumor originated from the adrenal gland (Figure 42b). Representative, macroscopic images of tumor locations are depicted in Figure 42c (left and middle). In contrast to other neuroblastoma models, no other primary tumor sites or macrometastases were observed. Notably, the IGF2BP1/MYCN transgene expression substantially elevated tumor burden per animal, with 19 tumors observed in 8 mice. Among these, 75% harbored tumors derived from the adrenal gland, 62.5% contained abdominal tumors and 50% showed tumors along the spine (Figure 42b). An example for a tumor along the spine is depicted in Figure 42c (right) indicated by the arrows. High iRFP signal and therefore IGF2BP1 expression in these tumors was confirmed using near-infrared imaging. Mice harboring tumors along the spine experienced paralysis of the hind legs, probably due to compression of the spinal cord. Histological examination of the tumors confirmed neuroblastoma characteristic small round blue tumor cell morphology and elevated nuclear Phox2b protein expression (Figure 42d).

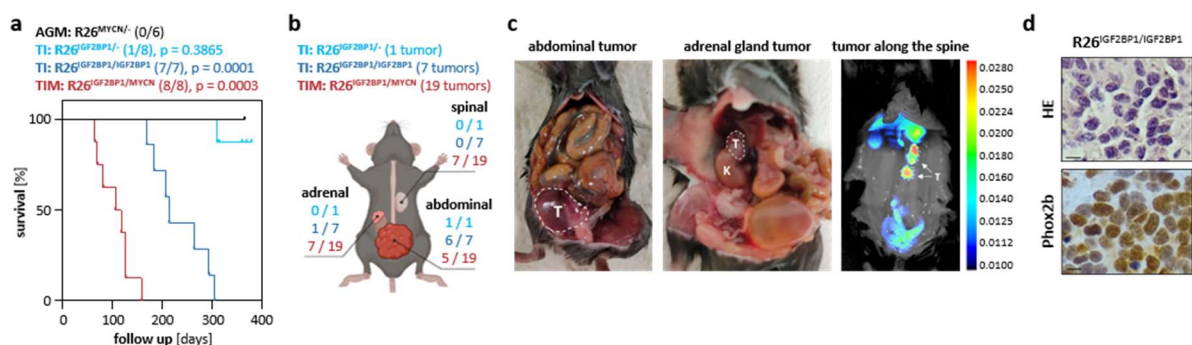


Figure 42: IGF2BP1 induces neuroblastoma tumor formation. (a) Kaplan-Meier survival analysis of heterozygous (cyan, $n = 8$) and homozygous (blue, $n = 7$) $R26^{IGF2BP1}$, heterozygous $R26^{MYCN}$ (black, $n = 6$) and double transgenic $R26^{IGF2BP1/MYCN}$ (red, $n = 8$) mice. Numbers in brackets indicate tumor bearing mice. (b) Scheme of tumor locations and burden within mice. (c) Representative images of tumors in the abdomen (left), in the adrenal gland (middle) or along the spine (right). Fluorescence intensity of iRFP is shown in the right picture (red = high). T - tumor, K - kidney (d) Representative images of hematoxylin and eosin staining (HE, top) and Phox2b immunohistochemistry (bottom) indicative for neuroblastoma in $R26^{IGF2BP1/IGF2BP1}$ mice (bars: 40 μ m).

To validate the expression of the transgenes and understand the molecular characteristics of the induced tumors, various analyses were performed. Western blot analysis confirmed upregulation of IGF2BP1/Igf2bp1 at the protein level in non-tumorous adrenal glands (AI) and further increased in tumors (TI, Figure 43a). Notably, IGF2BP1 transgene expression resulted in a moderate (AI) to strong (TI) upregulation of murine Mycn protein expression. In comparison, MYCN transgene expression was low in R26^{MYCN/-} adrenal glands (AGM) and accordingly this model failed to induce malignancies. However, in IGF2BP1/MYCN-transgenic adrenal glands (AIM) and tumors (TIM), MYCN/Mycn protein abundance was substantially increased, although protein expression was barely associated with abundance of the respective mRNAs (Figure 43b). This supports previously findings in cell culture, suggesting that IGF2BP1 not only regulates MYCN mRNA fate, but also modulates MYCN protein turnover in a probably indirect manner (chapter 4.6.4).

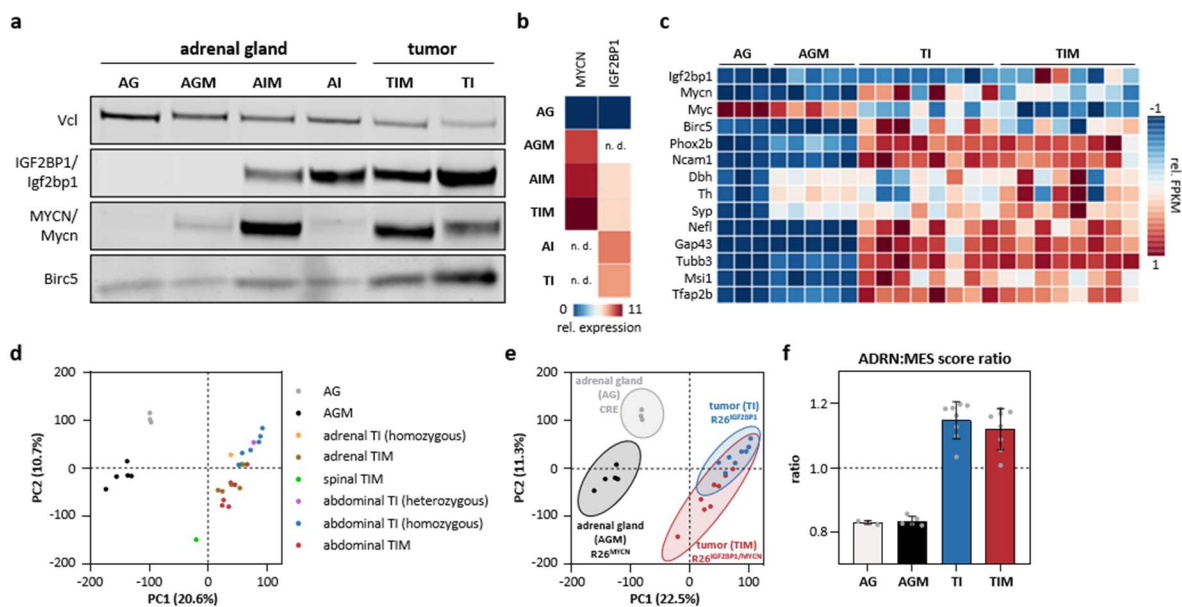


Figure 43: IGF2BP1-induced tumors express neuroblastoma marker genes. (a) Western blot analysis of IGF2BP1 and MYCN transgene expression in tumors and adrenal glands of representative mice ($n = 1$). (b) RT-qPCR analysis of human IGF2BP1 and MYCN mRNA in indicated mouse tissues/tumors (n. d. - not determined). (c) Heatmap depicting row-scaled FPKM values of indicated murine mRNAs in adrenal glands and tumors. (d, e) PCA of mouse adrenal glands and transgenic tumors split by their location (d) or by one tumor per mouse (e). (f) Ratio of adrenergic (ADRN) to mesenchymal (MES) signature of mouse adrenal glands and transgenic tumors. AG - adrenal gland, AGM - adrenal gland from R26^{MYCN/-}, AIM - adrenal gland from R26^{IGF2BP1/MYCN}, AI - adrenal gland from R26^{IGF2BP1}, TIM - tumor from R26^{IGF2BP1/MYCN}, TI - tumor from R26^{IGF2BP1}

Consistent with IGF2BP1/MYCN-driven expression of chromosome 17q oncogenes, Birc5 protein was significantly upregulated in tumors (Figure 43a). RNA analysis confirmed upregulation of murine Mycn, especially in IGF2BP1-induced tumors, while Myc expression was diminished (Figure 43c). Moreover, murine Igf2bp1 was slightly and Birc5 strongly increased in tumors derived from both models. Furthermore, several neuroblastoma marker genes such as Phox2b, Ncam1 or Dbh were substantially increased in IGF2BP1- and IGF2BP1/MYCN-induced tumors, while in MYCN-expressing adrenal glands no or only slight upregulation could be observed. These findings provided strong evidence that

neuroblastoma was induced in both models, which was further supported by elevated expression of sympatho-adrenal (e.g. *Th*), neural (e.g. *Gap43*), neural stem cell (e.g. *Msi1*) and neural crest cell markers (e.g. *Tfap2b*) among others (Althoff *et al.* 2015, Lignell *et al.* 2017). Principal component analysis (PCA) of RNA-seq data from all IGF2BP1- and IGF2BP1/MYCN-induced tumors as well as normal and MYCN-transgenic adrenal glands revealed clear separation of normal adrenal gland tissue, non-tumorous adrenal glands and tumors (Figure 43d). However, IGF2BP1- and IGF2BP1/MYCN-induced tumors clustered together, indicating that gene expression of tumors is largely independent of location and transgene combination. Re-evaluation, considering only one tumor per animal, confirmed the overall results (Figure 43e). Investigation of previously published adrenergic (ADRN) versus mesenchymal-like (MES) gene expression signatures (van Groningen *et al.* 2017) revealed a mesenchymal-like pattern in normal and MYCN-transgenic adrenal glands (Figure 43f). In contrast, both IGF2BP1- and IGF2BP1/MYCN-induced tumors exhibited an adrenergic neuroblastoma signature. In conclusion, these findings demonstrate a high similarity of gene expression profiles between IGF2BP1- and IGF2BP1/MYCN-induced tumors. Moreover, this provides the first evidence that IGF2BP1 is a strong oncogene in neuroblastoma, which induces tumor formation on its own and synergizes with MYCN in promoting tumor development.

Gene set enrichment analysis (Subramanian *et al.* 2005) based on RNA-seq data was conducted to gain insights into the molecular pathways and gene expression patterns associated with IGF2BP1- and IGF2BP1/MYCN-induced tumors. A substantial upregulation of pro-proliferative gene sets, such as E2F targets and G2/M checkpoint, was observed in tumors compared to normal adrenal glands (Figure 44a left). Concurrently, tumor-suppressive gene sets, including the p53 and apoptosis pathways, were downregulated. Consistent with the marked elevation of MYCN/*Mycn* expression in these tumors, the canonical MYC/N-driven gene expression (MYC targets V1) was significantly upregulated. In contrast, MYCN-transgenic adrenal glands exhibited an opposite effect on these hallmark gene sets, indicating a strong IGF2BP1/MYCN-dependent induction and progression of tumors. Intriguingly, there was a prominent association of hallmark normalized enrichment scores (NES) between tumors. This, however, was not observed in comparison to MYCN-transgenic adrenal glands, further supporting the gene expression similarity between IGF2BP1- and IGF2BP1/MYCN-induced tumors as well as the pivotal role of IGF2BP1 in promoting neuroblastoma growth in a MYCN-dependent manner (Figure 44b). To gain more insights into the specific gene signatures associated with these tumors, GSEA was conducted using larger curated gene set collections, the human C2 and mouse M2 (Figure 44c). GSEA in C2 revealed upregulation of gene signatures characteristic of pediatric cancer and MYC/N-driven gene expression in both tumor models (Figure 44a middle). Strikingly, IGF2BP1- but not IGF2BP1/MYCN-induced tumors showed upregulation of gene sets associated with neuroblastoma copy number gain. One of the strongest upregulated gene sets in C2 was the DREAM target pathway

(Fischer *et al.* 2016), which partially overlaps with the hallmark gene set E2F targets. Despite known cross-talk of MYC/N and E2F-driven gene expression, this supports IGF2BP1-dependent stimulation of RB-E2F-controlled cell cycle genes, as previously reported (Müller *et al.* 2020), and suggests an additional role of IGF2BP1 in activating DREAM-repressed cell cycle genes. Supporting this observation, several analyzed genes, including BIRC5 and AURKA, both canonical DREAM targets, were upregulated in transgenic tumors (Figure 44d).

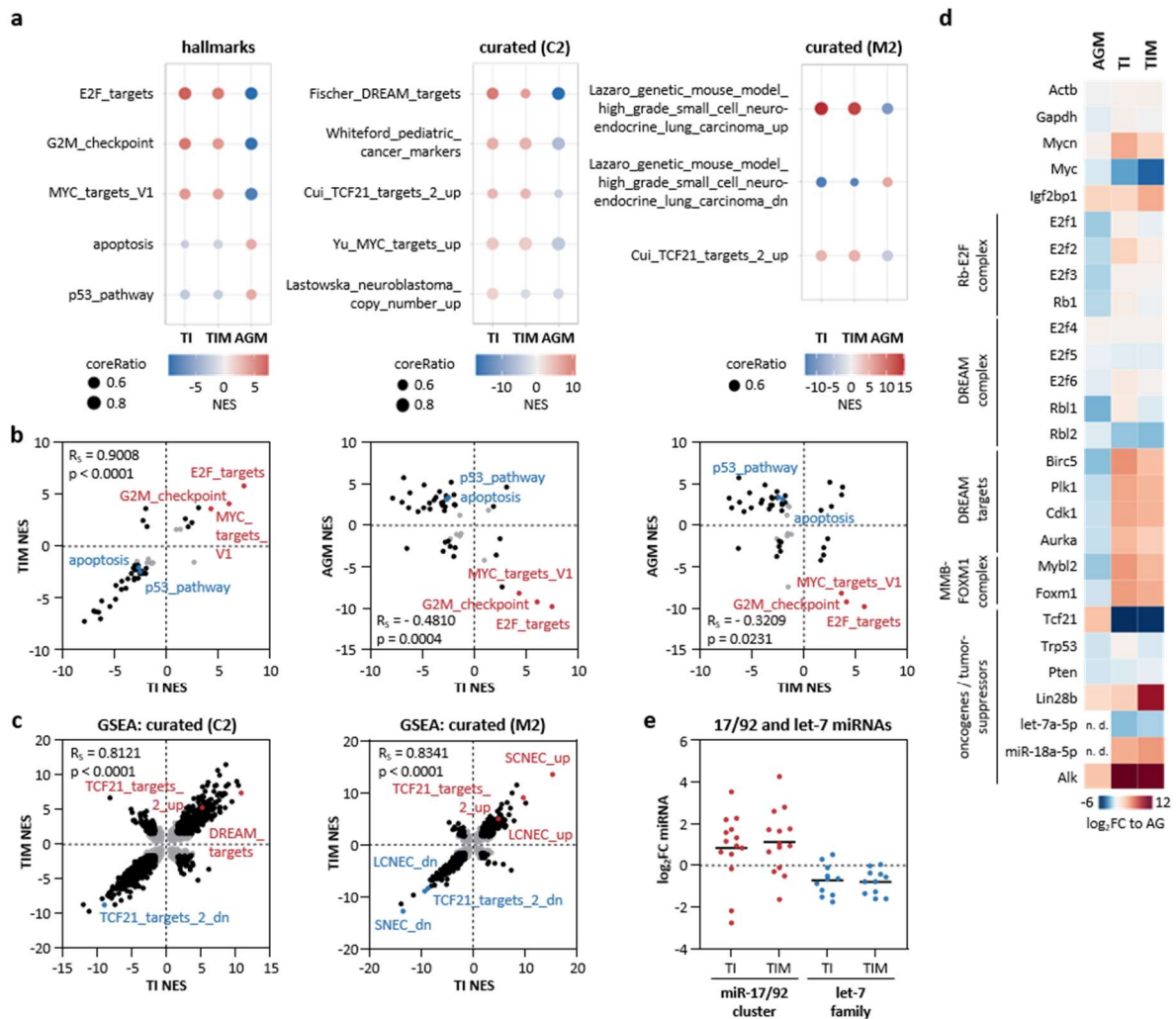


Figure 44: GSEA confirmed similarity of IGF2BP1- and IGF2BP1/MYC-induced tumors. (a) Selected hallmark (left), human C2 (middle) and mouse M2 (right) gene sets in TI, TIM and AGM mice based on GSEA. (b) Correlation of NES values of hallmark genes sets between TI and TIM (left), TI and AGM (middle) as well as TIM and AGM (right). Non-significant gene sets are depicted in grey. Spearman correlation coefficient and p-values are indicated. (c) Correlation of NES values of C2 (left) and M2 (right) gene sets between TI and TIM. Non-significant gene sets are depicted in grey. Spearman correlation coefficient and p-values are indicated. (d) RNA-seq analysis of indicated mRNAs presented as \log_2 fold change (\log_2 FC) compared to wildtype adrenal glands. (e) \log_2 FC of miRNAs from the miR-17-92 cluster (red) and let-7 family (blue) between TI or TIM and normal adrenal gland tissue. SCNEC/LCNEC - genetic mouse model of high-grade small/large-cell neuroendocrine lung carcinoma

Another highly deregulated pathway was TCF21-controlled gene expression. Accordingly, the expression of TCF21, a crucial developmental transcription factor and strong tumor suppressor (Ao *et al.* 2020), was essentially abolished in both tumor models (Figure 44d). GSEA in M2 further confirmed

TCF21-dependency and revealed similarities with high-grade small- (SCNEC) and large-cell (LCNEC) neuroendocrine lung carcinoma mouse models (Figure 44a right). These were derived by combined deletion of two key tumor suppressors, e.g. Pten and p53, or the combination of these losses with disturbing E2F-/DREAM-repression of cell cycle gene by deleting Rb1 or Rbl1/Rbl2 (Lazaro *et al.* 2019). In the IGF2BP1- and IGF2BP1/MYCN-induced neuroblastoma tumors, only Rbl2 was decreased, whereas Trp53, Rb1, Rbl1 and Pten mRNA expression remained largely unchanged (Figure 44d). The downregulation of Rbl2, a key target of the MYC/N-driven miR-17-92 cluster (Tseng *et al.* 2018), instructed an analysis of miRNA expression in both tumor models. Consistent with the upregulation of MYCN/Mycn, most members of the pro-tumorigenic miR-17-92 cluster were upregulated in IGF2BP1- and IGF2BP1/MYCN-induced tumors (Figure 44e). This upregulation strongly supports the strong impact of IGF2BP1 in disrupting the miRNA-dependent degradation of MYCN and presumably other mRNAs. In contrast, the rather tumor-suppressive let-7 miRNA family was overall decreased, which likely involves the modest to strong upregulation of Lin28b in tumors, a powerful suppressor of let-7 miRNA biogenesis (Figure 44d).

4.8.2 IGF2BP1 induces chromosomal aberrations syntenic to human disease

GSEA revealed that genes upregulated in IGF2BP1-induced tumors are also upregulated in human neuroblastoma by copy number gain. To investigate the genomic landscape associated with these tumors and normal tissue, sWGS was performed. In line with the lack of tumor induction in MYCN-only transgenic animals, no chromosomal aberrations were observed in adrenal glands compared to wildtype tissue (Figure 45a). In contrast, IGF2BP1/MYCN-induced tumors exhibited modest gains at murine chromosome 11 (< 20%) and pronounced gains at chromosome 6 (up to 50%), with minimal deletions observed (Figure 45b). Notably, murine chromosome 11q corresponds to the human chromosome 17q region and contains the *Igf2bp1* locus. Similarly, most parts of the murine chromosome 6 correspond to human chromosomes 7 and 12. Given that chromosome 17q and 7 are frequently gained in neuroblastoma (Table 22), these aberrations likely support the formation of neuroblastoma, but remain modest, probably due to the transgenic induction of two oncogenes and reduced tumor latency. Transgene expression may be enhanced further by amplification at chromosome 6, harboring the *Rosa26* locus, the integration site of the transgene cassettes. IGF2BP1-induced tumors stood out by substantially expanded chromosomal aberrations (Figure 45c). Only few deletions were observed on chromosomes 4, 9, 14 and 16. More strikingly, substantial gains were present at chromosomes 1, 6, 11q, 12 and 17. Murine chromosome 4q contains parts of human chromosome 1, where 1p deletions (e.g. harboring the miR-34a locus) are common in neuroblastoma. Similarly, chromosomes 9, 14 and 16 harbor genes located on human chromosome 3, which is frequently lost in human disease. Additionally, murine chromosome 9 contains parts of human

chromosome 11, another region with deletions in neuroblastoma. Furthermore, murine chromosomes 1, 6, 12 and 17 correspond to parts of human chromosome 2, with murine chromosome 12 harboring the *Mycn* locus. The strongest gains were observed for chromosome 11q, which is analogous to human chromosome 17q, including *Igf2bp1*. These findings suggest the acquisition of two strong oncogenic features, *MYCN* amplification and 17q gain, of neuroblastoma development through transgenic overexpression of IGF2BP1. To gain an overall picture of genomic aberration comparable to human disease, a chromosomal lift-over analysis was performed (Figure 45d). This analysis indicated that IGF2BP1 induces neuroblastoma reminiscent to human disease, including key chromosomal gains at 2p (*MYCN*) and 17q (*IGF2BP1*), as well as deletions at chromosome 1p, 3 and 11q. These observations highlight the relevance of IGF2BP1 overexpression in driving neuroblastoma tumorigenesis and support the suitability of the transgenic mouse model as a valuable tool for studying neuroblastoma development and genomic alterations contributing to the disease as well as suggest the respective mouse models as an appropriate tool for evaluating IGF2BP1-centered therapeutic approaches.

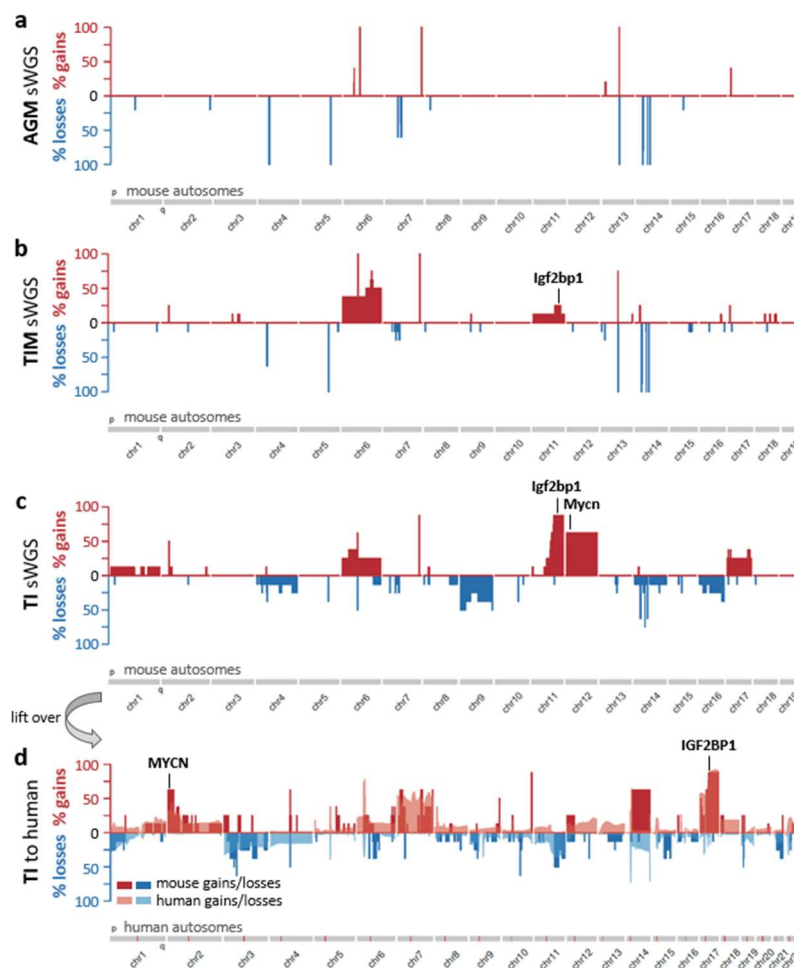


Figure 45: IGF2BP1-induced tumors harbor chromosomal aberrations syntenic to human neuroblastoma. (a-c) Frequency (%) of DNA copy number gains (red) and losses (blue) for murine chromosomes 1 to 19 in *MYCN*-transgenic adrenal glands (a), IGF2BP1/*MYCN*-induced tumors (b) or IGF2BP1-induced tumors (c) compared to wildtype adrenal glands. **(d)** Lift-over of the IGF2BP1-induced aberrations to the human genome (chromosomes 1 to 22). Overlay of human neuroblastoma sWGS is depicted in transparent colors. Murine and human IGF2BP1 and *MYCN* loci are indicated.

5. Discussion

IGF2BP1 and neuroblastoma: a nexus of tumorigenesis and therapeutic innovation

IGF2BP1, a prominent oncofetal mRNA-binding protein, is characterized by its pronounced expression in various cancers and its critical involvement in multiple developmental and cellular processes, including neural crest cell migration, neurite outgrowth modulation and stem-cell property regulation within the LIN28/let-7 signaling network (Yaniv and Yisraeli 2002, Yaniv *et al.* 2003, Perycz *et al.* 2011, Bell *et al.* 2013, Busch *et al.* 2016). Central to its oncogenic role is IGF2BP1's post-transcriptional stabilization of mRNAs, a mechanism that safeguards its target transcripts from miRNA-mediated degradation, a mechanism enhancing the expression of oncogenes like MYCN and pro-oncogenic factors like E2F1 (Noubissi *et al.* 2006, Köbel *et al.* 2007, Busch *et al.* 2016, Müller *et al.* 2018, Müller *et al.* 2020). Notably, IGF2BP1's regulatory influence encompasses diverse cancer types and is highly conserved in neuroblastoma (Bell *et al.* 2015). Within the scope of neuroblastoma, an investigation of RBPs in MYCN-amplified versus non-amplified tumors unveiled the upregulation of IGF2BP1 specifically in MNA tumors (Bell *et al.* 2020). This highlighted IGF2BP1 as a strong candidate oncogene since the *IGF2BP1* gene is located at the most frequently gained chromosomal region in neuroblastoma, 17q. In line with these findings, IGF2BP1 emerged as the prime candidate among essential genes located on chromosome 17 in this study (Figure 14, Table 23). Analyses of a cohort comprising 100 primary neuroblastoma tumors corroborated the increased expression of IGF2BP1 in aggressive subgroups such as MNA, INSS-stage 4 or cases marked by unbalanced 17q gain, as prior suggested (Bell *et al.* 2015; Figure 15). Furthermore, IGF2BP1's potential as an independent prognostic factor in predicting poor patient survival was confirmed, highlighting its significance as an oncogenic driver and as a promising target for therapeutic intervention. Functional analyses confirmed IGF2BP1's regulatory impact on proliferation and the self-renewal capacity of neuroblastoma cells, corroborating its effects in other malignancies (Köbel *et al.* 2007, Müller *et al.* 2018). This consistency was evident in the observed reduction of neuroblastoma cell line growth in both 2D and 3D cell culture models upon IGF2BP1 knockout or inhibition (Figure 25). Notably, this not only reduced cell viability but also marginally increased apoptosis. In support of this, IGF2BP1 deletion or inhibition also decreased growth of subcutaneous neuroblastoma xenografts (Figure 26, Figure 27). Collectively, these findings emphasize the pivotal role of IGF2BP1 in neuroblastoma tumorigenesis and substantiate its position as a promising therapeutic target. The convergence of *in vitro* and *in vivo* evidence accentuates the multifaceted potential of targeting IGF2BP1 for restraining neuroblastoma progression and potentially improving patient outcomes.

IGF2BP1 as guardian: uncoupling MYCN expression from miRNA regulation

A comprehensive analysis of miRNA expression profiles in primary neuroblastoma samples unveiled distinct miRNA expression signatures that effectively distinguish between MNA and nMNA tumors (Figure 17). This study successfully validated previously known miRNAs deregulated in MNA tumors, including members of the miR-17-92 cluster, let-7 family, miR-542, miR-9, miR-181a/b, miR-628-5p and miR-137-3p (Table 30; Schulte *et al.* 2008, Schulte *et al.* 2010, Mestdagh *et al.* 2010, Ma *et al.* 2010, Buechner and Einvik 2012, Fuziwara and Kimura 2015, Powers *et al.* 2016, Megiorni *et al.* 2017). In contrast to the prevailing notion that MYCN-regulatory miRNAs are predominantly downregulated in MNA neuroblastoma, supporting its high expression (Beckers *et al.* 2015b), the current investigation revealed a contrary trend with a majority of previously identified MYCN-targeting miRNAs being upregulated in MNA tumors. Particularly, the miR-17-92 cluster members emerged as prominent examples to this phenomenon (Figure 17, Figure 18). Notably, this is consistent with the established role of MYC transcription factors in stimulating this miRNA cluster via direct binding to E-Box elements in the promoter region (Schulte *et al.* 2008, Fuziwara and Kimura 2015). This research outcome strongly indicates that elevated MYCN expression in MNA neuroblastoma is not only supported by the downregulation of MYCN-regulatory miRNAs. Rather, it implies a mechanism that limits MYCN downregulation through these miRNAs.

The miTRAP experiments conducted in neuroblastoma and MYCN-expressing glioblastoma cell lines further validated the association of miR-17-92 cluster members with the MYCN 3'UTR, identifying these as prime candidates for targeting (Figure 18, Table 31). Surprisingly, despite their substantial abundance, let-7 family members exhibited only moderate enrichment with the MYCN 3'UTR in miTRAP studies. This suggests a more pivotal role of the miR-17-92 cluster and puts the postulated dominant role of the let-7 family into question. Along these lines, these findings challenge the previously postulated concept of the MYCN mRNA acting as a miRNA decoy, particularly for sequestering let-7 miRNAs (Powers *et al.* 2016). Reporter studies conclusively demonstrate that the MYCN 3'UTR lacks decoy activity, as evidenced by unaltered behavior of fluorescence reporter in response to the overexpression of GFP-tagged MYCN 3'UTR (Figure 19). This finding is consistent with the established influence of MYCN in promoting LIN28B expression (Beckers *et al.* 2015a), a potent suppressor of let-7 biogenesis (Viswanathan *et al.* 2008, Piskounova *et al.* 2011) and an inducer of neuroblastoma (Molenaar *et al.* 2012a). Particularly in MNA neuroblastoma, the co-upregulation of both MYCN protein and the miR-17-92 cluster highlights the intricate regulation of MYCN expression. This indicates a pivotal role of multilayered control of MYCN expression by trans-acting factors, including RBPs, which, like miRNAs, exert their control predominantly via the MYCN 3'UTR.

In this study, two RBPs were investigated that previously were reported to control MYCN expression in neuroblastoma, ELAVL4 and IGF2BP1 (Lazarova *et al.* 1999, Bell *et al.* 2015, Samaraweera *et al.* 2017). ELAVL4 showed decreased expression in MNA neuroblastoma (Figure 20), potentially due to losses at chromosome 1p, considering its location at 1p33-p32.3. Conversely, IGF2BP1 exhibited elevated expression in MNA neuroblastoma, consistent with earlier reports in primary tumors, MYC/N-driven transcriptional regulation and conserved oncofetal expression pattern (Noubissi *et al.* 2010, Bell *et al.* 2013, Bell *et al.* 2015). MNA neuroblastoma is considered an aggressive and de-differentiated disease. In this respect, the downregulation of ELAVL4 is consistent with its proposed role in promoting neural differentiation (Pascale *et al.* 2008), whereas the upregulation or *de novo* synthesis of IGF2BP1 is consistent with its known functions in various advanced, de-differentiated malignancies, as exemplified in anaplastic thyroid carcinoma (Haase *et al.* 2021). Moreover, IGF2BP1 shortens the G1 cell cycle phase and all members of the IGF2BP family were proposed to enhance a high self-renewal potential in stem cell-like lineages potentially, but not exclusively, relying on the enhancement of MYC (Müller *et al.* 2020, Samuels *et al.* 2020). The analysis of MYCN-3'UTR reporter studies emphasizes the influence of both ELAVL4 and IGF2BP1 in the modulation of MYCN expression through 3'UTR-dependent mechanisms (Figure 19). This is consistent with the reported role of ELAVL4 in antagonizing downregulation of MYCN expression by miR-17 and roles in 3'UTR-dependent enhancement of mRNA translation in neural and neuroblastoma-derived cells (Lazarova *et al.* 1999, Samaraweera *et al.* 2017). However, stimulation of MYCN-3'UTR reporter expression by ELAVL4 remained essentially unaffected by inactivating of the potentially overlapping miR-17 targeting sites. This suggests that ELAVL4 potentially regulates MYCN mRNA either by impairing other miRNAs, through a largely miRNA-independent mechanism or by enhancing mRNA translation in a 3'UTR-dependent manner. In contrast, the RNA-dependent regulation of MYCN-3'UTR reporters by IGF2BP1 is dependent on miRNA-mediated control, particularly involving miR-17 and other miRNAs.

This study successfully demonstrated the direct binding of IGF2BP1 to the MYCN mRNA through miTRAP and RIP experiments (Figure 21). Additional mRNA decay and luciferase reporter assays validated IGF2BP1's function in stabilizing the MYCN mRNA and safeguarding it from miRNA-induced degradation (Figure 22, Figure 23). Notably, IGF2BP1 also indirectly influenced the stabilization of MYCN protein turnover by promoting E2F/DREAM-regulated genes such as AURKA, PLK1 and CDK1 (Figure 35). In conclusion, these findings collectively substantiate the role of IGF2BP1 as a potent miRNA antagonist that upregulates MYCN mRNA and protein expression in neuroblastoma. This research advances our understanding of the complex regulatory network governing neuroblastoma initiation and progression, emphasizing the significance of miRNA-mediated deregulation and selective modulation of oncogene expression as driving forces in the disease.

IGF2BP1 and m⁶A modification: a unique binding preference without a clear motif

Recent investigations have identified IGF2BP1 as a novel m⁶A reader protein (Huang *et al.* 2018a). Intriguingly, certain target mRNAs, such as MYC or E2F1 (Huang *et al.* 2018a, Müller *et al.* 2020), appear to be regulated in an m⁶A-dependent manner by IGF2BP1. The postulated m⁶A reader function of IGF2BP1 remains a mystery since the protein lacks a classical m⁶A-binding domain (e.g. YTH domain) designed for sensing this modification. Nonetheless, IGF2BP1 has demonstrated a distinct preference for binding to m⁶A-modified mRNAs, which was independent of secondary structures, at least in the case of the MYC mRNA (Huang *et al.* 2018a). This intriguing observation raises the critical inquiry of how IGF2BP1 engages with m⁶A modifications. It was suggested that the KH3-4 di-domain is indispensable for m⁶A binding (Huang *et al.* 2018a), which is also the region with the greatest affinity for RNA binding (Farina *et al.* 2003). However, no conserved binding motif for IGF2BP1 was discovered yet, but could potentially include the RRACH motif for m⁶A modification. Alternatively, it is plausible that the KH3-4 di-domain within IGF2BP1 function as m⁶A-reader domain like the original YTH domain. Neither of these explanations offers a definitive rationale, necessitating further experiments to elucidate the underlying mechanism. Another mode of action could be the “m⁶A switch”, which is proposed for other RBPs (Sun *et al.* 2019). Thereby, the modification of the RNA induces a conformational change, exposing binding motifs for specific RBPs. In such a case, IGF2BP1 would not directly bind the m⁶A modification, but rather in its proximity and binding would be enhanced in the presence of the modification as it is exemplified for MYC (Huang *et al.* 2018a). This mode of binding would fit to IGF2BP1 as it is reported that IGF2BPs force their target mRNAs in a specific conformation upon binding (Chao *et al.* 2010). If this conformational change is also induced by the m⁶A modification, binding would be enhanced for IGF2BP1. In addition, the lack of a clear binding motif for years could indicate a motif-independent binding and may suggest that IGF2BPs bind their target mRNAs via specific conformations. This is supported by the fact that IGF2BPs are suggested to bind thousands of RNAs (Conway *et al.* 2016, Van Nostrand *et al.* 2016). Notably, the investigation into MYCN expression dynamics in neuroblastoma has suggested that IGF2BP1 predominantly influence MYCN expression through pathways independent of the m⁶A modification (Figure 24). In conclusion, the recent unveiling of IGF2BP1's engagement as an m⁶A reader adds a layer of complexity to the understanding of post-transcriptional gene regulation. While the exact mechanism of IGF2BP1's interaction with m⁶A-modified RNA remains enigmatic, its potential role in modulating MYCN expression appears largely independent of this modification since even upon depletion of the key writers of m⁶A modifications (METTL3/14) MYCN expression is mostly unaltered.

Unleashing the power of IGF2BP1 and MYCN: forging a potent feedforward loop

MYCN is the most studied and most important oncogene in neuroblastoma and its amplification is detected in a substantial proportion of cases (Maris and Matthay 1999, Park *et al.* 2010, Huang and Weiss 2013). Exploration of publicly available MYCN ChIP-seq data across various neuroblastoma cell lines (Oki *et al.* 2018) unveiled MYCN binding sites within the IGF2BP1 promoter region, as previously shown for MYC (Noubissi *et al.* 2010). This direct regulatory connection between MYCN and IGF2BP1 was further substantiated through nascent transcript synthesis assay and in TH-MYCN transgenic mice (Figure 16), confirming recent discoveries in breast cancer research (Shi *et al.* 2022). However, the depletion of MYCN led to an approximately 50% reduction in both IGF2BP1 protein and RNA expression. This observation suggests that additional transcriptional regulators influence the synthesis of IGF2BP1. To date, MYC/N, CTNNB1/TCF4 and EGR2 were shown to promote IGF2BP1 expression (Noubissi *et al.* 2006, Ying *et al.* 2021). Notably, MYCN depletion had minimal effect on CTNNB1 expression, which could be a potential explanation for the remaining IGF2BP1 expression. Intriguingly, an analysis of public ChIP-seq data via the ChIP-atlas (<https://chip-atlas.org/>) encompassing neural cell types, including neuroblastoma cell lines, spotlights numerous transcription factors binding to the IGF2BP1 promoter region. Among these, key neuroblastoma core regulatory circuit members, including GATA3, PHOX2B, HAND2, TBX2 and TFAP2B, emerged, all of which are upregulated in IGF2BP1-induced transgenic tumors. Further RNA-seq analysis illustrated the upregulation of GATA3 and HAND2 in MYCN-depleted BE(2)-C cells, which potentially rescues – at least partially – IGF2BP1 synthesis upon MYCN depletion. However, additional in depth analyses are required to decipher the complex transcriptional and likely epigenetic regulation of IGF2BP1 synthesis in cancer.

This study provides insight into the self-promoting feedforward loop between IGF2BP1 and MYCN in the context of tumorigenesis. The vast majority of MYCN-targeting miRNAs, predominantly the miR-17-92 cluster, are upregulated in MNA neuroblastoma. To counter the degradation orchestrated by these miRNAs, RBPs, particularly IGF2BP1, function as protective shields, inhibiting miRNA-directed downregulation. This protective role leads to increased mRNA stability, likely elevated mRNA translation and consequently to enhanced MYCN expression. Furthermore, IGF2BP1 itself is under direct transcriptional regulation by MYCN. This symbiotic relationship between the two proteins manifests as a transcriptional/post-transcriptional feedforward loop, effectively uncoupling MYCN expression from miRNA-dependent regulation (Figure 46).

On the edge of transformation: unraveling IGF2BP1's multifaceted influence in pediatric cancers

Moreover, the current study underscores the significance of the IGF2BP1/MYCN network, as both proteins exhibit overlapping downstream targets. This collaboration results in the enhancement of MYCN-driven transcription and IGF2BP1-mediated mRNA stabilization of oncogenic factors. Many of

these, including *NME1*, *PYCR1*, *TK1*, *BIRC5* and *TOP2A*, are located on chromosome 17q, exhibit upregulation in adverse neuroblastoma subgroups and are associated with poor patient survival (Islam *et al.* 2000, Chen *et al.* 2016, Huang *et al.* 2018a, Yogev *et al.* 2019, Adam *et al.* 2020; Figure 28, Figure 30). While certain genes, like *BIRC5* or *TOP2A*, were not identified as neuroblastoma-specific essential genes, direct targeting of these could pose challenges due to potential general toxicity. In contrast, *TK1* and *NME1* have been reported as IGF2BP1 or MYCN target transcripts, respectively (Godfried *et al.* 2002, Huang *et al.* 2018a, Shen *et al.* 2022). However, the other 17q gained genes are novel candidate targets for IGF2BP1- or MYCN-dependent regulation. Of the 177 identified neuroblastoma essential genes, two that were not examined in this study, *PRR11* and *CANT1*, have been previously reported as conserved IGF2BP1 target mRNAs in cancer (Glaß *et al.* 2021). Additionally, this list encompasses *ALYREF*, another chromosome 17q gene, suggested to drive oncogenesis by modulation MYCN protein turnover (Nagy *et al.* 2021). The here proposed regulatory network predominantly acts on both the transcriptional and post-transcriptional level of gene expression. The synergy between MYCN and IGF2BP1 is particularly pivotal in MNA disease, but it holds potential even in non-amplified and MYC/N-expressing neuroblastoma models, as shown in the case of NBL-S. The effectiveness relies on the broad spectrum of targets impacted by MYCN and IGF2BP1, which ultimately leads to escalated oncogene expression. The culmination of the IGF2BP1/MYCN-driven network results in an “oncogene storm”, likely contributing to genome destabilization. This emphasizes the impact of MYCN/IGF2BP1 synergy in reprogramming gene expression, irrespective of underlying genomic perturbations.

Moreover, IGF2BP1 plays a role in impeding apoptosis induced by DNA-damaging agents such as YM-155 and Doxorubicin. Overexpression of *BIRC5* in glioma cells led to increased DNA repair via non-homologous end joining and other IGF2BP1 targets, namely PPM1D (Wip-1) and *TOP2A*, are implicated in chromosome stability and apoptosis (Conde *et al.* 2017, Pechackova *et al.* 2017, Zhang *et al.* 2020). Consequently, IGF2BP1 might contribute to genomic instability by hampering apoptosis, potentially leading to the observed chromosomal gains in IGF2BP1-expressing murine and human tumors. Notably, IGF2BP1 governs cell death in rhabdomyosarcoma by regulating the translation of *clAP1* (*BIRC2*), a gene functionally related to *BIRC5* (Faye *et al.* 2015). Furthermore, in *Drosophila*, IGF2BP1 expression is imperative for allowing proliferation driven by transcription factors and preventing cellular dysfunction in brain cancer-initiating cells (Yang *et al.* 2017). Thus, it is plausible that IGF2BP1 facilitates MYC/N-driven proliferation in various contexts, including neuroblastoma, embryonal neuroblasts and other pediatric cancers reliant on MYC/N and characterized by aberrations at chromosome 17q, like rhabdomyosarcoma and medulloblastoma, as well as carcinoma in general.

Next to inhibition of apoptosis, IGF2BP1 was recently shown to modulate immune escape in hepatocellular and gastric cancer (Liu *et al.* 2022, Tang *et al.* 2023). IGF2BP1 overexpression led to

stabilization of the PD-L1 mRNA, therefore inhibiting activation of immune cells. Furthermore, MDM2 was shown to be an IGF2BP1 target transcript (Mu *et al.* 2022) and can induce protein degradation of IRF1 in ovarian carcinoma (unpublished data from Dr. Nadine Bley). Decreased IRF1 expression led to lower presentation of MHC class I molecules at the surface of tumor cells. Together with increased PD-L1 expression, this provides an effective escape mechanism of the host immune system, which can be targeted through IGF2BP1.

Navigating DREAM and E2F: IGF2BP1's dual role in cell cycle progression

Another notable finding centers on the robust correlation of IGF2BP1 and the G2/M checkpoint as well as the DREAM target gene cluster (Figure 33). Notably, the gene expression profile associated with IGF2BP1 is remarkably similar to that of MYBL2/FOXM1, the core transcriptional factors governing the activation of G2/M DREAM targets (Table 25; Fischer *et al.* 2016). Furthermore, IGF2BP1-transgenic mice showed substantial upregulation of the G2/M checkpoint and DREAM target gene sets, along with increased MYBL2 and FOXM1 expression levels (Figure 44). This pattern was further confirmed through IGF2BP1 knockdown analysis across different cancer cell line entities, consistently revealing a pronounced correlation with DREAM targets. The gene set attributed to DREAM targets partially overlaps with the E2F hallmark gene set, which is strongly influenced by IGF2BP1 due to its role in post-transcriptional regulation of E2F1/2/3 (Müller *et al.* 2020). Intriguingly, the downregulation of key kinases within the G2/M checkpoint was prominently observed upon IGF2BP1 depletion, implying potential direct regulation by IGF2BP1. Nevertheless, the in part preliminary results derived by luciferase reporter and RIP assays revealed only modest association between IGF2BP1 and these kinases (Figure 34). For instance, while PLK1 appeared substantially decreased by perturbing IGF2BP1, RIP assays failed to confirm strong association of IGF2BP1 with the PLK1 mRNA. Similar results were observed with AURKA, a gene implicated in the stability of chromosomes and apoptosis and recently suggested as a conserved IGF2BP1 target, like PLK1 and CDK1 (Glaß *et al.* 2021). Despite indications of influence on AURKA via knockdown and luciferase assays, the RIP analyses across three cell lines suggested an absence of direct binding between IGF2BP1 and AURKA mRNA. Nevertheless, these genes possess strong CLIP data for IGF2BP1 binding contradicting the results from the RNA immunoprecipitation. Possible explanations could be the experimental setup (cross-linking versus transient interaction), the sensitivity of the detection (high-throughput sequencing versus RT-qPCR) or RNA accessibility.

These discrepancies could potentially be reconciled if IGF2BP1 directly regulates MYBL2 and/or FOXM1 transcription factors, as these kinases are prominent targets of the MMB-FOXM1 complex. Moreover, FOXM1 has been previously proposed as a conserved target of IGF2BP1 (Glaß *et al.* 2021). Therefore, further investigations are imperative to elucidate the potential regulation of MYBL2 and FOXM1 by

IGF2BP1. Collectively, these findings indicate that IGF2BP1 might stimulate RB-E2F-controlled cell cycle genes via E2F1/2/3, further suggesting an additional role in activating DREAM-repressed cell cycle genes, potentially through MYBL2 and FOXM1. Consequently, IGF2BP1's involvement would span the entire cell cycle, not merely limited to G1/S transition as previously reported.

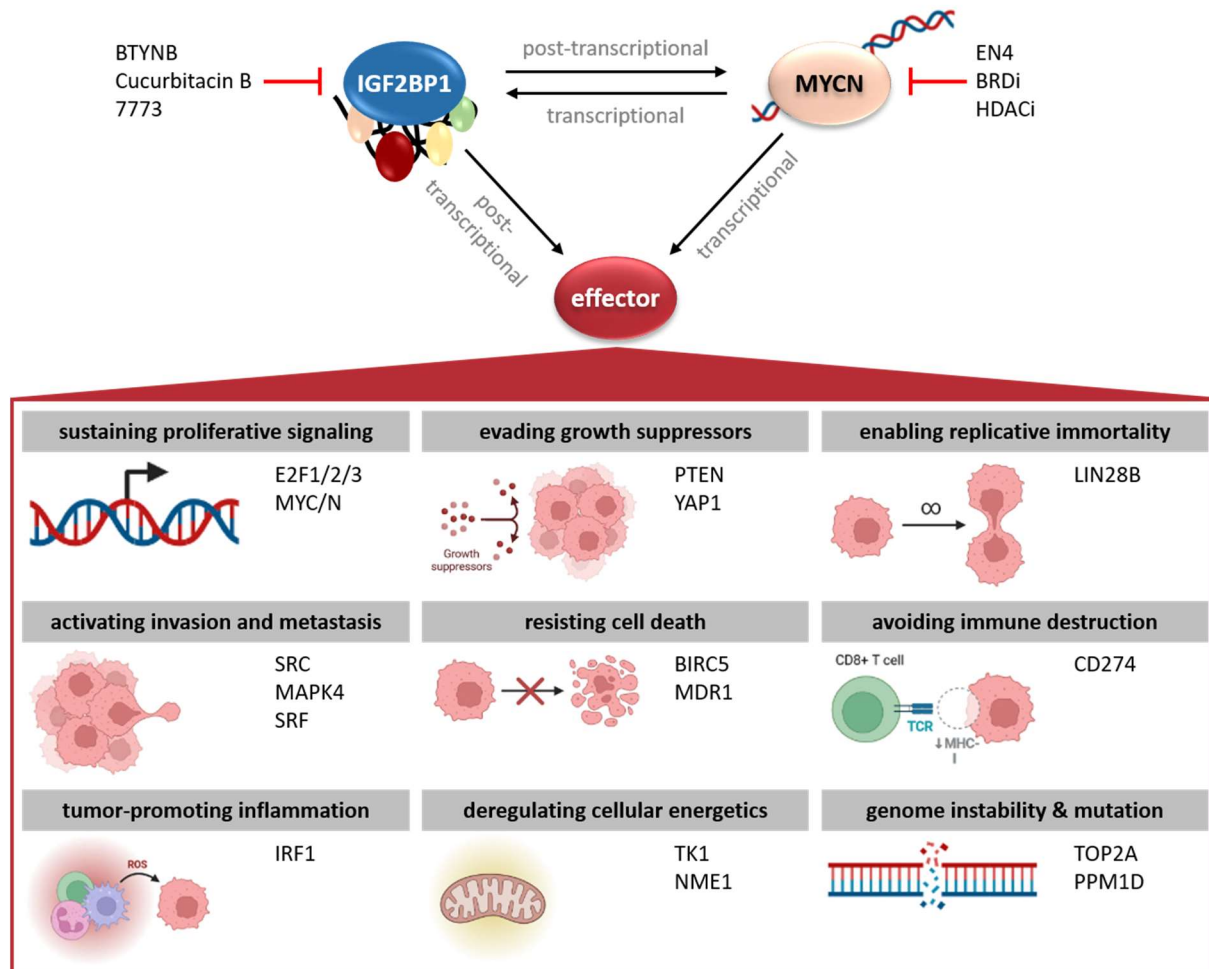


Figure 46: Feedforward loop between IGF2BP1 and MYCN influences the hallmarks of cancer. Scheme of the self-reinforcing feedforward loop of IGF2BP1 and MYCN, including shared downstream targets encompassing nearly all hallmarks of cancer and therapeutic potentials to disrupt this network.

In summary, this study uncovers the complex network between IGF2BP1 and MYCN, shedding light on their collaboration in the progression of neuroblastoma. The interplay between these proteins extends to downstream targets, leading to enhanced expression of various oncogenic factors encompassing nearly all hallmarks of cancer (Figure 46). This synergy has major impact beyond MNA disease and likely also influences other molecular subtypes of neuroblastoma, for instances when MYCN is upregulated by translocation as seen in NBL-S cells (Zimmerman *et al.* 2018). Irrespective of the amplification status of *MYCN*, the strong synergy between IGF2BP1 and MYCN unleashes an "oncogene storm". This likely promotes genomic instability, highlighting the relevance of the IGF2BP1/MYCN crosstalk in reprogramming gene expression to foster the expression of aggressive diseases. Additionally, IGF2BP1's role in impeding apoptosis and its broader implications in various cancers

emphasize its multifaceted impact. However, IGF2BP1's role in G1/S transition, the shortening of G1 phases and the here revealed role in modulating the G2/M checkpoint and DREAM target genes highlights its complex role in cell cycle regulation, calling for further investigation into the regulatory mechanisms at play.

IGF2BP1's tumorigenic prowess: dose dependency and genomic instability

The available literature on IGF2BP1 transgenic mouse models remains limited, particularly in the context of neuroblastoma. Presently, only three distinct IGF2BP1 transgenic mouse models have been documented. Firstly, an overexpression model inducing mammary carcinoma in lactating mice was established within 60 weeks, utilizing the WAP promoter to drive IGF2BP1 expression (Tessier *et al.* 2004). Secondly, knockout of IGF2BP1 by gene trap yielded significant effects in mice, including enhanced embryonal lethality, dwarfism of survivors and impaired gut development (Hansen *et al.* 2004). Additionally, complete IGF2BP1 knockout were reported to be embryonal lethal (International Mouse Phenotyping Consortium). Thirdly, a murine model involving intestine-specific knockdown of *Igf2bp1* resulted in a marked reduction of tumor formation in the *Apc*^{Min/+} mouse model, which pertains to intestinal tumorigenesis (Hamilton *et al.* 2013). Likewise, in *Drosophila melanogaster*, loss-of-function mutations in dIMP (the orthologue of IGF2BP1/2/3) were found to be lethal during zygotic stage (Boylan *et al.* 2008). Moreover, in *Drosophila* embryos, dIMP expression was identified as a prerequisite for the induction of neuroblast tumor growth by the transcription factor chinmo (Narbonne-Reveau *et al.* 2016).

To date, transgenic models of neuroblastoma primarily entail the overexpression of MYCN, *Lin28b* or mutant ALK, utilizing different driver lines (Weiss *et al.* 1997, Berry *et al.* 2012, Heukamp *et al.* 2012, Molenaar *et al.* 2012a, Althoff *et al.* 2015, Ueda *et al.* 2016). However, in this study, the capacity of IGF2BP1 to robustly induce neuroblastoma tumor formation was established using a C57BL6/NCrl background (Figure 41), with a strictly dose-dependent response to IGF2BP1 levels. Higher incidence and shorter latency were observed specifically in mice homozygous for IGF2BP1 (Figure 42). Notably, these tumors exhibited severe genomic aberrations reminiscent of human disease (Figure 45), including gains on chromosome 11q (human chromosome 17q) and 12 (including the *Mycn* locus). Additionally, a comparative analysis with existing transgenic neuroblastoma models revealed high similarity between the LSL-*IGF2BP1* and the LSL-*ALK*^{F1174L} model. Both models induced tumor formation with extended latency and substantial genomic aberrations (Heukamp *et al.* 2012). In contrast, the LSL-*Lin28b* and *MYCN* models exhibited faster tumor onset with fewer chromosomal rearrangements (De Wilde *et al.* 2018). The reliance on genomic events in these mouse models suggests a weaker oncogenic potential for *IGF2BP1* and mutant *ALK*, necessitating a secondary hit for tumor initiation. Intriguingly, the co-expression of human *MYCN* in conjunction with either *IGF2BP1* or *ALK*^{F1174L}

significantly shortened tumor latency and reduced genomic aberrations, indicating the compensatory role of *MYCN* overexpression as a secondary hit. Interestingly, regardless of the transgene employed (various *ALK* models or *IGF2BP1*), co-expression of *MYCN* consistently resulted in a 100% tumor incidence, underscoring the pivotal role of *MYCN* in neuroblastoma. This is supported by findings from homozygous TH-*MYCN* mice, which demonstrated higher incidence, shorter latency and fewer genomic aberrations compared to their heterozygous counterparts (Rasmuson *et al.* 2012). This suggests that *MYCN* amplification, generally considered a later event in neuroblastoma development, necessitates a prerequisite state of genomic instability in normal cells. However, overexpressing transgenic *MYCN* at sufficiently high levels, as seen in homozygous TH-*MYCN* mice, seems to circumvent this prerequisite. In contrast, *LIN28B*, a potent oncogene, exhibits distinct behavior, as evidenced by the LSL-*Lin28b* model's limited genomic aberrations, implying that *LIN28B* may not require a secondary hit for tumor initiation (Molenaar *et al.* 2012a). This may be due to the broad impact of *LIN28B* on gene expression by downregulation of let-7 miRNA family, which likely affects hundreds of target genes, including *IGF2BP1* (Boyerinas *et al.* 2008, Viswanathan *et al.* 2008). Collectively, these findings indicate that *ALK* mutation or *IGF2BP1* overexpression can trigger genomic instability, leading to chromosomal aberrations, including *MYCN* amplification, culminating in tumor formation. The co-expression of either of these factors with *MYCN* obviates the need for destabilization, resulting in accelerated and aggressive tumor formation avoid of genomic aberrations. In addition, *IGF2BP1* was recently shown to modulate *ATRX* expression (Yu *et al.* 2021). Thereby, *IGF2BP1* can contribute to alternative telomere lengthening and subsequent immortalization of cells. In support with that, *IGF2BP1* can also influence *TERT* expression by enhancing *MYCN* expression, contributing to stabilization of chromosome ends.

This study did not yield tumors within the LSL-*MYCN* model, contrary to prior reports (Althoff *et al.* 2015). This discrepancy is likely attributed to the mouse strain used in the study, although it was previously proposed that LSL-*MYCN* models induce tumors regardless of genetic background. Mice in this study were of a C57BL6/NCrl background, while the LSL-*Lin28b* and TH-*MYCN* mouse models were conducted on the more tumor-susceptible 129x1/SvJ strain. Furthermore, the published LSL-*MYCN* model encompassed a mixed C57BL6 x 129x1/SvJ background. The only other model demonstrating tumor formation on a pure C57BL6 background was the LSL-*ALK*^{F1174L} model, whereas models such as TH-*ALK*^{F1174L} or a transgenic knockin of *ALK*^{R1275Q} failed to induce tumors. Evidently, the C57BL6 strain demonstrated a lower tumor penetrance in neuroblastoma mouse models, leading to a drop in tumor incidence from 20-50% to 0-10% in heterozygous TH-*MYCN* mice (Weiss *et al.* 2000, Rasmuson *et al.* 2012). Thus, the choice of the mouse strain obviously influences the capability of tumor formation.

The more aggressive *MYCN* and *Lin28b* mouse models displayed the emergence of multiple tumors across different regions, including the adrenal glands and various ganglia in the neck, chest and the abdomen (e.g. ganglion celiacum, superior cervical ganglion). In line with this, *IGF2BP1/MYCN*-expressing mice also developed multiple tumors originating from the adrenal glands or peripheral nerves. Conversely, mice expressing *IGF2BP1* alone predominantly developed a single abdominal tumor, with no additional primary sites or macrometastases detected.

Investigation into chromosomal aberrations across all neuroblastoma mouse models revealed a prevalence of gains over losses. Losses were predominantly found on chromosome 4q and 9 in LSL-*ALK*^{F1174L} and LSL-*IGF2BP1* tumors, supporting the hypothesis that secondary events are essential for tumor formation. These regions correspond to human chromosome 1p36 and 11q, respectively, both frequently lost in neuroblastoma and potentially harboring tumor suppressor genes. Additionally, numerous murine chromosomes (5, 9, 14 and 16) exhibited deletions across various models, corresponding to human chromosome 3 or 4 regions, which are commonly lost in neuroblastoma. The most frequent chromosomal gain observed in all transgenic neuroblastoma models pertained to murine chromosome 11q, which is syntenic to the human chromosome 17q harboring the *IGF2BP1/Igf2bp1* locus. This chromosomal aberration is also the most frequent in human, highlighting its significance in neuroblastoma initiation and progression (Bown *et al.* 1999). Among the mouse models, the LSL-*IGF2BP1* model displayed the most substantial gains, reinforcing the notion of a secondary hit. Other recurrent chromosomal aberrations included gains on chromosome 3 (omnipresent except for *IGF2BP1*-induced tumors), 6 (*MYCN* and *IGF2BP1* models) and 12 (particularly LSL-*ALK*^{F1174L} and LSL-*IGF2BP1* models), corresponding to human chromosomes 1q, 2p, 7, 12p and 14q. These aberrations encompass well-known genomic events like 1q gain in MNA disease, whole chromosome 7 gain in up to 50% of cases or *MYCN* amplification on chromosome 2p (Figure 12, Table 22). Notably, this amplification likely contributed essentially to enhanced protein and mRNA expression of *Mycn* in *IGF2BP1*-induced tumors (Figure 43).

Assessing the overall expression patterns of LSL-*IGF2BP1* and LSL-*IGF2BP1/MYCN* tumors revealed striking similarities, as determined through PCA and GSEA (Figure 43, Figure 44). Pro-proliferative gene sets, such as E2F targets, G2/M checkpoint, *MYC* targets or Fischer DREAM targets, were markedly upregulated. Conversely, anti-proliferative gene sets encompassing p53 pathway and apoptosis were downregulated. This is in line with RNA-seq data obtained from *IGF2BP1* knockdown in neuroblastoma and other carcinoma cell lines, which highlights the inverse modulation of these gene sets, offering plausible explanation for tumor growth. Additionally, the gene expression patterns observed in transgenic tumors closely mirrored those of human disease and other transgenic mouse models, emphasizing the marked upregulation of neuroblastoma marker genes like *Phox2b*, *Ncam1*, *Syp*, *Th* or

Dbh (Figure 44). Furthermore, characteristic histological findings were noted, including the small round blue tumor cell morphology and elevated nuclear Phox2b expression (Figure 42). In summary, *IGF2BP1*-induced tumors resemble neuroblastoma disease in terms of expression pattern, origin and genetics, similarly to other transgenic neuroblastoma models previously reported.

Targeting IGF2BP1: a promising therapeutic avenue for cancer progression

The inhibition of IGF2BP1 function represents a novel potentially powerful approach for targeting cancer progression. Several characteristics of IGF2BP1 underscore its promising potential as a therapeutic target: 1) its high expression across a broad range of cancers, 2) its association with unfavorable clinical outcomes, 3) its role in promoting metastasis and 4) its minimal expression in normal adult tissue. Consequently, IGF2BP1's distinct properties position it as an appealing candidate for pharmacological inhibition, as specific inhibitors are expected to result in minimal off-target effects. To date, three small molecular inhibitors have been reported to target IGF2BP1: BTYNB, 7773 and cucurbitacin B (Mahapatra *et al.* 2017, Wallis *et al.* 2022, Liu *et al.* 2022). Of these, CuB and BTYNB have been evaluated for *in vivo* activity in H22 hepatocellular carcinoma or ES-2 ovarian cancer cell lines, respectively (Müller *et al.* 2020, Liu *et al.* 2022). In this study, the effectiveness of IGF2BP1 inhibition was explored in the context of neuroblastoma cell lines and xenograft models. BTYNB demonstrated EC₅₀ values in the anticipated range of approximately 5 μM and treatment of both 2D and 3D cells resulted in decreased viability and growth, consistent with prior reports (Figure 23, Figure 25, Figure 27). In subcutaneous xenografts, BTYNB-induced inhibition yielded comparable results to those achieved by an IGF2BP1 knockout cell line, underlining the potential of BTYNB as a therapeutic agent for cancer progression. Moreover, for the first time, BTYNB was evaluated *in vivo* by intra-peritoneal (systemic) and intra-tumoral (local) application in PDX or xenograft models, respectively. Systemic treatment with BTYNB showed expected trends towards hampered tumor growth but remained non-significant. This likely indicates unfavorable pharmacokinetics of the lead compound, potentially involving limited stability and substantial adsorption by plasma proteins. However, local treatment of subcutaneous xenograft tumors with BTYNB yielded a significant reduction in tumor growth, highlighting the great potential of inhibiting IGF2BP1 for cancer therapy (Figure 27). Further investigations aiming to enhance BTYNB's pharmacokinetic properties are necessary for more effective *in vivo* testing. By comparison, the covalent inhibitor CuB demonstrated anti-proliferative activity *in vivo* through intra-peritoneal application, indicating better pharmacokinetics than BTYNB. The compound 7773 has not been investigated *in vivo* so far.

It is important to note that monotherapies with IGF2BP1 inhibitors are unlikely to be sufficient for complete tumor eradication for various reasons. Nonetheless, even partial disruption of IGF2BP1-mRNA binding has broad impact on the expression of oncogenic factors. IGF2BP1 inhibition affects

genes that are either currently not, indirectly or directly targetable, such as MYC/N or BIRC5, respectively. As a common essential gene, it is not surprising that BIRC5 inhibition through YM-155 (Nakahara *et al.* 2007), explored in multiple clinical trials, has been hampered by issues of toxicity and low efficacy (Li *et al.* 2019). The inhibition of IGF2BP1, either alone or in combination with YM-155, could potentially mitigate these challenges. Indeed, this study revealed additive effects of BTYNB and YM-155 across various cancer types, reducing the adverse effects of high YM-155 concentrations and enhancing therapeutic efficacy in combined therapy (Figure 40). Moreover, prior research has demonstrated the benefits of combined IGF2BP1 and TOP2A inhibition, achieved through BTYNB and Doxorubicin, respectively (Bell *et al.* 2015, Biegel *et al.* 2021). TOP2A inhibitors like Doxorubicin are already employed in high-risk neuroblastoma therapy and augmentation of their effectiveness through combined drug regimens could yield improved outcome. In line with this, the inhibition of IGF2BP1 by BTYNB proved advantageous when combined with other standard-of-care drugs for neuroblastoma treatment such as Etoposide or Vincristine (Biegel *et al.* 2021). Furthermore, BTYNB potentiated the efficacy of CDK inhibitors, as evidenced by studies involving Palbociclib (CDK4/6) and Dinaciclib (CDK2/9) in ovarian cancer or neuroblastoma, respectively (Müller *et al.* 2020, Biegel *et al.* 2021). Additionally, the knockout of IGF2BP1 sensitized neuroblastoma cell lines to the BRD inhibitor Mivebresib (Figure 37). The synergistic effects observed upon indirect targeting of MYC/N through BRD inhibitors and IGF2BP1 through BTYNB provide an additional avenue for combined treatment strategies. The potential of HDAC inhibitors, especially HDAC1-3, to reduce MYCN expression and increase p21-dependent apoptosis or direct MYC/N inhibition through EN4 adds another layer to this combined therapy approach (Figure 36, Figure 38, Figure 39, Table 27). Thus, the simultaneous inhibition of IGF2BP1 and HDAC or MYC/N could potentially improve patient outcomes.

In conclusion, impairing IGF2BP1 expression or function through knockdown, knockout or inhibition sensitizes cancer cells to a range of therapeutic agents. These include BRD inhibitors, CDK inhibitors, HDAC inhibitors and neuroblastoma standard-of-care drugs, resulting in additive to synergistic effects in combined treatment. This implies a conserved underlying mechanism by which IGF2BP1 modulates drug sensitivity. Indeed, IGF2BP1 was shown to enhance the stability of MDR1 mRNA by inhibiting endonucleolytic digestion through binding to the CRD (Sparanese and Lee 2007). As MDR1 is linked to multidrug resistance phenotype in cultured cells and human cancers, this association provides a plausible explanation (Ambudkar *et al.* 2003). Consistent with this, MDR1 mRNA expression was substantially reduced upon IGF2BP1 depletion in different cancer cell lines, including BE(2)-C and KELLY neuroblastoma cell lines. Interestingly, MDR1 is located on chromosome 7q21, a region commonly gained in human neuroblastoma and deregulated in multiple neuroblastoma transgenic mouse models, including the newly established LSL-*IGF2BP1* model. In addition, IGF2BP1 enhances MDM2 expression (Mu *et al.* 2022), which in turn results in upregulation of MDR1 (Kondo *et al.* 1996).

However, contrary to expectations, MDR1 mRNA expression was reduced in MNA and stage 4 human as well as mouse transgenic neuroblastoma tumors. Moreover, there was no apparent correlation between IGF2BP1 and MDR1 mRNA expression and low MDR1 expression was associated with poor overall and event-free survival, in contrast to the hypothesized relationship. It is worth noting that MDR1 resistance is often acquired in cell lines and animal models and the RNA-seq data from analyzed tumor cohorts primarily consists of primary, untreated tumors, which might limit their insights. Another mechanism by which IGF2BP1 could modulate drug resistance is the MRP protein. No direct association of IGF2BP1 and MRP has been shown so far, but MYCN enhances MRP expression, thereby decreasing the sensitivity to therapeutics (Norris *et al.* 1996, Norris *et al.* 1997). As IGF2BP1 influences MYCN expression, a mediation of drug resistance is possible. Further investigations are required to decipher the mechanism by which IGF2BP1 mediates drug sensitivity.

IGF2BP1 inhibition holds the potential to improve the treatment outcomes for neuroblastoma patients through several mechanisms. For patients classified as low- and intermediate-risk, who generally respond well to existing treatment regimens, the immediate inclusion of IGF2BP1 inhibitors may not be imperative. Nevertheless, integrating these inhibitors into current therapeutic strategies could lead to reduced dosages of chemotherapeutic agents, thereby mitigating potential side effects. The utilization of IGF2BP1 inhibitors is particularly promising for high-risk patients, as this study has established a strong reliance on an oncogenic role for IGF2BP1 within this subgroup. Incorporating an IGF2BP1 inhibitor as part of the initial treatment alongside conventional drugs such as etoposide or vincristine could lower the required chemotherapeutic concentrations, potentially improving overall patient tolerance to treatment. This approach may also enhance the responsiveness of more patients to induction therapy. Another avenue involves integrating IGF2BP1 inhibitors into maintenance regimens designed to address minimal residual disease. This study reveals that IGF2BP1 knockout or inhibition leads to delayed tumor engraftment and reduced proliferation of neuroblastoma cells. Consequently, IGF2BP1 inhibition could effectively impede the growth of unresected tumor masses or relapse. This treatment strategy could also be explored in combination with ongoing experimental approaches like isotretinoin, anti-GD2 antibodies or DFMO. However, the effectiveness of these combinations would require thorough *in vitro* testing. Moreover, IGF2BP1 inhibitors may prove valuable in cases of relapsed or refractory disease, helping to overcome the chemoresistance often observed in these tumors. Beyond the aforementioned combinations, IGF2BP1 inhibitors have demonstrated synergistic effects with emerging therapeutics such as BRD inhibitors. This synergy may be expanded to other classes of compounds, including ALK, HDAC, AURKA or DNA methylation inhibitors. Such combinations could result in the coordinated downregulation of multiple oncogenic targets, subsequently impeding tumor progression. Additionally, IGF2BP1 inhibition can modify the recognition of tumor cells by the immune system, potentially harnessing the power of the body's

natural defense mechanisms to combat cancer. Although these approaches require rigorous *in vitro* and *in vivo* validation before therapeutic application in humans, the prospects for IGF2BP1 inhibitors are indeed promising and further research should be conducted in this field. Finally, it is worth noting that BTYNB is still a lead compound and needs more detailed analyses and improvement in context of pharmacokinetics, binding and off-targets.

6. References

- Acheson, Ann, Conover, Joanne C, Fandl, James P, DeChiara, Thomas M, Russell, Michelle, Thadani, Anu, Squinto, Stephen P, Yancopoulos, George D, and Lindsay, Ronald M. 1995. "A BDNF autocrine loop in adult sensory neurons prevents cell death." *Nature* 374 (6521):450-453.
- Adam, K., Lesperance, J., Hunter, T., and Zage, P. E. 2020. "The Potential Functional Roles of NME1 Histidine Kinase Activity in Neuroblastoma Pathogenesis." *Int J Mol Sci* 21 (9). doi: 10.3390/ijms21093319.
- Alaminos, Miguel, Davalos, Veronica, Cheung, Nai-Kong V, Gerald, William L, and Esteller, Manel. 2004. "Clustering of gene hypermethylation associated with clinical risk groups in neuroblastoma." *Journal of the National Cancer Institute* 96 (16):1208-1219.
- Althoff, K., Beckers, A., Bell, E., Nortmeyer, M., Thor, T., Sprussel, A., Lindner, S., De Preter, K., Florin, A., Heukamp, L. C., Klein-Hitpass, L., Astrahantseff, K., Kumps, C., Speleman, F., Eggert, A., Westermann, F., Schramm, A., and Schulte, J. H. 2015. "A Cre-conditional MYCN-driven neuroblastoma mouse model as an improved tool for preclinical studies." *Oncogene* 34 (26):3357-68. doi: 10.1038/onc.2014.269.
- Altungoz, Oguz, Aygun, Nevim, Tumer, Sait, Ozer, Erdener, Olgun, Nur, and Sakizli, Meral. 2007. "Correlation of modified Shimada classification with MYCN and 1p36 status detected by fluorescence in situ hybridization in neuroblastoma." *Cancer genetics and cytogenetics* 172 (2):113-119.
- Ambudkar, S. V., Kimchi-Sarfaty, C., Sauna, Z. E., and Gottesman, M. M. 2003. "P-glycoprotein: from genomics to mechanism." *Oncogene* 22 (47):7468-85. doi: 10.1038/sj.onc.1206948.
- Amente, S., Milazzo, G., Sorrentino, M. C., Ambrosio, S., Di Palo, G., Lania, L., Perini, G., and Majello, B. 2015. "Lysine-specific demethylase (LSD1/KDM1A) and MYCN cooperatively repress tumor suppressor genes in neuroblastoma." *Oncotarget* 6 (16):14572-83. doi: 10.18632/oncotarget.3990.
- Amiel, Jeanne, Béatrice, Attié-Bitach, Tania, Trang, Ha, de Pontual, Loïc, Gener, Blanca, Trochet, Delphine, Etchevers, Heather, Ray, Pierre, and Simonneau, Michel. 2003. "Polyalanine expansion and frameshift mutations of the paired-like homeobox gene PHOX2B in congenital central hypoventilation syndrome." *Nature genetics* 33 (4):459-461.
- Amler, Lukas C, and Schwab, Manfred. 1989. "Amplified N-myc in human neuroblastoma cells is often arranged as clustered tandem repeats of differently recombined DNA." *Molecular and cellular biology* 9 (11):4903-4913.
- Amler, Lukas C, Shibasaki, Yoshiro, Savelyeva, Larisa, and Schwab, Manfred. 1992. "Amplification of the N-myc gene in human neuroblastomas: tandemly repeated amplicons within homogeneously staining regions on different chromosomes with the retention of single copy gene at the resident site." *Mutation Research/Reviews in Genetic Toxicology* 276 (3):291-297.
- Ando, Kiyohiro, Ohira, Miki, Ozaki, Toshinori, Nakagawa, Atsuko, Akazawa, Kohei, Suenaga, Yusuke, Nakamura, Yohko, Koda, Tadayuki, Kamijo, Takehiko, and Murakami, Yoshinori. 2008. "Expression of TSLC1, a candidate tumor suppressor gene mapped to chromosome 11q23, is downregulated in unfavorable neuroblastoma without promoter hypermethylation." *International journal of cancer* 123 (9):2087-2094.
- Ao, X., Ding, W., Zhang, Y., Ding, D., and Liu, Y. 2020. "TCF21: a critical transcription factor in health and cancer." *J Mol Med (Berl)* 98 (8):1055-1068. doi: 10.1007/s00109-020-01934-7.
- Asgharzadeh, Shahab, Salo, Jill A, Ji, Lingyun, Oberthuer, André, Fischer, Matthias, Berthold, Frank, Hadjidanil, Michael, Liu, Cathy Wei-Yao, Metelitsa, Leonid S, and Pique-Regi, Roger. 2012. "Clinical significance of tumor-associated inflammatory cells in metastatic neuroblastoma." *Journal of Clinical Oncology* 30 (28):3525.
- Astuti, Dewi, Agathangelou, Angelo, Honorio, Sofia, Dallol, Ashraf, Martinsson, Tommy, Kogner, Per, Cummins, Carole, Neumann, Hartmut PH, Voutilainen, Raimo, and Dahia, Patricia. 2001. "RASSF1A promoter region CpG island hypermethylation in pheochromocytomas and neuroblastoma tumours." *Oncogene* 20 (51):7573-7577.
- Attiyeh, Edward F, London, Wendy B, Mossé, Yael P, Wang, Qun, Winter, Cynthia, Khazi, Deepa, McGrady, Patrick W, Seeger, Robert C, Look, A Thomas, and Shimada, Hiroyuki. 2005. "Chromosome 1p and 11q deletions and outcome in neuroblastoma." *New England Journal of Medicine* 353 (21):2243-2253.
- Aygun, Nevim. 2017. "Acquired chromosomal abnormalities and their potential formation mechanisms in solid tumours." *Chromosomal abnormalities-a hallmark manifestation of genomic instability. InTech*:27-70.
- Bader, Scott A, Fasching, Clare, Brodeur, Garrett M, and Stanbridge, Eric J. 1991. "Dissociation of suppression of tumorigenicity and differentiation in vitro effected by transfer of single human chromosomes into human neuroblastoma cells." *Cell growth & differentiation: the molecular biology journal of the American Association for Cancer Research* 2 (5):245-255.
- Baker, D. L., Schmidt, M. L., Cohn, S. L., Maris, J. M., London, W. B., Buxton, A., Stram, D., Castleberry, R. P., Shimada, H., Sandler, A., Shamberger, R. C., Look, A. T., Reynolds, C. P., Seeger, R. C., Matthay, K. K., and Children's Oncology, Group. 2010. "Outcome after reduced chemotherapy for intermediate-risk neuroblastoma." *N Engl J Med* 363 (14):1313-23. doi: 10.1056/NEJMoa1001527.
- Balis, F. M., Thompson, P. A., Mosse, Y. P., Blaney, S. M., Minard, C. G., Weigel, B. J., and Fox, E. 2017. "First-dose and steady-state pharmacokinetics of orally administered crizotinib in children with solid tumors: a report on ADVL0912 from the Children's Oncology Group Phase 1/Pilot Consortium." *Cancer Chemother Pharmacol* 79 (1):181-187. doi: 10.1007/s00280-016-3220-6.
- Bannister, Andrew J, and Kouzarides, Tony. 2011. "Regulation of chromatin by histone modifications." *Cell research* 21 (3):381-395.
- Barbacid, M. 1995. "Neurotrophic factors and their receptors." *Curr Opin Cell Biol* 7 (2):148-55. doi: 10.1016/0955-0674(95)80022-0.
- Barr, E. K., and Applebaum, M. A. 2018. "Genetic Predisposition to Neuroblastoma." *Children (Basel)* 5 (9). doi: 10.3390/children5090119.
- Bate-Eya, Laurel T, Gierman, Hincio J, Ebus, Marli E, Koster, Jan, Caron, Huib N, Versteeg, Rogier, Dolman, M Emmy M, and Molenaar, Jan J. 2017. "Enhancer of zeste homologue 2 plays an important role in neuroblastoma cell survival independent of its histone methyltransferase activity." *European Journal of Cancer* 75:63-72.
- Baylin, Stephen B, and Jones, Peter A. 2011. "A decade of exploring the cancer epigenome—biological and translational implications." *Nature Reviews Cancer* 11 (10):726-734.
- Baylin, Stephen B, and Jones, Peter A. 2016. "Epigenetic determinants of cancer." *Cold Spring Harbor perspectives in biology* 8 (9):a019505.
- Beckers, A., Van Peer, G., Carter, D. R., Gartlgruber, M., Herrmann, C., Agarwal, S., Helmsmoortel, H. H., Althoff, K., Molenaar, J. J., Cheung, B. B., Schulte, J. H., Benoit, Y., Shohet, J. M., Westermann, F., Marshall, G. M., Vandesompele, J., De Preter, K., and Speleman, F. 2015a. "MYCN-driven regulatory mechanisms controlling LIN28B in neuroblastoma." *Cancer Lett* 366 (1):123-32. doi: 10.1016/j.canlet.2015.06.015.

6. References

- Beckers, A., Van Peer, G., Carter, D. R., Mets, E., Althoff, K., Cheung, B. B., Schulte, J. H., Mestdagh, P., Vandesompele, J., Marshall, G. M., De Preter, K., and Speleman, F. 2015b. "MYCN-targeting miRNAs are predominantly downregulated during MYCN-driven neuroblastoma tumor formation." *Oncotarget* 6 (7):5204-16. doi: 10.18632/oncotarget.2477.
- Beckwith, J Bruce, and Perrin, Eugene V. 1963. "In situ neuroblastomas: a contribution to the natural history of neural crest tumors." *The American journal of pathology* 43 (6):1089.
- Bell, J. L., Hagemann, S., Holien, J. K., Liu, T., Nagy, Z., Schulte, J. H., Misiak, D., and Hüttelmaier, S. 2020. "Identification of RNA-Binding Proteins as Targetable Putative Oncogenes in Neuroblastoma." *Int J Mol Sci* 21 (14). doi: 10.3390/ijms21145098.
- Bell, J. L., Turlapati, R., Liu, T., Schulte, J. H., and Hüttelmaier, S. 2015. "IGF2BP1 harbors prognostic significance by gene gain and diverse expression in neuroblastoma." *J Clin Oncol* 33 (11):1285-93. doi: 10.1200/JCO.2014.55.9880.
- Bell, J. L., Wächter, K., Mühleck, B., Pazaitis, N., Köhn, M., Lederer, M., and Hüttelmaier, S. 2013. "Insulin-like growth factor 2 mRNA-binding proteins (IGF2BPs): post-transcriptional drivers of cancer progression?" *Cell Mol Life Sci* 70 (15):2657-75. doi: 10.1007/s00018-012-1186-z.
- Beltran, H. 2014. "The N-myc Oncogene: Maximizing its Targets, Regulation, and Therapeutic Potential." *Mol Cancer Res* 12 (6):815-22. doi: 10.1158/1541-7786.MCR-13-0536.
- Bernstein, P. L., Herrick, D. J., Prokipcak, R. D., and Ross, J. 1992. "Control of c-myc mRNA half-life in vitro by a protein capable of binding to a coding region stability determinant." *Genes Dev* 6 (4):642-54. doi: 10.1101/gad.6.4.642.
- Berry, T., Luther, W., Bhatnagar, N., Jamin, Y., Poon, E., Sanda, T., Pei, D., Sharma, B., Vetharoy, W. R., Hallsworth, A., Ahmad, Z., Barker, K., Moreau, L., Webber, H., Wang, W., Liu, Q., Perez-Atayde, A., Rodig, S., Cheung, N. K., Raynaud, F., Hallberg, B., Robinson, S. P., Gray, N. S., Pearson, A. D., Eccles, S. A., Chesler, L., and George, R. E. 2012. "The ALK(F1174L) mutation potentiates the oncogenic activity of MYCN in neuroblastoma." *Cancer Cell* 22 (1):117-30. doi: 10.1016/j.ccr.2012.06.001.
- Betson, N., Hajahmed, M., Gebretsadek, T., Ndebele, K., Ahmad, H. A., Tchounwou, P. B., Spiegelman, V. S., and Noubissi, F. K. 2022. "Inhibition of insulin-like growth factor 2 mRNA-binding protein 1 sensitizes colorectal cancer cells to chemotherapeutics." *FASEB Bioadv* 4 (12):816-829. doi: 10.1096/fba.2021-00069.
- Biegel, J. M., Dhamdhere, M., Gao, S., Gowda, C. P., Kawasawa, Y. I., and Spiegelman, V. S. 2021. "Inhibition of the mRNA-Binding Protein IGF2BP1 Suppresses Proliferation and Sensitizes Neuroblastoma Cells to Chemotherapeutic Agents." *Front Oncol* 11:608816. doi: 10.3389/fonc.2021.608816.
- Binz, Nicolas, Shalaby, T., Rivera, P., Shin-Ya, K., and Grotzer, MA. 2005. "Telomerase inhibition, telomere shortening, cell growth suppression and induction of apoptosis by telomestatin in childhood neuroblastoma cells." *European journal of cancer* 41 (18):2873-2881.
- Bird, Adrian. 2002. "DNA methylation patterns and epigenetic memory." *Genes & development* 16 (1):6-21.
- Biswas, J., Patel, V. L., Bhaskar, V., Chao, J. A., Singer, R. H., and Eliscovich, C. 2019. "The structural basis for RNA selectivity by the IMP family of RNA-binding proteins." *Nat Commun* 10 (1):4440. doi: 10.1038/s41467-019-12193-7.
- Bleeker, Gitta, Tytgat, Godelieve AM, Adam, Judit A, Caron, Huib N, Kremer, Leontien CM, Hooft, Lotty, and van Dalen, Elvira C. 2015. "123I-MIBG scintigraphy and 18F-FDG-PET imaging for diagnosing neuroblastoma." *Cochrane Database of Systematic Reviews* (9).
- Bley, N., Schott, A., Muller, S., Misiak, D., Lederer, M., Fuchs, T., Assmann, C., Glass, M., Ihling, C., Sinz, A., Pazaitis, N., Wickenhauser, C., Vetter, M., Ungurs, O., Strauss, H. G., Thomssen, C., and Hüttelmaier, S. 2020. "IGF2BP1 is a targetable SRC/MAPK-dependent driver of invasive growth in ovarian cancer." *RNA Biol*:1-13. doi: 10.1080/15476286.2020.1812894.
- Blomen, V. A., Majek, P., Jae, L. T., Bigenzahn, J. W., Nieuwenhuis, J., Staring, J., Sacco, R., van Diemen, F. R., Olk, N., Stukalov, A., Marceau, C., Janssen, H., Carette, J. E., Bennett, K. L., Colinge, J., Superti-Furga, G., and Brummelkamp, T. R. 2015. "Gene essentiality and synthetic lethality in haploid human cells." *Science* 350 (6264):1092-6. doi: 10.1126/science.aac7557.
- Boeva, V., Louis-Brennetot, C., Peltier, A., Durand, S., Pierre-Eugene, C., Raynal, V., Etchevers, H. C., Thomas, S., Lermine, A., Daudigeos-Dubus, E., Geoerger, B., Orth, M. F., Grunewald, T. G. P., Diaz, E., Ducos, B., Surdez, D., Carcaboso, A. M., Medvedeva, I., Deller, T., Combaret, V., Lapouble, E., Pierron, G., Grossetete-Lalami, S., Baulande, S., Schliermacher, G., Barillot, E., Rohrer, H., Delattre, O., and Janoueix-Lerosey, I. 2017. "Heterogeneity of neuroblastoma cell identity defined by transcriptional circuitries." *Nat Genet* 49 (9):1408-1413. doi: 10.1038/ng.3921.
- Bogen, Dominik, Brunner, Clemens, Walder, Diana, Ziegler, Andrea, Abbasi, Reza, Ladenstein, Ruth L, Noguera, Rosa, Martinsson, Tommy, Amann, Gabriele, and Schilling, Freimut H. 2016. "The genetic tumor background is an important determinant for heterogeneous MYCN-amplified neuroblastoma." *International journal of cancer* 139 (1):153-163.
- Boike, L., Cioffi, A. G., Majewski, F. C., Co, J., Henning, N. J., Jones, M. D., Liu, G., McKenna, J. M., Tallarico, J. A., Schirle, M., and Nomura, D. K. 2021. "Discovery of a Functional Covalent Ligand Targeting an Intrinsically Disordered Cysteine within MYC." *Cell Chem Biol* 28 (1):4-13 e17. doi: 10.1016/j.chembiol.2020.09.001.
- Bourdeaut, F., Trochet, D., Janoueix-Lerosey, I., Ribeiro, A., Deville, A., Coz, C., Michiels, J. F., Lyonnet, S., Amiel, J., and Delattre, O. 2005. "Germline mutations of the paired-like homeobox 2B (PHOX2B) gene in neuroblastoma." *Cancer Lett* 228 (1-2):51-8. doi: 10.1016/j.canlet.2005.01.055.
- Bourhis, Jean, Bénard, Jean, Hartmann, Oliver, Boccon-Gibod, Liliane, Lemerle, Jean, and Riou, Guy. 1989. "Correlation of MDR1 gene expression with chemotherapy in neuroblastoma." *JNCI: Journal of the National Cancer Institute* 81 (18):1401-1405.
- Bouzas-Rodriguez, Jimena, Cabrera, Jorge Ruben, Delloye-Bourgeois, Céline, Ichim, Gabriel, Delcros, Jean-Guy, Raquin, Marie-Anne, Rousseau, Raphaël, Combaret, Valérie, Bénard, Jean, and Tauszig-Delamasure, Servane. 2010. "Neurotrophin-3 production promotes human neuroblastoma cell survival by inhibiting TrkC-induced apoptosis." *The Journal of clinical investigation* 120 (3):850-858.
- Bown, N. 2001. "Neuroblastoma tumour genetics: clinical and biological aspects." *J Clin Pathol* 54 (12):897-910. doi: 10.1136/jcp.54.12.897.
- Bown, N., Cotterill, S., Lastowska, M., O'Neill, S., Pearson, A. D., Plantaz, D., Meddeb, M., Danglot, G., Brinkschmidt, C., Christiansen, H., Laureys, G., Speleman, F., Nicholson, J., Bernheim, A., Betts, D. R., Vandesompele, J., and Van Roy, N. 1999. "Gain of chromosome arm 17q and adverse outcome in patients with neuroblastoma." *N Engl J Med* 340 (25):1954-61. doi: 10.1056/NEJM199906243402504.
- Bown, N., Lastowska, M., Cotterill, S., O'Neill, S., Ellershaw, C., Roberts, P., Lewis, I., Pearson, A. D., Group, U. K. Cancer Cytogenetics, and the, U. K. Children's Cancer Study Group. 2001. "17q gain in neuroblastoma predicts adverse clinical outcome. U.K. Cancer Cytogenetics Group and the U.K. Children's Cancer Study Group." *Med Pediatr Oncol* 36 (1):14-9. doi: 10.1002/1096-911X(20010101)36:1<14::AID-MPO1005>3.0.CO;2-G.
- Boyerinas, B., Park, S. M., Shomron, N., Hedegaard, M. M., Vinther, J., Andersen, J. S., Feig, C., Xu, J., Burge, C. B., and Peter, M. E. 2008. "Identification of let-7-regulated oncofetal genes." *Cancer Res* 68 (8):2587-91. doi: 10.1158/0008-5472.CAN-08-0264.

6. References

- Boylan, K. L., Mische, S., Li, M., Marques, G., Morin, X., Chia, W., and Hays, T. S. 2008. "Motility screen identifies Drosophila IGF-II mRNA-binding protein--zipcode-binding protein acting in oogenesis and synaptogenesis." *PLoS Genet* 4 (2):e36. doi: 10.1371/journal.pgen.0040036.
- Brants, J. R., Ayoubi, T. A., Chada, K., Marchal, K., Van de Ven, W. J., and Petit, M. M. 2004. "Differential regulation of the insulin-like growth factor II mRNA-binding protein genes by architectural transcription factor HMGA2." *FEBS Lett* 569 (1-3):277-83. doi: 10.1016/j.febslet.2004.05.075.
- Braun, J., Misiak, D., Busch, B., Krohn, K., and Hüttelmaier, S. 2014. "Rapid identification of regulatory microRNAs by miTRAP (miRNA trapping by RNA in vitro affinity purification)." *Nucleic Acids Res* 42 (8):e66. doi: 10.1093/nar/gku127.
- Breen, C.J., O'meara, A., McDermott, M., Mullarkey, M., and Stallings, R.L. 2000. "Coordinate deletion of chromosome 3p and 11q in neuroblastoma detected by comparative genomic hybridization." *Cancer genetics and cytogenetics* 120 (1):44-49.
- Brinkschmidt, C., Poremba, C., Christiansen, H., Simon, R., Schäfer, K.L., Terpe, H.J., Lampert, F., Boecker, W., and Dockhorn-Dworniczak, B. 1998. "Comparative genomic hybridization and telomerase activity analysis identify two biologically different groups of 4s neuroblastomas." *British journal of cancer* 77 (12):2223-2229.
- Brockmann, M., Poon, E., Berry, T., Carstensen, A., Deubzer, H. E., Rycak, L., Jamin, Y., Thway, K., Robinson, S. P., Roels, F., Witt, O., Fischer, M., Chesler, L., and Eilers, M. 2013. "Small molecule inhibitors of aurora-a induce proteasomal degradation of N-myc in childhood neuroblastoma." *Cancer Cell* 24 (1):75-89. doi: 10.1016/j.ccr.2013.05.005.
- Brodeur, G. M. 2003. "Neuroblastoma: biological insights into a clinical enigma." *Nat Rev Cancer* 3 (3):203-16. doi: 10.1038/nrc1014.
- Brodeur, G. M. 2018. "Spontaneous regression of neuroblastoma." *Cell Tissue Res* 372 (2):277-286. doi: 10.1007/s00441-017-2761-2.
- Brodeur, G. M., Minturn, J. E., Ho, R., Simpson, A. M., Iyer, R., Varela, C. R., Light, J. E., Kolla, V., and Evans, A. E. 2009. "Trk receptor expression and inhibition in neuroblastomas." *Clin Cancer Res* 15 (10):3244-50. doi: 10.1158/1078-0432.CCR-08-1815.
- Brodeur, G. M., Pritchard, J., Berthold, F., Carlsen, N. L., Castel, V., Castelberry, R. P., De Bernardi, B., Evans, A. E., Favrot, M., Hedborg, F., and et al. 1993. "Revisions of the international criteria for neuroblastoma diagnosis, staging, and response to treatment." *J Clin Oncol* 11 (8):1466-77. doi: 10.1200/JCO.1993.11.8.1466.
- Brodeur, G. M., Seeger, R. C., Barrett, A., Berthold, F., Castleberry, R. P., D'Angio, G., De Bernardi, B., Evans, A. E., Favrot, M., Freeman, A. I., and et al. 1988. "International criteria for diagnosis, staging, and response to treatment in patients with neuroblastoma." *J Clin Oncol* 6 (12):1874-81. doi: 10.1200/JCO.1988.6.12.1874.
- Brodeur, Garrett M, and Bagatell, Rochelle. 2014. "Mechanisms of neuroblastoma regression." *Nature reviews Clinical oncology* 11 (12):704-713.
- Brodeur, Garrett M, Hayes, F Ann, Green, Alexander A, Casper, James T, Wasson, Jonathon, Wallach, Susan, and Seeger, Robert C. 1987. "Consistent N-myc copy number in simultaneous or consecutive neuroblastoma samples from sixty individual patients." *Cancer research* 47 (16):4248-4253.
- Brodeur, Garrett M, Maris, John M, Yamashiro, Darrell J, Hogarty, Michael D, and White, Peter S. 1997. "Biology and genetics of human neuroblastomas." *Journal of pediatric hematology/oncology* 19 (2):93-101.
- Brodeur, Garrett M, Seeger, Robert C, Schwab, Manfred, Varmus, Harold E, and Bishop, J Michael. 1984. "Amplification of N-myc in untreated human neuroblastomas correlates with advanced disease stage." *Science* 224 (4653):1121-1124.
- Buechner, J., and Einvik, C. 2012. "N-myc and noncoding RNAs in neuroblastoma." *Mol Cancer Res* 10 (10):1243-53. doi: 10.1158/1541-7786.MCR-12-0244.
- Bui, Chi-Bao, Le, Hoa Kim, Vu, Diem My, Truong, Kieu-Diem Dinh, Nguyen, Nhat Manh, Ho, Minh Anh Nguyen, and Truong, Dinh Quang. 2019. "ARID1A-SIN3A drives retinoic acid-induced neuroblastoma differentiation by transcriptional repression of TERT." *Molecular Carcinogenesis* 58 (11):1998-2007.
- Bunin, Greta R, WARD, ELIZABETH, KRAMER, SHIRA, RHEE, CHARLOTTE A, and MEADOWS, ANNA T. 1990. "Neuroblastoma and parental occupation." *American journal of epidemiology* 131 (5):776-780.
- Busch, B., Bley, N., Müller, S., Glaß, M., Misiak, D., Lederer, M., Vetter, M., Strauss, H. G., Thomssen, C., and Hüttelmaier, S. 2016. "The oncogenic triangle of HMGA2, LIN28B and IGF2BP1 antagonizes tumor-suppressive actions of the let-7 family." *Nucleic Acids Res* 44 (8):3845-64. doi: 10.1093/nar/gkw099.
- Cabanillas Stanchi, K. M., Bruchelt, G., Handgretinger, R., and Holzer, U. 2015. "Nifurtimox reduces N-Myc expression and aerobic glycolysis in neuroblastoma." *Cancer Biol Ther* 16 (9):1353-63. doi: 10.1080/15384047.2015.1070987.
- Cangemi, Giuliana, Reggiardo, Giorgio, Barco, Sebastiano, Barbagallo, Laura, Conte, Massimo, D'Angelo, Paolo, Bianchi, Maurizio, Favre, Claudio, Galleni, Barbara, and Melioli, Giovanni. 2012. "Prognostic value of ferritin, neuron-specific enolase, lactate dehydrogenase, and urinary and plasmatic catecholamine metabolites in children with neuroblastoma." *OncoTargets and therapy*:417-423.
- Capasso, Mario, Devoto, Marcella, Hou, Cuiping, Asgharzadeh, Shahab, Glessner, Joseph T, Attiyeh, Edward F, Mosse, Yael P, Kim, Cecilia, Diskin, Sharon J, and Cole, Kristina A. 2009. "Common variations in BARD1 influence susceptibility to high-risk neuroblastoma." *Nature genetics* 41 (6):718-723.
- Carén, Helena, Kryh, Hanna, Nethander, Maria, Sjöberg, Rose-Marie, Träger, Catarina, Nilsson, Staffan, Abrahamsson, Jonas, Kogner, Per, and Martinsson, Tommy. 2010. "High-risk neuroblastoma tumors with 11q-deletion display a poor prognostic, chromosome instability phenotype with later onset." *Proceedings of the National Academy of Sciences* 107 (9):4323-4328.
- Carlson, M. 2019. "org.Hs.eg.db: Genome wide annotation for Human." <https://bioconductor.org/packages/release/data/annotation/html/org.Hs.eg.db.html>.
- Carlson, M., and Maintainer, Bioconductor Package. 2015. "TxDb.Hsapiens.UCSC.hg19.knownGene: Annotation package for TxDb object(s)." <https://bioconductor.org/packages/release/data/annotation/html/TxDb.Hsapiens.UCSC.hg19.knownGene.html>.
- Caron, Huib. 1995. "Allelic loss of chromosome 1 and additional chromosome 17 material are both unfavourable prognostic markers in neuroblastoma." *Medical and pediatric oncology* 24 (4):215-221.
- Caron, Huib, van Sluis, Peter, Buschman, Roman, Pereira do Tanque, Ruth, Maes, Patricia, Beks, Loes, de Kraker, Jan, Voute, PA, Vergnaud, Gilles, and Westerveld, Andries. 1996. "Allelic loss of the short arm of chromosome 4 in neuroblastoma suggests a novel tumour suppressor gene locus." *Human genetics* 97:834-837.
- Caron, Huib, van Sluis, Peter, van Hoeve, Melanie, de Kraker, Jan, Bras, Johannes, Slater, Rosalyn, Mannens, Marcel, Voute, PA, Westerveld, Andries, and Versteeg, Rogier. 1993. "Allelic loss of chromosome 1p36 in neuroblastoma is of preferential maternal origin and correlates with N-myc amplification." *Nature genetics* 4 (2):187-190.
- Carpenter, E. L., and Mosse, Y. P. 2012. "Targeting ALK in neuroblastoma--preclinical and clinical advancements." *Nat Rev Clin Oncol* 9 (7):391-9. doi: 10.1038/nrclinonc.2012.72.

6. References

- Carrillo, C., Gonzalez, N. S., and Algranati, I. D. 2007. "Trypanosoma cruzi as a model system to study the expression of exogenous genes coding for polyamine biosynthetic enzymes. Induction of DFMO resistance in transgenic parasites." *Biochim Biophys Acta* 1770 (12):1605-11. doi: 10.1016/j.bbagen.2007.08.013.
- Carroll, Susan M, DeRose, Margaret L, Gaudray, Patrick, Moore, Charleen M, Needham-Vandevanter, Donald R, Von Hoff, Daniel D, and Wahl, Geoffrey M. 1988. "Double minute chromosomes can be produced from precursors derived from a chromosomal deletion." *Molecular and cellular biology*.
- Carvalho, L. 1973. "Spontaneous regression of an untreated neuroblastoma." *Br J Ophthalmol* 57 (11):832-5. doi: 10.1136/bjo.57.11.832.
- Castleberry, R. P. 1997. "Neuroblastoma." *Eur J Cancer* 33 (9):1430-7; discussion 1437-8. doi: 10.1016/s0959-8049(97)00308-0.
- Cattelani, Sara, Defferrari, Raffaella, Marsilio, Sonia, Bussolari, Rita, Candini, Olivia, Corradini, Francesca, Ferrari-Amorotti, Giovanna, Guerzoni, Clara, Pecorari, Luisa, and Menin, Chiara. 2008. "Impact of a single nucleotide polymorphism in the MDM2 gene on neuroblastoma development and aggressiveness: results of a pilot study on 239 patients." *Clinical cancer research* 14 (11):3248-3253.
- Cavalcante, R. G., and Sartor, M. A. 2017. "annotatr: genomic regions in context." *Bioinformatics* 33 (15):2381-2383. doi: 10.1093/bioinformatics/btx183.
- Cedar, Howard, and Bergman, Yehudit. 2009. "Linking DNA methylation and histone modification: patterns and paradigms." *Nature Reviews Genetics* 10 (5):295-304.
- Chao, J. A., Patskovsky, Y., Patel, V., Levy, M., Almo, S. C., and Singer, R. H. 2010. "ZBP1 recognition of beta-actin zipcode induces RNA looping." *Genes Dev* 24 (2):148-58. doi: 10.1101/gad.1862910.
- Charlet, J., Schneckeburger, M., Brown, K. W., and Diederich, M. 2012. "DNA demethylation increases sensitivity of neuroblastoma cells to chemotherapeutic drugs." *Biochem Pharmacol* 83 (7):858-65. doi: 10.1016/j.bcp.2012.01.009.
- Chava, S., Reynolds, C. P., Pathania, A. S., Gorantla, S., Poluektova, L. Y., Coulter, D. W., Gupta, S. C., Pandey, M. K., and Challagundla, K. B. 2020. "miR-15a-5p, miR-15b-5p, and miR-16-5p inhibit tumor progression by directly targeting MYCN in neuroblastoma." *Mol Oncol* 14 (1):180-196. doi: 10.1002/1878-0261.12588.
- Chen, J. M., Zhou, C. J., Ma, X. L., Guan, D. D., Yang, L. Y., Yue, P., and Gong, L. P. 2016. "[Abnormality of TOP2A expression and its gene copy number variations in neuroblastic tumors]." *Zhonghua Bing Li Xue Za Zhi* 45 (11):748-754. doi: 10.3760/cma.j.issn.0529-5807.2016.11.002.
- Chen, L., and Shan, G. 2021. "CircRNA in cancer: Fundamental mechanism and clinical potential." *Cancer Lett* 505:49-57. doi: 10.1016/j.canlet.2021.02.004.
- Chen, R. X., Chen, X., Xia, L. P., Zhang, J. X., Pan, Z. Z., Ma, X. D., Han, K., Chen, J. W., Judde, J. G., Deas, O., Wang, F., Ma, N. F., Guan, X., Yun, J. P., Wang, F. W., Xu, R. H., and Dan, Xie. 2019. "N(6)-methyladenosine modification of circSUN2 facilitates cytoplasmic export and stabilizes HMGA2 to promote colorectal liver metastasis." *Nat Commun* 10 (1):4695. doi: 10.1038/s41467-019-12651-2.
- Chen, S. T., Jeng, Y. M., Chang, C. C., Chang, H. H., Huang, M. C., Juan, H. F., Hsu, C. H., Lee, H., Liao, Y. F., Lee, Y. L., Hsu, W. M., and Lai, H. S. 2011. "Insulin-like growth factor II mRNA-binding protein 3 expression predicts unfavorable prognosis in patients with neuroblastoma." *Cancer Sci* 102 (12):2191-8. doi: 10.1111/j.1349-7006.2011.02100.x.
- Chen, Yuyan, Takita, Junko, Choi, Young Lim, Kato, Motohiro, Ohira, Miki, Sanada, Masashi, Wang, Lili, Soda, Manabu, Kikuchi, Akira, and Igarashi, Takashi. 2008. "Oncogenic mutations of ALK kinase in neuroblastoma." *Nature* 455 (7215):971-974.
- Chen, Z. X., Wallis, K., Fell, S. M., Sobrado, V. R., Hemmer, M. C., Ramsköld, D., Hellman, U., Sandberg, R., Kenchappa, R. S., Martinson, T., Johnsen, J. I., Kogner, P., and Schlisio, S. 2014. "RNA Helicase A Is a Downstream Mediator of KIF1Bβ Tumor-Suppressor Function in Neuroblastoma." *Cancer Discovery* 4 (4):434-451. doi: 10.1158/2159-8290.Cd-13-0362.
- Cheng, NC, Van Roy, Nadine, Chan, A, Beitsma, M, Westerveld, A, Speleman, Franki, and Versteeg, R. 1995. "Deletion mapping in neuroblastoma cell lines suggests two distinct tumor suppressor genes in the 1p35-36 region, only one of which is associated with N-myc amplification." *Oncogene* 10 (2):291-297.
- Cheung, N. K., Cheung, I. Y., Kushner, B. H., Ostrovnya, I., Chamberlain, E., Kramer, K., and Modak, S. 2012a. "Murine anti-GD2 monoclonal antibody 3F8 combined with granulocyte-macrophage colony-stimulating factor and 13-cis-retinoic acid in high-risk patients with stage 4 neuroblastoma in first remission." *J Clin Oncol* 30 (26):3264-70. doi: 10.1200/JCO.2011.41.3807.
- Cheung, N. K., Kushner, B. H., Cheung, I. Y., Kramer, K., Canete, A., Gerald, W., Bonilla, M. A., Finn, R., Yeh, S. J., and Larson, S. M. 1998. "Anti-(GD2) antibody treatment of minimal residual stage 4 neuroblastoma diagnosed at more than 1 year of age." *J Clin Oncol* 16 (9):3053-60. doi: 10.1200/JCO.1998.16.9.3053.
- Cheung, Nai-Kong V, Zhang, Jinghui, Lu, Charles, Parker, Matthew, Bahrami, Armita, Tickoo, Satish K, Heguy, Adriana, Pappo, Alberto S, Federico, Sara, and Dalton, James. 2012b. "Association of age at diagnosis and genetic mutations in patients with neuroblastoma." *Jama* 307 (10):1062-1071.
- Cheung, Nai-Kong V, Heller, Glenn, Kushner, Brian H, and Kramer, Kim. 1999. "Detection of neuroblastoma in bone marrow by immunocytology: is a single marrow aspirate adequate?" *Medical and Pediatric Oncology: The Official Journal of SIOP—International Society of Pediatric Oncology (Société Internationale d'Oncologie Pédiatrique* 32 (2):84-87.
- Christiansen, H, Sahin, K, Berthold, F, Hero, B, Terpe, H-J, and Lampert, F. 1995. "Comparison of DNA aneuploidy, chromosome 1 abnormalities, MYCN amplification and CD44 expression as prognostic factors in neuroblastoma." *European Journal of Cancer* 31 (4):541-544.
- Christiansen, J., Kolte, A. M., Hansen, Tv, and Nielsen, F. C. 2009. "IGF2 mRNA-binding protein 2: biological function and putative role in type 2 diabetes." *J Mol Endocrinol* 43 (5):187-95. doi: 10.1677/JME-09-0016.
- Ciaccio, R., De Rosa, P., Aloisi, S., Viggiano, M., Cimadom, L., Zadran, S. K., Perini, G., and Milazzo, G. 2021. "Targeting Oncogenic Transcriptional Networks in Neuroblastoma: From N-Myc to Epigenetic Drugs." *Int J Mol Sci* 22 (23). doi: 10.3390/ijms222312883.
- Clausen, N, Andersson, P, and Tommerup, N. 1989. "Familial occurrence of neuroblastoma, von Recklinghausen's neurofibromatosis, Hirschsprung's agangliosis and jaw-winking syndrome." *Acta Paediatrica* 78 (5):736-741.
- Cleynen, I., Brants, J. R., Peeters, K., Deckers, R., Debiec-Rychter, M., Sciort, R., Van de Ven, W. J., and Petit, M. M. 2007. "HMGA2 regulates transcription of the Imp2 gene via an intronic regulatory element in cooperation with nuclear factor-kappaB." *Mol Cancer Res* 5 (4):363-72. doi: 10.1158/1541-7786.MCR-06-0331.
- Cohen, Adam L, Piccolo, Stephen R, Cheng, Luis, Soldi, Rafaella, Han, Bing, Johnson, W Evan, and Bild, Andrea H. 2013. "Genomic pathway analysis reveals that EZH2 and HDAC4 represent mutually exclusive epigenetic pathways across human cancers." *BMC medical genomics* 6:1-13.
- Cohn, S. L., Pearson, A. D., London, W. B., Monclair, T., Ambros, P. F., Brodeur, G. M., Faldum, A., Hero, B., Ichihara, T., Machin, D., Mosseri, V., Simon, T., Garaventa, A., Castel, V., Matthay, K. K., and Force, Inrg Task. 2009. "The International Neuroblastoma Risk Group (INRG) classification system: an INRG Task Force report." *J Clin Oncol* 27 (2):289-97. doi: 10.1200/JCO.2008.16.6785.

6. References

- Combaret, V, Gross, N, Lasset, C, Balmas, K, Bouvier, R, Frappaz, D, Beretta-Brogna, C, Philip, T, Favrot, MC, and Coll, JL. 1997. "Clinical relevance of TRKA expression on neuroblastoma: comparison with N-MYC amplification and CD44 expression." *British journal of cancer* 75 (8):1151-1155.
- Conacci-Sorrell, M., McFerrin, L., and Eisenman, R. N. 2014. "An overview of MYC and its interactome." *Cold Spring Harb Perspect Med* 4 (1):a014357. doi: 10.1101/cshperspect.a014357.
- Conde, M., Michen, S., Wiedemuth, R., Klink, B., Schrock, E., Schackert, G., and Temme, A. 2017. "Chromosomal instability induced by increased BIRC5/Survivin levels affects tumorigenicity of glioma cells." *BMC Cancer* 17 (1):889. doi: 10.1186/s12885-017-3932-y.
- Conway, A. E., Van Nostrand, E. L., Pratt, G. A., Aigner, S., Wilbert, M. L., Sundararaman, B., Freese, P., Lambert, N. J., Sathe, S., Liang, T. Y., Essex, A., Landais, S., Burge, C. B., Jones, D. L., and Yeo, G. W. 2016. "Enhanced CLIP Uncovers IMP Protein-RNA Targets in Human Pluripotent Stem Cells Important for Cell Adhesion and Survival." *Cell Rep* 15 (3):666-679. doi: 10.1016/j.celrep.2016.03.052.
- Cook, Michael N, Olshan, Andrew F, Guess, Harry A, Savitz, David A, Poole, Charles, Blatt, Julie, Bondy, Melissa L, and Pollock, Brad H. 2004. "Maternal medication use and neuroblastoma in offspring." *American journal of epidemiology* 159 (8):721-731.
- Corvetta, Daisy, Chayka, Olesya, Gherardi, Samuele, D'Acunto, Cosimo W, Cantilena, Sandra, Valli, Emanuele, Piotrowska, Izabela, Perini, Giovanni, and Sala, Arturo. 2013. "Physical interaction between MYCN oncogene and polycomb repressive complex 2 (PRC2) in neuroblastoma: functional and therapeutic implications." *Journal of Biological Chemistry* 288 (12):8332-8341.
- Corvi, Raffaella, Amler, Lukas C, Savelyeva, Larissa, Gehring, Manuela, and Schwab, Manfred. 1994. "MYCN is retained in single copy at chromosome 2 band p23-24 during amplification in human neuroblastoma cells." *Proceedings of the National Academy of Sciences* 91 (12):5523-5527.
- Corvi, Raffaella, Savelyeva, Larissa, Breit, Stephen, Wenzel, Achim, Handgretinger, Rupert, Barak, Jaacov, Oren, Moshe, Amler, Lukas, and Schwab, Manfred. 1995a. "Non-syntenic amplification of MDM2 and MYCN in human neuroblastoma." *Oncogene* 10 (6):1081-1086.
- Corvi, Raffaella, Savelyeva, Larissa, and Schwab, Manfred. 1995b. "Duplication of N-MYC at its resident site 2p24 may be a mechanism of activation alternative to amplification in human neuroblastoma cells." *Cancer research* 55 (16):3471-3474.
- Cotterill, SJ, Pearson, ADJ, Pritchard, J, Foot, ABM, Roald, B, Kohler, JA, Imeson, J, Group, European Neuroblastoma Study, and Group, United Kingdom Children's Cancer Study. 2000. "Clinical prognostic factors in 1277 patients with neuroblastoma: results of The European Neuroblastoma Study Group 'Survey'1982-1992." *European journal of cancer* 36 (7):901-908.
- Coughlan, D., Gianferante, M., Lynch, C. F., Stevens, J. L., and Harlan, L. C. 2017. "Treatment and survival of childhood neuroblastoma: Evidence from a population-based study in the United States." *Pediatr Hematol Oncol* 34 (5):320-330. doi: 10.1080/08880018.2017.1373315.
- Croucher, J. L., Iyer, R., Li, N., Molteni, V., Loren, J., Gordon, W. P., Tuntland, T., Liu, B., and Brodeur, G. M. 2015. "TrkB inhibition by GNF-4256 slows growth and enhances chemotherapeutic efficacy in neuroblastoma xenografts." *Cancer Chemother Pharmacol* 75 (1):131-41. doi: 10.1007/s00280-014-2627-1.
- Cui, Hongjuan, Hu, Bo, Li, Tai, Ma, Jun, Alam, Goleeta, Gunning, William T, and Ding, Han-Fei. 2007. "Bmi-1 is essential for the tumorigenicity of neuroblastoma cells." *The American journal of pathology* 170 (4):1370-1378.
- Cunningham, F., Achuthan, P., Akanni, W., Allen, J., Amode, M. R., Armean, I. M., Bennett, R., Bhai, J., Billis, K., Boddu, S., Cummins, C., Davidson, C., Dodiya, K. J., Gall, A., Giron, C. G., Gil, L., Grego, T., Haggerty, L., Haskell, E., Hourlier, T., Izuogu, O. G., Janacek, S. H., Juettemann, T., Kay, M., Laird, M. R., Lavidas, I., Liu, Z., Loveland, J. E., Marugan, J. C., Maurel, T., McMahon, A. C., Moore, B., Morales, J., Mudge, J. M., Nuhn, M., Ogeh, D., Parker, A., Parton, A., Patricio, M., Abdul Salam, A. I., Schmitt, B. M., Schuilenburg, H., Sheppard, D., Sparrow, H., Stapleton, E., Szuba, M., Taylor, K., Threadgold, G., Thormann, A., Vullo, A., Walts, B., Winterbottom, A., Zadissa, A., Chakiachvili, M., Frankish, A., Hunt, S. E., Kostadima, M., Langridge, N., Martin, F. J., Muffato, M., Perry, E., Ruffier, M., Staines, D. M., Trevanion, S. J., Aken, B. L., Yates, A. D., Zerbino, D. R., and Flicek, P. 2019. "Ensembl 2019." *Nucleic Acids Res* 47 (D1):D745-D751. doi: 10.1093/nar/gky1113.
- Cunningham, F., Allen, J. E., Allen, J., Alvarez-Jarreta, J., Amode, M. R., Armean, I. M., Austine-Orimoloye, O., Azov, A. G., Barnes, I., Bennett, R., Berry, A., Bhai, J., Bignell, A., Billis, K., Boddu, S., Brooks, L., Charkhchi, M., Cummins, C., Da Rin Fioretto, L., Davidson, C., Dodiya, K., Donaldson, S., El Houdaigui, B., El Naboulsi, T., Fatima, R., Giron, C. G., Genev, T., Martinez, J. G., Gujjarro-Clarke, C., Gymer, A., Hardy, M., Hollis, Z., Hourlier, T., Hunt, T., Juettemann, T., Kaikala, V., Kay, M., Lavidas, I., Le, T., Lemos, D., Marugan, J. C., Mohanan, S., Mushtaq, A., Naven, M., Ogeh, D. N., Parker, A., Parton, A., Perry, M., Pilizota, I., Prosovetskaia, I., Sakthivel, M. P., Salam, A. I. A., Schmitt, B. M., Schuilenburg, H., Sheppard, D., Perez-Silva, J. G., Stark, W., Steed, E., Sutinen, K., Sukumaran, R., Sumathipala, D., Suner, M. M., Szpak, M., Thormann, A., Tricoli, F. F., Urbina-Gomez, D., Veidenberg, A., Walsh, T. A., Walts, B., Willhoft, N., Winterbottom, A., Wass, E., Chakiachvili, M., Flint, B., Frankish, A., Giorgetti, S., Haggerty, L., Hunt, S. E., GR, I. Sley, Loveland, J. E., Martin, F. J., Moore, B., Mudge, J. M., Muffato, M., Perry, E., Ruffier, M., Tate, J., Thybert, D., Trevanion, S. J., Dyer, S., Harrison, P. W., Howe, K. L., Yates, A. D., Zerbino, D. R., and Flicek, P. 2022. "Ensembl 2022." *Nucleic Acids Res* 50 (D1):D988-D995. doi: 10.1093/nar/gkab1049.
- Dagil, R., Ball, N. J., Ogrodowicz, R. W., Hobor, F., Purkiss, A. G., Kelly, G., Martin, S. R., Taylor, I. A., and Ramos, A. 2019. "IMP1 KH1 and KH2 domains create a structural platform with unique RNA recognition and re-modelling properties." *Nucleic Acids Res* 47 (8):4334-4348. doi: 10.1093/nar/gkz136.
- Dai, N. 2020. "The Diverse Functions of IMP2/IGF2BP2 in Metabolism." *Trends Endocrinol Metab* 31 (9):670-679. doi: 10.1016/j.tem.2020.05.007.
- Dai, N., Christiansen, J., Nielsen, F. C., and Avruch, J. 2013. "mTOR complex 2 phosphorylates IMP1 cotranslationally to promote IGF2 production and the proliferation of mouse embryonic fibroblasts." *Genes Dev* 27 (3):301-12. doi: 10.1101/gad.209130.112.
- Dai, N., Rapley, J., Angel, M., Yanik, M. F., Blower, M. D., and Avruch, J. 2011. "mTOR phosphorylates IMP2 to promote IGF2 mRNA translation by internal ribosomal entry." *Genes Dev* 25 (11):1159-72. doi: 10.1101/gad.2042311.
- Dai, N., Zhao, L., Wrighting, D., Kramer, M., Majithia, A., Wang, Y., Cracan, V., Borges-Rivera, D., Mootha, V. K., Nahrendorf, M., Thorburn, D. R., Minichiello, L., Altshuler, D., and Avruch, J. 2015. "IGF2BP2/IMP2-Deficient mice resist obesity through enhanced translation of Ucp1 mRNA and Other mRNAs encoding mitochondrial proteins." *Cell Metab* 21 (4):609-21. doi: 10.1016/j.cmet.2015.03.006.
- De Bernardi, B., Mosseri, V., Rubie, H., Castel, V., Foot, A., Ladenstein, R., Laureys, G., Beck-Popovic, M., de Lacerda, A. F., Pearson, A. D., De Kraker, J., Ambros, P. F., de Rycke, Y., Conte, M., Bruzzi, P., Michon, J., and Group, Siop Europe Neuroblastoma. 2008. "Treatment of localised resectable neuroblastoma. Results of the LNESG1 study by the SIOP Europe Neuroblastoma Group." *Br J Cancer* 99 (7):1027-33. doi: 10.1038/sj.bjc.6604640.
- De los Santos, M., Zambrano, A., and Aranda, A. 2007. "Combined effects of retinoic acid and histone deacetylase inhibitors on human neuroblastoma SH-SY5Y cells." *Mol Cancer Ther* 6 (4):1425-32. doi: 10.1158/1535-7163.MCT-06-0623.

6. References

- De Wilde, B., Beckers, A., Lindner, S., Kristina, A., De Preter, K., Depuydt, P., Mestdagh, P., Sante, T., Lefever, S., Hertwig, F., Peng, Z., Shi, L. M., Lee, S., Vandermarliere, E., Martens, L., Menten, B., Schramm, A., Fischer, M., Schulte, J., Vandesompele, J., and Speleman, F. 2018. "The mutational landscape of MYCN, Lin28b and ALK(F1174L) driven murine neuroblastoma mimics human disease." *Oncotarget* 9 (9):8334-8349. doi: 10.18632/oncotarget.23614.
- Decaestecker, B., Denecker, G., Van Neste, C., Dolman, E. M., Van Loocke, W., Gartlgruber, M., Nunes, C., De Vloed, F., Depuydt, P., Verboom, K., Rombaut, D., Loontjens, S., De Wyn, J., Kholosy, W. M., Koopmans, B., Essing, A. H. W., Herrmann, C., Dreidax, D., Durinck, K., Deforce, D., Van Nieuwerburgh, F., Henssen, A., Versteeg, R., Boeva, V., Schleiermacher, G., van Nes, J., Mestdagh, P., Vanhauwaert, S., Schulte, J. H., Westermann, F., Molenaar, J. J., De Preter, K., and Speleman, F. 2018. "TBX2 is a neuroblastoma core regulatory circuitry component enhancing MYCN/FOXO1 reactivation of DREAM targets." *Nat Commun* 9 (1):4866. doi: 10.1038/s41467-018-06699-9.
- Decock, Anneleen, Ongenaert, Maté, De Wilde, Bram, Brichard, Bénédicte, Noguera, Rosa, Speleman, Frank, and Vandesompele, Jo. 2016. "Stage 4S neuroblastoma tumors show a characteristic DNA methylation portrait." *Epigenetics* 11 (10):761-771.
- Degrauwe, N., Schlumpf, T. B., Janiszewska, M., Martin, P., Cauderay, A., Provero, P., Riggi, N., Suva, M. L., Paro, R., and Stamenkovic, I. 2016. "The RNA Binding Protein IMP2 Preserves Glioblastoma Stem Cells by Preventing let-7 Target Gene Silencing." *Cell Rep* 15 (8):1634-47. doi: 10.1016/j.celrep.2016.04.086.
- Dhillon, S. 2015. "Dinutuximab: first global approval." *Drugs* 75 (8):923-7. doi: 10.1007/s40265-015-0399-5.
- Diskin, S. J., Capasso, M., Schnepf, R. W., Cole, K. A., Attiyeh, E. F., Hou, C., Diamond, M., Carpenter, E. L., Winter, C., Lee, H., Jagannathan, J., Latorre, V., Iolascon, A., Hakonarson, H., Devoto, M., and Maris, J. M. 2012. "Common variation at 6q16 within HACE1 and LIN28B influences susceptibility to neuroblastoma." *Nat Genet* 44 (10):1126-30. doi: 10.1038/ng.2387.
- Diskin, Sharon J, Capasso, Mario, Diamond, Maura, Oldridge, Derek A, Conkrite, Karina, Bosse, Kristopher R, Russell, Mike R, Iolascon, Achille, Hakonarson, Hakon, and Devoto, Marcella. 2014. "Rare variants in TP53 and susceptibility to neuroblastoma." *Journal of the National Cancer Institute* 106 (4):dju047.
- Diskin, Sharon J, Hou, Cuiping, Glessner, Joseph T, Attiyeh, Edward F, Laudenslager, Marci, Bosse, Kristopher, Cole, Kristina, Mossé, Yaël P, Wood, Andrew, and Lynch, Jill E. 2009. "Copy number variation at 1q21. 1 associated with neuroblastoma." *Nature* 459 (7249):987-991.
- Dondero, Alessandra, Pastorino, Fabio, Della Chiesa, Mariella, Corrias, Maria Valeria, Morandi, Fabio, Pistoia, Vito, Olive, Daniel, Bellora, Francesca, Locatelli, Franco, and Castellano, Aurora. 2016. "PD-L1 expression in metastatic neuroblastoma as an additional mechanism for limiting immune surveillance." *Oncoimmunology* 5 (1):e1064578.
- Donnelly, C. J., Willis, D. E., Xu, M., Tep, C., Jiang, C., Yoo, S., Schanen, N. C., Kirn-Safran, C. B., van Minnen, J., English, A., Yoon, S. O., Bassell, G. J., and Twiss, J. L. 2011. "Limited availability of ZBP1 restricts axonal mRNA localization and nerve regeneration capacity." *EMBO J* 30 (22):4665-77. doi: 10.1038/emboj.2011.347.
- Doyen, J., Falk, A. T., Floquet, V., Herault, J., and Hannoun-Levi, J. M. 2016. "Proton beams in cancer treatments: Clinical outcomes and dosimetric comparisons with photon therapy." *Cancer Treat Rev* 43:104-12. doi: 10.1016/j.ctrv.2015.12.007.
- Doyle, G. A., Betz, N. A., Leeds, P. F., Fleisig, A. J., Prokipcak, R. D., and Ross, J. 1998. "The c-myc coding region determinant-binding protein: a member of a family of KH domain RNA-binding proteins." *Nucleic Acids Res* 26 (22):5036-44. doi: 10.1093/nar/26.22.5036.
- Doyle, M., and Kiebler, M. A. 2011. "Mechanisms of dendritic mRNA transport and its role in synaptic tagging." *EMBO J* 30 (17):3540-52. doi: 10.1038/emboj.2011.278.
- DuBois, S. G., Marachelian, A., Fox, E., Kudgus, R. A., Reid, J. M., Groshen, S., Malvar, J., Bagatell, R., Wagner, L., Maris, J. M., Hawkins, R., Courtier, J., Lai, H., Goodarzian, F., Shimada, H., Czarnecki, S., Tsao-Wei, D., Matthay, K. K., and Mosse, Y. P. 2016. "Phase I Study of the Aurora A Kinase Inhibitor Alisertib in Combination With Irinotecan and Temozolomide for Patients With Relapsed or Refractory Neuroblastoma: A NANT (New Approaches to Neuroblastoma Therapy) Trial." *J Clin Oncol* 34 (12):1368-75. doi: 10.1200/JCO.2015.65.4889.
- DuBois, Steven G, Geier, Ethan, Batra, Vandana, Yee, Sook Wah, Neuhaus, John, Segal, Mark, Martinez, Daniel, Pawel, Bruce, Yanik, Greg, and Naranjo, Arlene. 2012. "Evaluation of norepinephrine transporter expression and metaiodobenzylguanidine avidity in neuroblastoma: a report from the Children's Oncology Group." *International journal of molecular imaging* 2012.
- DuBois, Steven G, Kalika, Yan, Lukens, John N, Brodeur, Garrett M, Seeger, Robert C, Atkinson, James B, Haase, Gerald M, Black, C Thomas, Perez, Carlos, and Shimada, Hiroyuki. 1999. "Metastatic sites in stage IV and IVS neuroblastoma correlate with age, tumor biology, and survival." *Journal of pediatric hematology/oncology* 21 (3):181-189.
- Durbin, A. D., Zimmerman, M. W., Dharia, N. V., Abraham, B. J., Iniguez, A. B., Weichert-Leahey, N., He, S., Krill-Burger, J. M., Root, D. E., Vazquez, F., Tsherniak, A., Hahn, W. C., Golub, T. R., Young, R. A., Look, A. T., and Stegmaier, K. 2018. "Selective gene dependencies in MYCN-amplified neuroblastoma include the core transcriptional regulatory circuitry." *Nat Genet* 50 (9):1240-1246. doi: 10.1038/s41588-018-0191-z.
- Durinck, S., Spellman, P. T., Birney, E., and Huber, W. 2009. "Mapping identifiers for the integration of genomic datasets with the R/Bioconductor package biomaRt." *Nat Protoc* 4 (8):1184-91. doi: 10.1038/nprot.2009.97.
- Edsjö, Anders, Nilsson, Helén, Vandesompele, Jo, Karlsson, Jenny, Pattyn, Filip, Culp, Lloyd A, Speleman, Frank, and Pålman, Sven. 2004. "Neuroblastoma cells with overexpressed MYCN retain their capacity to undergo neuronal differentiation." *Laboratory investigation* 84 (4):406-417.
- Eggert, Angelika, Grotzer, Michael A, Ikegaki, Naohiko, Liu, Xing-ge, Evans, Audrey E, and Brodeur, Garrett M. 2000. "Expression of neurotrophin receptor TrkA inhibits angiogenesis in neuroblastoma." *Medical and Pediatric Oncology: The Official Journal of SIOP—International Society of Pediatric Oncology (Société Internationale d'Oncologie Pédiatrique)* 35 (6):569-572.
- Ejaskär, K, Aburatani, H, Abrahamsson, J, Kogner, P, and Martinsson, T. 1998. "Loss of heterozygosity of 3p markers in neuroblastoma tumours implicate a tumour-suppressor locus distal to the FHIT gene." *British journal of cancer* 77 (11):1787-1791.
- Elcheva, I., Goswami, S., Noubissi, F. K., and Spiegelman, V. S. 2009. "CRD-BP protects the coding region of betaTrCP1 mRNA from miR-183-mediated degradation." *Mol Cell* 35 (2):240-6. doi: 10.1016/j.molcel.2009.06.007.
- Eleveld, T. F., Oldridge, D. A., Bernard, V., Koster, J., Colmet Daage, L., Diskin, S. J., Schild, L., Bentahar, N. B., Bellini, A., Chicard, M., Lapouble, E., Combaret, V., Legoix-Ne, P., Michon, J., Pugh, T. J., Hart, L. S., Rader, J., Attiyeh, E. F., Wei, J. S., Zhang, S., Naranjo, A., Gastier-Foster, J. M., Hogarty, M. D., Asgharzadeh, S., Smith, M. A., Guidry-Auvil, J. M., Watkins, T. B., Zwijnenburg, D. A., Ebus, M. E., van Sluis, P., Hakkert, A., van Wezel, E., van der Schoot, C. E., Westerhout, E. M., Schulte, J. H., Tytgat, G. A., Dolman, M. E., Janoueix-Lerosey, I., Gerhard, D. S., Caron, H. N., Delattre, O., Khan, J., Versteeg, R., Schleiermacher, G., Molenaar, J. J., and Maris, J. M. 2015. "Relapsed neuroblastomas show frequent RAS-MAPK pathway mutations." *Nat Genet* 47 (8):864-71. doi: 10.1038/ng.3333.

6. References

- Emanuel, Beverly S, Balaban, Gloria, Boyd, Jennifer P, Grossman, Abraham, Negishi, Manabu, Parmiter, Annette, and Glick, Mary Catherine. 1985. "N-myc amplification in multiple homogeneously staining regions in two human neuroblastomas." *Proceedings of the National Academy of Sciences* 82 (11):3736-3740.
- Ennajdaoui, H., Howard, J. M., Sterne-Weiler, T., Jahanbani, F., Coyne, D. J., Uren, P. J., Dargyte, M., Katzman, S., Draper, J. M., Wallace, A., Cazarez, O., Burns, S. C., Qiao, M., Hinck, L., Smith, A. D., Toloue, M. M., Blencowe, B. J., Penalva, L. O., and Sanford, J. R. 2016. "IGF2BP3 Modulates the Interaction of Invasion-Associated Transcripts with RISC." *Cell Rep* 15 (9):1876-83. doi: 10.1016/j.celrep.2016.04.083.
- Eom, T., Antar, L. N., Singer, R. H., and Bassell, G. J. 2003. "Localization of a beta-actin messenger ribonucleoprotein complex with zipcode-binding protein modulates the density of dendritic filopodia and filopodial synapses." *J Neurosci* 23 (32):10433-44. doi: 10.1523/JNEUROSCI.23-32-10433.2003.
- Esteller, Manel. 2008. "Epigenetics in cancer." *New England Journal of Medicine* 358 (11):1148-1159.
- Evans, A. E., D'Angio, G. J., and Randolph, J. 1971. "A proposed staging for children with neuroblastoma. Children's cancer study group A." *Cancer* 27 (2):374-8. doi: 10.1002/1097-0142(197102)27:2<374::aid-cncr2820270221>3.0.co;2-g.
- Farina, K. L., Hüttelmaier, S., Musunuru, K., Darnell, R., and Singer, R. H. 2003. "Two ZBP1 KH domains facilitate beta-actin mRNA localization, granule formation, and cytoskeletal attachment." *J Cell Biol* 160 (1):77-87. doi: 10.1083/jcb.200206003.
- Faye, M. D., Beug, S. T., Graber, T. E., Earl, N., Xiang, X., Wild, B., Langlois, S., Michaud, J., Cowan, K. N., Korneluk, R. G., and Holcik, M. 2015. "IGF2BP1 controls cell death and drug resistance in rhabdomyosarcomas by regulating translation of cIAP1." *Oncogene* 34 (12):1532-41. doi: 10.1038/onc.2014.90.
- Fetahu, I. S., and Taschner-Mandl, S. 2021. "Neuroblastoma and the epigenome." *Cancer Metastasis Rev* 40 (1):173-189. doi: 10.1007/s10555-020-09946-y.
- Fischer, M., Grossmann, P., Padi, M., and DeCaprio, J. A. 2016. "Integration of TP53, DREAM, MMB-FOXM1 and RB-E2F target gene analyses identifies cell cycle gene regulatory networks." *Nucleic Acids Res* 44 (13):6070-86. doi: 10.1093/nar/gkw523.
- Foley, N. H., Bray, I. M., Tivnan, A., Bryan, K., Murphy, D. M., Buckley, P. G., Ryan, J., O'Meara, A., O'Sullivan, M., and Stallings, R. L. 2010. "MicroRNA-184 inhibits neuroblastoma cell survival through targeting the serine/threonine kinase AKT2." *Mol Cancer* 9:83. doi: 10.1186/1476-4598-9-83.
- Fong, Chin-to, Dracopoli, Nicholas C, White, Peter S, Merrill, Pauline T, Griffith, Rogers C, Housman, David E, and Brodeur, Garrett M. 1989. "Loss of heterozygosity for the short arm of chromosome 1 in human neuroblastomas: correlation with N-myc amplification." *Proceedings of the National Academy of Sciences* 86 (10):3753-3757.
- Fong, Chin-to, White, Peter S, Peterson, Karen, Sapienza, Carmen, Cavenee, Webster K, Kern, Scott E, Vogelstein, Bert, Cantor, Alan B, Look, A Thomas, and Brodeur, Garrett M. 1992. "Loss of heterozygosity for chromosomes 1 or 14 defines subsets of advanced neuroblastomas." *Cancer research* 52 (7):1780-1785.
- Franke, Folker, Rudolph, Bärbel, Christiansen, Holger, Harbott, Jochen, and Lampert, Fritz. 1986. "Tumour karyotype may be important in the prognosis of human neuroblastoma." *Journal of cancer research and clinical oncology* 111:266-272.
- Fujita, T., Igarashi, J., Okawa, E. R., Gotoh, T., Manne, J., Kolla, V., Kim, J., Zhao, H., Pawel, B. R., London, W. B., Maris, J. M., White, P. S., and Brodeur, G. M. 2008. "CHD5, a tumor suppressor gene deleted from 1p36.31 in neuroblastomas." *J Natl Cancer Inst* 100 (13):940-9. doi: 10.1093/jnci/djn176.
- Fuziwara, C. S., and Kimura, E. T. 2015. "Insights into Regulation of the miR-17-92 Cluster of miRNAs in Cancer." *Front Med (Lausanne)* 2:64. doi: 10.3389/fmed.2015.00064.
- Galardi, A., Colletti, M., Businaro, P., Quintarelli, C., Locatelli, F., and Di Giannatale, A. 2018. "MicroRNAs in Neuroblastoma: Biomarkers with Therapeutic Potential." *Curr Med Chem* 25 (5):584-600. doi: 10.2174/0929867324666171003120335.
- Gardina, P. J., Lo, K. C., Lee, W., Cowell, J. K., and Turpaz, Y. 2008. "Ploidy status and copy number aberrations in primary glioblastomas defined by integrated analysis of allelic ratios, signal ratios and loss of heterozygosity using 500K SNP Mapping Arrays." *BMC Genomics* 9:489. doi: 10.1186/1471-2164-9-489.
- Gatta, Gemma, Botta, Laura, Rossi, Silvia, Aareleid, Tiit, Bielska-Lasota, Magdalena, Clavel, Jacqueline, Dimitrova, Nadya, Jakab, Zsuzsanna, Kaatsch, Peter, and Lacour, Brigitte. 2014. "Childhood cancer survival in Europe 1999–2007: results of EURO CARE-5—a population-based study." *The lancet oncology* 15 (1):35-47.
- Gel, B., and Serra, E. 2017. "karyoploteR: an R/Bioconductor package to plot customizable genomes displaying arbitrary data." *Bioinformatics* 33 (19):3088-3090. doi: 10.1093/bioinformatics/btx346.
- Geng, C., and Macdonald, P. M. 2006. "Imp associates with squid and Hrp48 and contributes to localized expression of gurken in the oocyte." *Mol Cell Biol* 26 (24):9508-16. doi: 10.1128/MCB.01136-06.
- George, R. E., Sanda, T., Hanna, M., Frohling, S., Luther, W., 2nd, Zhang, J., Ahn, Y., Zhou, W., London, W. B., McGrady, P., Xue, L., Zozulya, S., Gregor, V. E., Webb, T. R., Gray, N. S., Gilliland, D. G., Diller, L., Greulich, H., Morris, S. W., Meyerson, M., and Look, A. T. 2008a. "Activating mutations in ALK provide a therapeutic target in neuroblastoma." *Nature* 455 (7215):975-8. doi: 10.1038/nature07397.
- George, Rani E, Sanda, Takaomi, Hanna, Megan, Fröhling, Stefan, li, William Luther, Zhang, Jianming, Ahn, Yebin, Zhou, Wenjun, London, Wendy B, and McGrady, Patrick. 2008b. "Activating mutations in ALK provide a therapeutic target in neuroblastoma." *Nature* 455 (7215):975-978.
- George, RE, and Squire, JA. 2000. "Structure of the MYCN amplicon." *Neuroblastoma. Elsevier Science BV Amsterdam*:85-100.
- Gerstberger, S., Hafner, M., and Tuschl, T. 2014. "A census of human RNA-binding proteins." *Nat Rev Genet* 15 (12):829-45. doi: 10.1038/nrg3813.
- Gestblom, C., Grynfeld, A., Ora, I., Ortoft, E., Larsson, C., Axelson, H., Sandstedt, B., Cserjesi, P., Olson, E. N., and Pahlman, S. 1999. "The basic helix-loop-helix transcription factor dHAND, a marker gene for the developing human sympathetic nervous system, is expressed in both high- and low-stage neuroblastomas." *Lab Invest* 79 (1):67-79.
- Git, A., Allison, R., Perdiguero, E., Nebreda, A. R., Houliston, E., and Standart, N. 2009. "Vg1RBP phosphorylation by Erk2 MAP kinase correlates with the cortical release of Vg1 mRNA during meiotic maturation of Xenopus oocytes." *RNA* 15 (6):1121-33. doi: 10.1261/rna.1195709.
- Glaß, M., Misiak, D., Bley, N., Müller, S., Hagemann, S., Busch, B., Rausch, A., and Hüttelmaier, S. 2021. "IGF2BP1, a Conserved Regulator of RNA Turnover in Cancer." *Front Mol Biosci* 8:632219. doi: 10.3389/fmolb.2021.632219.
- Godfried, M. B., Veenstra, M., v Sluis, P., Boon, K., v Asperen, R., Hermus, M. C., v Schaik, B. D., Voute, T. P., Schwab, M., Versteeg, R., and Caron, H. N. 2002. "The N-myc and c-myc downstream pathways include the chromosome 17q genes nm23-H1 and nm23-H2." *Oncogene* 21 (13):2097-101. doi: 10.1038/sj.onc.1205259.

6. References

- Goldstein, Lori J, Fojo, Antonio T, Ueda, Kazumitsu, Crist, William, Green, Alexander, Brodeur, Garrett, Pastan, Ira, and Gottesman, Michael M. 1990. "Expression of the multidrug resistance, MDR1, gene in neuroblastomas." *Journal of Clinical Oncology* 8 (1):128-136.
- Gonzalez Malagon, Sandra G, and Liu, Karen J. 2018. "ALK and GSK3: shared features of neuroblastoma and neural crest cells." *Journal of experimental neuroscience* 12:1179069518792499.
- Goswami, S., Tarapore, R. S., Poenitzsch Strong, A. M., TeSlaa, J. J., Grinblat, Y., Setaluri, V., and Spiegelman, V. S. 2015. "MicroRNA-340-mediated degradation of microphthalmia-associated transcription factor (MITF) mRNA is inhibited by coding region determinant-binding protein (CRD-BP)." *J Biol Chem* 290 (1):384-95. doi: 10.1074/jbc.M114.590158.
- Grobner, S. N., Worst, B. C., Weischenfeldt, J., Buchhalter, I., Kleinheinz, K., Rudneva, V. A., Johann, P. D., Balasubramanian, G. P., Segura-Wang, M., Brabetz, S., Bender, S., Hutter, B., Sturm, D., Pfaff, E., Hubschmann, D., Zipprich, G., Heinold, M., Eils, J., Lawerenz, C., Erkek, S., Lambo, S., Waszak, S., Blattmann, C., Borkhardt, A., Kuhlen, M., Eggert, A., Fulda, S., Gessler, M., Wegert, J., Kappler, R., Baumhoer, D., Burdach, S., Kirschner-Schwabe, R., Kontny, U., Kulozik, A. E., Lohmann, D., Hettmer, S., Eckert, C., Bielack, S., Nathrath, M., Niemeyer, C., Richter, G. H., Schulte, J., Siebert, R., Westermann, F., Molenaar, J. J., Vassal, G., Witt, H., Project, ICGC PedBrain-Seq, Project, ICGC Mmm1-Seq, Burkhardt, B., Kratz, C. P., Witt, O., van Tilburg, C. M., Kramm, C. M., Fleischhack, G., Dirksen, U., Rutkowski, S., Fruhwald, M., von Hoff, K., Wolf, S., Klingebiel, T., Koscielniak, E., Landgraf, P., Koster, J., Resnick, A. C., Zhang, J., Liu, Y., Zhou, X., Waanders, A. J., Zwijnenburg, D. A., Raman, P., Brors, B., Weber, U. D., Northcott, P. A., Pajtler, K. W., Kool, M., Piro, R. M., Korbel, J. O., Schlesner, M., Eils, R., Jones, D. T. W., Lichter, P., Chavez, L., Zapatka, M., and Pfister, S. M. 2018. "The landscape of genomic alterations across childhood cancers." *Nature* 555 (7696):321-327. doi: 10.1038/nature25480.
- Grovas, Alfred, Fremgen, Amy, Rauck, Amanda, Ruymann, Frederick B, Hutchinson, Carol L, Winchester, David P, and Menck, Herman R. 1997. "The National Cancer Data Base report on patterns of childhood cancers in the United States." *Cancer: Interdisciplinary International Journal of the American Cancer Society* 80 (12):2321-2332.
- Gu, L., Zhang, H., He, J., Li, J., Huang, M., and Zhou, M. 2012. "MDM2 regulates MYCN mRNA stabilization and translation in human neuroblastoma cells." *Oncogene* 31 (11):1342-53. doi: 10.1038/onc.2011.343.
- Gu, W., Wells, A. L., Pan, F., and Singer, R. H. 2008. "Feedback regulation between zipcode binding protein 1 and beta-catenin mRNAs in breast cancer cells." *Mol Cell Biol* 28 (16):4963-74. doi: 10.1128/MCB.00266-08.
- Guo, Chun, White, Peter S, Hogarty, Michael D, Brodeur, Garrett M, Gerbing, Robert, Stram, Daniel O, and Maris, John M. 2000. "Deletion of 11q23 is a frequent event in the evolution of MYCN single-copy high-risk neuroblastomas." *Medical and Pediatric Oncology: The Official Journal of SIOP—International Society of Pediatric Oncology (Société Internationale d'Oncologie Pédiatrique* 35 (6):544-546.
- Guo, Chun, White, Peter S, Weiss, Matthew J, Hogarty, Michael D, Thompson, Patricia M, Stram, Daniel O, Gerbing, Robert, Matthay, Katherine K, Seeger, Robert C, and Brodeur, Garrett M. 1999. "Allelic deletion at 11q23 is common in MYCN single copy neuroblastomas." *Oncogene* 18 (35):4948-4957.
- Gurney, James G, Ross, Julie A, Wall, Donna A, Bleyer, W Archie, Severson, Richard K, and Robison, Leslie L. 1997. "Infant cancer in the US: histology-specific incidence and trends, 1973 to 1992." *Journal of pediatric hematology/oncology* 19 (5):428-432.
- Gustafson, W. C., Meyerowitz, J. G., Nekritz, E. A., Chen, J., Benes, C., Charron, E., Simonds, E. F., Seeger, R., Matthay, K. K., Hertz, N. T., Eilers, M., Shokat, K. M., and Weiss, W. A. 2014. "Drugging MYCN through an allosteric transition in Aurora kinase A." *Cancer Cell* 26 (3):414-427. doi: 10.1016/j.ccr.2014.07.015.
- Gutschner, T., Hammerle, M., Pazaitis, N., Bley, N., Fiskin, E., Uckelmann, H., Heim, A., Grobner, M., Hofmann, N., Geffers, R., Skawran, B., Longerich, T., Breuhahn, K., Schirmacher, P., Muhleck, B., Hüttelmaier, S., and Diederichs, S. 2014. "Insulin-like growth factor 2 mRNA-binding protein 1 (IGF2BP1) is an important protumorigenic factor in hepatocellular carcinoma." *Hepatology* 59 (5):1900-11. doi: 10.1002/hep.26997.
- Haase, J., Misiak, D., Bauer, M., Pazaitis, N., Braun, J., Potschke, R., Mensch, A., Bell, J. L., Dralle, H., Siebolts, U., Wickenhauser, C., Lorenz, K., and Hüttelmaier, S. 2020. "IGF2BP1 is the first positive marker for anaplastic thyroid carcinoma diagnosis." *Mod Pathol*. doi: 10.1038/s41379-020-0630-0.
- Hackett, C. S., Hodgson, J. G., Law, M. E., Fridlyand, J., Osoegawa, K., de Jong, P. J., Nowak, N. J., Pinkel, D., Albertson, D. G., Jain, A., Jenkins, R., Gray, J. W., and Weiss, W. A. 2003. "Genome-wide array CGH analysis of murine neuroblastoma reveals distinct genomic aberrations which parallel those in human tumors." *Cancer Res* 63 (17):5266-73.
- Hafner, M., Landthaler, M., Burger, L., Khorshid, M., Hausser, J., Berninger, P., Rothballer, A., Ascano, M., Jr., Jungkamp, A. C., Munschauer, M., Ulrich, A., Wardle, G. S., Dewell, S., Zavolan, M., and Tuschl, T. 2010. "Transcriptome-wide identification of RNA-binding protein and microRNA target sites by PAR-CLIP." *Cell* 141 (1):129-41. doi: 10.1016/j.cell.2010.03.009.
- Hailat, Nabil, Keim, David R, Melhem, Randa F, Zhu, XIAO-XIANG, Eckerskorn, Christoph, Brodeur, Garrett M, Reynolds, C Patrick, Seeger, Robert C, Lottspeich, Friedrich, and Strahler, John R. 1991. "High levels of p19/nm23 protein in neuroblastoma are associated with advanced stage disease and with N-myc gene amplification." *The Journal of clinical investigation* 88 (1):341-345.
- Hamilton, K. E., Noubissi, F. K., Katti, P. S., Hahn, C. M., Davey, S. R., Lundsmith, E. T., Klein-Szanto, A. J., Rhim, A. D., Spiegelman, V. S., and Rustgi, A. K. 2013. "IMP1 promotes tumor growth, dissemination and a tumor-initiating cell phenotype in colorectal cancer cell xenografts." *Carcinogenesis* 34 (11):2647-54. doi: 10.1093/carcin/bgt217.
- Hammer, N. A., Hansen, Tv, Byskov, A. G., Rajpert-De Meyts, E., Grondahl, M. L., Bredkjaer, H. E., Wewer, U. M., Christiansen, J., and Nielsen, F. C. 2005. "Expression of IGF-II mRNA-binding proteins (IMPs) in gonads and testicular cancer." *Reproduction* 130 (2):203-12. doi: 10.1530/rep.1.00664.
- Hammerle, M., Gutschner, T., Uckelmann, H., Ozgur, S., Fiskin, E., Gross, M., Skawran, B., Geffers, R., Longerich, T., Breuhahn, K., Schirmacher, P., Stoecklin, G., and Diederichs, S. 2013. "Posttranscriptional destabilization of the liver-specific long noncoding RNA HULC by the IGF2 mRNA-binding protein 1 (IGF2BP1)." *Hepatology* 58 (5):1703-12. doi: 10.1002/hep.26537.
- Hann, Hie-Won L, Evans, Audrey E, Siegel, Stuart E, Wong, Kwan Y, Sather, Harland, Dalton, Andree, Hammond, Denman, and Seeger, Robert C. 1985. "Prognostic importance of serum ferritin in patients with Stages III and IV neuroblastoma: the Childrens Cancer Study Group experience." *Cancer research* 45 (6):2843-2848.
- Hansen, T. V., Hammer, N. A., Nielsen, J., Madsen, M., Dalbaeck, C., Wewer, U. M., Christiansen, J., and Nielsen, F. C. 2004. "Dwarfism and impaired gut development in insulin-like growth factor II mRNA-binding protein 1-deficient mice." *Mol Cell Biol* 24 (10):4448-64. doi: 10.1128/MCB.24.10.4448-4464.2004.
- Hansford, L. M., Thomas, W. D., Keating, J. M., Burkhardt, C. A., Peaston, A. E., Norris, M. D., Haber, M., Armati, P. J., Weiss, W. A., and Marshall, G. M. 2004. "Mechanisms of embryonal tumor initiation: distinct roles for Mycn expression and MYCN amplification." *Proc Natl Acad Sci U S A* 101 (34):12664-9. doi: 10.1073/pnas.0401083101.
- Hart, T., Brown, K. R., Sircoulomb, F., Rottapel, R., and Moffat, J. 2014. "Measuring error rates in genomic perturbation screens: gold standards for human functional genomics." *Mol Syst Biol* 10:733. doi: 10.1525/msb.20145216.

6. References

- Hasan, Md Kamrul, Nafady, Asmaa, Takatori, Atsushi, Kishida, Satoshi, Ohira, Miki, Suenaga, Yusuke, Hossain, Shamim, Akter, Jesmin, Ogura, Atsushi, and Nakamura, Yohko. 2013. "ALK is a MYCN target gene and regulates cell migration and invasion in neuroblastoma." *Scientific reports* 3 (1):3450.
- Haupt, Ygal, Maya, Ruth, Kazaz, Anat, and Oren, Moshe. 1997. "Mdm2 promotes the rapid degradation of p53." *Nature* 387 (6630):296-299.
- Henrich, Kai-Oliver, Bauer, Tobias, Schulte, Johannes, Ehemann, Volker, Deubzer, Hedwig, Gogolin, Sina, Muth, Daniel, Fischer, Matthias, Benner, Axel, and König, Rainer. 2011. "CAMTA1, a 1p36 tumor suppressor candidate, inhibits growth and activates differentiation programs in neuroblastoma cells." *Cancer research* 71 (8):3142-3151.
- Henrich, Kai-Oliver, Fischer, Matthias, Mertens, Daniel, Benner, Axel, Wiedemeyer, Ruprecht, Brors, Benedikt, Oberthuer, André, Berthold, Frank, Wei, Jun Stephen, and Khan, Javed. 2006. "Reduced expression of CAMTA1 correlates with adverse outcome in neuroblastoma patients." *Clinical cancer research* 12 (1):131-138.
- Henrich, Kai-Oliver, Schwab, Manfred, and Westermann, Frank. 2012. "1p36 tumor suppression—a matter of dosage?" *Cancer research* 72 (23):6079-6088.
- Henssen, A., Althoff, K., Odersky, A., Beckers, A., Koche, R., Speleman, F., Schafers, S., Bell, E., Nortmeyer, M., Westermann, F., De Preter, K., Florin, A., Heukamp, L., Spruessel, A., Astrahaneff, K., Lindner, S., Sadowski, N., Schramm, A., Astorgues-Xerri, L., Riveiro, M. E., Eggert, A., Cvitkovic, E., and Schulte, J. H. 2016. "Targeting MYCN-Driven Transcription By BET-Bromodomain Inhibition." *Clin Cancer Res* 22 (10):2470-81. doi: 10.1158/1078-0432.CCR-15-1449.
- Heukamp, L. C., Thor, T., Schramm, A., De Preter, K., Kumps, C., De Wilde, B., Odersky, A., Peifer, M., Lindner, S., Spruessel, A., Pattyn, F., Mestdagh, P., Menten, B., Kuhfittig-Kulle, S., Kunkele, A., König, K., Meder, L., Chatterjee, S., Ullrich, R. T., Schulte, S., Vandesompele, J., Speleman, F., Buttner, R., Eggert, A., and Schulte, J. H. 2012. "Targeted expression of mutated ALK induces neuroblastoma in transgenic mice." *Sci Transl Med* 4 (141):141ra91. doi: 10.1126/scitranslmed.3003967.
- Higashi, Mayumi, Kolla, Venkatadri, Iyer, Radhika, Naraparaju, Koumudi, Zhuang, Tiangang, Kolla, Sriharsha, and Brodeur, Garrett M. 2015. "Retinoic acid-induced CHD5 upregulation and neuronal differentiation of neuroblastoma." *Molecular cancer* 14 (1):1-10.
- Hirai, Misako, Yoshida, Sadao, Kashiwagi, Hironobu, Kawamura, Tomonori, Ishikawa, Tomoyoshi, Kaneko, Michio, Ohkawa, Haruo, Nakagawara, Akira, Miwa, Masanao, and Uchida, Kazuhiko. 1999. "1q23 gain is associated with progressive neuroblastoma resistant to aggressive treatment." *Genes, Chromosomes and Cancer* 25 (3):261-269.
- Hisashige, Akinori. 2014. "Effectiveness of nationwide screening program for neuroblastoma in Japan." *Global Journal of Health Science* 6 (4):94.
- Hiyama, E, Hiyama, K, Ohtsu, K, Yamaoka, H, Ichikawa, T, Shay, JW, and Yokoyama, T. 1997. "Telomerase activity in neuroblastoma: is it a prognostic indicator of clinical behaviour?" *European Journal of Cancer* 33 (12):1932-1936.
- Hiyama, Eiso, Hiyama, Keiko, Yokoyama, Takashi, Matsuura, Yuichiro, Piatyszek, Mieczyslaw A, and Shay, Jerry W. 1995. "Correlating telomerase activity levels with human neuroblastoma outcomes." *Nature medicine* 1 (3):249-255.
- Hiyama, Eiso, Iehara, Tomoko, Sugimoto, Tooru, Fukuzawa, Masahiro, Hayashi, Yutaka, Sasaki, Fumiaki, Sugiyama, Masahiko, Kondo, Satoshi, Yoneda, Akihiro, and Yamaoka, Hiroaki. 2008. "Effectiveness of screening for neuroblastoma at 6 months of age: a retrospective population-based cohort study." *The Lancet* 371 (9619):1173-1180.
- Ho, R., Eggert, A., Hishiki, T., Minturn, J. E., Ikegaki, N., Foster, P., Camoratto, A. M., Evans, A. E., and Brodeur, G. M. 2002. "Resistance to chemotherapy mediated by TrkB in neuroblastomas." *Cancer Res* 62 (22):6462-6.
- Hodges, Courtney, Kirkland, Jacob G, and Crabtree, Gerald R. 2016. "The many roles of BAF (mSWI/SNF) and PBAF complexes in cancer." *Cold Spring Harbor perspectives in medicine* 6 (8):a026930.
- Hogarty, M. D., Norris, M. D., Davis, K., Liu, X., Evageliou, N. F., Hayes, C. S., Pawel, B., Guo, R., Zhao, H., Sekyere, E., Keating, J., Thomas, W., Cheng, N. C., Murray, J., Smith, J., Sutton, R., Venn, N., London, W. B., Buxton, A., Gilmour, S. K., Marshall, G. M., and Haber, M. 2008. "ODC1 is a critical determinant of MYCN oncogenesis and a therapeutic target in neuroblastoma." *Cancer Res* 68 (23):9735-45. doi: 10.1158/0008-5472.CAN-07-6866.
- Honda, Reiko, Tanaka, Hirofumi, and Yasuda, Hideyo. 1997. "Oncoprotein MDM2 is a ubiquitin ligase E3 for tumor suppressor p53." *FEBS letters* 420 (1):25-27.
- Hosoi, Gaku, Hara, Junichi, Okamura, Takayuki, Osugi, Yuko, Ishihara, Shigehiko, Fukuzawa, Masahiro, Okada, Akira, Okada, Shintaro, and Tawa, Akio. 1994. "Low frequency of the p53 gene mutations in neuroblastoma." *Cancer* 73 (12):3087-3093.
- Hosono, Y., Niknafs, Y. S., Prensner, J. R., Iyer, M. K., Dhanasekaran, S. M., Mehra, R., Pitchiaya, S., Tien, J., Escara-Wilke, J., Poliakov, A., Chu, S. C., Saleh, S., Sankar, K., Su, F., Guo, S., Qiao, Y., Freier, S. M., Bui, H. H., Cao, X., Malik, R., Johnson, T. M., Beer, D. G., Feng, F. Y., Zhou, W., and Chinnaiyan, A. M. 2017. "Oncogenic Role of THOR, a Conserved Cancer/Testis Long Non-coding RNA." *Cell* 171 (7):1559-1572 e20. doi: 10.1016/j.cell.2017.11.040.
- Hua, Zhongyan, Gu, Xiao, Dong, Yudi, Tan, Fei, Liu, Zhihui, Thiele, Carol J, and Li, Zhijie. 2016. "PI3K and MAPK pathways mediate the BDNF/TrkB-increased metastasis in neuroblastoma." *Tumor Biology* 37:16227-16236.
- Huang, H., Weng, H., Sun, W., Qin, X., Shi, H., Wu, H., Zhao, B. S., Mesquita, A., Liu, C., Yuan, C. L., Hu, Y. C., Hüttelmaier, S., Skibbe, J. R., Su, R., Deng, X., Dong, L., Sun, M., Li, C., Nachtergaele, S., Wang, Y., Hu, C., Ferchen, K., Greis, K. D., Jiang, X., Wei, M., Qu, L., Guan, J. L., He, C., Yang, J., and Chen, J. 2018a. "Recognition of RNA N(6)-methyladenosine by IGF2BP proteins enhances mRNA stability and translation." *Nat Cell Biol* 20 (3):285-295. doi: 10.1038/s41556-018-0045-z.
- Huang, M., and Weiss, W. A. 2013. "Neuroblastoma and MYCN." *Cold Spring Harb Perspect Med* 3 (10):a014415. doi: 10.1101/cshperspect.a014415.
- Huang, Q., Guo, H., Wang, S., Ma, Y., Chen, H., Li, H., Li, J., Li, X., Yang, F., Qiu, M., Zhao, S., and Wang, J. 2020. "A novel circular RNA, circXPO1, promotes lung adenocarcinoma progression by interacting with IGF2BP1." *Cell Death Dis* 11 (12):1031. doi: 10.1038/s41419-020-03237-8.
- Huang, X., Zhang, H., Guo, X., Zhu, Z., Cai, H., and Kong, X. 2018b. "Insulin-like growth factor 2 mRNA-binding protein 1 (IGF2BP1) in cancer." *J Hematol Oncol* 11 (1):88. doi: 10.1186/s13045-018-0628-y.
- Hüttelmaier, S., Zenklusen, D., Lederer, M., Dichtenberg, J., Lorenz, M., Meng, X., Bassell, G. J., Condeelis, J., and Singer, R. H. 2005. "Spatial regulation of beta-actin translation by Src-dependent phosphorylation of ZBP1." *Nature* 438 (7067):512-5. doi: 10.1038/nature04115.
- Ianevski, A., Giri, A. K., and Aittokallio, T. 2020. "SynergyFinder 2.0: visual analytics of multi-drug combination synergies." *Nucleic Acids Res* 48 (W1):W488-W493. doi: 10.1093/nar/gkaa216.
- Ichimiya, Shigno, Nimura, Yoshinori, Seki, Naohiko, Ozaki, Toshifumi, Nagase, Takahiro, and Nakagawara, Akira. 2001. "Downregulation of hASH1 is associated with the retinoic acid-induced differentiation of human neuroblastoma cell lines." *Medical and Pediatric Oncology: The Official Journal of SIOP—International Society of Pediatric Oncology (Société Internationale d'Oncologie Pédiatrique)* 36 (1):132-134.

6. References

- Infarinato, Nicole R, Park, Jin H, Krytska, Kateryna, Ryles, Hannah T, Sano, Renata, Szigety, Katherine M, Li, Yimei, Zou, Helen Y, Lee, Nathan V, and Smeal, Tod. 2016. "The ALK/ROS1 inhibitor PF-06463922 overcomes primary resistance to crizotinib in ALK-driven neuroblastoma." *Cancer discovery* 6 (1):96-107.
- Inomistova, M. V., Khranovska, N. M., Skachkova, O. V., Klymniuk, G. I., Demydov, S. V., and Svergun, N. M. 2016. "MiR-137 expression in neuroblastoma: a role in clinical course and outcome." *Biopolymers and Cell* 32 (3):222-228. doi: 10.7124/bc.000924.
- Ireland, Christine M. 1989. "Activated N-ras oncogenes in human neuroblastoma." *Cancer Research* 49 (20):5530-5533.
- Irwin, M. S., and Park, J. R. 2015. "Neuroblastoma: paradigm for precision medicine." *Pediatr Clin North Am* 62 (1):225-56. doi: 10.1016/j.pcl.2014.09.015.
- Islam, A., Kageyama, H., Takada, N., Kawamoto, T., Takayasu, H., Isogai, E., Ohira, M., Hashizume, K., Kobayashi, H., Kaneko, Y., and Nakagawara, A. 2000. "High expression of Survivin, mapped to 17q25, is significantly associated with poor prognostic factors and promotes cell survival in human neuroblastoma." *Oncogene* 19 (5):617-23. doi: 10.1038/sj.onc.1203358.
- Isogai, Eriko, Ohira, Miki, Ozaki, Toshinori, Oba, Shigeyuki, Nakamura, Yohko, and Nakagawara, Akira. 2011. "Oncogenic LMO3 collaborates with HEN2 to enhance neuroblastoma cell growth through transactivation of Mash1." *PLoS one* 6 (5):e19297.
- Iyer, R., Wehrmann, L., Golden, R. L., Naraparaju, K., Croucher, J. L., MacFarland, S. P., Guan, P., Kolla, V., Wei, G., Cam, N., Li, G., Hornby, Z., and Brodeur, G. M. 2016. "Entrectinib is a potent inhibitor of Trk-driven neuroblastomas in a xenograft mouse model." *Cancer Lett* 372 (2):179-86. doi: 10.1016/j.canlet.2016.01.018.
- Jamal, A., Hassan Dalhat, M., Jahan, S., Choudhry, H., and Imran Khan, M. 2023. "BTYNB, an inhibitor of RNA binding protein IGF2BP1 reduces proliferation and induces differentiation of leukemic cancer cells." *Saudi J Biol Sci* 30 (3):103569. doi: 10.1016/j.sjbs.2023.103569.
- Janoueix-Lerosey, I., Lequin, D., Brugieres, L., Ribeiro, A., de Pontual, L., Combaret, V., Raynal, V., Puisieux, A., Schleiermacher, G., Pierron, G., Valteau-Couanet, D., Frebourg, T., Michon, J., Lyonnet, S., Amiel, J., and Delattre, O. 2008. "Somatic and germline activating mutations of the ALK kinase receptor in neuroblastoma." *Nature* 455 (7215):967-70. doi: 10.1038/nature07398.
- Jögi, Annika, Øra, Ingrid, Nilsson, Helén, Lindeheim, Åsa, Makino, Yuichi, Poellinger, Lorenz, Axelson, Håkan, and Pålman, Sven. 2002. "Hypoxia alters gene expression in human neuroblastoma cells toward an immature and neural crest-like phenotype." *Proceedings of the National Academy of Sciences* 99 (10):7021-7026.
- Johnson, Maureen R, Look, A Thomas, DeClue, Jeffrey E, Valentine, Marcus B, and Lowy, Douglas R. 1993. "Inactivation of the NF1 gene in human melanoma and neuroblastoma cell lines without impaired regulation of GTP. Ras." *Proceedings of the National Academy of Sciences* 90 (12):5539-5543.
- Jonson, L., Christiansen, J., Hansen, T. V. O., Vikesa, J., Yamamoto, Y., and Nielsen, F. C. 2014. "IMP3 RNP safe houses prevent miRNA-directed HMG2 mRNA decay in cancer and development." *Cell Rep* 7 (2):539-551. doi: 10.1016/j.celrep.2014.03.015.
- Jonson, L., Vikesaa, J., Krogh, A., Nielsen, L. K., Hansen, Tv, Borup, R., Johnsen, A. H., Christiansen, J., and Nielsen, F. C. 2007. "Molecular composition of IMP1 ribonucleoprotein granules." *Mol Cell Proteomics* 6 (5):798-811. doi: 10.1074/mcp.M600346-MCP200.
- Joshi, Vijay V, Larkin, Ernest W, Holbrook, C Tate, Silverman, Jan F, Norris, H Thomas, Cantor, Alan B, Shuster, Jonathan J, Brodeur, Garrett M, Look, A Thomas, and Hayes, F Ann. 1993. "Correlation between morphologic and other prognostic markers of neuroblastoma a study of histologic grade, DNA index, N-myc gene copy number, and lactic dehydrogenase in patients in the pediatric oncology group." *Cancer* 71 (10):3173-3181.
- Jung, H., Yoon, B. C., and Holt, C. E. 2012. "Axonal mRNA localization and local protein synthesis in nervous system assembly, maintenance and repair." *Nat Rev Neurosci* 13 (5):308-24. doi: 10.1038/nrn3210.
- Kanda, Teru, Sullivan, Kevin F, and Wahl, Geoffrey M. 1998. "Histone-GFP fusion protein enables sensitive analysis of chromosome dynamics in living mammalian cells." *Current Biology* 8 (7):377-385.
- Keshelava, N, Seeger, RC, and Reynolds, CP. 1997. "Drug resistance in human neuroblastoma cell lines correlates with clinical therapy." *European Journal of Cancer* 33 (12):2002-2006.
- Keshelava, Nino, Zuo, Juan J, Chen, Ping, Waidyaratne, Sitara N, Luna, Marian C, Gomer, Charles J, Triche, Timothy J, and Reynolds, C Patrick. 2001. "Loss of p53 function confers high-level multidrug resistance in neuroblastoma cell lines." *Cancer research* 61 (16):6185-6193.
- Kholodenko, Irina V, Kalinovsky, Daniel V, Doronin, Igor I, Deyev, Sergey M, and Kholodenko, Roman V. 2018. "Neuroblastoma origin and therapeutic targets for immunotherapy." *Journal of immunology research* 2018.
- Kim, D., Langmead, B., and Salzberg, S. L. 2015. "HISAT: a fast spliced aligner with low memory requirements." *Nat Methods* 12 (4):357-60. doi: 10.1038/nmeth.3317.
- Kim, M. K., and Carroll, W. L. 2004. "Autoregulation of the N-myc gene is operative in neuroblastoma and involves histone deacetylase 2." *Cancer* 101 (9):2106-15. doi: 10.1002/cncr.20626.
- Kim, Nam W, Piatyszek, Mieczyslaw A, Prowse, Karen R, Harley, Calvin B, West, Michael D, Ho, Peter LC, Coviello, Gina M, Wright, Woodring E, Weinrich, Scott L, and Shay, Jerry W. 1994. "Specific association of human telomerase activity with immortal cells and cancer." *Science* 266 (5193):2011-2015.
- Kinzler, Kenneth W. 1998. "The genetics basis of human cancer." *Colorectal Tumors*:565-587.
- Klambauer, G., Schwarzbauer, K., Mayr, A., Clevert, D. A., Mitterecker, A., Bodenhofer, U., and Hochreiter, S. 2012. "cn.MOPS: mixture of Poissons for discovering copy number variations in next-generation sequencing data with a low false discovery rate." *Nucleic Acids Res* 40 (9):e69. doi: 10.1093/nar/gks003.
- Knudson Jr, ALFRED G, and Strong, LC1762170. 1972. "Mutation and cancer: neuroblastoma and pheochromocytoma." *American journal of human genetics* 24 (5):514.
- Köbel, M., Weidensdorfer, D., Reinke, C., Lederer, M., Schmitt, W. D., Zeng, K., Thomssen, C., Hauptmann, S., and Hüttelmaier, S. 2007. "Expression of the RNA-binding protein IMP1 correlates with poor prognosis in ovarian carcinoma." *Oncogene* 26 (54):7584-9. doi: 10.1038/sj.onc.1210563.
- Kocak, H., Ackermann, S., Hero, B., Kahlert, Y., Oberthuer, A., Juraeva, D., Roels, F., Theissen, J., Westermann, F., Deubzer, H., Ehemann, V., Brors, B., Odenthal, M., Berthold, F., and Fischer, M. 2013. "Hox-C9 activates the intrinsic pathway of apoptosis and is associated with spontaneous regression in neuroblastoma." *Cell Death Dis* 4:e586. doi: 10.1038/cddis.2013.84.
- Köhn, M., Lederer, M., Wächter, K., and Hüttelmaier, S. 2010. "Near-infrared (NIR) dye-labeled RNAs identify binding of ZBP1 to the noncoding Y3-RNA." *RNA* 16 (7):1420-8. doi: 10.1261/rna.2152710.
- Kondo, S., Kondo, Y., Hara, H., Kaakaji, R., Peterson, J. W., Morimura, T., Takeuchi, J., and Barnett, G. H. 1996. "mdm2 gene mediates the expression of mdrl gene and P-glycoprotein in a human glioblastoma cell line." *Br J Cancer* 74 (8):1263-8. doi: 10.1038/bjc.1996.527.

6. References

- Kong, Xiao-Tang, Choi, Seung Hoon, Inoue, Akira, Xu, Feng, Chen, TAO, Takita, Junko, Yokota, Jun, Bessho, Fumio, Yanagisawa, Masayoshi, and Hanada, Ryoji. 1997. "Expression and mutational analysis of the DCC, DPC4, and MADR2/JV18-1 genes in neuroblastoma." *Cancer research* 57 (17):3772-3778.
- Koyama, Hiroshi, Zhuang, Tiangang, Light, Jennifer E, Kolla, Venkatadri, Higashi, Mayumi, McGrady, Patrick W, London, Wendy B, and Brodeur, Garrett M. 2012. "Mechanisms of CHD5 Inactivation in neuroblastomas." *Clinical cancer research* 18 (6):1588-1597.
- Kozomara, A., Birgaoanu, M., and Griffiths-Jones, S. 2019. "miRBase: from microRNA sequences to function." *Nucleic Acids Res* 47 (D1):D155-D162. doi: 10.1093/nar/gky1141.
- Kubbutat, Michael HG, Jones, Stephen N, and Vousden, Karen H. 1997. "Regulation of p53 stability by Mdm2." *Nature* 387 (6630):299-303.
- Kuo, Y. T., Liu, Y. L., Adebayo, B. O., Shih, P. H., Lee, W. H., Wang, L. S., Liao, Y. F., Hsu, W. M., Yeh, C. T., and Lin, C. M. 2015. "JARID1B Expression Plays a Critical Role in Chemoresistance and Stem Cell-Like Phenotype of Neuroblastoma Cells." *PLoS One* 10 (5):e0125343. doi: 10.1371/journal.pone.0125343.
- Kurihara, Sho, Hiyama, Eiso, Onitake, Yoshiyuki, Yamaoka, Emi, and Hiyama, Keiko. 2014. "Clinical features of ATRX or DAXX mutated neuroblastoma." *Journal of Pediatric Surgery* 49 (12):1835-1838.
- Kuroda, Hiroshi, Sugimoto, Tohru, Ueda, Kazumitsu, Tsuchida, Shigeki, Horii, Yoshihiro, Inazawa, Johji, Sato, Kiyomi, and Sawada, Tadashi. 1991. "Different drug sensitivity in two neuroblastoma cell lines established from the same patient before and after chemotherapy." *International journal of cancer* 47 (5):732-737.
- Kushner, B. H., Kramer, K., Modak, S., and Cheung, N. K. 2006. "Irinotecan plus temozolomide for relapsed or refractory neuroblastoma." *J Clin Oncol* 24 (33):5271-6. doi: 10.1200/JCO.2006.06.7272.
- Kushner, B. H., Kramer, K., Modak, S., Qin, L. X., and Cheung, N. K. 2010. "Differential impact of high-dose cyclophosphamide, topotecan, and vincristine in clinical subsets of patients with chemoresistant neuroblastoma." *Cancer* 116 (12):3054-60. doi: 10.1002/cncr.25232.
- Kushner, B. H., Modak, S., Kramer, K., Basu, E. M., Roberts, S. S., and Cheung, N. K. 2013. "Ifosfamide, carboplatin, and etoposide for neuroblastoma: a high-dose salvage regimen and review of the literature." *Cancer* 119 (3):665-71. doi: 10.1002/cncr.27783.
- Kushner, Brian H, Gilbert, Fred, and Helson, Lawrence. 1986. "Familial neuroblastoma. Case reports, literature review, and etiologic considerations." *Cancer* 57 (9):1887-1893.
- Kuzyk, A., Booth, S., Righolt, C., Mathur, S., Gartner, J., and Mai, S. 2015. "MYCN overexpression is associated with unbalanced copy number gain, altered nuclear location, and overexpression of chromosome arm 17q genes in neuroblastoma tumors and cell lines." *Genes Chromosomes Cancer* 54 (10):616-28. doi: 10.1002/gcc.22273.
- Ladenstein, R. L., Poetschger, U., Luksch, R., Brock, P., Castel, V., Yaniv, I., Papadakis, V., Laureys, G., Malis, J., Balwierz, W., Ruud, E., Kogner, P., Schroeder, H., Lacerda, A. Forjaz De, Popovic, M. Beck, Bician, P., Garami, M., Trahair, T., Pearson, A. D., and Couanet, D. Valteau. 2011. "Busulphan-melphalan as a myeloablative therapy (MAT) for high-risk neuroblastoma: Results from the HR-NBL1/SIOPEN trial." *Journal of Clinical Oncology* 29 (18_suppl):2-2. doi: 10.1200/jco.2011.29.18_suppl.2.
- Langmead, B., and Salzberg, S. L. 2012. "Fast gapped-read alignment with Bowtie 2." *Nat Methods* 9 (4):357-9. doi: 10.1038/nmeth.1923.
- Lasorella, Anna, Boldrini, Renata, Dominici, Carlo, Donfrancesco, Alberto, Yokota, Yoshifumi, Inserra, Alessandro, and Iavarone, Antonio. 2002. "Id2 is critical for cellular proliferation and is the oncogenic effector of N-myc in human neuroblastoma." *Cancer research* 62 (1):301-306.
- Łastowska, M, Van Roy, Nadine, Bown, N, Speleman, Franki, Roberts, P, Lunec, J, Strachan, T, Pearson, ADJ, and Jackson, MS. 2001. "Molecular cytogenetic definition of 17q translocation breakpoints in neuroblastoma." *Medical and Pediatric Oncology: The Official Journal of SIOP—International Society of Pediatric Oncology (Société Internationale d'Oncologie Pédiatrique)* 36 (1):20-23.
- Łastowska, Maria, Cotterill, Simon, Bown, Nick, Cullinane, Catherine, Variend, Sadick, Lunec, John, Strachan, Tom, Pearson, Andrew DJ, and Jackson, Michael S. 2002. "Breakpoint position on 17q identifies the most aggressive neuroblastoma tumors." *Genes, Chromosomes and Cancer* 34 (4):428-436.
- Lazaro, S., Perez-Crespo, M., Lorz, C., Bernardini, A., Oteo, M., Enguita, A. B., Romero, E., Hernandez, P., Tomas, L., Morcillo, M. A., Paramio, J. M., and Santos, M. 2019. "Differential development of large-cell neuroendocrine or small-cell lung carcinoma upon inactivation of 4 tumor suppressor genes." *Proc Natl Acad Sci U S A* 116 (44):22300-22306. doi: 10.1073/pnas.1821745116.
- Lazarova, D. L., Spengler, B. A., Biedler, J. L., and Ross, R. A. 1999. "HuD, a neuronal-specific RNA-binding protein, is a putative regulator of N-myc pre-mRNA processing/stability in malignant human neuroblasts." *Oncogene* 18 (17):2703-10. doi: 10.1038/sj.onc.1202621.
- Lee, Soo Hyun, Kim, Jung-Sun, Zheng, Siyuan, Huse, Jason T, Bae, Joon Seol, Lee, Ji Won, Yoo, Keon Hee, Koo, Hong Hoe, Kyung, Sungkyu, and Park, Woong-Yang. 2017. "ARID1B alterations identify aggressive tumors in neuroblastoma." *Oncotarget* 8 (28):45943.
- Leek, J. T., Johnson, W. E., Parker, H. S., Jaffe, A. E., and Storey, J. D. 2012. "The sva package for removing batch effects and other unwanted variation in high-throughput experiments." *Bioinformatics* 28 (6):882-3. doi: 10.1093/bioinformatics/bts034.
- Lemm, I., and Ross, J. 2002. "Regulation of c-myc mRNA decay by translational pausing in a coding region instability determinant." *Mol Cell Biol* 22 (12):3959-69. doi: 10.1128/MCB.22.12.3959-3969.2002.
- Li, B., Zhu, L., Lu, C., Wang, C., Wang, H., Jin, H., Ma, X., Cheng, Z., Yu, C., Wang, S., Zuo, Q., Zhou, Y., Wang, J., Yang, C., Lv, Y., Jiang, L., and Qin, W. 2021. "circNDUFB2 inhibits non-small cell lung cancer progression via destabilizing IGF2BPs and activating anti-tumor immunity." *Nat Commun* 12 (1):295. doi: 10.1038/s41467-020-20527-z.
- Li, C, Xu, ZL, Zhao, Z, An, Q, Wang, L, Yu, Y, and Piao, DX. 2017a. "ARID1A gene knockdown promotes neuroblastoma migration and invasion." *Neoplasma* 64 (3):367-376.
- Li, F., Aljhdali, I., and Ling, X. 2019. "Cancer therapeutics using survivin BIRC5 as a target: what can we do after over two decades of study?" *J Exp Clin Cancer Res* 38 (1):368. doi: 10.1186/s13046-019-1362-1.
- Li, Yuanyuan, Ohira, Miki, Zhou, Yong, Xiong, Teng, Luo, Wen, Yang, Chao, Li, Xiangchun, Gao, Zhibo, Zhou, Rui, and Nakamura, Yohko. 2017b. "Genomic analysis-integrated whole-exome sequencing of neuroblastomas identifies genetic mutations in axon guidance pathway." *Oncotarget* 8 (34):56684.
- Li, Zhenghao, Takenobu, Hisanori, Setyawati, Amallia Nuggetsiana, Akita, Nobuhiro, Haruta, Masayuki, Satoh, Shunpei, Shinno, Yoshitaka, Chikaraishi, Koji, Mukae, Kyosuke, and Akter, Jesmin. 2018. "EZH2 regulates neuroblastoma cell differentiation via NTRK1 promoter epigenetic modifications." *Oncogene* 37 (20):2714-2727.
- Liao, B., Hu, Y., Herrick, D. J., and Brewer, G. 2005. "The RNA-binding protein IMP-3 is a translational activator of insulin-like growth factor II leader-3 mRNA during proliferation of human K562 leukemia cells." *J Biol Chem* 280 (18):18517-24. doi: 10.1074/jbc.M500270200.
- Liao, Y., Smyth, G. K., and Shi, W. 2014. "featureCounts: an efficient general purpose program for assigning sequence reads to genomic features." *Bioinformatics* 30 (7):923-30. doi: 10.1093/bioinformatics/btt656.
- Liberzon, A., Birger, C., Thorvaldsdottir, H., Ghandi, M., Mesirov, J. P., and Tamayo, P. 2015. "The Molecular Signatures Database (MSigDB) hallmark gene set collection." *Cell Syst* 1 (6):417-425. doi: 10.1016/j.cels.2015.12.004.

6. References

- Liberzon, A., Subramanian, A., Pinchback, R., Thorvaldsdottir, H., Tamayo, P., and Mesirov, J. P. 2011. "Molecular signatures database (MSigDB) 3.0." *Bioinformatics* 27 (12):1739-40. doi: 10.1093/bioinformatics/btr260.
- Lignell, A., Kerosuo, L., Streichan, S. J., Cai, L., and Bronner, M. E. 2017. "Identification of a neural crest stem cell niche by Spatial Genomic Analysis." *Nat Commun* 8 (1):1830. doi: 10.1038/s41467-017-01561-w.
- Liu, Y., Guo, Q., Yang, H., Zhang, X. W., Feng, N., Wang, J. K., Liu, T. T., Zeng, K. W., and Tu, P. F. 2022. "Allosteric Regulation of IGF2BP1 as a Novel Strategy for the Activation of Tumor Immune Microenvironment." *ACS Cent Sci* 8 (8):1102-1115. doi: 10.1021/acscentsci.2c00107.
- Liu, Z., Chen, S. S., Clarke, S., Veschi, V., and Thiele, C. J. 2020. "Targeting MYCN in Pediatric and Adult Cancers." *Front Oncol* 10:623679. doi: 10.3389/fonc.2020.623679.
- Livak, K. J., and Schmittgen, T. D. 2001. "Analysis of relative gene expression data using real-time quantitative PCR and the 2(-Delta Delta C(T)) Method." *Methods* 25 (4):402-8. doi: 10.1006/meth.2001.1262.
- London, W. B., Castel, V., Monclair, T., Ambros, P. F., Pearson, A. D., Cohn, S. L., Berthold, F., Nakagawara, A., Ladenstein, R. L., Iehara, T., and Matthay, K. K. 2011. "Clinical and biologic features predictive of survival after relapse of neuroblastoma: a report from the International Neuroblastoma Risk Group project." *J Clin Oncol* 29 (24):3286-92. doi: 10.1200/JCO.2010.34.3392.
- Longo, L., Panza, E., Schena, F., Seri, M., Devoto, M., Romeo, G., Bini, C., Pappalardo, G., Tonini, G. P., and Perri, P. 2007. "Genetic predisposition to familial neuroblastoma: identification of two novel genomic regions at 2p and 12p." *Hum Hered* 63 (3-4):205-11. doi: 10.1159/000099997.
- Look, A Thomas, Hayes, F Ann, Nitschke, Ruprecht, McWilliams, Nancy B, and Green, Alexander A. 1984. "Cellular DNA content as a predictor of response to chemotherapy in infants with unresectable neuroblastoma." *New England Journal of Medicine* 311 (4):231-235.
- Look, A Thomas, Hayes, F Ann, Shuster, Jonathan J, Douglass, Edwin C, Castleberry, Robert P, Bowman, LC, Smith, EI, and Brodeur, GM. 1991. "Clinical relevance of tumor cell ploidy and N-myc gene amplification in childhood neuroblastoma: a Pediatric Oncology Group study." *Journal of Clinical Oncology* 9 (4):581-591.
- Lu, Ziyang, Tian, Yufeng, Salwen, Helen R, Chlenski, Alexandre, Godley, Lucy A, Raj, J Usha, and Yang, Qiwei. 2013. "Histone lysine methyltransferase EHMT2 is involved in proliferation, apoptosis, cell invasion and DNA methylation of human neuroblastoma cells." *Anti-cancer drugs* 24 (5):484.
- Luttikhuis, MEM, Powell, JE, Rees, SA, Genus, Tracey, Chughtai, S, Ramani, Pramila, Mann, JR, and McConville, CM. 2001. "Neuroblastomas with chromosome 11q loss and single copy MYCN comprise a biologically distinct group of tumours with adverse prognosis." *British journal of cancer* 85 (4):531-537.
- Lutz, W., Stohr, M., Schurmann, J., Wenzel, A., Lohr, A., and Schwab, M. 1996. "Conditional expression of N-myc in human neuroblastoma cells increases expression of alpha-prothymosin and ornithine decarboxylase and accelerates progression into S-phase early after mitogenic stimulation of quiescent cells." *Oncogene* 13 (4):803-12.
- Ma, L., Young, J., Prabhala, H., Pan, E., Mestdagh, P., Muth, D., Teruya-Feldstein, J., Reinhardt, F., Onder, T. T., Valastyan, S., Westermann, F., Speleman, F., Vandesompele, J., and Weinberg, R. A. 2010. "miR-9, a MYC/MYCN-activated microRNA, regulates E-cadherin and cancer metastasis." *Nat Cell Biol* 12 (3):247-56. doi: 10.1038/ncb2024.
- Mac, Susanna M, D'Cunha, Caroline A, and Farnham, Peggy J. 2000. "Direct recruitment of N-myc to target gene promoters." *Molecular Carcinogenesis: Published in cooperation with the University of Texas MD Anderson Cancer Center* 29 (2):76-86.
- Mahaira, L. G., Katsara, O., Pappou, E., Iliopoulou, E. G., Fortis, S., Antsaklis, A., Fotinopoulos, P., Baxevas, C. N., Papamichail, M., and Perez, S. A. 2014. "IGF2BP1 expression in human mesenchymal stem cells significantly affects their proliferation and is under the epigenetic control of TET1/2 demethylases." *Stem Cells Dev* 23 (20):2501-12. doi: 10.1089/scd.2013.0604.
- Mahapatra, L., Andruska, N., Mao, C., Le, J., and Shapiro, D. J. 2017. "A Novel IMP1 Inhibitor, BTYNB, Targets c-Myc and Inhibits Melanoma and Ovarian Cancer Cell Proliferation." *Transl Oncol* 10 (5):818-827. doi: 10.1016/j.tranon.2017.07.008.
- Maizels, Y., Oberman, F., Miloslavski, R., Ginzach, N., Berman, M., and Yisraeli, J. K. 2015. "Localization of cofilin mRNA to the leading edge of migrating cells promotes directed cell migration." *J Cell Sci* 128 (10):1922-33. doi: 10.1242/jcs.163972.
- Majzner, R. G., Simon, J. S., Grosso, J. F., Martinez, D., Pawel, B. R., Santi, M., Merchant, M. S., Georger, B., Hezam, I., Marty, V., Vielh, P., Daugaard, M., Sorensen, P. H., Mackall, C. L., and Maris, J. M. 2017. "Assessment of programmed death-ligand 1 expression and tumor-associated immune cells in pediatric cancer tissues." *Cancer* 123 (19):3807-3815. doi: 10.1002/cncr.30724.
- Manohar, C. F., Short, M. L., Nguyen, A., Nguyen, N. N., Chagnovich, D., Yang, Q., and Cohn, S. L. 2002. "HuD, a neuronal-specific RNA-binding protein, increases the in vivo stability of MYCN RNA." *J Biol Chem* 277 (3):1967-73. doi: 10.1074/jbc.M106966200.
- Maris, J. M. 2010. "Recent advances in neuroblastoma." *N Engl J Med* 362 (23):2202-11. doi: 10.1056/NEJMra0804577.
- Maris, J. M., and Matthay, K. K. 1999. "Molecular biology of neuroblastoma." *J Clin Oncol* 17 (7):2264-79. doi: 10.1200/JCO.1999.17.7.2264.
- Maris, JM, Hogarty, MD, Bagatell, R, and Cohn, SL. 2007. Neuroblastoma *Lancet* 369 (9579): 2106–2120.
- Maris, JM, Kyemba, SM, Rebbeck, TR, White, PS, Sulman, EP, Jensen, SJ, Allen, C, Biegel, JA, and Brodeur, GM. 1997. "Molecular genetic analysis of familial neuroblastoma." *European Journal of Cancer* 33 (12):1923-1928.
- Maris, John M, Weiss, Matthew J, Mosse, Yael, Hii, George, Guo, Chun, White, Peter S, Hogarty, Michael D, Mirensky, Tamar, Brodeur, Garrett M, and Rebbeck, Timothy R. 2002. "Evidence for a hereditary neuroblastoma predisposition locus at chromosome 16p12–13." *Cancer research* 62 (22):6651-6658.
- Marshall, G. M., Carter, D. R., Cheung, B. B., Liu, T., Mateos, M. K., Meyerowitz, J. G., and Weiss, W. A. 2014. "The prenatal origins of cancer." *Nat Rev Cancer* 14 (4):277-89. doi: 10.1038/nrc3679.
- Marshall, Glenn M, Liu, Pei Y, Gherardi, Samuele, Scarlett, Christopher J, Bedalov, Antonio, Xu, Ning, Iraci, Nuncio, Valli, Emanuele, Ling, Dora, and Thomas, Wayne. 2011. "SIRT1 promotes N-Myc oncogenesis through a positive feedback loop involving the effects of MKP3 and ERK on N-Myc protein stability." *PLoS genetics* 7 (6):e1002135.
- Matsumoto, Kazue, Wada, Randal K, Yamashiro, Joyce M, Kaplan, David R, and Thiele, Carol J. 1995. "Expression of brain-derived neurotrophic factor and p145TrkB affects survival, differentiation, and invasiveness of human neuroblastoma cells." *Cancer research* 55 (8):1798-1806.
- Matthay, K. K., Maris, J. M., Schleiermacher, G., Nakagawara, A., Mackall, C. L., Diller, L., and Weiss, W. A. 2016. "Neuroblastoma." *Nat Rev Dis Primers* 2:16078. doi: 10.1038/nrdp.2016.78.
- Matthay, K. K., Villablanca, J. G., Seeger, R. C., Stram, D. O., Harris, R. E., Ramsay, N. K., Swift, P., Shimada, H., Black, C. T., Brodeur, G. M., Gerbing, R. B., and Reynolds, C. P. 1999. "Treatment of high-risk neuroblastoma with intensive chemotherapy, radiotherapy, autologous bone marrow transplantation, and 13-cis-retinoic acid. Children's Cancer Group." *N Engl J Med* 341 (16):1165-73. doi: 10.1056/NEJM199910143411601.

6. References

- Matthay, Katherine K, Yanik, Gregory, Messina, Julia, Quach, Alekist, Huberty, John, Cheng, Su-Chun, Veatch, Janet, Goldsby, Robert, Brophy, Patricia, and Kersun, Leslie S. 2007. "Phase II study on the effect of disease sites, age, and prior therapy on response to iodine-131-metaiodobenzylguanidine therapy in refractory neuroblastoma." *Journal of clinical oncology* 25 (9):1054-1060.
- Mayr, C., and Bartel, D. P. 2009. "Widespread shortening of 3'UTRs by alternative cleavage and polyadenylation activates oncogenes in cancer cells." *Cell* 138 (4):673-84. doi: 10.1016/j.cell.2009.06.016.
- Mazloom, A., Louis, C. U., Nuchtern, J., Kim, E., Russell, H., Allen-Rhoades, W., Krance, R., and Paulino, A. C. 2014. "Radiation therapy to the primary and postinduction chemotherapy MIBG-avid sites in high-risk neuroblastoma." *Int J Radiat Oncol Biol Phys* 90 (4):858-62. doi: 10.1016/j.ijrobp.2014.07.019.
- McDermott, Suzanne, Salzberg, Deborah C, Anderson, Anna Paige, Shaw, Timothy, and Lead, Jamie. 2015. "Systematic review of chromium and nickel exposure during pregnancy and impact on child outcomes." *Journal of Toxicology and Environmental Health, Part A* 78 (21-22):1348-1368.
- Meddeb, Mounira, Danglot, Gisèle, Chudoba, Ise, Vénuat, Anne-Marie, Bénard, Jean, Avet-Loiseau, Hervé, Vasseur, Béatrice, Le Paslier, Denis, Terrier-Lacombe, Marie-Jose, and Hartmann, Olivier. 1996. "Additional copies of a 25 Mb chromosomal region originating from 17q23.1-17qter are present in 90% of high-grade neuroblastomas." *Genes, Chromosomes and Cancer* 17 (3):156-165.
- Megiorni, F., Colaiacovo, M., Cialfi, S., McDowell, H. P., Guffanti, A., Camero, S., Felsani, A., Losty, P. D., Pizer, B., Shukla, R., Cappelli, C., Ferrara, E., Pizzuti, A., Moles, A., and Dominici, C. 2017. "A sketch of known and novel MYCN-associated miRNA networks in neuroblastoma." *Oncol Rep* 38 (1):3-20. doi: 10.3892/or.2017.5701.
- Mei, H., Lin, Z. Y., and Tong, Q. S. 2014. "The roles of microRNAs in neuroblastoma." *World J Pediatr* 10 (1):10-6. doi: 10.1007/s12519-014-0448-2.
- Melaiu, O., Mina, M., Chierici, M., Boldrini, R., Jurman, G., Romania, P., D'Alicandro, V., Benedetti, M. C., Castellano, A., Liu, T., Furlanello, C., Locatelli, F., and Fruci, D. 2017. "PD-L1 Is a Therapeutic Target of the Bromodomain Inhibitor JQ1 and, Combined with HLA Class I, a Promising Prognostic Biomarker in Neuroblastoma." *Clin Cancer Res* 23 (15):4462-4472. doi: 10.1158/1078-0432.CCR-16-2601.
- Meltzer, SJ, O'Doherty, SP, Frantz, CN, Smolinski, K, Yin, J, Cantor, AB, Liu, J, Valentine, M, Brodeur, GM, and Berg, PE. 1996. "Allelic imbalance on chromosome 5q predicts long-term survival in neuroblastoma." *British journal of cancer* 74 (12):1855-1861.
- Menegaux, Florence, Olshan, Andrew F, Neglia, Joseph P, Pollock, Brad H, and Bondy, Melissa L. 2004. "Day care, childhood infections, and risk of neuroblastoma." *American journal of epidemiology* 159 (9):843-851.
- Mestdagh, P., Fredlund, E., Pattyn, F., Schulte, J. H., Muth, D., Vermeulen, J., Kumps, C., Schlierf, S., De Preter, K., Van Roy, N., Noguera, R., Laureys, G., Schramm, A., Eggert, A., Westermann, F., Speleman, F., and Vandesompele, J. 2010. "MYCN/c-MYC-induced microRNAs repress coding gene networks associated with poor outcome in MYCN/c-MYC-activated tumors." *Oncogene* 29 (9):1394-404. doi: 10.1038/onc.2009.429.
- Meyer, M., and Kircher, M. 2010. "Illumina sequencing library preparation for highly multiplexed target capture and sequencing." *Cold Spring Harb Protoc* 2010 (6):pdb prot5448. doi: 10.1101/pdb.prot5448.
- Meyers, R. M., Bryan, J. G., McFarland, J. M., Weir, B. A., Sizemore, A. E., Xu, H., Dharia, N. V., Montgomery, P. G., Cowley, G. S., Pantel, S., Goodale, A., Lee, Y., Ali, L. D., Jiang, G., Lubonja, R., Harrington, W. F., Strickland, M., Wu, T., Hawes, D. C., Zhivich, V. A., Wyatt, M. R., Kalani, Z., Chang, J. J., Okamoto, M., Stegmaier, K., Golub, T. R., Boehm, J. S., Vazquez, F., Root, D. E., Hahn, W. C., and Tsherniak, A. 2017. "Computational correction of copy number effect improves specificity of CRISPR-Cas9 essentiality screens in cancer cells." *Nat Genet* 49 (12):1779-1784. doi: 10.1038/ng.3984.
- Mlakar, V., Dupanloup, I., Gonzales, F., Papangelopoulou, D., Ansari, M., and Gumy-Pause, F. 2024. "17q Gain in Neuroblastoma: A Review of Clinical and Biological Implications." *Cancers (Basel)* 16 (2). doi: 10.3390/cancers16020338.
- Molenaar, J. J., Domingo-Fernandez, R., Ebus, M. E., Lindner, S., Koster, J., Drabek, K., Mestdagh, P., van Sluis, P., Valentijn, L. J., van Nes, J., Broekmans, M., Haneveld, F., Volckmann, R., Bray, I., Heukamp, L., Sprussel, A., Thor, T., Kieckbusch, K., Klein-Hitpass, L., Fischer, M., Vandesompele, J., Schramm, A., van Noesel, M. M., Varesio, L., Speleman, F., Eggert, A., Stallings, R. L., Caron, H. N., Versteeg, R., and Schulte, J. H. 2012a. "LIN28B induces neuroblastoma and enhances MYCN levels via let-7 suppression." *Nat Genet* 44 (11):1199-206. doi: 10.1038/ng.2436.
- Molenaar, Jan J, Domingo-Fernández, Raquel, Ebus, Marli E, Lindner, Sven, Koster, Jan, Drabek, Ksenija, Mestdagh, Pieter, van Sluis, Peter, Valentijn, Linda J, and van Nes, Johan. 2012b. "LIN28B induces neuroblastoma and enhances MYCN levels via let-7 suppression." *Nature genetics* 44 (11):1199-1206.
- Molenaar, Jan J, Koster, Jan, Zwijnenburg, Danny A, Van Sluis, Peter, Valentijn, Linda J, Van Der Ploeg, Ida, Hamdi, Mohamed, Van Nes, Johan, Westerman, Bart A, and Van Arkel, Jennemiek. 2012c. "Sequencing of neuroblastoma identifies chromothripsis and defects in neurogenesis genes." *Nature* 483 (7391):589-593.
- Moley, Jeffrey F, Brother, Michele B, Wells, Samuel A, Spengler, Barbara A, Biedler, June L, and Brodeur, Garrett M. 1991. "Low frequency of ras gene mutations in neuroblastomas, pheochromocytomas, and medullary thyroid cancers." *Cancer research* 51 (6):1596-1599.
- Monclair, T., Brodeur, G. M., Ambros, P. F., Brisse, H. J., Cecchetto, G., Holmes, K., Kaneko, M., London, W. B., Matthay, K. K., Nuchtern, J. G., von Schweinitz, D., Simon, T., Cohn, S. L., Pearson, A. D., and Force, Inrg Task. 2009. "The International Neuroblastoma Risk Group (INRG) staging system: an INRG Task Force report." *J Clin Oncol* 27 (2):298-303. doi: 10.1200/JCO.2008.16.6876.
- Mongroo, P. S., Noubissi, F. K., Cuatrecasas, M., Kalabis, J., King, C. E., Johnstone, C. N., Bowser, M. J., Castells, A., Spiegelman, V. S., and Rustgi, A. K. 2011. "IMP-1 displays cross-talk with K-Ras and modulates colon cancer cell survival through the novel proapoptotic protein CYFIP2." *Cancer Res* 71 (6):2172-82. doi: 10.1158/0008-5472.CAN-10-3295.
- Moore, N. F., Azarova, A. M., Bhatnagar, N., Ross, K. N., Drake, L. E., Frumm, S., Liu, Q. S., Christie, A. L., Sanda, T., Chesler, L., Kung, A. L., Gray, N. S., Stegmaier, K., and George, R. E. 2014. "Molecular rationale for the use of PI3K/AKT/mTOR pathway inhibitors in combination with crizotinib in ALK-mutated neuroblastoma." *Oncotarget* 5 (18):8737-49. doi: 10.18632/oncotarget.2372.
- Mosse, Y. P., Deyell, R. J., Berthold, F., Nagakawara, A., Ambros, P. F., Monclair, T., Cohn, S. L., Pearson, A. D., London, W. B., and Matthay, K. K. 2014. "Neuroblastoma in older children, adolescents and young adults: a report from the International Neuroblastoma Risk Group project." *Pediatr Blood Cancer* 61 (4):627-35. doi: 10.1002/pbc.24777.
- Mosse, Y. P., Laudenslager, M., Khazi, D., Carlisle, A. J., Winter, C. L., Rappaport, E., and Maris, J. M. 2004. "Germline PHOX2B mutation in hereditary neuroblastoma." *Am J Hum Genet* 75 (4):727-30. doi: 10.1086/424530.
- Mossé, Yaël P, Laudenslager, Marci, Longo, Luca, Cole, Kristina A, Wood, Andrew, Attiyeh, Edward F, Laquaglia, Michael J, Sennett, Rachel, Lynch, Jill E, and Perri, Patrizia. 2008. "Identification of ALK as a major familial neuroblastoma predisposition gene." *Nature* 455 (7215):930-935.

6. References

- Mossé, Yael P, Lim, Megan S, Voss, Stephan D, Wilner, Keith, Ruffner, Katherine, Laliberte, Julie, Rolland, Delphine, Balis, Frank M, Maris, John M, and Weigel, Brenda J. 2013. "Safety and activity of crizotinib for paediatric patients with refractory solid tumours or anaplastic large-cell lymphoma: a Children's Oncology Group phase 1 consortium study." *The lancet oncology* 14 (6):472-480.
- Mu, H., Cai, S., Wang, X., Li, H., Zhang, L., Li, H., and Xiang, W. 2022. "RNA binding protein IGF2BP1 mediates oxidative stress-induced granulosa cell dysfunction by regulating MDM2 mRNA stability in an m(6)A-dependent manner." *Redox Biol* 57:102492. doi: 10.1016/j.redox.2022.102492.
- Mueller-Pillasch, F., Lacher, U., Wallrapp, C., Micha, A., Zimmerhackl, F., Hameister, H., Varga, G., Friess, H., Buchler, M., Beger, H. G., Vila, M. R., Adler, G., and Gress, T. M. 1997. "Cloning of a gene highly overexpressed in cancer coding for a novel KH-domain containing protein." *Oncogene* 14 (22):2729-33. doi: 10.1038/sj.onc.1201110.
- Mueller, S., Yang, X., Sottero, T. L., Gragg, A., Prasad, G., Polley, M. Y., Weiss, W. A., Matthay, K. K., Davidoff, A. M., DuBois, S. G., and Haas-Kogan, D. A. 2011. "Cooperation of the HDAC inhibitor vorinostat and radiation in metastatic neuroblastoma: efficacy and underlying mechanisms." *Cancer Lett* 306 (2):223-9. doi: 10.1016/j.canlet.2011.03.010.
- Mujoo, K., Cheresch, D. A., Yang, H. M., and Reisfeld, R. A. 1987. "Disialoganglioside GD2 on human neuroblastoma cells: target antigen for monoclonal antibody-mediated cytotoxicity and suppression of tumor growth." *Cancer Res* 47 (4):1098-104.
- Müller, S., Bley, N., Busch, B., Glaß, M., Lederer, M., Misiak, C., Fuchs, T., Wedler, A., Haase, J., Bertoldo, J. B., Michl, P., and Hüttelmaier, S. 2020. "The oncofetal RNA-binding protein IGF2BP1 is a druggable, post-transcriptional super-enhancer of E2F-driven gene expression in cancer." *Nucleic Acids Res* 48 (15):8576-8590. doi: 10.1093/nar/gkaa653.
- Müller, S., Bley, N., Glaß, M., Busch, B., Rousseau, V., Misiak, D., Fuchs, T., Lederer, M., and Hüttelmaier, S. 2018. "IGF2BP1 enhances an aggressive tumor cell phenotype by impairing miRNA-directed downregulation of oncogenic factors." *Nucleic Acids Res* 46 (12):6285-6303. doi: 10.1093/nar/gky229.
- Müller, S., Glaß, M., Singh, A. K., Haase, J., Bley, N., Fuchs, T., Lederer, M., Dahl, A., Huang, H., Chen, J., Posern, G., and Hüttelmaier, S. 2019. "IGF2BP1 promotes SRF-dependent transcription in cancer in a m6A- and miRNA-dependent manner." *Nucleic Acids Res* 47 (1):375-390. doi: 10.1093/nar/gky1012.
- Munro, T. P., Kwon, S., Schnapp, B. J., and St Johnston, D. 2006. "A repeated IMP-binding motif controls oskar mRNA translation and anchoring independently of Drosophila melanogaster IMP." *J Cell Biol* 172 (4):577-88. doi: 10.1083/jcb.200510044.
- Murphy, D. M., Buckley, P. G., Bryan, K., Das, S., Alcock, L., Foley, N. H., Prenter, S., Bray, I., Watters, K. M., Higgins, D., and Stallings, R. L. 2009. "Global MYCN transcription factor binding analysis in neuroblastoma reveals association with distinct E-box motifs and regions of DNA hypermethylation." *PLoS One* 4 (12):e8154. doi: 10.1371/journal.pone.0008154.
- Nagy, Z., Seneviratne, J. A., Kanikevich, M., Chang, W., Mayoh, C., Venkat, P., Du, Y., Jiang, C., Salib, A., Koach, J., Carter, D. R., Mittra, R., Liu, T., Parker, M. W., Cheung, B. B., and Marshall, G. M. 2021. "An ALYREF-MYCN coactivator complex drives neuroblastoma tumorigenesis through effects on USP3 and MYCN stability." *Nat Commun* 12 (1):1881. doi: 10.1038/s41467-021-22143-x.
- Nakagawara, A. 1998a. "Molecular basis of spontaneous regression of neuroblastoma: role of neurotrophic signals and genetic abnormalities." *Human cell* 11 (3):115-124.
- Nakagawara, A. 1998b. "The NGF story and neuroblastoma." *Med Pediatr Oncol* 31 (2):113-5. doi: 10.1002/(sici)1096-911x(199808)31:2<113::aid-mpo14>3.0.co;2-o.
- Nakagawara, A. 2004. "Neural crest development and neuroblastoma: the genetic and biological link." *Prog Brain Res* 146:233-42. doi: 10.1016/s0079-6123(03)46015-9.
- Nakagawara, A., Arima-Nakagawara, M., Scavarda, N. J., Azar, C. G., Cantor, A. B., and Brodeur, G. M. 1993. "Association between high levels of expression of the TRK gene and favorable outcome in human neuroblastoma." *N Engl J Med* 328 (12):847-54. doi: 10.1056/NEJM199303253281205.
- Nakagawara, A., Arima, M., Azar, C. G., Scavarda, N. J., and Brodeur, G. M. 1992. "Inverse relationship between trk expression and N-myc amplification in human neuroblastomas." *Cancer Res* 52 (5):1364-8.
- Nakagawara, A., Azar, C. G., Scavarda, N. J., and Brodeur, G. M. 1994. "Expression and function of TRK-B and BDNF in human neuroblastomas." *Mol Cell Biol* 14 (1):759-67. doi: 10.1128/mcb.14.1.759-767.1994.
- Nakagawara, A., Li, Y., Izumi, H., Muramori, K., Inada, H., and Nishi, M. 2018. "Neuroblastoma." *Jpn J Clin Oncol* 48 (3):214-241. doi: 10.1093/jjco/hyx176.
- Nakagawara, Akira, Kadomatsu, Kenji, Sato, Shin-ichi, Kohno, Kimitoshi, Takano, Hiroshi, and Kuwano, Michihiko. 1991. "Inverse expression of MYCN and mdr-1 in human neuroblastoma." *Progress in Clinical and Biological Research* 366:11-19.
- Nakaguro, Masato, Kiyonari, Shinichi, Kishida, Satoshi, Cao, Dongliang, Murakami-Tonami, Yuko, Ichikawa, Hitoshi, Takeuchi, Ichiro, Nakamura, Shigeo, and Kadomatsu, Kenji. 2015. "Nucleolar protein PES 1 is a marker of neuroblastoma outcome and is associated with neuroblastoma differentiation." *Cancer science* 106 (3):237-243.
- Nakahara, T., Kita, A., Yamanaka, K., Mori, M., Amino, N., Takeuchi, M., Tominaga, F., Hatakeyama, S., Kinoyama, I., Matsuhisa, A., Kudoh, M., and Sasamata, M. 2007. "YM155, a novel small-molecule survivin suppressant, induces regression of established human hormone-refractory prostate tumor xenografts." *Cancer Res* 67 (17):8014-21. doi: 10.1158/0008-5472.CAN-07-1343.
- Naraparaju, K., Kolla, V., Zhuang, T., Higashi, M., Iyer, R., Kolla, S., Okawa, E. R., Blobel, G. A., and Brodeur, G. M. 2016. "Role of microRNAs in epigenetic silencing of the CHD5 tumor suppressor gene in neuroblastomas." *Oncotarget* 7 (13):15977-85. doi: 10.18632/oncotarget.7434.
- Narbonne-Reveau, K., Lanet, E., Dillard, C., Foppolo, S., Chen, C. H., Parrinello, H., Rialle, S., Sokol, N. S., and Maurange, C. 2016. "Neural stem cell-encoded temporal patterning delineates an early window of malignant susceptibility in Drosophila." *Elife* 5. doi: 10.7554/eLife.13463.
- Ngo, L. H., Bert, A. G., Dredge, B. K., Williams, T., Murphy, V., Li, W., Hamilton, W. B., Carey, K. T., Toubia, J., Pillman, K. A., Liu, D., Desogus, J., Chao, J. A., Deans, A. J., Goodall, G. J., and Wickramasinghe, V. O. 2024. "Nuclear export of circular RNA." *Nature* 627 (8002):212-220. doi: 10.1038/s41586-024-07060-5.
- Nielsen, J., Adolph, S. K., Rajpert-De Meyts, E., Lykke-Andersen, J., Koch, G., Christiansen, J., and Nielsen, F. C. 2003. "Nuclear transit of human zipcode-binding protein IMP1." *Biochem J* 376 (Pt 2):383-91. doi: 10.1042/BJ20030943.
- Nielsen, J., Christiansen, J., Lykke-Andersen, J., Johnsen, A. H., Wewer, U. M., and Nielsen, F. C. 1999. "A family of insulin-like growth factor II mRNA-binding proteins represses translation in late development." *Mol Cell Biol* 19 (2):1262-70. doi: 10.1128/MCB.19.2.1262.
- Nielsen, J., Kristensen, M. A., Willemoes, M., Nielsen, F. C., and Christiansen, J. 2004. "Sequential dimerization of human zipcode-binding protein IMP1 on RNA: a cooperative mechanism providing RNP stability." *Nucleic Acids Res* 32 (14):4368-76. doi: 10.1093/nar/gkh754.
- Nishino, J., Kim, S., Zhu, Y., Zhu, H., and Morrison, S. J. 2013. "A network of heterochronic genes including Imp1 regulates temporal changes in stem cell properties." *Elife* 2:e00924. doi: 10.7554/eLife.00924.

- Norris, MD, Bordow, SB, Haber, PS, Marshall, GM, Kavallaris, M, Madafiglio, J, Cohn, SL, Salwen, H, Schmidt, ML, and Hipfner, DR. 1997. "Evidence that the MYCN oncogene regulates MRP gene expression in neuroblastoma." *European Journal of Cancer* 33 (12):1911-1916.
- Norris, Murray D, Bordow, Sharon B, Marshall, Glenn M, Haber, Paul S, Cohn, Susan L, and Haber, Michelle. 1996. "Expression of the gene for multidrug-resistance-associated protein and outcome in patients with neuroblastoma." *New England Journal of Medicine* 334 (4):231-238.
- Noubissi, F. K., Elcheva, I., Bhatia, N., Shakoory, A., Ougolkov, A., Liu, J., Minamoto, T., Ross, J., Fuchs, S. Y., and Spiegelman, V. S. 2006. "CRD-BP mediates stabilization of betaTrCP1 and c-myc mRNA in response to beta-catenin signalling." *Nature* 441 (7095):898-901. doi: 10.1038/nature04839.
- Noubissi, F. K., Nikiforov, M. A., Colburn, N., and Spiegelman, V. S. 2010. "Transcriptional Regulation of CRD-BP by c-myc: Implications for c-myc Functions." *Genes Cancer* 1 (10):1074-82. doi: 10.1177/1947601910395581.
- Nuchtern, J. G. 2006. "Perinatal neuroblastoma." *Semin Pediatr Surg* 15 (1):10-6. doi: 10.1053/j.sempedsurg.2005.11.003.
- Nuchtern, J. G., London, W. B., Barnewolt, C. E., Naranjo, A., McGrady, P. W., Geiger, J. D., Diller, L., Schmidt, M. L., Maris, J. M., Cohn, S. L., and Shamberger, R. C. 2012. "A prospective study of expectant observation as primary therapy for neuroblastoma in young infants: a Children's Oncology Group study." *Ann Surg* 256 (4):573-80. doi: 10.1097/SLA.0b013e31826cbbdb.
- O'Neill, Seamus, Ekstrom, Lori, Lastowska, Maria, Roberts, Paul, Brodeur, Garrett M, Kees, Ursula R, Schwab, Manfred, and Bown, Nick. 2001. "MYCN amplification and 17q in neuroblastoma: evidence for structural association." *Genes, Chromosomes and Cancer* 30 (1):87-90.
- Ochiai, H, Takenobu, H, Nakagawa, A, Yamaguchi, Y, Kimura, M, Ohira, M, Okimoto, Y, Fujimura, Y, Koseki, H, and Kohno, Y. 2010. "Bmi1 is a MYCN target gene that regulates tumorigenesis through repression of KIF1B β and TSLC1 in neuroblastoma." *Oncogene* 29 (18):2681-2690.
- Oehme, I., Deubzer, H. E., Wegener, D., Pickert, D., Linke, J. P., Hero, B., Kopp-Schneider, A., Westermann, F., Ulrich, S. M., von Deimling, A., Fischer, M., and Witt, O. 2009. "Histone deacetylase 8 in neuroblastoma tumorigenesis." *Clin Cancer Res* 15 (1):91-9. doi: 10.1158/1078-0432.CCR-08-0684.
- Oehme, Ina, Linke, Jan-Peter, Böck, Barbara C, Milde, Till, Lodrini, Marco, Hartenstein, Bettina, Wiegand, Inga, Eckert, Christian, Roth, Wilfried, and Kool, Marcel. 2013. "Histone deacetylase 10 promotes autophagy-mediated cell survival." *Proceedings of the National Academy of Sciences* 110 (28):E2592-E2601.
- Oki, S., Ohta, T., Shioi, G., Hatanaka, H., Ogasawara, O., Okuda, Y., Kawaji, H., Nakaki, R., Sese, J., and Meno, C. 2018. "ChIP-Atlas: a data-mining suite powered by full integration of public ChIP-seq data." *EMBO Rep* 19 (12). doi: 10.15252/embr.201846255.
- Oleynikov, Y., and Singer, R. H. 2003. "Real-time visualization of ZBP1 association with beta-actin mRNA during transcription and localization." *Curr Biol* 13 (3):199-207. doi: 10.1016/s0960-9822(03)00044-7.
- Otto, T., Horn, S., Brockmann, M., Eilers, U., Schuttrumpf, L., Popov, N., Kenney, A. M., Schulte, J. H., Beijersbergen, R., Christiansen, H., Berwanger, B., and Eilers, M. 2009. "Stabilization of N-Myc is a critical function of Aurora A in human neuroblastoma." *Cancer Cell* 15 (1):67-78. doi: 10.1016/j.ccr.2008.12.005.
- Padovan-Merhar, Olivia M, Raman, Pichai, Ostrovnyaya, Irina, Kalletta, Karthik, Rubnitz, Kaitlyn R, Sanford, Eric M, Ali, Siraj M, Miller, Vincent A, Mossé, Yael P, and Granger, Meaghan P. 2016. "Enrichment of targetable mutations in the relapsed neuroblastoma genome." *PLoS genetics* 12 (12):e1006501.
- Pan, F., Hüttelmaier, S., Singer, R. H., and Gu, W. 2007. "ZBP2 facilitates binding of ZBP1 to beta-actin mRNA during transcription." *Mol Cell Biol* 27 (23):8340-51. doi: 10.1128/MCB.00972-07.
- Papadopoulos, K. P., Lopez-Jimenez, J., Smith, S. E., Steinberg, J., Keating, A., Sasse, C., Jie, F., and Thyss, A. 2016. "A multicenter phase II study of sepantromium bromide (YM155) plus rituximab in patients with relapsed aggressive B-cell Non-Hodgkin lymphoma." *Leuk Lymphoma* 57 (8):1848-55. doi: 10.3109/10428194.2015.1113275.
- Park, J. R., Eggert, A., and Caron, H. 2010. "Neuroblastoma: biology, prognosis, and treatment." *Hematol Oncol Clin North Am* 24 (1):65-86. doi: 10.1016/j.hoc.2009.11.011.
- Park, Jeong A, and Cheung, Nai-Kong V. 2020. "Targets and antibody formats for immunotherapy of neuroblastoma." *Journal of Clinical Oncology* 38 (16):1836.
- Park, Julie R., Kreissman, Susan G., London, Wendy B., Naranjo, Arlene, Cohn, Susan Lerner, Hogarty, Michael D., Tenney, Sheena Cretella, Haas-Kogan, Daphne, Shaw, Peter John, Geiger, James Duncan, Doski, John J, Gorges, Sandra Wootton, Khanna, Geetika, Voss, Stephan D., Maris, John M., Grupp, Stephan A., and Diller, Lisa. 2016. "A phase III randomized clinical trial (RCT) of tandem myeloablative autologous stem cell transplant (ASCT) using peripheral blood stem cell (PBSC) as consolidation therapy for high-risk neuroblastoma (HR-NB): A Children's Oncology Group (COG) study." *Journal of Clinical Oncology* 34 (18_suppl):LBA3-LBA3. doi: 10.1200/JCO.2016.34.18_suppl.LBA3.
- Pascale, A., Amadio, M., and Quattrone, A. 2008. "Defining a neuron: neuronal ELAV proteins." *Cell Mol Life Sci* 65 (1):128-40. doi: 10.1007/s00018-007-7017-y.
- Patapoutian, Ardem, and Reichardt, Louis F. 2001. "Trk receptors: mediators of neurotrophin action." *Current opinion in neurobiology* 11 (3):272-280.
- Patel, V. L., Mitra, S., Harris, R., Buxbaum, A. R., Lionnet, T., Brenowitz, M., Girvin, M., Levy, M., Almo, S. C., Singer, R. H., and Chao, J. A. 2012. "Spatial arrangement of an RNA zipcode identifies mRNAs under post-transcriptional control." *Genes Dev* 26 (1):43-53. doi: 10.1101/gad.177428.111.
- Patil, H., Saha, A., Senda, E., Cho, K. I., Haque, M., Yu, M., Qiu, S., Yoon, D., Hao, Y., Peachey, N. S., and Ferreira, P. A. 2014. "Selective impairment of a subset of Ran-GTP-binding domains of ran-binding protein 2 (Ranbp2) suffices to recapitulate the degeneration of the retinal pigment epithelium (RPE) triggered by Ranbp2 ablation." *J Biol Chem* 289 (43):29767-89. doi: 10.1074/jbc.M114.586834.
- Pattyn, A., Morin, X., Cremer, H., Goridis, C., and Brunet, J. F. 1999. "The homeobox gene Phox2b is essential for the development of autonomic neural crest derivatives." *Nature* 399 (6734):366-70. doi: 10.1038/20700.
- Pearson, A. D., Pinkerton, C. R., Lewis, I. J., Imeson, J., Ellershaw, C., Machin, D., European Neuroblastoma Study, Group, Children's, Cancer, and Leukaemia, Group. 2008. "High-dose rapid and standard induction chemotherapy for patients aged over 1 year with stage 4 neuroblastoma: a randomised trial." *Lancet Oncol* 9 (3):247-56. doi: 10.1016/S1470-2045(08)70069-X.
- Pechackova, S., Burdova, K., and Macurek, L. 2017. "WIP1 phosphatase as pharmacological target in cancer therapy." *J Mol Med (Berl)* 95 (6):589-599. doi: 10.1007/s00109-017-1536-2.

6. References

- Peifer, Martin, Hertwig, Falk, Roels, Frederik, Dreidax, Daniel, Gartlgruber, Moritz, Menon, Roopika, Krämer, Andrea, Roncaioli, Justin L, Sand, Frederik, and Heuckmann, Johannes M. 2015. "Telomerase activation by genomic rearrangements in high-risk neuroblastoma." *Nature* 526 (7575):700-704.
- Pelengaris, S., Khan, M., and Evan, G. 2002. "c-MYC: more than just a matter of life and death." *Nat Rev Cancer* 2 (10):764-76. doi: 10.1038/nrc904.
- Peng, S., Chen, L. L., Lei, X. X., Yang, L., Lin, H., Carmichael, G. G., and Huang, Y. 2011. "Genome-wide studies reveal that Lin28 enhances the translation of genes important for growth and survival of human embryonic stem cells." *Stem Cells* 29 (3):496-504. doi: 10.1002/stem.591.
- Perez, C. A., Matthay, K. K., Atkinson, J. B., Seeger, R. C., Shimada, H., Haase, G. M., Stram, D. O., Gerbing, R. B., and Lukens, J. N. 2000. "Biologic variables in the outcome of stages I and II neuroblastoma treated with surgery as primary therapy: a children's cancer group study." *J Clin Oncol* 18 (1):18-26. doi: 10.1200/JCO.2000.18.1.18.
- Perycz, M., Urbanska, A. S., Krawczyk, P. S., Parobczak, K., and Jaworski, J. 2011. "Zipcode binding protein 1 regulates the development of dendritic arbors in hippocampal neurons." *J Neurosci* 31 (14):5271-85. doi: 10.1523/JNEUROSCI.2387-10.2011.
- Peuchmaur, M., d'Amore, E. S., Joshi, V. V., Hata, J., Roald, B., Dehner, L. P., Gerbing, R. B., Stram, D. O., Lukens, J. N., Matthay, K. K., and Shimada, H. 2003. "Revision of the International Neuroblastoma Pathology Classification: confirmation of favorable and unfavorable prognostic subsets in ganglioneuroblastoma, nodular." *Cancer* 98 (10):2274-81. doi: 10.1002/cncr.11773.
- Pietras, Alexander, Hansford, Loen M, Johnsson, A Sofie, Bridges, Esther, Sjölund, Jonas, Gisselsson, David, Rehn, Matilda, Beckman, Siv, Noguera, Rosa, and Navarro, Samuel. 2009. "HIF-2 α maintains an undifferentiated state in neural crest-like human neuroblastoma tumor-initiating cells." *Proceedings of the National Academy of Sciences* 106 (39):16805-16810.
- Piskounova, E., Polytarouch, C., Thornton, J. E., LaPierre, R. J., Pothoulakis, C., Hagan, J. P., Iliopoulos, D., and Gregory, R. I. 2011. "Lin28A and Lin28B inhibit let-7 microRNA biogenesis by distinct mechanisms." *Cell* 147 (5):1066-79. doi: 10.1016/j.cell.2011.10.039.
- Piunti, Andrea, and Shilatifard, Ali. 2016. "Epigenetic balance of gene expression by Polycomb and COMPASS families." *Science* 352 (6290):aad9780.
- Pizzo, Philip A, and Poplack, David G. 2015. *Principles and practice of pediatric oncology*: Lippincott Williams & Wilkins.
- Powers, J. T., Tsanov, K. M., Pearson, D. S., Roels, F., Spina, C. S., Ebricht, R., Seligson, M., de Soysa, Y., Cahan, P., Theissen, J., Tu, H. C., Han, A., Kurek, K. C., LaPier, G. S., Osborne, J. K., Ross, S. J., Cesana, M., Collins, J. J., Berthold, F., and Daley, G. Q. 2016. "Multiple mechanisms disrupt the let-7 microRNA family in neuroblastoma." *Nature* 535 (7611):246-51. doi: 10.1038/nature18632.
- Pugh, T. J., Morozova, O., Attiyeh, E. F., Asgharzadeh, S., Wei, J. S., Auclair, D., Carter, S. L., Cibulskis, K., Hanna, M., Kiezun, A., Kim, J., Lawrence, M. S., Lichtenstein, L., McKenna, A., Peadarallu, C. S., Ramos, A. H., Shefler, E., Sivachenko, A., Sougnez, C., Stewart, C., Ally, A., Birol, I., Chiu, R., Corbett, R. D., Hirst, M., Jackman, S. D., Kamoh, B., Khodabakshi, A. H., Krzywinski, M., Lo, A., Moore, R. A., Mungall, K. L., Qian, J., Tam, A., Thiessen, N., Zhao, Y., Cole, K. A., Diamond, M., Diskin, S. J., Mosse, Y. P., Wood, A. C., Ji, L., Sposto, R., Badgett, T., London, W. B., Moyer, Y., Gastier-Foster, J. M., Smith, M. A., Guidry Auvil, J. M., Gerhard, D. S., Hogarty, M. D., Jones, S. J., Lander, E. S., Gabriel, S. B., Getz, G., Seeger, R. C., Khan, J., Marra, M. A., Meyerson, M., and Maris, J. M. 2013. "The genetic landscape of high-risk neuroblastoma." *Nat Genet* 45 (3):279-84. doi: 10.1038/ng.2529.
- Puissant, A., Frumm, S. M., Alexe, G., Bassil, C. F., Qi, J., Chanthery, Y. H., Nekritz, E. A., Zeid, R., Gustafson, W. C., Greninger, P., Garnett, M. J., McDermott, U., Benes, C. H., Kung, A. L., Weiss, W. A., Bradner, J. E., and Stegmaier, K. 2013. "Targeting MYCN in neuroblastoma by BET bromodomain inhibition." *Cancer Discov* 3 (3):308-23. doi: 10.1158/2159-8290.CD-12-0418.
- Raabe, EH, Laudenslager, M, Winter, C, Wasserman, N, Cole, K, LaQuaglia, M, Maris, DJ, Mosse, YP, and Maris, JM. 2008. "Prevalence and functional consequence of PHOX2B mutations in neuroblastoma." *Oncogene* 27 (4):469-476.
- Rasmuson, A., Segerstrom, L., Nethander, M., Finnman, J., Elfman, L. H., Javanmardi, N., Nilsson, S., Johnsen, J. I., Martinsson, T., and Kogner, P. 2012. "Tumor development, growth characteristics and spectrum of genetic aberrations in the TH-MYCN mouse model of neuroblastoma." *PLoS One* 7 (12):e51297. doi: 10.1371/journal.pone.0051297.
- Rauch, A., Hennig, D., Schafer, C., Wirth, M., Marx, C., Heinzl, T., Schneider, G., and Kramer, O. H. 2014. "Survivin and YM155: how faithful is the liaison?" *Biochim Biophys Acta* 1845 (2):202-20. doi: 10.1016/j.bbcan.2014.01.003.
- Rayburn, Elizabeth, Zhang, Ruiwen, He, Jie, and Wang, Hui. 2005. "MDM2 and human malignancies: expression, clinical pathology, prognostic markers, and implications for chemotherapy." *Current cancer drug targets* 5 (1):27-41.
- Reale, Michael A, Reyes-Mugica, Miguel, Pierceall, William E, Rubinstein, Michael C, Hedrick, Lora, Cohn, Susan L, Nakagawara, Akira, Brodeur, Garrett M, and Fearon, Eric R. 1996. "Loss of DCC expression in neuroblastoma is associated with disease dissemination." *Clinical cancer research: an official journal of the American Association for Cancer Research* 2 (7):1097-1102.
- Reiter, Jill L, and Brodeur, Garrett M. 1996. "High-Resolution Mapping of a 130-kb Core Region of theMYCNAmplicon in Neuroblastomas." *Genomics* 32 (1):97-103.
- Reiter, Jill L, and Brodeur, Garrett M. 1998. "MYCN is the only highly expressed gene from the core amplified domain in human neuroblastomas." *Genes, Chromosomes and Cancer* 23 (2):134-140.
- Ritchie, M. E., Phipson, B., Wu, D., Hu, Y., Law, C. W., Shi, W., and Smyth, G. K. 2015. "limma powers differential expression analyses for RNA-sequencing and microarray studies." *Nucleic Acids Res* 43 (7):e47. doi: 10.1093/nar/gkv007.
- Robinson, M. D., McCarthy, D. J., and Smyth, G. K. 2010. "edgeR: a Bioconductor package for differential expression analysis of digital gene expression data." *Bioinformatics* 26 (1):139-40. doi: 10.1093/bioinformatics/btp616.
- Robinson, M. D., and Oshlack, A. 2010. "A scaling normalization method for differential expression analysis of RNA-seq data." *Genome Biol* 11 (3):R25. doi: 10.1186/gb-2010-11-3-r25.
- Ross, A. F., Olyynikov, Y., Kislauskis, E. H., Taneja, K. L., and Singer, R. H. 1997. "Characterization of a beta-actin mRNA zipcode-binding protein." *Mol Cell Biol* 17 (4):2158-65. doi: 10.1128/MCB.17.4.2158.
- Ru, Y., Kechris, K. J., Tabakoff, B., Hoffman, P., Radcliffe, R. A., Bowler, R., Mahaffey, S., Rossi, S., Calin, G. A., Bemis, L., and Theodorescu, D. 2014. "The multiMiR R package and database: integration of microRNA-target interactions along with their disease and drug associations." *Nucleic Acids Res* 42 (17):e133. doi: 10.1093/nar/gku631.
- Runge, S., Nielsen, F. C., Nielsen, J., Lykke-Andersen, J., Wewer, U. M., and Christiansen, J. 2000. "H19 RNA binds four molecules of insulin-like growth factor II mRNA-binding protein." *J Biol Chem* 275 (38):29562-9. doi: 10.1074/jbc.M001156200.
- Russell, Mike R, Penikis, Annalise, Oldridge, Derek A, Alvarez-Dominguez, Juan R, McDaniel, Lee, Diamond, Maura, Padovan, Olivia, Raman, Pichai, Li, Yimei, and Wei, Jun S. 2015. "CASC15-S is a tumor suppressor lncRNA at the 6p22 neuroblastoma susceptibility locus." *Cancer research* 75 (15):3155-3166.
- Ryden, M, Sehgal, R, Dominici, C, Schilling, FH, Ibanez, CF, and Kogner, P. 1996. "Expression of mRNA for the neurotrophin receptor trkC in neuroblastomas with favourable tumour stage and good prognosis." *British journal of cancer* 74 (5):773-779.

6. References

- Saint-Andre, V., Federation, A. J., Lin, C. Y., Abraham, B. J., Reddy, J., Lee, T. I., Bradner, J. E., and Young, R. A. 2016. "Models of human core transcriptional regulatory circuitries." *Genome Res* 26 (3):385-96. doi: 10.1101/gr.197590.115.
- Saito-Ohara, F., Imoto, I., Inoue, J., Hosoi, H., Nakagawara, A., Sugimoto, T., and Inazawa, J. 2003. "PPM1D is a potential target for 17q gain in neuroblastoma." *Cancer Res* 63 (8):1876-83.
- Samaraweera, L., Spengler, B. A., and Ross, R. A. 2017. "Reciprocal antagonistic regulation of N-myc mRNA by miR17 and the neuronal-specific RNA-binding protein HuD." *Oncol Rep* 38 (1):545-550. doi: 10.3892/or.2017.5664.
- Sampson, V. B., Rong, N. H., Han, J., Yang, Q., Aris, V., Soteropoulos, P., Petrelli, N. J., Dunn, S. P., and Krueger, L. J. 2007. "MicroRNA let-7a down-regulates MYC and reverts MYC-induced growth in Burkitt lymphoma cells." *Cancer Res* 67 (20):9762-70. doi: 10.1158/0008-5472.CAN-07-2462.
- Samuels, T. J., Jarvelin, A. I., Ish-Horowicz, D., and Davis, I. 2020. "Imp/IGF2BP levels modulate individual neural stem cell growth and division through myc mRNA stability." *Elife* 9. doi: 10.7554/eLife.51529.
- Satoh, T., Okamoto, I., Miyazaki, M., Morinaga, R., Tsuya, A., Hasegawa, Y., Terashima, M., Ueda, S., Fukuoka, M., Ariyoshi, Y., Saito, T., Masuda, N., Watanabe, H., Taguchi, T., Kakiyama, T., Aoyama, Y., Hashimoto, Y., and Nakagawa, K. 2009. "Phase I study of YM155, a novel survivin suppressant, in patients with advanced solid tumors." *Clin Cancer Res* 15 (11):3872-80. doi: 10.1158/1078-0432.CCR-08-1946.
- Saulnier Sholler, G. L., Brard, L., Straub, J. A., Dorf, L., Illeyne, S., Koto, K., Kalkunte, S., Bosenberg, M., Ashikaga, T., and Nishi, R. 2009. "Nifurtimox induces apoptosis of neuroblastoma cells in vitro and in vivo." *J Pediatr Hematol Oncol* 31 (3):187-93. doi: 10.1097/MPH.0b013e3181984d91.
- Sausen, Mark, Leary, Rebecca J, Jones, Siân, Wu, Jian, Reynolds, C Patrick, Liu, Xueyuan, Blackford, Amanda, Parmigiani, Giovanni, Diaz Jr, Luis A, and Papadopoulos, Nickolas. 2013. "Integrated genomic analyses identify ARID1A and ARID1B alterations in the childhood cancer neuroblastoma." *Nature genetics* 45 (1):12-17.
- Savelyeva, L, Corvi, R, and Schwab, M. 1994. "Translocation involving 1p and 17q is a recurrent genetic alteration of human neuroblastoma cells." *American journal of human genetics* 55 (2):334.
- Sawada, Tadashi, Todo, Shinjiro, Fujita, Katsutoshi, Iino, Shigeru, Imashuku, Shinsaku, and Kusunoki, Tomoichi. 1982. "Mass screening of neuroblastoma in infancy." *American Journal of Diseases of Children* 136 (8):710-712.
- Schilling, Freimut H, Spix, Claudia, Berthold, Frank, Erttmann, Rudolf, Fehse, Natalja, Hero, Barbara, Klein, Gisela, Sander, Johannes, Schwarz, Kerstin, and Treuner, Joern. 2002. "Neuroblastoma screening at one year of age." *New England Journal of Medicine* 346 (14):1047-1053.
- Schleiermacher, G, Mosseri, V, London, WB, Maris, JM, Brodeur, GM, Attiyeh, E, Haber, M, Khan, J, Nakagawara, A, and Speleman, Franki. 2012. "Segmental chromosomal alterations have prognostic impact in neuroblastoma: a report from the INRG project." *British journal of cancer* 107 (8):1418-1422.
- Schleiermacher, Gudrun, Javanmardi, Niloufar, Bernard, Virginie, Leroy, Quentin, Cappel, Julie, Frio, T Rio, Pierron, Gaëlle, Lapouble, Eve, Combaret, Valérie, and Speleman, Frank. 2014. "Emergence of new ALK mutations at relapse of neuroblastoma." *J Clin Oncol* 32 (25):2727-2734.
- Schleiermacher, Gudrun, Peter, Martine, Michon, Jean, Hugot, Jean-Pierre, Vielh, Philippe, Zucker, Jean-Michel, Magdelénat, Henri, Thomas, Gilles, and Delattre, Olivier. 1994. "Two distinct deleted regions on the short arm of chromosome 1 in neuroblastoma." *Genes, Chromosomes and Cancer* 10 (4):275-281.
- Schlisio, S., Kenchappa, R. S., Vredeveld, L. C. W., George, R. E., Stewart, R., Greulich, H., Shahriari, K., Nguyen, N. V., Pigny, P., Dahia, P. L., Pomeroy, S. L., Maris, J. M., Look, A. T., Meyerson, M., Peeper, D. S., Carter, B. D., and Kaelin, W. G. 2008. "The kinesin KIF1B β acts downstream from EglN3 to induce apoptosis and is a potential 1p36 tumor suppressor." *Genes & Development* 22 (7):884-893. doi: 10.1101/gad.1648608.
- Schmidt, Mary Lou, Lukens, John N, Seeger, Robert C, Brodeur, Garrett M, Shimada, Hiroyuki, Gerbing, Robert B, Stram, Daniel O, Perez, Carlos, Haase, Gerald M, and Matthay, Katherine K. 2000. "Biologic factors determine prognosis in infants with stage IV neuroblastoma: a prospective Children's Cancer Group study." *Journal of Clinical Oncology* 18 (6):1260-1268.
- Schneider, T., Hung, L. H., Aziz, M., Wilmen, A., Thaum, S., Wagner, J., Janowski, R., Müller, S., Schreiner, S., Friedhoff, P., Hüttelmaier, S., Niessing, D., Sattler, M., Schlundt, A., and Bindereif, A. 2019. "Combinatorial recognition of clustered RNA elements by the multidomain RNA-binding protein IMP3." *Nat Commun* 10 (1):2266. doi: 10.1038/s41467-019-09769-8.
- Schnepp, R. W., and Diskin, S. J. 2016. "LIN28B: an orchestrator of oncogenic signaling in neuroblastoma." *Cell Cycle* 15 (6):772-4. doi: 10.1080/15384101.2015.1137712.
- Schnepp, R. W., Khurana, P., Attiyeh, E. F., Raman, P., Chodosh, S. E., Oldridge, D. A., Gagliardi, M. E., Conkrite, K. L., Asgharzadeh, S., Seeger, R. C., Madison, B. B., Rustgi, A. K., Maris, J. M., and Diskin, S. J. 2015. "A LIN28B-RAN-AURKA Signaling Network Promotes Neuroblastoma Tumorigenesis." *Cancer Cell* 28 (5):599-609. doi: 10.1016/j.ccell.2015.09.012.
- Schramm, Alexander, Köster, Johannes, Assenov, Yassen, Althoff, Kristina, Peifer, Martin, Mahlow, Ellen, Odersky, Andrea, Beisser, Daniela, Ernst, Corinna, and Henssen, Anton G. 2015. "Mutational dynamics between primary and relapse neuroblastomas." *Nature genetics* 47 (8):872-877.
- Schulte, J. H., Horn, S., Otto, T., Samans, B., Heukamp, L. C., Eilers, U. C., Krause, M., Astrahantseff, K., Klein-Hitpass, L., Buettner, R., Schramm, A., Christiansen, H., Eilers, M., Eggert, A., and Berwanger, B. 2008. "MYCN regulates oncogenic MicroRNAs in neuroblastoma." *Int J Cancer* 122 (3):699-704. doi: 10.1002/ijc.23153.
- Schulte, J. H., Schowe, B., Mestdagh, P., Kaderali, L., Kalaghatgi, P., Schlierf, S., Vermeulen, J., Brockmeyer, B., Pajtler, K., Thor, T., de Preter, K., Speleman, F., Morik, K., Eggert, A., Vandesompele, J., and Schramm, A. 2010. "Accurate prediction of neuroblastoma outcome based on miRNA expression profiles." *Int J Cancer* 127 (10):2374-85. doi: 10.1002/ijc.25436.
- Schwab, M., Alitalo, K., Klemptner, K. H., Varmus, H. E., Bishop, J. M., Gilbert, F., Brodeur, G., Goldstein, M., and Trent, J. 1983. "Amplified DNA with limited homology to myc cellular oncogene is shared by human neuroblastoma cell lines and a neuroblastoma tumour." *Nature* 305 (5931):245-8. doi: 10.1038/305245a0.
- Schwab, Manfred, Varmus, Harold E, Bishop, J Michael, Grzeschik, Karl-Heinz, Naylor, Susan L, Sakaguchi, Alan Y, Brodeur, Garrett, and Trent, Jeffrey. 1984. "Chromosome localization in normal human cells and neuroblastomas of a gene related to c-myc." *Nature* 308 (5956):288-291.
- Seeger, R. C., Brodeur, G. M., Sather, H., Dalton, A., Siegel, S. E., Wong, K. Y., and Hammond, D. 1985. "Association of multiple copies of the N-myc oncogene with rapid progression of neuroblastomas." *N Engl J Med* 313 (18):1111-6. doi: 10.1056/NEJM198510313131802.
- Seif, A. E., Naranjo, A., Baker, D. L., Bunin, N. J., Kletzel, M., Kretschmar, C. S., Maris, J. M., McGrady, P. W., von Allmen, D., Cohn, S. L., London, W. B., Park, J. R., Diller, L. R., and Grupp, S. A. 2013. "A pilot study of tandem high-dose chemotherapy with stem cell rescue as

- consolidation for high-risk neuroblastoma: Children's Oncology Group study ANBL00P1." *Bone Marrow Transplant* 48 (7):947-52. doi: 10.1038/bmt.2012.276.
- Serra, Alexandre, Häberle, Beate, König, Inke R, Kappler, Roland, Suttrop, Meinolf, Schackert, Hans K, Roesner, Dietmar, and Fitze, Guido. 2008. "Rare occurrence of PHOX2b mutations in sporadic neuroblastomas." *Journal of pediatric hematology/oncology* 30 (10):728-732.
- Shahbazi, Jeyran, Liu, Pei Y, Atmadibrata, Bernard, Bradner, James E, Marshall, Glenn M, Lock, Richard B, and Liu, Tao. 2016. "The bromodomain inhibitor JQ1 and the histone deacetylase inhibitor panobinostat synergistically reduce N-Myc expression and induce anticancer effects." *Clinical cancer research* 22 (10):2534-2544.
- Sharp, Susan E, Shulkin, Barry L, Gelfand, Michael J, Salisbury, Shelia, and Furman, Wayne L. 2009. "123I-MIBG scintigraphy and 18F-FDG PET in neuroblastoma." *Journal of Nuclear Medicine* 50 (8):1237-1243.
- Shen, Q., Xu, Z., Sun, G., Wang, H., and Zhang, L. 2022. "TFAP4 Activates IGF2BP1 and Promotes Progression of Non-Small Cell Lung Cancer by Stabilizing TK1 Expression through m6A Modification." *Mol Cancer Res* 20 (12):1763-1775. doi: 10.1158/1541-7786.MCR-22-0231.
- Shi, J., Zhang, Q., Yin, X., Ye, J., Gao, S., Chen, C., Yang, Y., Wu, B., Fu, Y., Zhang, H., Wang, Z., Wang, B., Zhu, Y., Wu, H., Yao, Y., Xu, G., Wang, Q., Wang, S., and Zhang, W. 2023. "Stabilization of IGF2BP1 by USP10 promotes breast cancer metastasis via CPT1A in an m6A-dependent manner." *Int J Biol Sci* 19 (2):449-464. doi: 10.7150/ijbs.76798.
- Shi, W., Tang, Y., Lu, J., Zhuang, Y., and Wang, J. 2022. "MIR210HG promotes breast cancer progression by IGF2BP1 mediated m6A modification." *Cell Biosci* 12 (1):38. doi: 10.1186/s13578-022-00772-z.
- Shimada, Hiroyuki, Ambros, Inge M, Dehner, Louis P, Hata, Jun-ichi, Joshi, Vijay V, Roald, Borghild, Stram, Daniel O, Gerbing, Robert B, Lukens, John N, and Matthay, Katherine K. 1999. "The international neuroblastoma pathology classification (the Shimada system)." *Cancer: Interdisciplinary International Journal of the American Cancer Society* 86 (2):364-372.
- Shimada, Hiroyuki, Chatten, Jane, Newton, William A, Sachs, Nancy, Hamoudi, Ala B, Chiba, Tsuneo, Marsden, Henry B, and Misugi, Kazuaki. 1984. "Histopathologic prognostic factors in neuroblastic tumors: definition of subtypes of ganglioneuroblastoma and an age-linked classification of neuroblastomas." *JNCI: Journal of the National Cancer Institute* 73 (2):405-416.
- Shimada, Hiroyuki, Umehara, Shunsuke, Monobe, Yasumasa, Hachitanda, Yoichi, Nakagawa, Atsuko, Goto, Shoko, Gerbing, Robert B, Stram, Daniel O, Lukens, John N, and Matthay, Katherine K. 2001. "International neuroblastoma pathology classification for prognostic evaluation of patients with peripheral neuroblastic tumors: a report from the Children's Cancer Group." *Cancer* 92 (9):2451-2461.
- Shojaei-Brosseau, Taraneh, Chompret, Agnès, Abel, Anne, de Vathaire, Florent, Raquin, Marie-Anne, Brugières, Laurence, Feunteun, Jean, Hartmann, Olivier, and Bonaïti-Pellié, Catherine. 2004. "Genetic epidemiology of neuroblastoma: a study of 426 cases at the Institut Gustave-Roussy in France." *Pediatric blood & cancer* 42 (1):99-105.
- Sholler, G. L. S., Ferguson, W., Bergendahl, G., Bond, J. P., Neville, K., Eslin, D., Brown, V., Roberts, W., Wada, R. K., Oesterheld, J., Mitchell, D., Foley, J., Parikh, N. S., Eshun, F., Zage, P., Rawwas, J., Sencer, S., Pankiewicz, D., Quinn, M., Rich, M., Junewick, J., and Kravaka, J. M. 2018. "Maintenance DFMO Increases Survival in High Risk Neuroblastoma." *Sci Rep* 8 (1):14445. doi: 10.1038/s41598-018-32659-w.
- Smith, V., and Foster, J. 2018. "High-Risk Neuroblastoma Treatment Review." *Children (Basel)* 5 (9). doi: 10.3390/children5090114.
- Song, T., Zheng, Y., Wang, Y., Katz, Z., Liu, X., Chen, S., Singer, R. H., and Gu, W. 2015. "Specific interaction of KIF11 with ZBP1 regulates the transport of beta-actin mRNA and cell motility." *J Cell Sci* 128 (5):1001-10. doi: 10.1242/jcs.161679.
- Sorrentino, S., Gigliotti, A. R., Sementa, A. R., Morsellino, V., Conte, M., Erminio, G., Buffa, P., Granata, C., Mazzocco, K., Garaventa, A., and De Bernardi, B. 2014. "Neuroblastoma in the adult: the Italian experience with 21 patients." *J Pediatr Hematol Oncol* 36 (8):e499-505. doi: 10.1097/MPH.0000000000000144.
- Sparanese, D., and Lee, C. H. 2007. "CRD-BP shields c-myc and MDR-1 RNA from endonucleolytic attack by a mammalian endoribonuclease." *Nucleic Acids Res* 35 (4):1209-21. doi: 10.1093/nar/gkl1148.
- Spitz, R., Hero, B., Ernestus, K., and Berthold, F. 2003. "Deletions in chromosome arms 3p and 11q are new prognostic markers in localized and 4s neuroblastoma." *Clin Cancer Res* 9 (1):52-8.
- Srivatsan, Eri S, Ying, Kuang Lin, and Seeger, Robert C. 1993. "Deletion of chromosome 11 and of 14q sequences in neuroblastoma." *Genes, Chromosomes and Cancer* 7 (1):32-37.
- Stallings, R. L., Howard, J., Dunlop, A., Mullarkey, M., McDermott, M., Breatnach, F., and O'Meara, A. 2003. "Are gains of chromosomal regions 7q and 11p important abnormalities in neuroblastoma?" *Cancer Genet Cytogenet* 140 (2):133-7. doi: 10.1016/s0165-4608(02)00681-7.
- Stanton, B. R., Perkins, A. S., Tessarollo, L., Sassoon, D. A., and Parada, L. F. 1992. "Loss of N-myc function results in embryonic lethality and failure of the epithelial component of the embryo to develop." *Genes Dev* 6 (12A):2235-47. doi: 10.1101/gad.6.12a.2235.
- Stephens, Philip J, Greenman, Chris D, Fu, Beiyuan, Yang, Fengtang, Bignell, Graham R, Mudie, Laura J, Pleasance, Erin D, Lau, King Wai, Beare, David, and Stebbings, Lucy A. 2011. "Massive genomic rearrangement acquired in a single catastrophic event during cancer development." *cell* 144 (1):27-40.
- Stiller, Charles A. 2016. "Epidemiology of childhood tumours." *The surgery of childhood tumors*:7-18.
- Stöhr, N., Köhn, M., Lederer, M., Glaß, M., Reinke, C., Singer, R. H., and Hüttelmaier, S. 2012. "IGF2BP1 promotes cell migration by regulating MK5 and PTEN signaling." *Genes Dev* 26 (2):176-89. doi: 10.1101/gad.177642.111.
- Stöhr, N., Lederer, M., Reinke, C., Meyer, S., Hatzfeld, M., Singer, R. H., and Hüttelmaier, S. 2006. "ZBP1 regulates mRNA stability during cellular stress." *J Cell Biol* 175 (4):527-34. doi: 10.1083/jcb.200608071.
- Stokowy, T., Eszlinger, M., Swierniak, M., Fujarewicz, K., Jarzab, B., Paschke, R., and Krohn, K. 2014. "Analysis options for high-throughput sequencing in miRNA expression profiling." *BMC Res Notes* 7:144. doi: 10.1186/1756-0500-7-144.
- Strother, D. R., London, W. B., Schmidt, M. L., Brodeur, G. M., Shimada, H., Thorner, P., Collins, M. H., Tagge, E., Adkins, S., Reynolds, C. P., Murray, K., Lavey, R. S., Matthay, K. K., Castleberry, R., Maris, J. M., and Cohn, S. L. 2012. "Outcome after surgery alone or with restricted use of chemotherapy for patients with low-risk neuroblastoma: results of Children's Oncology Group study P9641." *J Clin Oncol* 30 (15):1842-8. doi: 10.1200/JCO.2011.37.9990.
- Subramanian, A., Tamayo, P., Mootha, V. K., Mukherjee, S., Ebert, B. L., Gillette, M. A., Paulovich, A., Pomeroy, S. L., Golub, T. R., Lander, E. S., and Mesirov, J. P. 2005. "Gene set enrichment analysis: a knowledge-based approach for interpreting genome-wide expression profiles." *Proc Natl Acad Sci U S A* 102 (43):15545-50. doi: 10.1073/pnas.0506580102.
- Sugio, Kenji, Nakagawara, Akira, and Sasazuki, Takehiko. 1991. "Association of expression between N-myc gene and major histocompatibility complex class I gene in surgically resected human neuroblastoma." *Cancer* 67 (5):1384-1388.
- Sun, G., Lu, J., Zhang, C., You, R., Shi, L., Jiang, N., Nie, D., Zhu, J., Li, M., and Guo, J. 2017. "MiR-29b inhibits the growth of glioma via MYCN dependent way." *Oncotarget* 8 (28):45224-45233. doi: 10.18632/oncotarget.16780.

6. References

- Sun, L., Fazal, F. M., Li, P., Broughton, J. P., Lee, B., Tang, L., Huang, W., Kool, E. T., Chang, H. Y., and Zhang, Q. C. 2019. "RNA structure maps across mammalian cellular compartments." *Nat Struct Mol Biol* 26 (4):322-330. doi: 10.1038/s41594-019-0200-7.
- Taggart, Denah R, Han, Myo M, Quach, Alekist, Groshen, Susan, Ye, Wei, Villablanca, Judith G, Jackson, Hollie A, Aparici, Carina Mari, Carlson, David, and Maris, John. 2009. "Comparison of iodine-123 metaiodobenzylguanidine (MIBG) scan and [18F] fluorodeoxyglucose positron emission tomography to evaluate response after iodine-131 MIBG therapy for relapsed neuroblastoma." *Journal of clinical oncology* 27 (32):5343.
- Takeda, Osamu, Homma, Chieko, Maseki, Nobuo, Sakurai, Masaharu, Kanda, Naotoshi, Schwab, Manfred, Nakamura, Yusuke, and Kaneko, Yasuhiko. 1994. "There may be two tumor suppressor genes on chromosome arm 1p closely associated with biologically distinct subtypes of neuroblastoma." *Genes, Chromosomes and Cancer* 10 (1):30-39.
- Takemoto, J., Kuda, M., Kohashi, K., Yamada, Y., Koga, Y., Kinoshita, I., Souza, R., Taguchi, T., and Oda, Y. 2019. "HuC/D expression in small round cell tumors and neuroendocrine tumors: a useful tool for distinguishing neuroblastoma from childhood small round cell tumors." *Hum Pathol* 85:162-167. doi: 10.1016/j.humpath.2018.11.004.
- Takita, Junko, Hayashi, Yasuhide, Kohno, Takashi, Yamaguchi, Naohito, Hanada, Ryoji, Yamamoto, Keiko, and Yokota, Jun. 1997. "Deletion map of chromosome 9 and p16 (CDKN2A) gene alterations in neuroblastoma." *Cancer research* 57 (5):907-912.
- Takita, Junko, Yang, Hong Wei, Bessho, Fumio, Hanada, Ryoji, Yamamoto, Keiko, Kidd, Vincent, Teitz, Tal, Wei, Tie, and Hayashi, Yasuhide. 2000. "Absent or reduced expression of the caspase 8 gene occurs frequently in neuroblastoma, but not commonly in Ewing sarcoma or rhabdomyosarcoma." *Medical and Pediatric Oncology: The Official Journal of SIOP—International Society of Pediatric Oncology (Société Internationale d'Oncologie Pédiatrique)* 35 (6):541-543.
- Tanaka, Takeo, Slamon, Dennis J, Shimoda, Hiroko, Waki, Chiaki, Kawaguchi, Yoshinori, Tanaka, Yoshito, and Ida, Noriaki. 1988. "Expression of Ha-ras oncogene products in human neuroblastomas and the significant correlation with a patient's prognosis." *Cancer research* 48 (4):1030-1034.
- Tang, B., Bi, L., Xu, Y., Cao, L., and Li, X. 2023. "N(6)-Methyladenosine (m(6)A) Reader IGF2BP1 Accelerates Gastric Cancer Development and Immune Escape by Targeting PD-L1." *Mol Biotechnol*. doi: 10.1007/s12033-023-00896-8.
- Tang, Z., Kang, B., Li, C., Chen, T., and Zhang, Z. 2019. "GEPIA2: an enhanced web server for large-scale expression profiling and interactive analysis." *Nucleic Acids Res* 47 (W1):W556-W560. doi: 10.1093/nar/gkz430.
- Tee, A. E., Ling, D., Nelson, C., Atmadibrata, B., Dinger, M. E., Xu, N., Mizukami, T., Liu, P. Y., Liu, B., Cheung, B., Pasquier, E., Haber, M., Norris, M. D., Suzuki, T., Marshall, G. M., and Liu, T. 2014. "The histone demethylase JMJD1A induces cell migration and invasion by up-regulating the expression of the long noncoding RNA MALAT1." *Oncotarget* 5 (7):1793-804. doi: 10.18632/oncotarget.1785.
- Teitz, Tal, Wei, Tie, Valentine, Marcus B, Vanin, Elio F, Grenet, Jose, Valentine, Virginia A, Behm, Frederick G, Look, A Thomas, Lahti, Jill M, and Kidd, Vincent J. 2000. "Caspase 8 is deleted or silenced preferentially in childhood neuroblastomas with amplification of MYCN." *Nature medicine* 6 (5):529-535.
- Tessier, C. R., Doyle, G. A., Clark, B. A., Pitot, H. C., and Ross, J. 2004. "Mammary tumor induction in transgenic mice expressing an RNA-binding protein." *Cancer Res* 64 (1):209-14. doi: 10.1158/0008-5472.can-03-2927.
- The, Inge, Murthy, Anita E, Hannigan, Gregory E, Jacoby, Lee B, Menon, Anil G, Gusella, James F, and Bernards, Andre. 1993. "Neurofibromatosis type 1 gene mutations in neuroblastoma." *Nature genetics* 3 (1):62-66.
- Thompson, Daria, Vo, Kieuhoa T, London, Wendy B, Fischer, Matthias, Ambros, Peter F, Nakagawara, Akira, Brodeur, Garrett M, Matthay, Katherine K, and DuBois, Steven G. 2016. "Identification of patient subgroups with markedly disparate rates of MYCN amplification in neuroblastoma: A report from the International Neuroblastoma Risk Group project." *Cancer* 122 (6):935-945.
- Thompson, PM, Seifried, BA, Kyemba, SK, Jensen, SJ, Guo, C, Maris, JM, Brodeur, GM, Stram, DO, Seeger, RC, and Gerbing, R. 2001. "Loss of heterozygosity for chromosome 14q in neuroblastoma." *Medical and Pediatric Oncology: The Official Journal of SIOP—International Society of Pediatric Oncology (Société Internationale d'Oncologie Pédiatrique)* 36 (1):28-31.
- Tivnan, Amanda, Tracey, Lorraine, Buckley, Patrick G, Alcock, Leah C, Davidoff, Andrew M, and Stallings, Raymond L. 2011. "MicroRNA-34a is a potent tumor suppressor molecule in vivo in neuroblastoma." *BMC cancer* 11 (1):1-11.
- Tolbert, V. P., Coggins, G. E., and Maris, J. M. 2017. "Genetic susceptibility to neuroblastoma." *Curr Opin Genet Dev* 42:81-90. doi: 10.1016/j.gde.2017.03.008.
- Tolcher, A. W., Mita, A., Lewis, L. D., Garrett, C. R., Till, E., Daud, A. I., Patnaik, A., Papadopoulos, K., Takimoto, C., Bartels, P., Keating, A., and Antonia, S. 2008. "Phase I and pharmacokinetic study of YM155, a small-molecule inhibitor of survivin." *J Clin Oncol* 26 (32):5198-203. doi: 10.1200/JCO.2008.17.2064.
- Toledano, H., D'Alterio, C., Czech, B., Levine, E., and Jones, D. L. 2012. "The let-7-imp axis regulates ageing of the Drosophila testis stem-cell niche." *Nature* 485 (7400):605-10. doi: 10.1038/nature11061.
- Tomioka, N, Oba, S, Ohira, M, Misra, A, Fridlyand, J, Ishii, S, Nakamura, Y, Isogai, E, Hirata, T, and Yoshida, Y. 2008. "Novel risk stratification of patients with neuroblastoma by genomic signature, which is independent of molecular signature." *Oncogene* 27 (4):441-449.
- Tonini, G. P., and Capasso, M. 2020. "Genetic predisposition and chromosome instability in neuroblastoma." *Cancer Metastasis Rev* 39 (1):275-285. doi: 10.1007/s10555-020-09843-4.
- Tonini, Gian Paolo, Boni, Luca, Pession, Annalisa, and Rogers, David. 1997. "MYCN On cogene Amplification in Neuroblastom a Is Associated VVith VVorse Prognosis, Except in Stage 4s: The Italian Experience VVith 295 Children." *Journal of clinical oncology* 15 (1):85-93.
- Trieselmann, N., Armstrong, S., Rauw, J., and Wilde, A. 2003. "Ran modulates spindle assembly by regulating a subset of TPX2 and Kid activities including Aurora A activation." *J Cell Sci* 116 (Pt 23):4791-8. doi: 10.1242/jcs.00798.
- Trochet, Delphine, Bourdeaut, Franck, Janoueix-Lerosey, Isabelle, Deville, Anne, De Pontual, Loïc, Schleiermacher, Gudrun, Coze, Carole, Philip, Nicole, Frébourg, Thierry, and Munnich, Arnold. 2004. "Germline mutations of the paired-like homeobox 2B (PHOX2B) gene in neuroblastoma." *The American Journal of Human Genetics* 74 (4):761-764.
- Tsai, M. Y., Wiese, C., Cao, K., Martin, O., Donovan, P., Ruderman, J., Prigent, C., and Zheng, Y. 2003. "A Ran signalling pathway mediated by the mitotic kinase Aurora A in spindle assembly." *Nat Cell Biol* 5 (3):242-8. doi: 10.1038/ncb936.
- Tseng, Alexander M., Mahnke, Amanda H., Salem, Nihal A., and Miranda, Rajesh C. 2018. "Noncoding RNA Regulatory Networks, Epigenetics, and Programming Stem Cell Renewal and Differentiation: Implications for Stem Cell Therapy." In *Epigenetics in Human Disease*, 20. Academic Press.
- Tweddle, Deborah A, Malcolm, Archie J, Bown, Nick, Pearson, Andrew DJ, and Lunec, John. 2001. "Evidence for the development of p53 mutations after cytotoxic therapy in a neuroblastoma cell line." *Cancer research* 61 (1):8-13.
- Ueda, T., Nakata, Y., Yamasaki, N., Oda, H., Sentani, K., Kanai, A., Onishi, N., Ikeda, K., Sera, Y., Honda, Z. I., Tanaka, K., Sata, M., Ogawa, S., Yasui, W., Saya, H., Takita, J., and Honda, H. 2016. "ALK(R1275Q) perturbs extracellular matrix, enhances cell invasion and leads to the development of neuroblastoma in cooperation with MYCN." *Oncogene* 35 (34):4447-58. doi: 10.1038/nc.2015.519.

6. References

- Valentijn, Linda J, Koppen, Arjen, van Asperen, Ronald, Root, Heather A, Haneveld, Franciska, and Versteeg, Rogier. 2005. "Inhibition of a new differentiation pathway in neuroblastoma by copy number defects of N-myc, Cdc42, and nm23 genes." *Cancer research* 65 (8):3136-3145.
- Valentijn, Linda J, Koster, Jan, Zwijnenburg, Danny A, Hasselt, Nancy E, Van Sluis, Peter, Volckmann, Richard, Van Noesel, Max M, George, Rani E, Tytgat, Godelieve AM, and Molenaar, Jan J. 2015. "TERT rearrangements are frequent in neuroblastoma and identify aggressive tumors." *Nature genetics* 47 (12):1411-1414.
- van Groningen, T., Koster, J., Valentijn, L. J., Zwijnenburg, D. A., Akogul, N., Hasselt, N. E., Broekmans, M., Haneveld, F., Nowakowska, N. E., Bras, J., van Noesel, C. J. M., Jongejan, A., van Kampen, A. H., Koster, L., Baas, F., van Dijk-Kerkhoven, L., Huizer-Smit, M., Lecca, M. C., Chan, A., Lakeman, A., Molenaar, P., Volckmann, R., Westerhout, E. M., Hamdi, M., van Sluis, P. G., Ebus, M. E., Molenaar, J. J., Tytgat, G. A., Westerman, B. A., van Nes, J., and Versteeg, R. 2017. "Neuroblastoma is composed of two super-enhancer-associated differentiation states." *Nat Genet* 49 (8):1261-1266. doi: 10.1038/ng.3899.
- van Limpt, V., Schramm, A., van Lakeman, A., Sluis, P., Chan, A., van Noesel, M., Baas, F., Caron, H., Eggert, A., and Versteeg, R. 2004. "The Phox2B homeobox gene is mutated in sporadic neuroblastomas." *Oncogene* 23 (57):9280-8. doi: 10.1038/sj.onc.1208157.
- Van Nostrand, E. L., Pratt, G. A., Shishkin, A. A., Gelboin-Burkhart, C., Fang, M. Y., Sundaraman, B., Blue, S. M., Nguyen, T. B., Surka, C., Elkins, K., Stanton, R., Rigo, F., Guttman, M., and Yeo, G. W. 2016. "Robust transcriptome-wide discovery of RNA-binding protein binding sites with enhanced CLIP (eCLIP)." *Nat Methods* 13 (6):508-14. doi: 10.1038/nmeth.3810.
- Van Roy, Nadine, Cheng, NC, Laureys, Genevieve, Opendakker, Ghislain, Versteeg, R, and Speleman, Franki. 1995. "Molecular cytogenetic analysis of 1; 17 translocations in neuroblastoma." *European Journal of Cancer* 31 (4):530-535.
- Van Roy, Nadine, Laureys, Geneviève, Cheng, Ngan Ching, Willem, Pascale, Opendakker, Ghislain, Versteeg, Rogier, and Speleman, Frank. 1994. "1; 17 translocations and other chromosome 17 rearrangements in human primary neuroblastoma tumors and cell lines." *Genes, Chromosomes and Cancer* 10 (2):103-114.
- Van Roy, Nadine, Laureys, Genevieve, Van Gele, Mireille, Opendakker, Ghislain, Miura, Retsu, van der Drift, Pauline, Chan, Alvin, Versteeg, Rogier, and Speleman, Franki. 1997. "Analysis of 1; 17 translocation breakpoints in neuroblastoma: implications for mapping of neuroblastoma genes." *European Journal of Cancer* 33 (12):1974-1978.
- Vandesompele, J., Baudis, M., De Preter, K., Van Roy, N., Ambros, P., Bown, N., Brinkschmidt, C., Christiansen, H., Combaret, V., Lastowska, M., Nicholson, J., O'Meara, A., Plantaz, D., Stallings, R., Brichard, B., Van den Broecke, C., De Bie, S., De Paepe, A., Laureys, G., and Speleman, F. 2005. "Unequivocal delineation of clinicogenetic subgroups and development of a new model for improved outcome prediction in neuroblastoma." *J Clin Oncol* 23 (10):2280-99. doi: 10.1200/JCO.2005.06.104.
- Venkatraman, E. S., and Olshen, A. B. 2007. "A faster circular binary segmentation algorithm for the analysis of array CGH data." *Bioinformatics* 23 (6):657-63. doi: 10.1093/bioinformatics/btl646.
- Vikesaa, J., Hansen, T. V., Jonson, L., Borup, R., Wewer, U. M., Christiansen, J., and Nielsen, F. C. 2006. "RNA-binding IMPs promote cell adhesion and invadopodia formation." *EMBO J* 25 (7):1456-68. doi: 10.1038/sj.emboj.7601039.
- Virchow, R. 1864. "Hyperplasie der Zirbel und der Nebennieren." *Die Krankhaften Geschwulste* 2:1864-1865.
- Viswanathan, S. R., Daley, G. Q., and Gregory, R. I. 2008. "Selective blockade of microRNA processing by Lin28." *Science* 320 (5872):97-100. doi: 10.1126/science.1154040.
- Vo, Kieuhoa T, Matthay, Katherine K, Neuhaus, John, London, Wendy B, Hero, Barbara, Ambros, Peter F, Nakagawara, Akira, Miniati, Doug, Wheeler, Kate, and Pearson, Andrew DJ. 2014. "Clinical, biologic, and prognostic differences on the basis of primary tumor site in neuroblastoma: a report from the international neuroblastoma risk group project." *Journal of clinical oncology* 32 (28):3169.
- Vogan, Kyle, Bernstein, Mark, Leclerc, Jean-Marie, Brisson, Linda, Brossard, Josee, Brodeur, Garrett M, Pelletier, Jerry, and Gros, Philippe. 1993. "Absence of p53 gene mutations in primary neuroblastomas." *Cancer research* 53 (21):5269-5273.
- Wächter, K., Köhn, M., Stöhr, N., and Hüttelmaier, S. 2013. "Subcellular localization and RNP formation of IGF2BPs (IGF2 mRNA-binding proteins) is modulated by distinct RNA-binding domains." *Biol Chem* 394 (8):1077-90. doi: 10.1515/hsz-2013-0111.
- Waldeck, K., Cullinane, C., Ardley, K., Shortt, J., Martin, B., Tothill, R. W., Li, J., Johnstone, R. W., McArthur, G. A., Hicks, R. J., and Wood, P. J. 2016. "Long term, continuous exposure to panobinostat induces terminal differentiation and long term survival in the TH-MYCIN neuroblastoma mouse model." *Int J Cancer* 139 (1):194-204. doi: 10.1002/ijc.30056.
- Wallis, N., Oberman, F., Shurrush, K., Germain, N., Greenwald, G., Gershon, T., Pearl, T., Abis, G., Singh, V., Singh, A., Sharma, A. K., Barr, H. M., Ramos, A., Spiegelman, V. S., and Yisraeli, J. K. 2022. "Small molecule inhibitor of IGF2bp1 represses Kras and a pro-oncogenic phenotype in cancer cells." *RNA Biol* 19 (1):26-43. doi: 10.1080/15476286.2021.2010983.
- Wang, Chunxi, Liu, Zhihui, Woo, Chan-Wook, Li, Zhijie, Wang, Lifeng, Wei, Jun S, Marquez, Victor E, Bates, Susan E, Jin, Qihuang, and Khan, Javed. 2012. "EZH2 Mediates epigenetic silencing of neuroblastoma suppressor genes CASZ1, CLU, RUNX3, and NGFR." *Cancer research* 72 (1):315-324.
- Wang, G., Edwards, H., Caldwell, J. T., Buck, S. A., Qing, W. Y., Taub, J. W., Ge, Y., and Wang, Z. 2013. "Panobinostat synergistically enhances the cytotoxic effects of cisplatin, doxorubicin or etoposide on high-risk neuroblastoma cells." *PLoS One* 8 (9):e76662. doi: 10.1371/journal.pone.0076662.
- Wang, J. J., Chen, D. X., Zhang, Y., Xu, X., Cai, Y., Wei, W. Q., Hao, J. J., and Wang, M. R. 2023. "Elevated expression of the RNA-binding protein IGF2BP1 enhances the mRNA stability of INHBA to promote the invasion and migration of esophageal squamous cancer cells." *Exp Hematol Oncol* 12 (1):75. doi: 10.1186/s40164-023-00429-8.
- Wang, Kai, Diskin, Sharon J, Zhang, Haitao, Attiyeh, Edward F, Winter, Cynthia, Hou, Cuiping, Schnepf, Robert W, Diamond, Maura, Bosse, Kristopher, and Mayes, Patrick A. 2011. "Integrative genomics identifies LMO1 as a neuroblastoma oncogene." *Nature* 469 (7329):216-220.
- Wei, J. S., Song, Y. K., Durinck, S., Chen, Q. R., Cheuk, A. T., Tsang, P., Zhang, Q., Thiele, C. J., Slack, A., Shohet, J., and Khan, J. 2008. "The MYCN oncogene is a direct target of miR-34a." *Oncogene* 27 (39):5204-13. doi: 10.1038/ncr.2008.154.
- Weidensdorfer, D., Stöhr, N., Baude, A., Lederer, M., Köhn, M., Schierhorn, A., Buchmeier, S., Wahle, E., and Hüttelmaier, S. 2009. "Control of c-myc mRNA stability by IGF2BP1-associated cytoplasmic RNPs." *RNA* 15 (1):104-15. doi: 10.1261/rna.1175909.
- Weiss, W. A., Aldape, K., Mohapatra, G., Feuerstein, B. G., and Bishop, J. M. 1997. "Targeted expression of MYCN causes neuroblastoma in transgenic mice." *EMBO J* 16 (11):2985-95. doi: 10.1093/emboj/16.11.2985.
- Weiss, W. A., Godfrey, T., Francisco, C., and Bishop, J. M. 2000. "Genome-wide screen for allelic imbalance in a mouse model for neuroblastoma." *Cancer Res* 60 (9):2483-7.
- Welch, C, Chen, Y, and Stallings, RL. 2007. "MicroRNA-34a functions as a potential tumor suppressor by inducing apoptosis in neuroblastoma cells." *Oncogene* 26 (34):5017-5022.

6. References

- Wenzel, A., Cziepluch, C., Hamann, U., Schurmann, J., and Schwab, M. 1991. "The N-Myc oncoprotein is associated in vivo with the phosphoprotein Max(p20/22) in human neuroblastoma cells." *EMBO J* 10 (12):3703-12. doi: 10.1002/j.1460-2075.1991.tb04938.x.
- White, PS, Thompson, PM, Seifried, BA, Sulman, EP, Jensen, SJ, Guo, C, Maris, JM, Hogarty, MD, Allen, C, and Biegel, JA. 2001. "Detailed molecular analysis of 1p36 in neuroblastoma." *Medical and Pediatric Oncology: The Official Journal of SIOP—International Society of Pediatric Oncology (Société Internationale d'Oncologie Pédiatrique)* 36 (1):37-41.
- Whittle, S. B., Smith, V., Doherty, E., Zhao, S., McCarty, S., and Zage, P. E. 2017. "Overview and recent advances in the treatment of neuroblastoma." *Expert Rev Anticancer Ther* 17 (4):369-386. doi: 10.1080/14737140.2017.1285230.
- Wilbert, M. L., Huelga, S. C., Kapeli, K., Stark, T. J., Liang, T. Y., Chen, S. X., Yan, B. Y., Nathanson, J. L., Hutt, K. R., Lovci, M. T., Kazan, H., Vu, A. Q., Massirer, K. B., Morris, Q., Hoon, S., and Yeo, G. W. 2012. "LIN28 binds messenger RNAs at GGAGA motifs and regulates splicing factor abundance." *Mol Cell* 48 (2):195-206. doi: 10.1016/j.molcel.2012.08.004.
- Witt, O., Deubzer, H. E., Lodrini, M., Milde, T., and Oehme, I. 2009. "Targeting histone deacetylases in neuroblastoma." *Curr Pharm Des* 15 (4):436-47. doi: 10.2174/138161209787315774.
- Wong, M., Tee, A. E. L., Milazzo, G., Bell, J. L., Poulos, R. C., Atmadibrata, B., Sun, Y., Jing, D., Ho, N., Ling, D., Liu, P. Y., Zhang, X. D., Hüttelmaier, S., Wong, J. W. H., Wang, J., Polly, P., Perini, G., Scarlett, C. J., and Liu, T. 2017. "The Histone Methyltransferase DOT1L Promotes Neuroblastoma by Regulating Gene Transcription." *Cancer Res* 77 (9):2522-2533. doi: 10.1158/0008-5472.CAN-16-1663.
- Woods, William G, Gao, Ru-Nie, Shuster, Jonathan J, Robison, Leslie L, Bernstein, Mark, Weitzman, Sheila, Bunin, Greta, Levy, Isra, Brossard, Josee, and Dougherty, Geoffrey. 2002. "Screening of infants and mortality due to neuroblastoma." *New England Journal of Medicine* 346 (14):1041-1046.
- Wright, James Homer. 1910. "Neurocytoma or neuroblastoma, a kind of tumor not generally recognized." *The Journal of experimental medicine* 12 (4):556.
- Xiang, Xuan, Mei, Hong, Zhao, Xiang, Pu, Jiarui, Li, Dan, Qu, Hongxia, Jiao, Wanju, Zhao, Jihe, Huang, Kai, and Zheng, Liduan. 2015. "miRNA-337-3p suppresses neuroblastoma progression by repressing the transcription of matrix metalloproteinase 14." *Oncotarget* 6 (26):22452.
- Xie, F., Huang, C., Liu, F., Zhang, H., Xiao, X., Sun, J., Zhang, X., and Jiang, G. 2021. "CircPTPRA blocks the recognition of RNA N(6)-methyladenosine through interacting with IGF2BP1 to suppress bladder cancer progression." *Mol Cancer* 20 (1):68. doi: 10.1186/s12943-021-01359-x.
- Xuan, J. J., Sun, W. J., Lin, P. H., Zhou, K. R., Liu, S., Zheng, L. L., Qu, L. H., and Yang, J. H. 2018. "RMBase v2.0: deciphering the map of RNA modifications from epitranscriptome sequencing data." *Nucleic Acids Res* 46 (D1):D327-D334. doi: 10.1093/nar/gkx934.
- Yamamoto, Keiko, Ohta, Shigeru, Ito, Etsuro, Hayashi, Yutaka, Asami, Tadashi, Mabuchi, Osamu, Higashigawa, Masamune, and Tanimura, Masako. 2002. "Marginal decrease in mortality and marked increase in incidence as a result of neuroblastoma screening at 6 months of age: cohort study in seven prefectures in Japan." *Journal of clinical oncology* 20 (5):1209-1214.
- Yamashiro, Darrell J, Nakagawara, Akira, Ikegaki, Naohiko, Liu, XG, and Brodeur, Garrett M. 1996. "Expression of TrkC in favorable human neuroblastomas." *Oncogene* 12 (1):37-41.
- Yang, C. P., Samuels, T. J., Huang, Y., Yang, L., Ish-Horowicz, D., Davis, I., and Lee, T. 2017. "Imp and Syp RNA-binding proteins govern decommitment of *Drosophila* neural stem cells." *Development* 144 (19):3454-3464. doi: 10.1242/dev.149500.
- Yang, J., Altahan, A. M., Hu, D., Wang, Y., Cheng, P. H., Morton, C. L., Qu, C., Nathwani, A. C., Shohet, J. M., Fotsis, T., Koster, J., Versteeg, R., Okada, H., Harris, A. L., and Davidoff, A. M. 2015. "The role of histone demethylase KDM4B in Myc signaling in neuroblastoma." *J Natl Cancer Inst* 107 (6):djv080. doi: 10.1093/jnci/djv080.
- Yang, J., Zhou, J., Li, C., and Wang, S. 2021. "Integrated analysis of the functions and prognostic values of RNA-binding proteins in neuroblastoma." *PLoS One* 16 (12):e0260876. doi: 10.1371/journal.pone.0260876.
- Yanik, G. A., Parisi, M. T., Shulkin, B. L., Naranjo, A., Kreissman, S. G., London, W. B., Villablanca, J. G., Maris, J. M., Park, J. R., Cohn, S. L., McGrady, P., and Matthay, K. K. 2013. "Semiquantitative mIBG scoring as a prognostic indicator in patients with stage 4 neuroblastoma: a report from the Children's oncology group." *J Nucl Med* 54 (4):541-8. doi: 10.2967/jnumed.112.112334.
- Yaniv, K., Fainsod, A., Kalcheim, C., and Yisraeli, J. K. 2003. "The RNA-binding protein Vg1 RBP is required for cell migration during early neural development." *Development* 130 (23):5649-61. doi: 10.1242/dev.00810.
- Yaniv, K., and Yisraeli, J. K. 2002. "The involvement of a conserved family of RNA binding proteins in embryonic development and carcinogenesis." *Gene* 287 (1-2):49-54. doi: 10.1016/s0378-1119(01)00866-6.
- Yano, H., and Chao, M. V. 2000. "Neurotrophin receptor structure and interactions." *Pharm Acta Helv* 74 (2-3):253-60. doi: 10.1016/s0031-6865(99)00036-9.
- Yates, B., Braschi, B., Gray, K. A., Seal, R. L., Tweedie, S., and Bruford, E. A. 2017. "Genenames.org: the HGNC and VGNC resources in 2017." *Nucleic Acids Res* 45 (D1):D619-D625. doi: 10.1093/nar/gkw1033.
- Ying, Y., Ma, X., Fang, J., Chen, S., Wang, W., Li, J., Xie, H., Wu, J., Xie, B., Liu, B., Wang, X., Zheng, X., and Xie, L. 2021. "EGR2-mediated regulation of m(6A) reader IGF2BP proteins drive RCC tumorigenesis and metastasis via enhancing S1PR3 mRNA stabilization." *Cell Death Dis* 12 (8):750. doi: 10.1038/s41419-021-04038-3.
- Yisraeli, J. K. 2005. "VICKZ proteins: a multi-talented family of regulatory RNA-binding proteins." *Biol Cell* 97 (1):87-96. doi: 10.1042/BC20040151.
- Yogev, O., Almeida, G. S., Barker, K. T., George, S. L., Kwok, C., Campbell, J., Zarowiecki, M., Klefogiannis, D., Smith, L. M., Hallsworth, A., Berry, P., Mocklinghoff, T., Webber, H. T., Danielson, L. S., Buttery, B., Calton, E. A., da Costa, B. M., Poon, E., Jamin, Y., Lise, S., Veal, G. J., Sebire, N., Robinson, S. P., Anderson, J., and Chesler, L. 2019. "In Vivo Modeling of Chemoresistant Neuroblastoma Provides New Insights into Chemorefractory Disease and Metastasis." *Cancer Res* 79 (20):5382-5393. doi: 10.1158/0008-5472.CAN-18-2759.
- Yoon, K. J., Danks, M. K., Ragsdale, S. T., Valentine, M. B., and Valentine, V. A. 2006. "Translocations of 17q21 approximately qter in neuroblastoma cell lines infrequently include the topoisomerase IIalpha gene." *Cancer Genet Cytogenet* 167 (1):92-4. doi: 10.1016/j.cancergencyto.2005.11.004.
- Yu, A. L., Gilman, A. L., Ozkaynak, M. F., London, W. B., Kreissman, S. G., Chen, H. X., Smith, M., Anderson, B., Villablanca, J. G., Matthay, K. K., Shimada, H., Grupp, S. A., Seeger, R., Reynolds, C. P., Buxton, A., Reisfeld, R. A., Gillies, S. D., Cohn, S. L., Maris, J. M., Sondel, P. M., and Children's Oncology, Group. 2010. "Anti-GD2 antibody with GM-CSF, interleukin-2, and isotretinoin for neuroblastoma." *N Engl J Med* 363 (14):1324-34. doi: 10.1056/NEJMoa0911123.
- Yu, F., Wei, J., Cui, X., Yu, C., Ni, W., Bungert, J., Wu, L., He, C., and Qian, Z. 2021. "Post-translational modification of RNA m6A demethylase ALKBH5 regulates ROS-induced DNA damage response." *Nucleic Acids Res* 49 (10):5779-5797. doi: 10.1093/nar/gkab415.

6. References

- Yu, G., Wang, L. G., Han, Y., and He, Q. Y. 2012. "clusterProfiler: an R package for comparing biological themes among gene clusters." *OMICS* 16 (5):284-7. doi: 10.1089/omi.2011.0118.
- Yu, Meng, Ohira, Miki, Li, Yuanyuan, Niizuma, Hidetaka, Oo, Myat Lin, Zhu, Yuyan, Ozaki, Toshinori, Isogai, Eriko, Nakamura, Yohko, and Koda, Tadayuki. 2009. "High expression of ncRAN, a novel non-coding RNA mapped to chromosome 17q25. 1, is associated with poor prognosis in neuroblastoma." *International journal of oncology* 34 (4):931-938.
- Zafar, A., Wang, W., Liu, G., Wang, X., Xian, W., McKeon, F., Foster, J., Zhou, J., and Zhang, R. 2021. "Molecular targeting therapies for neuroblastoma: Progress and challenges." *Med Res Rev* 41 (2):961-1021. doi: 10.1002/med.21750.
- Zeineldin, Maged, Federico, Sara, Chen, Xiang, Fan, Yiping, Xu, Beisi, Stewart, Elizabeth, Zhou, Xin, Jeon, Jongrye, Griffiths, Lyra, and Nguyen, Rosa. 2020. "MYCN amplification and ATRX mutations are incompatible in neuroblastoma." *Nature communications* 11 (1):913.
- Zeltzer, Paul M, Marangos, Paul J, Evans, Audrey E, and Schneider, Sandra L. 1986. "Serum neuron-specific enolase in children with neuroblastoma. Crelationship to stage and disease course." *Cancer* 57 (6):1230-1234.
- Zhang, H. L., Eom, T., Oleynikov, Y., Shenoy, S. M., Liebelt, D. A., Dichtenberg, J. B., Singer, R. H., and Bassell, G. J. 2001. "Neurotrophin-induced transport of a beta-actin mRNA complex increases beta-actin levels and stimulates growth cone motility." *Neuron* 31 (2):261-75. doi: 10.1016/s0896-6273(01)00357-9.
- Zhang, M., Liang, C., Chen, Q., Yan, H., Xu, J., Zhao, H., Yuan, X., Liu, J., Lin, S., Lu, W., and Wang, F. 2020. "Histone H2A phosphorylation recruits topoisomerase IIalpha to centromeres to safeguard genomic stability." *EMBO J* 39 (3):e101863. doi: 10.15252/embj.2019101863.
- Zhen, Z., Yang, K., Ye, L., You, Z., Chen, R., Liu, Y., and He, Y. 2017. "Suberoylanilide hydroxamic acid sensitizes neuroblastoma to paclitaxel by inhibiting thioredoxin-related protein 14-mediated autophagy." *Cancer Sci* 108 (7):1485-1492. doi: 10.1111/cas.13279.
- Zhi, F., Wang, R., Wang, Q., Xue, L., Deng, D., Wang, S., and Yang, Y. 2014. "MicroRNAs in neuroblastoma: small-sized players with a large impact." *Neurochem Res* 39 (4):613-23. doi: 10.1007/s11064-014-1247-9.
- Zhu, Qichao, and Center, Melvin S. 1994. "Cloning and sequence analysis of the promoter region of the MRP gene of HL60 cells isolated for resistance to adriamycin." *Cancer research* 54 (16):4488-4492.
- Zimmerman, K. A., Yancopoulos, G. D., Collum, R. G., Smith, R. K., Kohl, N. E., Denis, K. A., Nau, M. M., Witte, O. N., Toran-Allerand, D., Gee, C. E., and et al. 1986. "Differential expression of myc family genes during murine development." *Nature* 319 (6056):780-3. doi: 10.1038/319780a0.
- Zimmerman, M. W., Liu, Y., He, S., Durbin, A. D., Abraham, B. J., Easton, J., Shao, Y., Xu, B., Zhu, S., Zhang, X., Li, Z., Weichert-Leahey, N., Young, R. A., Zhang, J., and Look, A. T. 2018. "MYC Drives a Subset of High-Risk Pediatric Neuroblastomas and Is Activated through Mechanisms Including Enhancer Hijacking and Focal Enhancer Amplification." *Cancer Discov* 8 (3):320-335. doi: 10.1158/2159-8290.CD-17-0993.

7. Appendix

7.1 Supplementary Tables

Table 28: Human neuroblastoma tumor cohort.

ID	age at diagnosis (d)	dead or last follow up (d)	dead	clinical stage	MYCN amplification	17q unbalance	RNA-seq data	sWGS data
1	356	2121	-	1	-	+	+	+
2	1197	1456	-	1	-	-	+	+
3	98	776	-	1	-	-	+	+
4	298	590	-	1	-	-	+	+
5	1852	1631	-	1	-	-	+	+
6	95	54	-	1	-	-	+	+
7	42	729	-	1	-	-	+	+
8	254	509	-	1	-	-	+	+
9	0	345	-	1	-	-	+	+
10	32	185	-	1	-	-	+	+
11	179	294	-	1	-	-	+	+
12	300	2509	-	2	-	-	+	+
13	729	704	-	2	-	-	+	+
14	217	2539	-	3	-	-	+	+
15	1022	478	+	3	+	+	+	+
16	447	203	+	4	+	+	+	+
17	279	889	+	4	+	+	+	+
18	1575	262	+	4	+	+	+	+
19	2045	679	-	4	+	+	+	+
20	970	1202	+	4	-	+	+	+
21	1443	969	-	4	-	+	+	+
22	849	424	+	4	-	+	+	+
23	1383	1364	-	4	-	+	+	+
24	1812	834	-	4	-	+	+	+
25	1136	194	-	4	-	+	+	+
26	16	2482	-	4S	-	-	+	+
27	95	665	-	4S	-	-	+	+
28	0	560	-	4S	-	-	+	+
29	6	388	-	4S	-	-	+	+
30	65	211	-	4S	-	-	+	+
31	589	1648	-	1	-	-	+	+
32	75	1632	-	1	-	-	+	+
33	102	1452	-	1	-	-	+	+
34	12	1844	-	2	-	-	+	+
35	623	610	-	2	-	-	+	+
36	1726	354	-	2	-	-	+	+
37	492	995	-	2	-	-	+	+
38	701	881	-	2	-	-	-	+
39	518	785	-	3	-	-	+	+
40	282	1288	-	3	-	-	+	+
41	271	2067	-	3	-	-	+	+
42	310	103	+	3	+	-	+	+
43	1137	5548	-	3	+	+	+	+
44	2551	558	-	3	-	-	+	+
45	1742	2898	-	3	+	+	+	+
46	196	539	+	4	+	-	+	+
47	1904	207	+	4	+	-	+	+

48	n. d.	n. d.	n. d.	4	-	+	+	+
49	1162	1131	+	4	-	-	-	+
50	400	5801	-	4	-	+	+	+
51	476	5298	-	4	-	-	+	+
52	1644	3511	-	4	-	+	+	+
53	619	3357	-	4	-	-	+	+
54	497	2448	-	4	-	-	+	+
55	327	737	-	4	-	-	-	+
56	1537	1235	+	4	-	+	+	+
57	933	1445	+	4	-	+	+	+
58	279	889	+	4	+	+	+	+
59	2135	1063	+	4	-	+	+	+
60	633	454	+	4	+	+	+	+
61	790	329	+	4	-	+	+	+
62	447	203	+	4	+	+	+	+
63	308	3935	-	4S	-	-	+	+
64	243	2294	-	4S	-	+	+	+
65	41	1338	-	4S	-	-	+	+
66	133	627	-	4S	-	-	+	+
67	107	3571	-	4S	-	-	+	+
68	4	2494	-	4S	-	-	+	+
69	297	2050	-	4S	-	-	+	+
70	16	3540	-	1	-	-	+	+
71	0	2167	-	1	-	-	+	+
72	887	3703	-	1	-	-	+	+
73	41	2782	-	1	-	-	+	+
74	22	4014	-	1	-	-	+	+
75	224	3788	-	1	-	-	+	+
76	2041	4070	-	1	-	+	+	+
77	316	2557	-	1	-	-	+	+
78	263	2586	-	1	-	+	+	+
79	363	3139	-	2.1	-	+	+	+
80	1676	3627	-	2.2	-	-	+	+
81	129	2308	-	2.2	-	-	+	+
82	2143	1255	-	3	-	-	+	+
83	1224	943	-	3	-	-	+	+
84	1381	4675	-	3	-	-	+	+
85	1683	3290	-	3	-	-	+	+
86	860	3009	-	3	-	-	+	+
87	3866	2826	-	3	-	+	+	+
88	382	1450	-	4	-	+	+	+
89	1529	1118	+	4	-	+	+	+
90	2326	2465	-	4	-	+	+	+
91	2105	784	+	4	+	-	+	+
92	701	702	+	4	+	+	+	+
93	947	892	+	4	+	+	+	+
94	849	948	+	4	+	+	+	+
95	62	86	-	4S	-	-	+	+
96	46	1395	-	4S	-	-	+	+
97	3	4408	-	4S	-	-	+	+
98	84	1919	-	4S	-	-	+	+
99	73	3478	-	4S	-	-	+	+
100	50	2248	-	4S	-	-	+	+

Table 29: Transgenic mice.

sex	genotype	CRE	age (d)	tumor	abdominal tumor	adrenal tumor	spinal tumor	RNA-seq (run)	miRNA-seq	sWGS
f	wildtype	-	364	no				+ (1)		+
f	wildtype	-	364	no				+ (1)		+
f	wildtype	-	364	no				+ (1)		+
f	wildtype	-	464	no					+	
m	wildtype	-	465	no					+	
m	wildtype	-	465	no					+	
f	IGF2BP1 fl/wt	-	377	no						
f	IGF2BP1 fl/wt	-	377	no						
m	IGF2BP1 fl/wt	-	376	no						
f	IGF2BP1 fl/wt	-	371	no						
f	IGF2BP1 fl/wt	-	436	no						
m	IGF2BP1 fl/wt	-	436	no						
f	IGF2BP1 fl/wt	-	364	no						
f	IGF2BP1 fl/wt	-	364	no						
f	IGF2BP1 fl/fl	-	364	no						
f	IGF2BP1 fl/fl	-	364	no						
f	IGF2BP1 fl/fl	-	364	no						
m	IGF2BP1 fl/fl	-	364	no						
m	IGF2BP1 fl/fl	-	364	no						
m	IGF2BP1 fl/fl	-	364	no						
m	IGF2BP1 fl/wt	+	310	yes	1	0	0	+ (1)	+	+
m	IGF2BP1 fl/wt	+	310	no						
f	IGF2BP1 fl/wt	+	379	no						
f	IGF2BP1 fl/wt	+	369	no						
f	IGF2BP1 fl/wt	+	314	no						
m	IGF2BP1 fl/wt	+	360	no						
m	IGF2BP1 fl/wt	+	360	no						
f	IGF2BP1 fl/wt	+	360	no						
m	IGF2BP1 fl/fl	+	184	yes	1	0	0	+ (1)		+
m	IGF2BP1 fl/fl	+	294	yes	1	0	0	+ (1)	+	+
f	IGF2BP1 fl/fl	+	305	yes	0	1	0	+ (1)	+	+
m	IGF2BP1 fl/fl	+	207	yes	1	0	0	+ (2)	+	+
m	IGF2BP1 fl/fl	+	214	yes	1	0	0	+ (1)	+	+
m	IGF2BP1 fl/fl	+	264	yes	1	0	0	+ (1)	+	+
m	IGF2BP1 fl/fl	+	169	yes	1	0	0	+ (3)	+	+
f	MYCN fl/wt	+	365	no				+ (2)		+
f	MYCN fl/wt	+	365	no				+ (2)		+
f	MYCN fl/wt	+	365	no				+ (2)		+
m	MYCN fl/wt	+	365	no						
f	MYCN fl/wt	+	365	no				+ (2)		+
f	MYCN fl/wt	+	365	no				+ (2)		+
m	IGF2BP1 fl/wt; MYCN fl/wt	+	106	yes	0	1	0	+ (2)	+	+
m	IGF2BP1 fl/wt; MYCN fl/wt	+	65	yes	0	1	0	+ (2)	+	+
m	IGF2BP1 fl/wt; MYCN fl/wt	+	159	yes	1	1	1	+ (2)	+	+
m	IGF2BP1 fl/wt; MYCN fl/wt	+	127	yes	1	2	3	+ (3)	+	+
f	IGF2BP1 fl/wt; MYCN fl/wt	+	127	yes	0	0	2	+ (3)	+	+
m	IGF2BP1 fl/wt; MYCN fl/wt	+	70	yes	1	0	0	+ (3)	+	+
f	IGF2BP1 fl/wt; MYCN fl/wt	+	82	yes	1	1	0	+ (3)	+	+
m	IGF2BP1 fl/wt; MYCN fl/wt	+	118	yes	1	1	1	+ (3)	+	+

Table 30: List of oncogenic and tumor-suppressive miRNAs deregulated in MNA neuroblastoma.

oncomiRs			tumor suppressor miRs		
let-7a-3p	miR-199a-3p	miR-7704	miR-1197	miR-26b-5p	miR-487a-5p
let-7c-3p	miR-199a-5p	miR-7974	miR-128-2-5p	miR-30a-3p	miR-487b-5p
let-7c-5p	miR-199b-3p	miR-92a-1-5p	miR-129-1-3p	miR-30a-5p	miR-488-5p
miR-10394-3p	miR-199b-5p	miR-92a-3p	miR-129-5p	miR-30c-1-3p	miR-496
miR-10401-3p	miR-19a-3p	miR-92b-3p	miR-134-3p	miR-323a-3p	miR-539-5p
miR-1244	miR-20a-5p	miR-93-5p	miR-135a-3p	miR-323a-5p	miR-541-3p
miR-1270	miR-214-3p	miR-9-3p	miR-137-3p	miR-323b-3p	miR-542-3p
miR-1282	miR-25-3p	miR-9-5p	miR-148a-3p	miR-324-5p	miR-542-5p
miR-1304-3p	miR-25-5p		miR-149-5p	miR-328-3p	miR-574-3p
miR-130b-3p	miR-296-3p		miR-153-3p	miR-330-5p	miR-598-3p
miR-130b-5p	miR-3144-3p		miR-190a-5p	miR-3605-3p	miR-628-3p
miR-15b-5p	miR-3176		miR-196a-3p	miR-370-5p	miR-628-5p
miR-16-2-3p	miR-3182		miR-196a-5p	miR-379-5p	miR-654-5p
miR-17-5p	miR-320a-3p		miR-197-3p	miR-382-5p	miR-668-3p
miR-181a-2-3p	miR-345-5p		miR-204-5p	miR-3909	miR-6852-5p
miR-181a-3p	miR-34c-5p		miR-208b-3p	miR-412-5p	miR-744-3p
miR-181a-5p	miR-378a-3p		miR-210-5p	miR-432-3p	miR-744-5p
miR-181b-2-3p	miR-383-5p		miR-215-5p	miR-432-5p	miR-769-5p
miR-181b-3p	miR-4449		miR-217-5p	miR-433-3p	miR-770-5p
miR-181b-5p	miR-4510		miR-22-3p	miR-433-5p	miR-876-3p
miR-18a-3p	miR-551b-3p		miR-2355-5p	miR-450a-5p	miR-889-5p
miR-18a-5p	miR-561-5p		miR-26a-5p	miR-450b-5p	miR-95-3p

Table 31: Top 10 enriched miRNA at the MYCN 3'UTR using miTRAP.

BE(2)-C		KNS42	
hsa-miR-449a	hsa-miR-20b-5p	hsa-miR-106a-5p	hsa-miR-20a-5p
hsa-miR-17-5p	hsa-miR-20a-5p	hsa-miR-3619-5p	hsa-miR-29b-3p
hsa-miR-106a-5p	hsa-miR-29b-3p	hsa-miR-592	hsa-miR-106b-5p
hsa-miR-193b-3p	hsa-miR-16-5p	hsa-miR-193b-3p	hsa-miR-20b-5p
hsa-miR-1248	hsa-miR-106b-5p	hsa-miR-17-5p	hsa-miR-19a-3p

Table 32: Mutated miRNA seed regions within the MYCN 3'UTR.

miRNA site	3'UTR base pairs	reporter status
miR-34-5p	22-29	mut
miR-19-3p	31-38	mut
miR-29-3p	332-339	mut
miR-101-3p	493-500	mut
let-7-5p/miR-98-5p	505-511	mut
miR-101-3p	562-568	wt
miR-34-5p	579-585	mut
miR-302-3p	858-864	mut
miR-17-5p/20-5p/93-5p/106-5p	859-865	mut
let-7-5p/miR-98-5p	868-874	mut

7.2 List of figures

Figure 1: Overview of signaling and regulation pathways in high-risk neuroblastoma.	10
Figure 2: Somatic mutations in pediatric cancer.	12
Figure 3: Genetic model of neuroblastoma development.	14
Figure 4: LIN28B-RAN-AURKA-MYCN signaling network in neuroblastoma.	16
Figure 5: Prognostic factors and their contribution to survival probability.	19
Figure 6: Association of chromosomal aberrations in high-risk neuroblastoma.	20
Figure 7: Chromosome 17q breakpoints in neuroblastoma tumors.	22
Figure 8: The structure of the IGF2BP family.	35
Figure 9: Overview of IGF2BP1 regulation and function.	37
Figure 10: Expression of IGF2BP family members in human hippocampus development.	41
Figure 11: Expression and dependency for IGF2BP1 in human cancer.	43
Figure 12: The genomic landscape of neuroblastoma is predictive for patient outcome.	75
Figure 13: Unbalancing of chromosome 17.	76
Figure 14: Chromosome 17q harbors most neuroblastoma essential genes.	78
Figure 15: IGF2BP1 has prognostic relevance in different neuroblastoma subgroups, is highly expressed in aggressive neuroblastoma and correlates with MYCN abundance.	81
Figure 16: MYCN directly promotes IGF2BP1 transcription.	83
Figure 17: miRNA expression can distinguish between MNA and nMNA tumors.	85
Figure 18: miTRAP identified selective co-purified miRNAs with in vitro transcribed bait RNA.	87
Figure 19: IGF2BP1 and ELAVL4 are potent regulators of MYCN expression.	88
Figure 20: ELAVL4 is downregulated in aggressive neuroblastoma subtypes.	89
Figure 21: IGF2BP1 directly bind the MYCN mRNA.	90
Figure 22: IGF2BP1 stimulated MYCN expression is miRNA-dependent.	91
Figure 23: BTYNB disrupts IGF2BP1 stabilization of MYCN mRNA.	92
Figure 24: Regulation of MYCN by IGF2BP1 is largely m ⁶ A-independent.	93
Figure 25: Impairment of IGF2BP1 reduced neuroblastoma growth in vitro.	95
Figure 26: IGF2BP1 knockout impaired neuroblastoma xenograft growth.	96
Figure 27: BTYNB impaired neuroblastoma xenograft growth.	97
Figure 28: Identification of potential chromosome 17 downstream targets.	100
Figure 29: IGF2BP1 and MYCN promote oncogenic genes located on chromosome 17q.	100
Figure 30: Top 17q IGF2BP1/MYCN target genes are highly expressed in aggressive neuroblastoma.	101
Figure 31: IGF2BP1 regulate 17q essential neuroblastoma genes in a 3'UTR-dependent manner.	102
Figure 32: IGF2BP1- and MYC/N-dependent regulation is conserved across cancer.	103
Figure 33: Determination of potential IGF2BP1 and MYCN target kinases.	104
Figure 34: IGF2BP1 regulates G2/M checkpoint kinases in a 3'UTR-dependent manner.	105
Figure 35: IGF2BP1 enhances MYCN protein stability.	107
Figure 36: EN4 inhibits neuroblastoma growth and reduces MYCN transcriptional activity.	109
Figure 37: Combined BTYNB and BRD inhibition is beneficial.	110
Figure 38: HDAC inhibitors are efficient in reducing MYCN levels.	112
Figure 39: HDAC1-3 inhibitors are sufficient and necessary to impair MYCN expression.	113
Figure 40: BIRC5 and IGF2BP1 inhibition are beneficial in combination treatment.	114
Figure 41: Scheme of transgenic mouse system.	116
Figure 42: IGF2BP1 induces neuroblastoma tumor formation.	117
Figure 43: IGF2BP1-induced tumors express neuroblastoma marker genes.	118
Figure 44: GSEA confirmed similarity of IGF2BP1- and IGF2BP1/MYCN-induced tumors.	120
Figure 45: IGF2BP1-induced tumors harbor chromosomal aberrations syntenic to human neuroblastoma.	122
Figure 46: Feedforward loop between IGF2BP1 and MYCN influences the hallmarks of cancer.	130

7.3 List of tables

<i>Table 1: Risk stratification with the INRG staging system.....</i>	<i>7</i>
<i>Table 2: GEMMs of high-risk neuroblastoma.....</i>	<i>31</i>
<i>Table 3: Mice strains.....</i>	<i>48</i>
<i>Table 4: Parental cell lines.....</i>	<i>49</i>
<i>Table 5: Generated cell lines and clones.....</i>	<i>49</i>
<i>Table 6: Small molecule inhibitors.....</i>	<i>50</i>
<i>Table 7: Standard buffer.....</i>	<i>50</i>
<i>Table 8: Primary and secondary antibodies.....</i>	<i>51</i>
<i>Table 9: Cloning vectors and plasmids.....</i>	<i>52</i>
<i>Table 10: Oligonucleotides and restriction sites for cloning.....</i>	<i>53</i>
<i>Table 11: RT-qPCR primer.....</i>	<i>54</i>
<i>Table 12: Primers for genotyping.....</i>	<i>55</i>
<i>Table 13: siRNAs.....</i>	<i>55</i>
<i>Table 14: Standard systems and kits.....</i>	<i>56</i>
<i>Table 15: Instruments.....</i>	<i>57</i>
<i>Table 16: PCR reaction setup.....</i>	<i>63</i>
<i>Table 17: PCR program.....</i>	<i>63</i>
<i>Table 18: Ligation.....</i>	<i>64</i>
<i>Table 19: RT program.....</i>	<i>65</i>
<i>Table 20: RT-qPCR program.....</i>	<i>65</i>
<i>Table 21: In vitro transcription reaction mix.....</i>	<i>67</i>
<i>Table 22: Frequency of chromosomal aberrations in neuroblastoma.....</i>	<i>76</i>
<i>Table 23: Top 10 essential gene candidates by significance.....</i>	<i>79</i>
<i>Table 24: Hypergeometric testing for distribution of MNA neuroblastoma essential genes.....</i>	<i>79</i>
<i>Table 25: Selected IGF2BP1-associated transcription factors.....</i>	<i>82</i>
<i>Table 29: BTYNB stability.....</i>	<i>98</i>
<i>Table 27: Tested HDAC inhibitors.....</i>	<i>112</i>
<i>Table A1: Human neuroblastoma tumor cohort.....</i>	<i>XXVII</i>
<i>Table A2: Transgenic mice.....</i>	<i>XXIX</i>
<i>Table A3: List of oncogenic and tumor-suppressive miRNAs deregulated in MNA neuroblastoma.....</i>	<i>XXX</i>
<i>Table A4: Top 10 enriched miRNA at the MYCN 3'UTR using miTRAP.....</i>	<i>XXX</i>
<i>Table A5: Mutated miRNA seed regions within the MYCN 3'UTR.....</i>	<i>XXX</i>

7.4 List of abbreviations

3'UTR: 3' untranslated region; **5'UTR:** 5' untranslated region; **ADRN:** adrenergic; **AG:** adrenal gland; **AGM:** adrenal gland from LSL-MYCN mouse model; **AI:** adrenal gland from LSL-IGF2BP1 mouse model; **AIM:** adrenal gland from LSL-IGF2BP1/MYCN mouse model; **ASCR:** autologous stem cell rescue; **BRD:** bromodomain-containing protein; **BRDi:** BRD inhibitor; **BTYNB:** 2-(((5-bromo-2-thienyl)methylene)amino) benzamide; **CCR4-NOT:** Carbon Catabolite Repression - Negative On TATA-less; **cdNA:** complementary DNA; **CHIP:** chromatin immunoprecipitation; **CLIP:** cross-linking and immunoprecipitation; **CN:** copy number; **CRC:** core regulatory circuit; **CRD:** coding region instability determinant; **CRISPR/Cas9:** clustered regularly interspaced short palindromic repeats and CRISPR associated protein 9; **CuB:** cucurbitacin B; **DAC:** 5'-aza-3'-deoxycytidine; **DFMO:**

difluoromethylornithine; **DNA**: deoxyribonucleic acid; **dt**: doubling time; **EC₅₀**: half maximal effective concentration; **eCLIP**: enhanced crosslinking and immunoprecipitation; **FACS**: fluorescence-activated cell sorting; **FDA**: food and drug administration; **FDR**: false discovery rate; **FPKM**: fragments per kilobase of exon per million mapped fragments; **GD2**: disialoganglioside; **gDNA**: genomic DNA; **GEMM**: genetically engineered mouse model; **GFP**: green fluorescent protein; **GM-CSF**: granulocyte-macrophage colony-stimulating factor; **GSEA**: gene set enrichment analysis; **GWAS**: genome-wide association study; **HDAC**: histone deacetylase; **HDACi**: HDAC inhibitor; **hESCs**: human embryonic stem cells; **HR**: hazard ratio; **IDRF**: image-defined risk factor; **INRG**: International Neuroblastoma Risk Group; **INSS**: International Neuroblastoma Staging System; **i.p.**: intra-peritoneal; **iRFP**: infra-red fluorescent protein; **i.t.**: intra-tumoral; **KH**: hnRNPK homology; **KO**: knockout; **LC-MS/MS**: liquid chromatography-mass spectrometry/mass spectrometry; **LCNEC**: high-grade large-cell neuroendocrine lung carcinoma; **LIHC**: liver hepatocellular carcinoma; **lncRNA**: long non-coding RNA; **LSL**: loxP-stop-loxP; **LUAD**: lung adenocarcinoma; **m⁶A**: N⁶-methyladenosine; **MES**: mesenchymal; **MHC**: major histocompatibility complex; **miRNA**: micro RNA; **miTRAP**: miRNA trapping by RNA *in vitro* affinity purification; **MNA**: *MYCN*-amplified; **mRNA**: messenger RNA; **mRNP**: messenger ribonucleoprotein complex; **MS2-BP**: MS2-binding protein; **mut**: mutated; **NB**: neuroblastoma; **ncRNA**: non-coding RNA; **n. d.**: not determined; **NES**: normalized enrichment score; **nMNA**: non-*MYCN*-amplified; **n. s.**: not significant; **PAAD**: pancreatic adenocarcinoma; **PCA**: principal component analysis; **PCR**: polymerase chain reaction; **PDX**: patient-derived xenograft; **PRC**: polycomb repressive complex; **R26**: *Rosa26* locus; **RBP**: RNA-binding protein; **RIP**: RNA immunoprecipitation; **RNA**: ribonucleic acid; **RRM**: RNA recognition motif; **RT-qPCR**: reverse transcriptase quantitative PCR; **SCNEC**: high-grade small-cell neuroendocrine lung carcinoma; **s.c.**: subcutaneous; **SD**: standard deviation; **SEM**: standard error of mean; **SELEX**: systematic evolution of ligands by exponential enrichment; **sgRNA**: single guide RNA; **siRNA**: small interfering RNA; **SNP**: single nucleotide polymorphism; **sWGS**: shallow whole genome sequencing; **SWI/SNF**: Switch/Sucrose Non-Fermentable; **TCGA**: The Cancer Genome Atlas; **TI**: tumor from LSL-*IGF2BP1* mouse model; **TIM**: tumor from LSL-*IGF2BP1*/*MYCN* mouse model; **TMM**: trimmed mean of M values; **TPM**: transcripts per million; **wt**: wildtype; **ZIP**: zero interaction potency

7.5 List of publications / presentations

Publications

Bell JL, **Hagemann S**, Holien JK, Liu T, Nagy Z, Schulte JH, Misiak D, Hüttelmaier S.: “Identification of RNA-Binding Proteins as Targetable Putative Oncogenes in Neuroblastoma.” *Int J Mol Sci.* 2020 Jul 19;21(14):5098; doi: 10.3390/ijms21145098; PMID: 32707690

Ihling C, Tänzler D, **Hagemann S**, Kehlen A, Hüttelmaier S, Arlt C, Sinz A.: “Mass Spectrometric Identification of SARS-CoV-2 Proteins from Gargle Solution Samples of COVID-19 Patients.” *J Proteome Res.* 2020 Nov 6;19(11):4389-4392; doi: 10.1021/acs.jproteome.0c00280; PMID: 32568543

Glaß M, Misiak D, Bley N, Müller S, **Hagemann S**, Busch B, Rausch A, Hüttelmaier S.: “IGF2BP1, a Conserved Regulator of RNA Turnover in Cancer.” *Front Mol Biosci.* 2021 Mar 22;8:632219; doi: 10.3389/fmolb.2021.632219; PMID: 33829040

Misiak D*, **Hagemann S***, Bell JL, Busch B, Lederer M, Bley N, Schulte JH, Hüttelmaier S.: “The MicroRNA Landscape of MYCN-Amplified Neuroblastoma.” *Front Oncol.* 2021 May 7;11:647737; doi: 10.3389/fonc.2021.647737; PMID: 34026620 (* denoted shared first authorship)

Hagemann S, Misiak D, Bell JL, Fuchs T, Lederer MI, Bley N, Hämmerle M, Ghazy E, Sippl W, Schulte JH, Hüttelmaier S.: “IGF2BP1 induces neuroblastoma via a druggable feedforward loop with MYCN promoting 17q oncogene expression.” *Mol Cancer.* 2023 May 29;22(1):88; doi: 10.1186/s12943-023-01792-0; PMID: 37246217

Presentations

29.05. - 03.06.2018: RNA meeting, Berkeley, USA – “The perfect storm: IGF2BP1 and MYCN form a self-sustaining oncogenic network in neuroblastoma”

15. - 17.02.2023: AEK Cancer Congress, Kassel, Germany – “IGF2BP1 induces high-risk neuroblastoma and enhances oncogene expression”

30.05. - 04.06.2023: RNA meeting, Singapore, Singapore – “The RNA-binding protein IGF2BP1 induces high-risk neuroblastoma, enhances oncogene expression and has high pharmacological target potential”

7.6 Eidesstattliche Erklärung

Hiermit erkläre ich, dass ich meine Dissertationsschrift selbständig und ohne fremde Hilfe verfasst habe. Ich habe keine anderen als die von mir angegebenen Quellen und Hilfsmittel benutzt. Die aus den benutzten Werken wörtlich oder inhaltlich entnommenen Stellen habe ich als solche kenntlich gemacht.

Mit der vorliegenden Arbeit bewerbe ich mich erstmals um die Erlangung des Doktorgrades.

Halle (Saale)

Sven Hagemann

7.7 Curriculum vitae

Personal Details

Name: Sven Hagemann
Nationality: German

Scientific Education

2011 - 2014	Bachelor of Science studies in Biochemistry at the Martin-Luther-University Halle-Wittenberg
2014	Bachelor thesis under supervision of PD Dr. Stephan König at the Martin-Luther-University Halle Wittenberg Title: “Funktionelle und strukturelle Charakterisierung von Phosphoketolase aus <i>Lactobacillus pentosus</i> “
2014 - 2016	Master of Science studies in Biochemistry at the Martin-Luther-University Halle-Wittenberg
2016	Master thesis under supervision of Prof. Dr. Stefan Hüttelmaier at the Martin-Luther-University Halle-Wittenberg Title: “Analyse des feedback-Mechanismus von IGF2BP1 und MYCN im Neuroblastom“
2017 - 2024	Doctoral thesis in the laboratory of Prof. Dr. Stefan Hüttelmaier at the Martin-Luther-University Halle-Wittenberg